Special functions and dynamical systems in cosmology

Antonio d'Alfonso del Sordo

Department of Mathematics, University College London

A thesis submitted in partial fulfilment of
the requirements for the degree of

Doctor of Philosophy

Supervised by
Prof Christian G Böhmer

September 2025

Declaration

I, Antonio d'Alfonso del Sordo, confirm that the work presented in this thesis is my own. Where information has been derived from other sources, I confirm that this has been indicated in the thesis.

To my grandmothers

Abstract

From a mathematical perspective, questions in cosmology often reduce to solving ordinary differential equations. The theories of special functions and dynamical systems provide powerful tools for analysing these equations, enabling us to draw physical conclusions. We investigate two distinct problems: (i) computing the angular distance travelled by a test particle along an azimuthal geodesic in closed Friedmann-Lemaître-Robertson-Walker (FLRW) universes; (ii) studying the dynamical evolution of a cosmological model with a boundary-term coupling.

After reviewing exact solutions to the cosmological field equations and deriving the full set of FLRW geodesics, we compute an array of explicit formulae for the path of a photon over one cycle of expansion and recollapse in several scenarios. We begin with the simplest closed FLRW model with an arbitrary linear equation of state parameter and extend our analysis to include two-fluid models, a cosmological constant, and a massive particle. Special functions, particularly elliptic functions, naturally emerge in this context.

Next, we apply dynamical systems techniques to cosmological models incorporating a perfect fluid, a scalar field, and boundary terms. After reviewing the use of dynamical systems in dark energy models, we adopt Brown's formulation of the variational principle for relativistic fluids to introduce novel couplings. We focus on one specific coupling, which is particularly relevant to cosmology, as it behaves similarly to models where dark matter decays into dark energy, particularly in the case of a constant coupling. When the coupling is non-constant, however, it reveals a previously unseen, rich dynamical structure, featuring both early- and late-time accelerated expansion. Using well-known variables, we work in a two-dimensional phase space, allowing for a clear physical interpretation and draw analogies with existing models.

Whilst the first problem yields self-contained, complete results, the second opens several promising directions for future research.

Impact statement

This thesis investigates two main threads of research within mathematical cosmology. It falls within the broader EPSRC remit of Mathematical Physics, with the "aim to advance the strong intradisciplinary links to both pure and applied mathematics [... and to] encourage novel interactions between mathematical physics and new research challenges of national importance relating to EPSRC's outcomes, including through links to pure and applied mathematics and theoretical physics"; in particular, it contributes to our understanding of topics related to the nature of dark energy, dark matter, and the large-scale structure of the cosmos.

The main findings are based on two original research papers, namely [34, 37], published in peer-reviewed journals and have been presented to academic and general audiences alike, at conferences and more informal settings. Inside academia, this thesis deepens our understanding of the mathematical structures underlying cosmological models and the motion of particles. Secondly, it proposes theoretical models which exhibit similar behaviour to that seen in observational cosmology, particularly when it comes to the universe's accelerated expansion. A pressing question in modern physics is whether General Relativity is sufficient to describe gravity on cosmological scales; this thesis contributes to the growing body of work that modifies Einstein's theory of gravity in light of dark energy and dark matter.

From an educational standpoint, this thesis could be used to develop valuable teaching resources for undergraduate and postgraduate instruction in applied mathematics and theoretical physics, by providing concrete examples of mathematical techniques applied to cosmological contexts. For instance, the derivation presented in Section 3.4.1 lends itself to pedagogical use; special cases of this appear in standard undergraduate cosmology textbooks, and we show that the natural extension of that problem to universes with any type of matter content is also accessible at the undergraduate level. This derivation can be shared with educators by publishing it in the form of a short pedagogical article. Moreover, beyond academia, this particular result has outreach potential since the underlying concept is straightforward, and could be used to explain difficult concepts about cosmology to a lay audience, made accessible through Mathematica simulations which have already bee developed by the authors.

Acknowledgements

In ancient times, it was customary to begin works of literature with a call to the Muse (or to the Muses), seeking inspiration and guidance for creative endeavours. In a way, this was a form of acknowledgement, and thanks for their protection during the course of the creative journey. In the same spirit, I would like to thank the several muses and companions I had the honour and privilege to have by my side.

This work is supported by the Engineering and Physical Sciences Research Council EP/R513143/1 & EP/T517793/1.

Firstly, I would like to thank my supervisor, Prof Christian G Böhmer, for his kind guidance, his sustained encouragement, his reassuring words in times of need, and keeping my interest for research alive thanks to his supervisory skills.

I would also like to express my gratitude to my collaborators, Dr Betti Hartmann and Dr Erik Jensko, with whom it is always a pleasure to discuss research ideas. I am extremely grateful to my PhD mentor, Dr Cecilia Busuioc, for her generosity with her time, looking after me, listening to me, and offering advice.

After eight years at UCL, the Department of Mathematics has been a second home for me. The inspiring conversations I have had—from the mathematical to the mundane—have been numerous. I have had the pleasure to meet several people, whom I now call friends; I give my gratitude to them for making my journey meaningful and pleasant. Some of them kindly offered their help in proofreading earlier versions of this manuscript and provided valuable feedback; my thanks to Dr Isidoros Strouthos, Dr David Sheard, Dr Erik Jensko, and Sheila Maria Pérez García.

I am in debt to all the lecturers and teachers who have inspired me from school to university.

I will always be grateful to my family for their constant support, trusting my passions, and all the sacrifices they made to allow me to pursue them. I dedicate this work to my Nonna Assunta and the loving memory of my Nonna Lia; they were both Mathematics teachers at points in their lives, and engaged with a young me when discovering the beauty of mathematics.

To my friends, from Italy and here in London, for having been wonderful listeners and having been patient with me during the rollercoaster of life. To my goddaughter, Sophie Rose, who arrived

in the middle of my PhD and continues to bring light to my life ever since.

At the beginning of this PhD experience at UCL, I found my loving partner, David. Without his relentless support, patience which cannot be underestimated, profound belief in my abilities, and, most importantly, genuine love, I would not have made it to the end.

I count myself very lucky for all the people who have been my Muses during this journey, and I would like to wish them all well.

As ever,

UCL research paper declaration form

(1) **For a research manuscript that has already been published** (if not yet published, please skip to section 2)**:**

(a) **What is the title of the manuscript?**

[34] Azimuthal geodesics in closed FLRW cosmological models

[37] Cosmological fluids with boundary term couplings

(b) **Please include a link to or doi for the work:**

[34] https://doi.org/10.1103/PhysRevD.110.083504

[37] https://doi.org/10.1007/s10714-024-03260-6

(c) **Where was this work published?**

[34] Physical Review D

[37] General Relativity and Gravitation

(d) **Who published the work?**

[34] American Physical Society

[37] Springer Nature

(e) **When was the work published?**

[34] 1 October 2024

[37] 18 June 2024

(f) **List the manuscript's authors in the order they appear on the publication:**

[34] Christian G. Boehmer, Antonio d'Alfonso del Sordo, Betti Hartmann, Linus Elias Münch

[37] Christian G. Boehmer, Antonio d'Alfonso del Sordo

(g) **Was the work peer reviewed?**

[34] Yes

[37] Yes

(h) **Have you retained the copyright?**

[34] Yes, for publication in my thesis.

[37] Yes, for publication in my thesis.

(i) **Was an earlier form of the manuscript uploaded to a preprint server? If 'Yes', please give a link or doi.**

[34] https://arxiv.org/pdf/2404.18119

[37] https://arxiv.org/pdf/2404.05301

(2) **For a research manuscript prepared for publication but that has not yet been published** (if already published, please skip to section 3)**:**

(a) **What is the current title of the manuscript?**

[33] Azimuthal geodesics in closed FLRW cosmologies

(b) **Has the manuscript been uploaded to a preprint server? If 'Yes', please please give a link or doi.**

[33] https://arxiv.org/pdf/2401.04597

(c) **Where is the work intended to be published?**

[33] TBC

(d) **List the manuscript's authors in the intended authorship order:**

[33] Christian G Boehmer, Antonio d'Alfonso del Sordo, Betti Hartmann

(e) **Stage of publication:**

[33] TBC

(3) **For multi-authored work, please give a statement of contribution covering all authors** (if single-author, please skip to section 4)**:**

[33] **Christian G Boehmer**: conceptualisation (lead); formal analysis (equal); supervision (equal); writing - review and editing (equal).

Antonio d'Alfonso del Sordo: formal analysis (equal); writing - original draft; writing - review and editing (equal); funding acquisition.

Betti Hartmann: conceptualisation (supporting); supervision (equal); writing - review and editing (equal).

[34] **Christian G Boehmer**: conceptualisation (equal); supervision (equal); validation (equal); visualisation (supporting); writing - review and editing (equal).

Antonio d'Alfonso del Sordo: conceptualisation (equal); formal analysis (equal); visualisation (lead); writing - original draft (lead); writing - review and editing (equal); funding acquisition.

Betti Hartmann: conceptualisation (equal); supervision (equal); validation (equal); writing - review and editing (equal).

Linus Elias Münch: formal analysis (supporting).

[37] **Christian G Boehmer**: conceptualisation; supervision; validation; writing - original draft (equal); writing - review and editing (equal).

Antonio d'Alfonso del Sordo: formal analysis; funding acquisition; visualisation; writing - original draft (equal); writing - review and editing (equal).

(4) **In which chapter(s) of your thesis can this material be found?**

[33] Chapter 3

[34] Chapter 3

[37] Chapter 4

e-Signatures confirming that the information above is accurate

Candidate: Antonio d'Alfonso del Sordo

Date: 07 July 2025

Supervisor/Senior Author signature (where appropriate)**:**

[33] Christian G Böhmer

[34] Christian G Böhmer

[37] Christian G Böhmer

Date: 07 July 2025

Contents

List of figures

List of tables

0

Overview

Physical cosmology is the study of the universe as a whole; it has its foundations in Einstein's theory of General Relativity (GR), which formulates physical laws using pseudo-Riemannian geometry. In GR, the information regarding geometric and causal structure of spacetime, as well as its effects on gravity, is contained in the line element (or metric tensor). By imposing symmetries of homogeneity and isotropy, one obtains the Friedmann–Lemaître–Robertson–Walker (FLRW) metric [82, 117, 140–142, 166], which contains a time-dependent function, called the scale factor, describing the rate at which the universe expands or contracts.

This thesis studies systems of ordinary differential equations which emerge in the context of cosmology in two specific scenarios. The first is a set of four coupled second-order differential equations which describe the motion of test particles, such as photons, along geodesics through the FLRW spacetime. The second consists of Einstein's field equations—a set of ten coupled non-linear partial differential equations—which become a system of non-linear ordinary differential equations describing the (idealised) evolution of the universe that we observe. From a mathematical perspective, studying these two systems of equations requires different approaches.

In the more standard cases, these equations can be solved analytically, albeit with the use of non-elementary functions, or special functions [12, 14, 90], such as elliptic functions [50, 57, 58, 68, 69, 76, 135]. Special functions can be thought of as a generalisation of elementary functions, which appear naturally in some mathematical theories as well as physical applications. The meaning of the term 'special' is nebulous, and can vary between different contexts. For the purpose of this thesis, one can think of a special function as a function which satisfies a second-order ordinary differential equation. From this point of view, the 'elementary' functions like trigonometric, exponential, and logarithmic functions are the solutions of second-order ordinary differential equations *with constant coefficients*, or their inverses.

The FLRW metric describes a spatially maximally symmetric space of constant curvature evolving in time. The curvature of the spatial surfaces dictates the geometry of the universe on cosmic scales [87, 98, 112] and can take one of three forms: negative, zero, or positive; corresponding to an open, flat, or closed universe, respectively. The geometry of a closed universe, which is spatially a

sphere, allows for a scenario in which the universe expands up to a maximum size, before recollapsing during the so-called *big crunch*. This oscillatory behaviour was first noted by Friedmann [82]. In [96], Harrison provided a classification for FLRW models, including oscillatory universes. These models of a universe undergoing cycles of expansion and contraction were further explored in [21–24, 41]. In particular, in [22], the closed-universe recollapse conjecture—which states that, under certain conditions, the expanding universe could eventually reverse its course, contracting back to a highly dense state, and initiating a new cycle of expansion and contraction—was proposed as a potential solution to cosmological issues such as the *singularity problem*, which aims to understand what happened at the Big Bang.

While the prevailing observational evidence has strongly favoured a spatially flat universe over a closed one, recent observations have prompted a reconsideration of the possibility that the universe may in fact exhibit a closed geometry [13, 63–65, 84, 92, 147, 161, 162]. The 2018 PLANCK data set [6] slightly favours a closed universe. This is in contrast with the cosmic microwave background (CMB) lensing and baryon acoustic oscillations data; this tension reopened the debate over the curvature of the universe [92]. Moreover, closed universe models also seem to be good candidates to address the Hubble tension—the discrepancy between different measurements of the Hubble constant which describes the current rate of expansion of the universe—between supernovae observations and the CMB [92]. Analyses from the more recent DESI collaboration [5] of early- and late-time data, including baryon acoustic oscillations and Type Ia supernovae, also point towards a positive curvature constant. This motivates studying test particle motion in closed FLRW spacetimes. In this geometric setting, it is possible to study azimuthal geodesics; this type of geodesics has been studied extensively in the context of rotating systems and settings involving spherical symmetry, for example the motion of particles around massive objects such as black holes, see [49], where special functions arise [52, 113].

Beyond the large-scale curvature of the universe, there are many other phenomena which are of relevance to theoretical cosmology. Perhaps the most important of these at present are the observed early- and late-time accelerated expansions of the universe (usually referred to as *inflation* and *dark energy-dominated epoch*, respectively). Models which exhibit these phenomena correspond to cosmological field equations for which the task of obtaining analytical solutions is formidable. It is therefore useful to employ techniques from the theory of dynamical systems. This theory provides us with techniques to understand the qualitative behaviour of the solutions of a differential equation, or a system thereof, without finding them explicitly. The use of dynamical systems precedes the discovery of the accelerated expansion of the universe in 1998, and hence the concept of *dark energy*; see for example [164]. In more recent years, a review which deals with dark energy and modified theories of gravity through the lens of dynamical systems filled this

gap [28]. For a cosmological dynamical system to be physically relevant, we expect it to reflect the succession of the following epochs through some fixed points: inflation (early-time attractor), radiation-domination and matter-domination (usually saddle points), late-time inflation (late-time attractor). In Chapter 4, we apply dynamical systems techniques to cosmological field equations which derive from modifications of gravity.

Since the introduction of GR in 1915, several approaches to extending or modifying Einstein's theory have been proposed. This is due to the fact that (pseudo-)Riemannian geometry was a relatively novel subject when GR came about, hence it was interesting to consider what consequences the removal, or modification, of some of its assumptions would yield. As an example, from a theoretical point of view, in GR, one usually restricts the Lagrangian to be a linear function of the Ricci scalar, minimally coupled with matter. However, there is no reason, *a priori*, to assume such a restriction. So, one can modify the gravitational part of the action to allow non-linear corrections to the Lagrangian [47, 126]; this is the general approach followed by $f(R)$-theories of gravity [61, 149]. Some other extensions of GR increase the number of spacetime dimensions or introduce non-minimal matter couplings to boundary and topological terms [19, 35, 46, 53, 78, 86, 94, 132–134]. These are terms in the Lagrangian that describe how matter couples to geometrical quantities. Non-minimally coupled terms involving curvature vanish in the limit of special relativity.

Another approach is to consider dark energy as evidence for the incompleteness of GR and, hence, seek extensions or modifications of GR [104, 111, 145]. Towards the end of the last century, a further realisation was that not only is the universe expanding, but it is also accelerating. In 2011, Permutter, Riess, and Schmidt were awarded the Nobel Prize in physics for their discovery in 1998 [137, 138] of the accelerating expansion of the universe. Since this discovery, a plethora of models to elucidate this phenomenon has emerged. The addition of a positive cosmological constant, Λ, to the Einstein field equations, originally introduced by Einstein [70] for his static universe, is one of the most straightforward candidates for dark energy. This paves the way for the Λ Cold Dark Matter (ΛCDM) model. However, the ΛCDM model fails to explain why the inferred value of Λ is so small compared to the vacuum energy density expected from particle physics [167]. It is also unclear why its value is comparable to the matter density today; this constitutes the so-called *coincidence problem* [144, 172].

One way to begin to address this issue is to allow for a dynamical cosmological constant [56], that is, to introduce some dynamical field able to reproduce the late-time acceleration behaviour and mimic the properties of the cosmological constant. In order for it to agree with current observations, such a field must not interact through any of the Standard Model fundamental forces other than gravity, and must be invisible to the electromagnetic radiation, hence *dark* energy.

The simplest such model is a canonical scalar field, ϕ, with flat potential, $V(\phi)$, which drives the accelerated expansion of the universe. Any model of this type is referred to as *quintessence* [157], named after the fifth element in ancient and medieval philosophy, which was believed to be the fundamental substance of the universe and the source of all life and motion. Scalar fields play a major role in cosmology as they are also employed to characterise inflation, the early-time epoch of accelerated expansion [30, 152, 159], and dark matter, a hypothetical form of matter thought to account for approximately 85% of the matter content in the universe; see, for example, [125]. Several models to describe the dark energy interaction with dark matter have been proposed [20, 27, 45, 77, 89, 99, 136, 163]. It is worth mentioning that, the first and only observed elementary scalar particle (zero spin), as predicted by the Standard Model of particle physics, is the Higgs boson. This particle is associated with the Higgs field, a field that fills the entire Universe and gives mass to all elementary particles; its existence was confirmed in 2012 by the ATLAS and CMS experiments at the Large Hadron Collider (LHC) at CERN [1].

At the core of this thesis, there are two main aims:

(i) to compute the angular distance travelled by a test particle along an azimuthal geodesic in closed FLRW universes;

(ii) to study the dynamical evolution of a cosmological model with a boundary-term coupling.

For (i), we need special functions, and, for (ii), dynamical system techniques. These are both introduced in Chapter 1, where we provide a mathematical overview. Through a motivational example concerning the simple pendulum, we introduce dynamical systems first and, then, elliptic integrals and elliptic functions. Some of these results concerning what makes a special function *special* are quite classical, but surprisingly overlooked. We therefore provide an overview of these and show how complex analysis can help us understand the properties of these functions.

We are interested in the applications of these mathematical tools to cosmology, which we introduce in Chapter 2. We build the FLRW metric from symmetries, using mathematical objects from differential geometry. We then also review exact solutions to the cosmological field equations and show how dynamical systems techniques have been employed to understand simple models of scalar field cosmology used to describe inflation.

In Chapter 3, we address (i). We first derive the full set of FLRW geodesics, and we then compute an array of explicit formulae for the path of a photon over one cycle of expansion and recollapse for a closed FLRW universe in several scenarios. We first obtain a formula for the simplest model, which includes an arbitrary linear equation of state parameter and a vanishing cosmological constant. In Section 3.4.1, we find that the angular distance travelled by a ray of light starting at the beginning of the universe during the expansion and recollapse is given by

$\Delta\varphi = 2\pi/(1+3w)$, for an arbitrary linear equation of state parameter w, consistently with the well-known values of 2π for a matter-dominated universe and π for a radiation-dominated one.

We then broaden the scope to include the motion of a massless particle in two-fluid models; in the presence of a cosmological constant; and we also consider massive particles in a single fluid. For example, a massless particle travels an angular distance of $\Delta\varphi = \pi + 2\arcsin\big(1/\sqrt{4\xi+1}\big)$ in a universe filled with dust and radiation (see Section 3.4.3.1), and exactly half this distance when dust is replaced by stiff matter (see Section 3.4.3.2). Here, ξ measures the relative initial densities of the two fluids. When massive particles are considered, we must employ the special functions introduced in Chapter 1, and the cosmological notions from Chapter 2. The simplest is, perhaps, a massive particle in a radiation-filled universe, which traverses an angular distance of $\Delta\varphi = 2K(-\beta/L_z^2)$, where β is the initial radiation density, L_z is the angular momentum of the particle, and K is the complete elliptic integral of the first kind (see Section 3.4.5.2).

In Chapter 4, we apply dynamical systems techniques to cosmological models incorporating a perfect fluid, a scalar field, and boundary terms. After reviewing the use of dynamical systems in dark energy models, we adopt Brown's formulation of the variational principle for relativistic fluids to introduce novel couplings. We focus on a derivative coupling, for which the interaction Lagrangian density is of the form $\mathcal{L}_{\text{int}} = -\sqrt{-g}f(n,s,\phi)B^\mu\partial_\mu\phi$, which turns out to be particularly relevant to cosmology, as it behaves similarly to models where dark matter decays into dark energy, e.g. [54], particularly in the case of a constant coupling. We provide an analysis of this model for the matter-dominated and radiation-dominated cases in Section 4.4. Using well-known variables, we work in a two-dimensional phase space; and by applying a carefully chosen change of variables, we were able to arrive at a phase space which mirrors the one studied in [54]. These results demonstrate that our model can be seen as a natural extension of previous work.

When the coupling is non-constant, we consider an interaction function $f(n,\phi)$ which is proportional to $n^{\alpha(1+w)/2}V(\phi)^{-\alpha/2}$, for an exponential potential V. This reveals a previously unseen, rich dynamical structure, featuring both early- and late-time accelerated expansion, when $\alpha = 2$, which is discussed in Section 4.5. In contrast, when we consider the case $\alpha = -2$ in Section 4.7, it is necessary to re-write the models in terms of a different choice of variables; see also Section 4.6. Once this is done, the phase space looks similar to that from Section 4.5, but we have to apply a further restriction so that the values of the effective equation of state parameter are physically meaningful. In practice, this restricts the physical trajectories and is overall more limiting than the scenarios for $\alpha = 2$. Nevertheless, interesting phenomena do appear, for example, one choice of model parameters yields a universe with the so-called phantom dark energy, in which energy density increases over time.

Problem (i) yields self-contained, complete results, whereas Problem (ii) opens several promising

directions for future research. These are discussed in Chapter 5.

Notation and conventions

Unless otherwise specified, we employ standard relativistic notation throughout. The signature of the metric tensor $g_{\mu\nu}$ is assumed to be $(-,+,+,+)$, Greek indices are space-time indices taking $(0,1,2,3)$.

The coupling constant appearing in the Einstein field equations is denoted by $\kappa = 8\pi G/c^4$, where c is the speed of light and G the Newton's gravitational constant. Throughout, we use geometrised natural units with $c = 1$ and $G = 1$.

A dot will denote differentiation with respect to cosmological time. A prime denotes the derivative with respect to the argument. Sometimes the comma notation for partial derivatives is used $\phi_{,\mu} = \partial_\mu \phi$.

We will use the following without proof:

- Christoffel symbols for the metric $\mathrm{d}s^2 = g_{\mu\nu}\mathrm{d}x^\mu \mathrm{d}x^\nu$:

$$\Gamma^\rho_{\mu\nu} = \frac{1}{2} g^{\rho\sigma}\left(\frac{\partial g_{\mu\sigma}}{\partial x^\nu} + \frac{\partial g_{\nu\sigma}}{\partial x^\mu} - \frac{\partial g_{\mu\nu}}{\partial x^\sigma}\right); \tag{0.1}$$

- covariant derivative acting on a rank-2 tensor:

$$\nabla_\rho T_{\mu\nu} = \partial_\rho T_{\mu\nu} - \Gamma^\sigma_{\rho\mu} T_{\sigma\nu} - \Gamma^\sigma_{\rho\nu} T_{\mu\sigma}\,. \tag{0.2}$$

1

Mathematical overview

1.1 Introduction

In this thesis, a common theme is describing solutions to problems in cosmology using special functions. To provide some motivation for the need for special functions, and, in particular, elliptic integrals, we first consider the example of the *simple pendulum*[1]. It is one of the very first examples encountered in elementary mechanics courses, where the non-linearity of the differential equation which describes its motion is typically overcome by introducing a small-angle approximation. The use of dynamical systems techniques allows one to go further and investigate the large-angle regime qualitatively. The reason behind this pedagogical choice is the complexity encountered when we seek an analytic solution for all values of the angle. This complexity requires us to introduce *special functions*. In what follows, we illustrate how special functions naturally arise in the description of physical phenomena by looking carefully at the simple pendulum. This also serves to introduce the other main tool in this thesis, that is, dynamical systems techniques.

1.2 The simple pendulum

Let us begin by considering a particle of mass m attached to the end of a light (massless) inextensible string (or rod) of length ℓ, in the absence of damping and external driving. Let θ denote the angle from the downwards vertical to the pendulum string, as shown in Fig. 1.1.

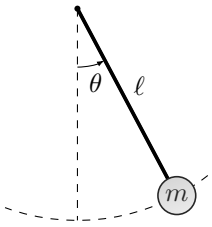

Fig. 1.1: The simple pendulum

[1]This is sometimes referred to as the *mathematical* or *ideal pendulum*, to distinguish it from the physical pendulum because of its modelling assumptions.

The forces acting on the mass are: the tension in the string; and the force of gravity, which can be decomposed into a radial component, $mg\cos\theta$, and a transverse component, $-mg\sin\theta$, where g is the acceleration due to gravity. There is no motion in the radial direction since the string is inextensible; whereas, in the transverse direction, by Newton's second law, the angular acceleration $\ell \mathrm{d}^2\theta/\mathrm{d}t^2$, is given by

$$m\ell\frac{\mathrm{d}^2\theta}{\mathrm{d}t^2} = -mg\sin\theta \implies \frac{\mathrm{d}^2\theta}{\mathrm{d}t^2} + \frac{g}{\ell}\sin\theta = 0\,. \tag{1.1}$$

By introducing the frequency $\omega = \sqrt{g/\ell}$ and a dimensionless time variable $\tau = \omega t$, Eq. (1.1) reads

$$\ddot{\theta} + \sin\theta = 0\,, \tag{1.2}$$

where the overdot denotes differentiation with respect to τ. This is a nonlinear first-order ordinary differential equation, which, as we shall see, is difficult to solve analytically since it requires the use of elliptic functions. Generally, to bypass this, one studies the behaviour of the pendulum for small oscillations about the equilibrium position, that is, $\theta \ll 1$ and $\sin\theta \approx \theta$. In this case, the solution is approximately simple harmonic motion of period 2π, that is, $\theta = A\sin(\tau + \phi)$, where A is the amplitude and ϕ is the phase of the oscillations. However, this does not hold for the large-angle regime. In order to analyse the behaviour of the pendulum, we will use dynamical systems techniques.

1.3 Dynamical systems

Classical dynamical systems can be thought of as systems of differential equations. Such dynamical systems are extremely interesting and useful objects of study, and are an important tool across pure and applied mathematics.

Let $\mathbf{f}$ be a vector field on a state space $X \subset \mathbb{R}^n$. The *autonomous differential equation* defined by a function $\mathbf{f}$ is

$$\dot{\mathbf{x}} = \mathbf{f}(\mathbf{x})\,, \quad \mathbf{x} \in X \subset \mathbb{R}^n. \tag{1.3}$$

Here the overdot represents the derivative with respect to a variable t, which can be interpreted as time. A solution $\mathbf{x}(t)$ to this system with initial condition $\mathbf{x}(0) = \mathbf{x}_0$ then models a particle which starts at $\mathbf{x}_0$ and moves with position $\mathbf{x}(t)$ such that its velocity vector is given by $\dot{\mathbf{x}} = \mathbf{f}(\mathbf{x})$. For a given $\mathbf{x}_0$, this is called a *trajectory*. Thus, the tangent vector to the solution curve, $\dot{\mathbf{x}}(t)$, is equal to the vector field $\mathbf{f}$ evaluated at the position $\mathbf{x}$ at time t, $\mathbf{f}(\mathbf{x}(t))$. When $\mathbf{f}$ is sufficiently 'nice', Eq. (1.3) with initial condition $\mathbf{x}(0) = \mathbf{x}_0$ admits a unique solution by the following theorem.

Theorem 1.1 (Picard–Lindelöf theorem [150, p. 150])

Let $\mathbf{f}\colon X \to \mathbb{R}^n$ *be a continuous function on an open set* $X \subset \mathbb{R}^n$*. Suppose that the partial derivatives* $\partial f_i/\partial x_j$ *exist and are continuous for* $1 \leq i, j \leq n$ *on* X*. Fix a point* $\mathbf{x}_0 \in X$*. Then, for the initial value problem* $\dot{\mathbf{x}} = \mathbf{f}(\mathbf{x})$ *with* $\mathbf{x}(0) = \mathbf{x}_0$*, there exists a unique solution* $\mathbf{x}(t)$ *defined on some interval* $t \in (-\tau, \tau)$ *for* $\tau > 0$*.*

An immediate corollary is that, when $\mathbf{f}$ has continuous partial derivatives, there is a unique trajectory through any point in X, and so no trajectory can intersect another trajectory, or itself, unless it is periodic. These hypotheses hold in many simple examples of dynamical systems, including that of the simple pendulum. In Chapter 4, we will encounter cosmological models for which the hypotheses of the Picard–Lindelöf theorem do not hold at all points in the phase space and trajectories can intersect. Such examples are known as *discontinuous* dynamical systems [80, 123]; and are systems for which, at some point, uniqueness is violated since there are at least two solutions satisfying the same initial condition, but are distinct on the interval $(-\tau, \tau)$.

As an example of this behaviour, consider the dynamical system given by

$$\dot{x} = \frac{|x|}{\sqrt{x^2 + y^2}}\,, \tag{1.4a}$$

$$\dot{y} = \frac{|y|}{\sqrt{x^2 + y^2}}\,, \tag{1.4b}$$

on $\mathbb{R}^2 \setminus \{(0,0)\}$. The phase portrait is shown in Figure 1.2. The right-hand sides of Eq. (1.4) are discontinuous at $(0,0)$, meaning that the limit $\lim_{(x,y)\to(0,0)}(\dot{x}, \dot{y})$ does not exist, and hence any extension of the dynamical system to $\mathbb{R}^2$ will fail to satisfy the hypotheses of Theorem 1.1. It is, however, possible to extend trajectories which approach $(0,0)$ in finite time across this singularity in a way consistent with Eq. (1.4). Fix an angle $0 \leq \alpha \leq \pi/2$, and consider the trajectory $\mathbf{x}_\alpha(t) = (t\cos(\alpha), t\sin(\alpha))$; this is the straight line passing through $(0,0)$ with constant unit speed, and making angle α to the x-axis. One can easily verify that $\mathbf{x}_\alpha(t)$ satisfies Eq. (1.4) for $t \neq 0$. Moreover, the limit, $\lim_{t\to 0}(\dot{x}, \dot{y})\big|_{\mathbf{x}_\alpha(t)}$, exists and equals $(\cos(\alpha), \sin(\alpha))$, so, in a rigorous sense, the trajectory $\mathbf{x}_\alpha(t)$ can be said to satisfy Eq. (1.4), considered on the whole of $\mathbb{R}^2$. This dynamical system, therefore, gives an instance where infinitely many distinct trajectories intersect at the same point, as shown in Fig. 1.2—this behaviour will also be observed in Section 4.5 and Section 4.7.

For now, let us return to the situation where the Picard–Lindelöf theorem does apply, and every point in the phase space determines a unique trajectory which passes through it. In this case, we can define the *flow*, which is a function that describes all trajectories simultaneously.

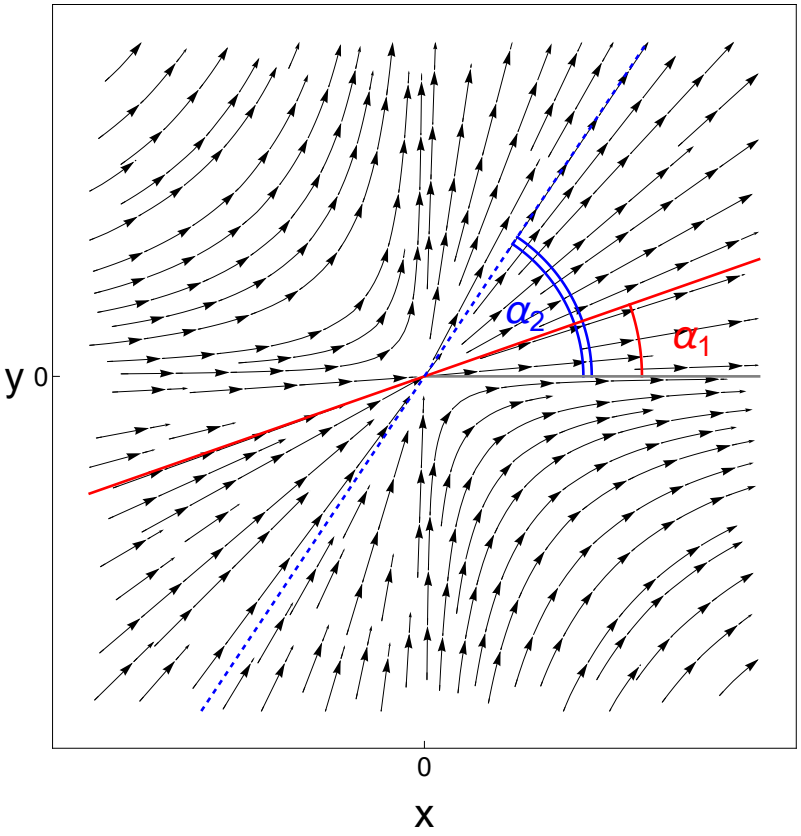

Fig. 1.2: Phase portrait of the dynamical system given in Eq. (1.4), whose right-hand side is discontinuous at the origin. The solid red line represents the trajectory $\mathbf{x}_{\alpha_1}(t)$, with $\alpha_1 = 0.35$, and the dashed blue line represents the trajectory $\mathbf{x}_{\alpha_2}(t)$, with $\alpha_2 = 1.5$. Note that the angles α_1 and α_2 are taken with respect to the x-axis.

Definition 1.2 (Flow): The *flow* of the dynamical system in Eq. (1.3) with $\mathbf{x}(0) = \mathbf{x}_0$ is the smooth mapping $\varphi(\mathbf{x}, t) : \mathbb{R}^n \times \mathbb{R} \to X$ such that $\varphi(\mathbf{x}, 0) = \mathbf{x}$ and

$$\varphi(\mathbf{x}, t + s) = \varphi(\varphi(\mathbf{x}, t), s) = \varphi(\varphi(\mathbf{x}, s), t) = \varphi(\mathbf{x}, s + t)\,. \tag{1.5}$$

The flow property in Eq. (1.5) says that travelling along a trajectory for some time s and then for some time t is the same as travelling for the time $s + t$. Hence,

$$\frac{\mathrm{d}}{\mathrm{d}t}\varphi(\mathbf{x}, t) = \mathbf{f}(\varphi(\mathbf{x}, t))\,, \tag{1.6}$$

for all t, such that the solution through $\mathbf{x}_0$ exists and $\varphi(\mathbf{x}_0, 0) = \mathbf{x}_0$. The flow generated by the vector field function $\mathbf{f}$ is a one-parameter diffeomorphism group for which $\mathbf{f}$ is the phase velocity vector field. The flow can be conceived as the motion of a fluid in phase space, whose representation is controlled by some stagnation points known as fixed points [85, 150].

A *fixed point* of a dynamical system is a point $\mathbf{x}^*$ such that $\mathbf{f}(\mathbf{x}^*) = \mathbf{0}$; this point is also known as *critical point*, *steady state*, or *equilibrium* of the system. To determine the behaviour of trajectories near the fixed points, we can linearise the system around its critical points, by using a Taylor

expansion for $\mathbf{f}$ in the neighbourhood of the fixed point, that is,

$$\mathbf{f}(\mathbf{x}) = \mathbf{f}(\mathbf{x}^*) + (\mathbf{x} - \mathbf{x}^*)\,\boldsymbol{\nabla}\mathbf{f}(\mathbf{x}^*) + o(|\mathbf{x} - \mathbf{x}^*|) = (\mathbf{x} - \mathbf{x}^*)\,\boldsymbol{\nabla}\mathbf{f}(\mathbf{x}^*) + o(|\mathbf{x} - \mathbf{x}^*|), \tag{1.7}$$

where $\mathbf{x} - \mathbf{x}^*$ is small, and we used the fact that $\mathbf{f}(\mathbf{x}^*) = \mathbf{0}$. Here $p(x) = o(q(x))$ as $x \to x_0$ means $\lim_{x\to x_0} |p(x)|/|q(x)| = 0$.

The eigenvalues of the matrix $\boldsymbol{\nabla}\mathbf{f}(\mathbf{x}^*)$, known as the *Jacobian* (or *stability*) *matrix*, contain the information about the local behaviour of $\mathbf{f}$ near $\mathbf{x}^*$. By the Hartman–Grobman theorem (or linearisation theorem), the dynamics of the linearised system and of the original system are qualitatively equivalent to one another; for details, see for example [16, 150, 169]. The stability or instability of the fixed point $\mathbf{x}^*$ depends on the eigenvalues of the Jacobian. In this thesis, we will only be concerned with two-dimensional dynamical systems; for this reason, let us provide the classification of fixed points in terms of the two eigenvalues of the Jacobian, λ_1 and λ_2, in Table 1.1.

Table 1.1: Classification of the critical points for a two-dimensional dynamical system according to the eigenvalues of the Jacobian λ_1 and λ_2.

Eigenvalues	Classification
$\lambda_1 < 0$, $\lambda_2 < 0$	stable node/sink/attractor
$\lambda_1 > 0$, $\lambda_2 > 0$	unstable node/source/repeller
$\lambda_1 < 0$, $\lambda_2 > 0$	saddle point
$\lambda_1 = 0$, $\lambda_2 > 0$	unstable point
$\lambda_1 = 0$, $\lambda_2 < 0$	non-hyperbolic (linear stability fails)
$\lambda_1 = \alpha + \mathrm{i}\beta$, $\lambda_2 = \alpha - \mathrm{i}\beta$	unstable spiral if $\alpha > 0$ and $\beta \neq 0$
$\lambda_1 = \alpha + \mathrm{i}\beta$, $\lambda_2 = \alpha - \mathrm{i}\beta$	stable spiral if $\alpha < 0$ and $\beta \neq 0$
$\lambda_1 = \mathrm{i}\beta$, $\lambda_2 = -\mathrm{i}\beta$	centre

Let us now return to the simple pendulum example and write Eq. (1.2) as two coupled first order differential equations

$$\dot{\theta} = v =: f(\theta, v)\,, \tag{1.8a}$$

$$\dot{v} = -\sin\theta =: g(\theta, v)\,, \tag{1.8b}$$

where v can be interpreted physically as the dimensionless angular velocity and f and g are analytic. It is now clear that the system involving the displacement angle θ and the angular velocity v, described by Eq. (1.8), is two dimensional. In particular, θ lies on a circle, and $\dot{\theta}$ in $\mathbb{R}$. So the state space can be thought of as an infinite cylinder $\mathbb{S}^1 \times \mathbb{R}$. We can now employ dynamical systems techniques to gain a qualitative insight into the system's behaviour. The fixed (or critical) points of the dynamical system in Eq. (1.8), that is those points for which $f(\theta, v) = g(\theta, v) \equiv 0$, are all of the form $(n\pi, 0)$, for $n \in \mathbb{Z}$. Due to the periodic nature of the pendulum, it suffices to consider the fixed points $(0, 0)$ and $(0, \pi)$, which are, respectively, Point O and Point A in Fig. 1.3.

The eigenvalues of the matrix

$$\begin{pmatrix} \dfrac{\partial f}{\partial \theta} & \dfrac{\partial g}{\partial \theta} \\ \dfrac{\partial f}{\partial v} & \dfrac{\partial g}{\partial v} \end{pmatrix} = \begin{pmatrix} 0 & -\cos\theta \\ 1 & 0 \end{pmatrix} \tag{1.9}$$

evaluated at the fixed points contain the information about the local behaviour of f and g near the fixed points. Since the eigenvalues at the origin $(0, 0)$ are purely imaginary, further analysis is needed to determine whether the fixed point is a centre or a spiral for the full nonlinear system; whereas the fixed point $(0, \pi)$ is a saddle because the eigenvalues are real with opposite signs. An extensive discussion on these techniques can be found in [15, 16, 85, 150], and, specifically, in the context of cosmology, in [18, 28].

To see that the origin is indeed a nonlinear centre, one can check that this fixed point is a local minimum of a conserved quantity, the energy; the level sets of this quantity are closed curves that encircle it; and hence, all trajectories near the centre must follow these closed curves. For the simple pendulum, there is no damping or friction, and hence, we can show that the energy for the system in Eq. (1.8) is conserved; systems for which a conservative quantity exists are called *conservative*. The existence of a conserved quantity (also called a constant of motion, or first integral) can be seen by multiplying Eq. (1.2) by $\dot{\theta}$ and integrating

$$\dot{\theta}\left(\ddot{\theta} + \sin\theta\right) = 0 \implies \frac{1}{2}\dot{\theta}^2 - \cos\theta = \mathcal{E}\,, \tag{1.10}$$

where $\mathcal{E}$ is a constant of integration and represents the total energy of the system. The closed curves defined by the contours of constant energy can be visualised by plotting the energy function

$$\mathcal{E}(\theta, v) = \frac{1}{2}v^2 - \cos\theta\,, \tag{1.11}$$

and coincide with the trajectories in the phase plane, as shown in Fig. 1.3. Point O corresponds to a state of stable equilibrium, that is, rest, and is a local minimum of Eq. (1.11). Around the origin, the phase space is foliated by invariant ellipses. This is consistent with the small-angle approximation reducing the equation of the pendulum to that of a simple harmonic oscillator. Point A represents an *inverted* pendulum at rest. We can also observe that the lowest energy state is when $\mathcal{E} = -1$; the critical energy state is when $\mathcal{E} = 1$, where the trajectories join the saddles; for $\mathcal{E} > 1$, the pendulum periodically whirls over the top.

A natural question to ask at this point is: can we go further and integrate Eq. (1.10)? Before proceeding, let θ_0 denote the highest angular position, where the kinetic energy is zero and the total energy is given by the value of potential energy. This means we may write Eq. (1.10) as

$$\frac{1}{2}\dot{\theta}^2 - \cos\theta = -\cos(\theta_0)\,. \tag{1.12}$$

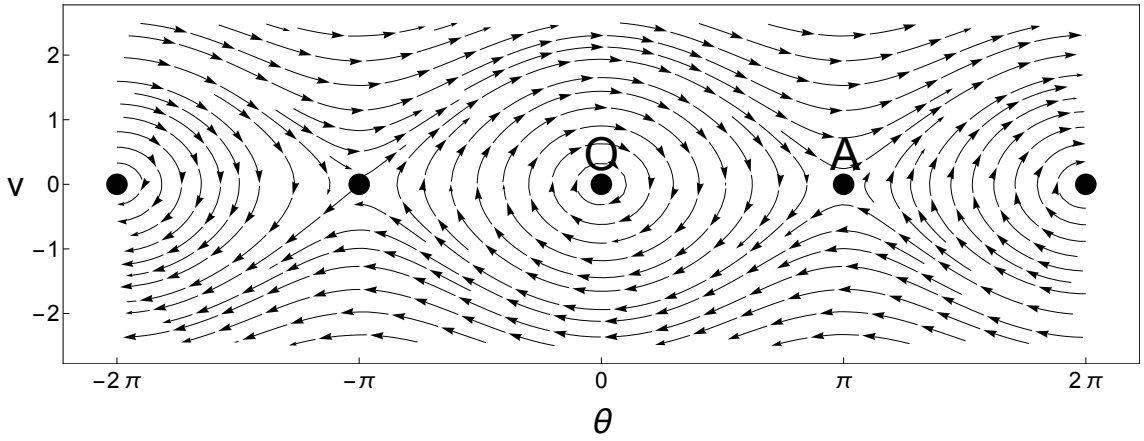

Fig. 1.3: Phase portrait of the pendulum. The trajectories indicated by arrows coincide with energy contours.

Solving for $\dot{\theta}$ gives

$$\tau = \int \mathrm{d}\tau = \int \frac{\mathrm{d}\theta}{\sqrt{2(\cos\theta - \cos\theta_0)}}\,. \tag{1.13}$$

Let us now employ the double-angle formula and rewrite $\cos(\theta) = 1 - 2\sin^2(\theta/2)$. Upon rearranging, and noting a quarter of a cycle is from $\theta = 0$ to $\theta = \theta_0$, this gives the period

$$T = 2\sqrt{\frac{\ell}{g}} \int_0^{\theta_0} \frac{\mathrm{d}\theta}{\sqrt{\sin^2(\theta_0/2) - \sin^2(\theta/2)}}\,. \tag{1.14}$$

Upon defining

$$x = \frac{\sin(\theta/2)}{\sin(\theta_0/2)}\,, \quad k = \sin\left(\frac{\theta_0}{2}\right), \tag{1.15}$$

which gives

$$\mathrm{d}x = \frac{1}{2k}\cos\left(\frac{\theta}{2}\right)\mathrm{d}\theta = \frac{1}{2k}\sqrt{1 - k^2x^2}\,\mathrm{d}\theta\,, \tag{1.16}$$

$$\sin^2\left(\frac{\theta_0}{2}\right) - \sin^2\left(\frac{\theta}{2}\right) = k^2(1 - x^2)\,. \tag{1.17}$$

Hence, Eq. (1.14) becomes

$$T = 2\sqrt{\frac{\ell}{g}} \int_0^1 \frac{\mathrm{d}x}{\sqrt{(1 - x^2)(1 - k^2x^2)}} =: 2\sqrt{\frac{\ell}{g}}K(k)\,. \tag{1.18}$$

This integral cannot be solved in terms of elementary functions, but it is a *special function* of its own: namely, the *complete elliptic integral of the first kind*, K, where k is the *elliptic modulus*. Since we defined $k = \sin(\theta_0/2)$, the period of the simple pendulum may be written as

$$T = 2\sqrt{\frac{\ell}{g}}K\left(\sin\left(\frac{\theta_0}{2}\right)\right). \tag{1.19}$$

When $\theta_0 \ll \pi/2$, i.e. $k \ll 1$, we find the expansion

$$T = 2\pi\sqrt{\frac{\ell}{g}}\left(1 + \frac{1}{4}k^2 + \frac{9}{64}k^4 + \cdots\right). \tag{1.20}$$

The first term of the expansion gives the well-known period of the simple pendulum obtained with the small-angle approximation.

We have therefore shown different ways to approach the study of the solutions of the ODE given in Eq. (1.2). In the following, we discuss how one can identify whether an elementary function can be integrated in finite terms to obtain an elementary antiderivative versus when its integral is a special function. Special functions permeate mathematical physics; we restrict our attention to those which we will be using later on in the context of cosmology.

1.4 What is an elementary function?

The problem outlined in the previous section presents us with the idea that there are some cases in which an analytic, closed-form, solution of an ODE can be found in terms of special functions. The adjective *special* is employed to distinguish these functions from the *elementary* functions. In particular, Liouville showed that some integrals cannot be expressed in terms of elementary functions, but require new functions to be introduced [122]. Liouville developed the theory of integration in finite terms in eleven papers published from 1833 to 1841; for a detailed account see [124]. Using Liouville's results, Chebyshev formulated a theorem (Theorem 1.10 below), which we shall use later on, to determine whether a binomial-type integral admits a solution in terms of elementary functions or not [154]; for a modern exposition, see [106, 127, 139]. Elementary functions were introduced by Liouville [108, 122]; to define them rigorously takes a considerable amount of work (see, for example, Chapter I in [139]). The definition we give below is sufficient for our present purposes, and is recursive in nature. Here, $\widehat{\mathbb{C}} = \mathbb{C} \cup \{\infty\}$ denotes the Riemann sphere; we allow ourselves to consider multi-valued complex functions.

Definition 1.3 (Elementary function): A polynomial, exponential, logarithmic, trigonometric, or inverse trigonometric function $f : \Omega \to \widehat{\mathbb{C}}$, where $\Omega \subseteq \widehat{\mathbb{C}}$, is *elementary* (in the sense of Liouville). If $f_1, f_2 : \Omega \to \widehat{\mathbb{C}}$ are elementary functions, then $f_1(z) + f_2(z)$, $f_1(z) - f_2(z)$, $f_1(z)f_2(z)$, $f_1(z)/f_2(z)$, $(f_1 \circ f_2)(z)$ are also elementary functions. Furthermore, if $f_0, f_1, \ldots, f_n : \Omega \to \widehat{\mathbb{C}}$ are finitely many elementary functions, then a (possibly multi-valued) function $g : \Omega \to \widehat{\mathbb{C}}$ which satisfies $f_0(z) + f_1(z)g(z) + \cdots + f_n(z)g(z)^n = 0$ is an elementary function. A function which cannot be obtained as a finite combination of the above operations is called *non-elementary*.

As an example, the function given by $\sqrt{e^z - \arctan(2z+1)}$ is elementary, and we will show below that the function K introduced in Eq. (1.18) is non-elementary. It is worth mentioning that both Laplace and Abel worked on the antiderivatives of elementary functions before Liouville. Moreover, elementary transcendental functions and their properties were surveyed by Euler in *Introductio in analysin infinitorum* [73]. At about the same time, interest in integrals of the form of that in Eq. (1.18) began, and more generally in differential equations of the form $(y'(x))^2 = f(x)$.

In 1834, Liouville proved an important theorem about the elementary integrals of algebraic functions, which we will introduce in Theorem 1.6 below. The first example of a non-elementary integral that he obtained as a result of his theorem was for

$$\int \frac{\mathrm{d}x}{\sqrt{(1-x^2)\,(1-k^2x^2)}}, \tag{1.21}$$

where k is a constant and $k^2 \notin \{0, 1\}$. In 1948, Ritt published *Integration in Finite Terms: Liouville's Theory of Elementary Methods* [139]. This textbook contains an account of the results produced by Liouville, Abel, and Chebyshev, as well as an introduction to the field of *differential algebra*. In 1968, an algebraic proof of Liouville's theorem was obtained by Rosenlicht [143].

We can now proceed to show the non-elementary character of the integral in Eq. (1.21), using some tools from complex analysis. The aim of the subsequent exposition is to provide a pedagogical introduction to these key ideas. For full rigour, the reader can refer to [139].

We want to study properties of integrals of real-valued functions, but it turns out to be necessary to move to the complex realm, where we can apply powerful tools from complex analysis. In particular, we use the fundamental theorem of algebra to guarantee the existence of roots of polynomial equations. We now introduce the following definitions.

Definition 1.4 (Algebraic function): A (possibly multi-valued) function $f : \Omega \to \widehat{\mathbb{C}}$, for $\Omega \subset \widehat{\mathbb{C}}$, is *algebraic* if it satisfies an irreducible relation

$$P\,(f(z), z) = 0\,, \tag{1.22}$$

where

$$P(w, z) = a_n(z)w^n + \cdots + a_1(z)w + a_0(z)\,, \tag{1.23}$$

where each a_i is a polynomial in z. By *irreducible*, we mean that the right hand-side of Eq. (1.23) cannot be written as the product of two non-constant polynomials in w and z.

As an example, functions defined in terms of polynomials, or functions like $\sqrt{x^2+1}$, are algebraic; exponentials, logarithms, and trigonometric functions are non-algebraic. All algebraic functions are elementary.

Let f be a non-constant algebraic (possibly multi-valued) function on $\widehat{\mathbb{C}}$. A point $z_0 \in \widehat{\mathbb{C}}$ is a *branch point* of f if f has more values on every punctured neighbourhood of z_0 than f has at z_0. In general, each point $z_0 \in \widehat{\mathbb{C}}$ is either a branch point, or there is some connected open subset $\Omega \subset \widehat{\mathbb{C}}$ containing z_0 and no branch points of f on which any branch f_* of f is either analytic or has a pole at z_0. In all cases, we can write f as a semi-infinite series

$$a_{p/m}(z - z_0)^{p/m} + a_{(p+1)/m}(z - z_0)^{(p+1)/m} + \cdots , \tag{1.24}$$

where $p, m \in \mathbb{Z}$, $m > 0$, and the coefficients $a_i \in \mathbb{C}$ with $a_{p/m} \neq 0$; we define $a_{q/m} = 0$ for $q < p$. In the case $z_0 = \infty$, we replace $(z - z_0)$ by $1/z$. Except when z_0 is a branch point, we can take $m = 1$. When it is a branch point, m is the number of sheets in a neighbourhood of z_0.

Definition 1.5 (Residue): The *residue* of f at z_0, up to a multiplicative constant coming from the choice of branch, is given by $\mathrm{Res}(f, z_0) = ma_{-1}$.

For our purposes, we are only interested in whether the residue is zero or not. Hence, it is sufficient to give the definition up to a multiplicative constant. For a fuller definition, see [139, Chapter II, Section 11]. Let us also introduce some key theorems without proof. The main theorem, due to Liouville, describes the forms that the integral of an algebraic function, $\int f(z)\,\mathrm{d}z$, must have if it is elementary. Since the integral is elementary, we must be able to write it in terms of rational functions, radicals, exponentials, and logarithms (note that trigonometric functions can be written in terms of complex exponentials). When we differentiate the integral $\int f(z)\,\mathrm{d}z$, we obtain an algebraic function which necessarily does not include any exponentials or logarithms.

We know that differentiating terms involving exponentials results in terms involving exponentials. So the integral $\int f(z)\,\mathrm{d}z$ cannot include exponentials. Differentiating the logarithm of an algebraic function does result in an algebraic function; but, if we differentiate a term involving nested logarithms, the result will involve logarithms, and hence not be algebraic. Intuitively, therefore, the elementary integral of an algebraic function must involve only algebraic functions and, possibly, single logarithms of algebraic functions. Liouville's theorem guarantees that this intuition is, in fact, correct.

Theorem 1.6 (Liouville's theorem)

Let $f(z)$ be an algebraic function and assume $\int f(z)\,\mathrm{d}z$ is elementary. Then

$$\int f(z)\,\mathrm{d}z = v_0(z) + c_1 \log(v_1(z)) + \cdots + c_r \log(v_r(z)) , \tag{1.25}$$

where $r > 0$ is an integer, c_i are constants, and each $v_i(z)$ is an algebraic function.

For a proof, see [139, p. 21]. When we apply Liouville's theorem, we in fact assume that the integral is not only elementary, but itself also algebraic, in which case the only term which appears on the right-hand side of Eq. (1.25) is $v_0(z)$. The following theorem, due to Abel, gives a precise description for the form of this algebraic function.

Theorem 1.7 (Abel's theorem)

Let $f(z)$ be an algebraic function and assume $\int f(z)\,\mathrm{d}z$ has the form given in Eq. (1.25). Then, each of the algebraic functions $v_i(z)$ is rational in z and f, with constant coefficients, and, in particular,

$$v_0 = A_0 + A_1 f + \cdots + A_{m-1} f^{m-1}\,, \tag{1.26}$$

where each A_i is a rational function of z only, and $m < \infty$ is the number of branches of f.

For a proof, see [139, p. 28]. In fact, Abel proved this theorem around ten years before Liouville published his work.

With a bit of further work, these theorems yield the following proposition, which is the main tool needed to show that the elliptic integral of the first kind is not elementary. This is also employed to prove the necessity aspect in the proof of Chebyshev's theorem (see Theorem 1.10). For a proof, see Appendix A.

Proposition 1.8 ([139, Chapter II, Section 12])

Let $f(z)$ be an algebraic function and assume $\int f(z)\,\mathrm{d}z$ is elementary, but not algebraic. Then, there is a point in $\widehat{\mathbb{C}}$ at which a branch of f has non-zero residue.

Now, let $k \notin \{0, 1\}$ be a constant and

$$\int \frac{\mathrm{d}z}{\sqrt{(1-z)^2(1-k^2z^2)}} =: \int f(z)\,\mathrm{d}z\,.$$

We are ready to show the following corollary. This will follow from Proposition 1.8 by showing that $\int f(z)\,\mathrm{d}z$ is not algebraic, but all of its residues are zero. Note, we can apply the proposition since the integrand is algebraic and satisfies

$$(1-z)^2(1-k^2z^2)f^2 - 1 = 0\,. \tag{1.27}$$

Corollary 1.9

The elliptic integral of the first kind, given in Eq. (1.21), is not elementary.

Proof. To show that the integral is non-elementary, we will proceed by contradiction. Let

$$y = \sqrt{(1-z^2)(1-k^2z^2)}\,, \tag{1.28}$$

which is algebraic with two branches. For a contradiction, assume that $\int 1/y\,\mathrm{d}z$ is algebraic. Then, by Theorem 1.7, and since y^2 is rational (in fact, polynomial),

$$\int \frac{1}{y}\,\mathrm{d}z = A_0 + \widetilde{A}_1 \frac{1}{y}\cdot\frac{y}{y} = A_0 + \frac{\widetilde{A}_1}{y^2}y = A_0 + A_1 y\,, \tag{1.29}$$

where A_0 and $A_1 = \widetilde{A}_1/y^2$ are rational functions of z. By differentiating Eq. (1.29), we obtain

$$\frac{1}{y} = \frac{\mathrm{d}A_0}{\mathrm{d}z} + \frac{\mathrm{d}}{\mathrm{d}z}\left(A_1 y\right) = \frac{\mathrm{d}A_0}{\mathrm{d}z} + y\frac{\mathrm{d}A_1}{\mathrm{d}z} + A_1\frac{\mathrm{d}y}{\mathrm{d}z}. \tag{1.30}$$

Since $\mathrm{d}\left(y^2\right)/\mathrm{d}z = 2y\mathrm{d}y/\mathrm{d}z$, we can write

$$\frac{1}{y} = \frac{\mathrm{d}A_0}{\mathrm{d}z} + y\frac{\mathrm{d}A_1}{\mathrm{d}z} + \frac{A_1}{2y}\frac{\mathrm{d}(y^2)}{\mathrm{d}z}\,. \tag{1.31}$$

Multiplying through by y yields

$$1 = \underbrace{\frac{\mathrm{d}A_0}{\mathrm{d}z}y}_{\text{Term 1}} + y^2\frac{\mathrm{d}A_1}{\mathrm{d}z} + \frac{A_1}{2}\frac{\mathrm{d}(y^2)}{\mathrm{d}z}\,. \tag{1.32}$$

All terms on the right-hand side, with the exception of Term 1, are rational in z. For the equality to hold, we must have $\mathrm{d}A_0/\mathrm{d}z = 0$, that is, A_0 is a constant. Hence, Eq. (1.30) becomes

$$\frac{1}{y} = \frac{\mathrm{d}}{\mathrm{d}z}(A_1 y)\,. \tag{1.33}$$

Now, the left-hand side of Eq. (1.33) is holomorphic in $\mathbb{C}$ away from $z \in \{\pm 1, \pm k^{-1}\}$, where it has poles of order $1/2$. Therefore, the right-hand side of Eq. (1.33) can only have poles at these points, but they must come from poles of order $n \in \mathbb{Z}^+$ of A_1. These will be poles of order $(n-1/2)$ in $A_1 y$, and of order $(n+1/2) > 1/2$ in $\mathrm{d}(A_1 z)/\mathrm{d}z$, a contradiction. Hence, $\int 1/y\,\mathrm{d}z$ is not algebraic.

The last thing to check is that $1/y$ has zero residue everywhere. We have already remarked that $1/y$ is holomorphic away from the branch points, so has zero residue at all finite points except possibly these—we also have to check $z = \infty$. Consider, as an example, $z = 1$. We can write

$$\frac{1}{y} = \frac{1}{\sqrt{(1-z)(1+z)(1-k^2z^2)}} = \frac{(1-z)^{-1/2}}{\sqrt{(1+z)(1-k^2z^2)}}\,, \tag{1.34}$$

and, near $z = 1$, the denominator is non-zero and analytic, so $1/y$ had an expansion starting with $(1-z)^{-1/2}$. Hence, the coefficient of $(1-z)^{-1}$ will be zero and $1/y$ has zero residue at this point. An almost identical argument holds at the other three branch points of y.

Finally, consider $z = \infty$, we can write

$$\frac{1}{y} = \frac{1}{z^2\sqrt{(1-1/z^2)\,(1-k^2/z^2)}} \overset{z^{-1}\mapsto z}{\longmapsto} \frac{z^2}{\sqrt{(1-z)^2(1-k^2z^2)}}\,, \tag{1.35}$$

so $1/y$ is holomorphic (in fact has a zero of order 2) at $z = 0$, and hence has zero residue. This contradicts Proposition 1.8, and, therefore, we can conclude that $\int 1/y \, \mathrm{d}z$ is non-elementary. □

We have therefore shown that the *elliptic integral of the first kind* cannot be expressed in terms of elementary functions. This motivates the introduction of *special functions*. It is worth remarking at this stage that special functions go beyond a mere neat symbolic stratagem. Their true power lies in their well-studied and classified properties, and the connections they have to one another, and how they emerge in a plethora of varied contexts.

We now state, without proof, a theorem due to Chebyshev, which allows us to determine whether the integral of a binomial is elementary just by looking at its powers. This will turn out to be a useful tool in Chapter 2 and Chapter 3. The proof of this result can be found in [139, p. 37]: the proof of sufficiency is due to Goldbach and Euler [127]; the proof of the necessity argument uses the same ideas of the Proof of Lemma 1.9, although it is a little more involved.

Theorem 1.10 (Chebyshev's theorem)

Let $p, q, r \in \mathbb{Q}$, $r \neq 0$, and $a, b \in \mathbb{R}$. The integral

$$\int x^p (a + bx^r)^q \, \mathrm{d}x \tag{1.36}$$

is elementary if and only if *at least one of* $\dfrac{p+1}{r}$, q, *or* $\dfrac{p+1}{r} + q$ *is an integer.*

1.5 Elliptic functions and other special functions

In Section 1.4, we showed that some types of integrals cannot be integrated in terms of elementary functions. To be able to write a closed formula, we need to introduce *special functions*. In the following, we showcase the key special functions, and their properties, which are relevant in the context of cosmology. Let us briefly return to the example of the simple pendulum, and in particular the conservation of energy, in Eq. (1.10). By making the substitution $z = \mathrm{e}^{\mathrm{i}\theta} \in \mathbb{C}$, we obtain $\dot{z} = \mathrm{i}\dot{\theta}\mathrm{e}^{i\theta} = \mathrm{i}\dot{\theta}z$. Recalling that $\cos(\theta) = (\mathrm{e}^{\mathrm{i}\theta} + \mathrm{e}^{-\mathrm{i}\theta})/2 = (z + z^{-1})/2$, Eq. (1.10) reads

$$\frac{1}{2}\left(\frac{\dot{z}}{\mathrm{i}z}\right)^2 - \frac{z + z^{-1}}{2} = \mathcal{E}\,. \tag{1.37}$$

Upon rearranging, we have

$$\dot{z}^2 = -z^3 - 2\mathcal{E}z^2 - z\,. \tag{1.38}$$

Let us now make the substitution

$$Z = -\frac{1}{4}\left(z + 2\frac{\mathcal{E}}{3}\right) \iff z = -\frac{2}{3}\left(\mathcal{E} + 6Z\right), \tag{1.39}$$

which allows us to rewrite Eq. (1.38) as

$$\dot{Z}^2 = 4Z^3 + \left(\frac{1}{4} - \frac{\mathcal{E}^2}{3}\right) Z + \frac{\mathcal{E}}{24} - \frac{\mathcal{E}^3}{27}\,. \tag{1.40}$$

Equation (1.40) illustrates how the pair $(Z, \dot{Z})$ lies on an *elliptic curve*, that is, an equation of the form $y^2 = x^3 + ax + b$ where a, b are constants. This equation can be thought of as the conservation of energy and is the standard form of the Weierstrass differential equation. For a visualisation of this in the context of the example of the pendulum, see [109]. In what follows, we introduce the key properties of elliptic functions and highlight the link between the different representations of the solutions to the simple pendulum.

1.5.1 *Elliptic functions*

Elliptic functions can be thought of as a generalisation of trigonometric functions, and they exhibit (doubly-)periodic behaviour. Their name is due to their natural appearance in the computation of the perimeter of an ellipse. Recall that a function which is complex-differentiable everywhere in an open subset $\Omega \subset \mathbb{C}$ except at isolated points, where it has poles, is said to be *meromorphic* in Ω.

Definition 1.11 (Elliptic functions): Let ω_1 and ω_2 be two nonzero complex numbers whose ratio is not a real number. Then any function f for which $f(z + 2\omega_1) = f(z)$ and $f(z + 2\omega_2) = f(z)$, for all z in the domain of f, is said to be *doubly periodic* with periods $2\omega_1$ and $2\omega_2$. If f is doubly periodic and meromorphic (in the whole of $\mathbb{C}$), then it is called an *elliptic function*.

A doubly periodic function is completely defined by its restriction to the fundamental parallelogram, that is, a parallelogram with vertices 0, $2\omega_1$, $2\omega_2$, $(2\omega_1 + 2\omega_2)$, as shown in Fig 1.4.

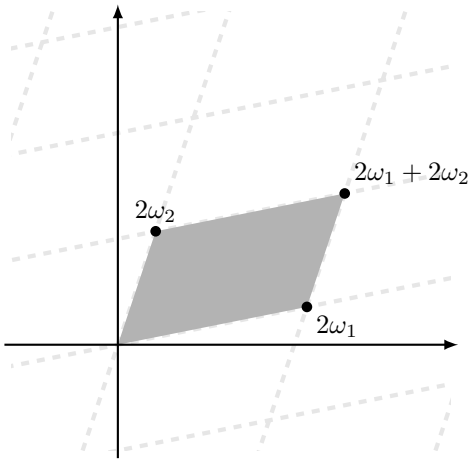

Fig. 1.4: Fundamental parallelogram.

For a discussion of the key properties of elliptic functions, consult [8, 90, 155, 168]. One

immediate property is Liouville's theorem for entire elliptic functions, which follows from his well-known theorem that any bounded entire (i.e. analytic at every point of $\mathbb{C}$) function is constant.

Theorem 1.12 (Liouville's theorem)

Any entire elliptic function is constant.

Proof. An entire function is bounded on any closed and bounded subset of $\mathbb{C}$. In particular, an entire elliptic function is bounded on the closure of its fundamental parallelogram. The fact that it is doubly periodic implies that the value at any point in $\mathbb{C}$ is the same as the value at some point in the fundamental parallelogram, so the function is bounded on the whole of $\mathbb{C}$. Applying Liouville's theorem from complex analysis yields the desired result. □

An example of an elliptic function is the Weierstrass $\wp$-function, which is defined by

$$\wp(z) \coloneqq \frac{1}{z^2} + \sum_{\substack{n,m\in\mathbb{Z}\\(n,m)\neq(0,0)}} \left(\frac{1}{(z-\Omega_{nm})^2} - \frac{1}{\Omega_{nm}^2} \right), \tag{1.41}$$

where $\Omega_{nm} = 2(m\omega_1 + n\omega_2)$. This function will feature in our subsequent computations of the azimuthal geodesics, in particular, in Section 3.4.4.1. The series in Eq. (1.41) converges uniformly on closed and bounded subsets of $\mathbb{C} \setminus \{\text{poles}\}$; the series has double poles at $z = \Omega_{mn}$. This means it can be differentiated term-by-term, which yields the series

$$\wp'(z) = -2 \sum_{m,n=-\infty}^{\infty} \frac{1}{\left(z - 2(m\omega_1 + n\omega_2)\right)^3},$$

which is also uniformly convergent and meromorphic. In fact, it can also be shown to be elliptic by replacing z with $z + 2\omega_j$ for $j \in \{1, 2\}$ and incrementing either the index m or the index n. We can conclude that $\wp'$ is therefore an elliptic function, and so is any polynomial of $\wp$ and $\wp'$. The only poles of such a polynomial are at $z = \Omega_{mn}$. Let us construct a polynomial of $\wp$ and $\wp'$ with no pole at the origin, which will therefore be entire. By Theorem 1.12, it is necessarily constant. We can observe that since $\wp$ is even, its Laurent expansion around $z = 0$ contains even powers only. As $z \to 0$, Eq. (1.41) gives

$$\wp(z) = \frac{1}{z^2} + 3 \sum_{\substack{n,m\in\mathbb{Z}\\(n,m)\neq(0,0)}} \Omega_{mn}^{-4}\, z^2 + 5 \sum_{\substack{n,m\in\mathbb{Z}\\(n,m)\neq(0,0)}} \Omega_{mn}^{-6}\, z^4 + \cdots, \tag{1.42}$$

and, hence,

$$\wp'(z) = -\frac{2}{z^3} + 6 \sum_{\substack{n,m\in\mathbb{Z}\\(n,m)\neq(0,0)}} \Omega_{mn}^{-4}\, z + 20 \sum_{\substack{n,m\in\mathbb{Z}\\(n,m)\neq(0,0)}} \Omega_{mn}^{-6}\, z^3 + \cdots. \tag{1.43}$$

Considering

$$(\wp')^2 - 4\wp^3 = -60 \sum_{\substack{n,m\in\mathbb{Z}\\(n,m)\neq(0,0)}} \Omega_{mn}^{-4}\,\frac{1}{z^2} - 140 \sum_{\substack{n,m\in\mathbb{Z}\\(n,m)\neq(0,0)}} \Omega_{mn}^{-6} + \mathcal{O}(z^2) \tag{1.44}$$

allows us to cancel leading order terms. Since the leading order of $\wp$ is $1/z^2$, Eq. (1.44) can be written as

$$(\wp')^2 - 4\wp^3 + 60 \sum_{\substack{n,m\in\mathbb{Z}\\(n,m)\neq(0,0)}} \Omega_{mn}^{-4}\,\wp + 140 \sum_{\substack{n,m\in\mathbb{Z}\\(n,m)\neq(0,0)}} \Omega_{mn}^{-6} = \mathcal{O}(z^2)\,, \tag{1.45}$$

where we note that the left-hand side of Eq. (1.45) is an entire elliptic function (no pole in any fundamental period parallelogram containing $z = 0$), and by Theorem 1.12, it is also constant. As $z \to 0$, $\mathcal{O}(z^2) \to 0$. Therefore, we have shown that the elliptic function $\wp$ satisfies the ODE

$$(\wp')^2 = 4\wp^3 - g_2\wp - g_3\,, \tag{1.46}$$

where the constants g_2 and g_3, known as the *invariants*, are given by

$$g_2 \coloneqq 60 \sum_{\substack{n,m\in\mathbb{Z}\\(n,m)\neq(0,0)}} \Omega_{mn}^{-4}\,, \qquad g_3 \coloneqq 140 \sum_{\substack{n,m\in\mathbb{Z}\\(n,m)\neq(0,0)}} \Omega_{mn}^{-6}\,. \tag{1.47}$$

Conversely, consider an ODE of the form

$$\left(\frac{\mathrm{d}y}{\mathrm{d}z}\right)^2 = 4y^3 - g_2 y - g_3\,, \tag{1.48}$$

where the right-hand side has three distinct roots as a cubic polynomial in y. Then, the general solution is given by $y(z) = \wp(z - z_0)$ for some constant $z_0 \in \mathbb{C}$, where the Ω_{mn} satisfy Eq. (1.47).

1.5.2 *Elliptic integrals*

From Eq. (1.46), we can separate the variables and write

$$z = \int_y^\infty \frac{\mathrm{d}t}{\sqrt{4t^3 - g_2 t - g_3}}\,, \tag{1.49}$$

where $y = \wp(z)$. Thus, $z = \wp^{-1}(y)$, that is, the inversion of the integral given in Eq. (1.49) gives rise to the Weierstrass $\wp$-function. The integral in Eq. (1.49) is elliptic, highlighting the connection between the Weierstrass $\wp$-function and elliptic integrals.

Definition 1.13 (Elliptic integral): An *elliptic integral* is an integral of the form

$$\int R\,(x, y)\,\mathrm{d}x\,, \tag{1.50}$$

where $R(x, y)$ is a rational function of two variables with degree greater than zero as a function of y and $y^2 = Q(x)$ is a polynomial in x of degree three or four with no repeated roots.

When the degree of Q is greater than four, the integral is called *hyperelliptic*; for more details see [44]. The elliptic integral we have just defined cannot, in general, be expressed in terms of elementary functions unless (i) $R(x, y)$ contains no odd powers of y, and (ii) y^2 has a repeated factor. We exclude those cases. We now show that all elliptic integrals can be expressed in terms of three integrals, namely, Legendre's elliptic integrals of the first, second, and third kind.

Let us note that a polynomial $p(x, y)$ can be written as

$$\begin{aligned} p(x,y) &= a_0(x) + a_1(x)y + a_2(x)y^2 + \cdots + a_n(x)y^n && (1.51)\\ &= \left(a_0(x) + a_2(x)y^2 + a_4(x)y^4 + \cdots\right) \\ &\qquad + y\left(a_1(x) + a_3(x)y^2 + a_5(x)y^4 + \cdots\right) && (1.52)\\ &= \left(a_0(x) + a_2(x)Q(x) + a_4(x)Q^2(x) + \cdots\right) \\ &\qquad + y\left(a_1(x) + a_3(x)Q(x) + a_5(x)Q^2(x) + \cdots\right). && (1.53) \end{aligned}$$

Therefore,

$$p(x,y) = p_1\left(x, Q(x)\right) + p_2\left(x, Q(x)\right) y\,, \tag{1.54}$$

for some polynomials p_1 and p_2 in x and $y^2 = Q(x)$. Therefore, without loss of generality, we can assume that the degree of R as a function of y is one.

Since R is a rational function, there are some polynomials a, b, c, and d in x such that

$$\begin{aligned} R(x,y) &= \frac{a(x)+b(x)y}{c(x)+d(x)y} = \frac{a(x)+b(x)y}{c(x)+d(x)y}\frac{c(x)-d(x)y}{c(x)-d(x)y} && (1.55)\\ &= \frac{(ac-bdy^2)+(-ac+bc)y}{c^2-d^2y^2} = \frac{ac-bdQ(x)}{c^2-d^2Q(x)} + \frac{-ac+bc}{c^2-d^2Q(x)}y && (1.56)\\ &= f(x) + g(x)y = f(x) + g(x)y\frac{y}{y} && (1.57)\\ &= f(x) + \left(g(x)y^2\right)\frac{1}{y} = f(x) + \frac{h(x)}{y}\,, && (1.58) \end{aligned}$$

for some rational functions f, g, and h, of x. We now note that only the integral $\int f(x)\,\mathrm{d}x$ can be evaluated by means of elementary functions. So our problem reduces to understanding the integral of the form $\int h(x)/y\,\mathrm{d}x$, where $y^2 = Q(x)$ is a polynomial in x of degree three or four with no repeated roots.

Before we proceed, recalling the example of the simple pendulum from Section 1.4, we would like to reduce these integrals to the case $Q(x) = (1-x^2)(1-k^2x^2)$. We have the following cases.

If $y^2 = Q(x) = (x-e_1)(x-e_2)(x-e_3)$, for some distinct e_i for $i \in \{1,2,3\}$, then the substitution $x = u^2 + e_1$ converts the differential to

$$\frac{\mathrm{d}x}{y} = \frac{2\,\mathrm{d}u}{\sqrt{(u^2+e_1-e_2)(u^2+e_1-e_3)}}\,. \tag{1.59}$$

So we can always convert the degree three case to the degree four case.

If $y^2 = Q(x) = (x-e_1)(x-e_2)(x-e_3)(x-e_4)$, then we can use an appropriate Möbius transformation to map $\{e_1, e_2, e_3, e_4\}$ to $\{1, -1, k^{-1}, -k^{-1}\}$. We first map the roots $z_i = e_i$ to $w_1 = 1$, $w_2 = -1$, $w_3 = k^{-1}$ through

$$\frac{z_2 - z_3}{z_2 - z_1}\frac{z - z_1}{z - z_3} = \frac{w_2 - w_3}{w_2 - w_1}\frac{w - w_1}{w - w_3}\,, \tag{1.60}$$

and solving for w gives a mapping $z_i \to w_i$ for $i \in \{1, 2, 3\}$. We then demand that a fourth point $z_4 = e_4$ be mapped to $w_4 = -k^{-1}$. This gives a quadratic equation for k. This procedure allows to re-write the integral in the required form. Calculations are omitted because they are very lengthy and provide no particular insight.

We have shown that we can reduce the problem to considering integrals of the form

$$\int h(x)\frac{\mathrm{d}y}{y}\,, \quad \text{where} \quad y^2 = (1-x^2)(1-k^2x^2)\,. \tag{1.61}$$

We now split the function h into its even and odd parts, namely, for rational functions h_1 and h_2,

$$h(x) \coloneqq h_1(x^2) + xh_2(x^2)\,, \tag{1.62}$$

which yields

$$\int h(x)\frac{\mathrm{d}x}{y} = \int \frac{h_1(x^2)\mathrm{d}x}{\sqrt{(1-x^2)(1-k^2x^2)}} + \int \frac{xh_2(x^2)\mathrm{d}x}{\sqrt{(1-x^2)(1-k^2x^2)}} = I_1 + I_2\,. \tag{1.63}$$

By employing the substitution $t = x^2$,

$$I_2 = \frac{1}{2}\int \frac{h_2(t)\mathrm{d}t}{\sqrt{(1-t)(1-k^2t)}}\,, \tag{1.64}$$

which is elementary, see for example [93, Chapter V, Section 3]. Let us now turn to I_1. The partial fractions decomposition of h_1 with complex coefficients is

$$h_1(x) = \sum_{j=1}^{n} a_j x^{2j} + \sum_{j=1}^{\ell}\sum_{m=1}^{m_j} \frac{b_{jm}}{(x^2 - c_j^2)^m}\,, \tag{1.65}$$

where a_j, b_{jm} and c_j are complex numbers, and ℓ, m_j integers. Thus the integral $\int h(x)/y\,\mathrm{d}x$ is a linear combination of integrals of the form

$$I_n = \int \frac{x^{2n}\mathrm{d}x}{\sqrt{(1-x^2)(1-k^2x^2)}}\,, \quad \text{and} \quad J_n = \int \frac{\mathrm{d}x}{(x^2-c^2)^n\sqrt{(1-x^2)(1-k^2x^2)}}\,, \quad n \geq 0\,. \tag{1.66}$$

By considering the derivative $(x^{2n}y)'$, a tedious calculation yields the recurrence relation

$$nI_{n-1} - \left(n + \frac{1}{2}\right)(k^2+1)I_n + (n+1)k^2 I_{n+1} = x^{2n}y + \text{constant}\,. \tag{1.67}$$

Similarly, the derivative of $y(x^2-c^2)^{-n}$ yields the recurrence relation for J_n [4, §17.1.5]

$$\begin{aligned}\frac{1}{2}k^2(3-2n)J_{n-2}+(3c-1)k^2-1(1-n)J_{n-1}\\ +\frac{1}{2}(1-2n)\left(\left(3c^2-2c\right)k^2-2c+1\right)J_n\\ -n(c-1)c\left(ck^2-1\right)J_{n+1}=y(x^2-c^2)^{-n}+\text{constant}\,.\end{aligned}\tag{1.68}$$

Consider

$$I_0=\int\frac{\mathrm{d}x}{\sqrt{(1-x^2)(1-k^2x^2)}}\,,\tag{1.69}$$

this is the elliptic integral of the first kind. Then, consider I_2:

$$I_2=\frac{1}{k^2}\int\frac{(1-(1-k^2x^2))}{\sqrt{(1-x^2)(1-k^2x^2)}}\,\mathrm{d}x\tag{1.70}$$

$$=\frac{1}{k^2}I_0-\frac{1}{k^2}\int\sqrt{\frac{1-k^2x^2}{1-x^2}}\,\mathrm{d}x\,,\tag{1.71}$$

a linear combination of the elliptic integral of the first kind I_0, and another non-elementary integral which we call an *elliptic integral of the second kind*. Lastly, the integral

$$J_1=\int\frac{\mathrm{d}x}{(x^2-c^2)\sqrt{(1-x^2)(1-k^2x^2)}}\tag{1.72}$$

is an elliptic integral of the third kind. We have thus proved the following theorem.

Theorem 1.14 (Legendre standard form)

Any elliptic integral is a linear combination of the following functions: integrals expressed by elementary functions, elliptic integrals of the first kind, elliptic integrals of the second kind, and elliptic integrals of the third kind.

This theorem is due to Legendre [116]; for a modern exposition, see [151, Theorem 2.2]. To simplify the form of the integrals in the Legendre form, we can make the change of variables $x=\sin\varphi$. Then,

$$x=\sin\varphi\implies\mathrm{d}x=\cos\varphi\,\mathrm{d}\varphi\tag{1.73}$$

$$\implies\sqrt{1-x^2}=\cos\varphi\tag{1.74}$$

$$\implies\sqrt{1-k^2x^2}=\sqrt{1-k^2\sin^2\varphi}\,.\tag{1.75}$$

Therefore, we obtain the following forms for the elliptic integrals of the first, second, and third kind

$$\int\frac{\mathrm{d}\varphi}{\sqrt{1-k^2\sin^2\varphi}}\,,\quad\int\frac{\sin^2\varphi\,\mathrm{d}\varphi}{\sqrt{1-k^2\sin^2\varphi}}\,,\quad\int\frac{\mathrm{d}\varphi}{(\sin^2\varphi-c^2)\sqrt{1-k^2\sin\varphi}}\,.\tag{1.76}$$

Note that, since

$$k^2 \int \frac{\sin^2\varphi \,\mathrm{d}\varphi}{\sqrt{1-k^2\sin\varphi}} = \int \frac{\mathrm{d}\varphi}{\sqrt{1-k^2\sin^2\varphi}} - \int \sqrt{1-k^2\sin^2\varphi}\,\mathrm{d}\varphi\,, \tag{1.77}$$

we take the integral $\int \sqrt{1-k^2\sin^2\varphi}\,\mathrm{d}\varphi$ to be the elliptic integral of the second kind. We gather the above together in the following definitions.

Definition 1.15 (Elliptic integrals of the first, second, and third kind): In the following, the number k is referred to as *the modulus*, and taken such that $0 < k < 1$. The variable φ is the *argument*, and usually taken to be $0 < \varphi \leq \pi/2$.

- The incomplete elliptic integral of the first kind is defined as

$$F(\varphi, k) \coloneqq \int_0^{\sin\varphi} \frac{\mathrm{d}t}{\sqrt{(1-t^2)(1-k^2t^2)}} = \int_0^{\varphi} \frac{\mathrm{d}\vartheta}{\sqrt{1-k^2\sin^2\vartheta}}\,. \tag{1.78}$$

- The incomplete elliptic integral of the second kind is defined as

$$E(\varphi, k) \coloneqq \int_0^{\sin\varphi} \sqrt{\frac{1-k^2t^2}{1-t^2}}\,\mathrm{d}t = \int_0^{\varphi} \sqrt{1-k^2\sin^2\vartheta}\,\mathrm{d}\vartheta\,. \tag{1.79}$$

- The incomplete elliptic integral of the third kind is defined as

$$\begin{aligned}\Pi(\varphi, \alpha^2, k) &\coloneqq \int_0^{\sin\varphi} \frac{\mathrm{d}t}{(1-\alpha^2t^2)\sqrt{(1-t^2)(1-k^2t^2)}} \\ &= \int_0^{\varphi} \frac{\mathrm{d}\vartheta}{(1-\alpha^2\sin^2\vartheta)\sqrt{1-k^2\sin^2\vartheta}}\,,\end{aligned} \tag{1.80}$$

  where $-\infty < \alpha^2 < \infty$.

When $\varphi = \pi/2$, i.e. when $\sin\varphi = 1$, the integrals in Eqs. (1.78)–(1.80) are said to be *complete* and one writes

- the complete elliptic function of the first kind as $K(k) \coloneqq F(\pi/2, k)$,
- the complete elliptic function of the second kind as $E(k) \coloneqq E(\pi/2, k)$,
- the complete elliptic function of the third kind as $\Pi(\alpha^2, k) \coloneqq \Pi(\pi/2, \alpha^2, k)$, $\alpha^2 \neq 1$.

Notice that, in the limiting case that $k \to 1$, the incomplete elliptic integral of the first kind, Eq. (1.78), gives $\operatorname{arcoth}(x)$, while, as $k \to 0$, it gives $\arcsin(x)$. In this sense, elliptic integrals can be viewed as generalisations of the inverse trigonometric or hyperbolic functions.

1.5.3 *Hypergeometric functions*

In Eq. (1.19), we expressed the period of the simple pendulum in terms of the complete elliptic integral of the first kind:

$$T = 2\sqrt{\frac{\ell}{g}} K\left(\sin\frac{\theta_0}{2}\right), \tag{1.81}$$

for some initial θ_0. In this section, we will show that T can be expressed in terms of another special function, the *hypergeometric function*. By the binomial theorem, the integrand becomes

$$\frac{1}{\sqrt{1-k^2\sin^2\vartheta}} = \sum_{n=0}^{\infty} \binom{-1/2}{n} (-1)^n k^{2n} \sin^{2n}(\vartheta)\,. \tag{1.82}$$

Integrating the right-hand side of Eq. (1.82) term by term, and using the identity that, for any natural number n,

$$\int_0^{\pi/2} \sin^{2n}(\vartheta)\,\mathrm{d}\vartheta = \frac{\pi}{2}(-1)^n \binom{-1/2}{n}, \tag{1.83}$$

we can write

$$K(k) = \frac{\pi}{2} \sum_{n=0}^{\infty} \frac{(1/2)_n\,(1/2)_n}{n!\,(1)_n} k^{2n}, \tag{1.84}$$

where we used the notation $(q)_n$ for the (rising) *Pochhammer symbol*, which is given by

$$(q)_n = \begin{cases} 1 & n = 0 \\ q(q+1)\cdots(q+n-1) & n > 0 \end{cases}. \tag{1.85}$$

We now introduce the *generalised hypergeometric function*, defined by the power series

$${}_pF_q(a_1,\ldots,a_p;b_1,\ldots,b_q;z) = \sum_{n=0}^{\infty} \frac{(a_1)_n\cdots(a_p)_n}{(b_1)_n\cdots(b_q)_n} \frac{z^n}{n!}\,, \tag{1.86}$$

where $a_j, b_k \in \mathbb{C}$. In particular, when $p = 2$ and $q = 1$, we have what is called *Gaussian* or *ordinary hypergeometric function* denoted by ${}_2F_1$. Therefore, Eq. (1.84) reduces to

$$K(k) = \frac{\pi}{2}\,{}_2F_1\left(\frac{1}{2},\frac{1}{2};1;k^2\right). \tag{1.87}$$

Similarly, one obtains

$$E(k) = \frac{\pi}{2}\,{}_2F_1\left(-\frac{1}{2},\frac{1}{2};1;k^2\right). \tag{1.88}$$

The name *hypergeometric* is due to the fact that this function can be considered as a generalisation of the geometric series. This can be seen by computing ${}_2F_1(1,1;1;z)$, that is,

$${}_2F_1(1,1;1;z) = \sum_{n=0}^{\infty} z^n = \frac{1}{1-z}\,. \tag{1.89}$$

Lastly, let us first recall that Euler's *gamma function* is defined as

$$\Gamma(z) = \int_0^\infty t^{z-1} \mathrm{e}^{-t} \mathrm{d}t \,, \tag{1.90}$$

where $\mathrm{Re}(z) > 0$. It can also be analytically continued to all complex numbers z except non-positive integers, and, when z is a positive integer, $z = n$, it satisfies $\Gamma(n+1) = n!$ or, more generally, $\Gamma(z+1) = z\Gamma(z)$. We remark that, when $z = 1$ and if $\mathrm{Re}(c) > \mathrm{Re}(a+b)$, the hypergeometric function reduces to a ratio of gamma functions of the form

$${}_2F_1\left(a, b; c; 1\right) = \frac{\Gamma\left(c\right)\Gamma\left(c-a-b\right)}{\Gamma\left(c-a\right)\Gamma\left(c-b\right)}. \tag{1.91}$$

This identity is known as *Gauss's summation theorem*. For more details, see [67, Chapter 15].

2

Cosmology

2.1 Introduction

Cosmology is the study of the universe as a whole, with the aim to understand its origin and evolution. The quest for understanding the cosmos has always raised fascinating questions, and the first theoretical models to describe our universe, though atavistic, date back to the 16th century BCE, in which the Mesopotamian civilisation envisaged a flat circular Earth surrounded by a cosmic ocean [101]. Several cosmological theories were proposed over the centuries, for example by the ancient Hindu civilisation (15th–11th century BCE), by the Babylonians (6th century BCE), and by the ancient Greeks (from the 6th century BCE onwards). Some of these ideas, for example of cyclic universes models, or on infinite universes, despite having their roots in myths, are still relevant to this day. It is therefore worth remarking that this thesis concerns *physical* cosmology, that is, the scientific study of the universe as a whole in alignment with the laws of physics.

In the second decade of the last century, thanks to the mathematical foundations of Einstein's general theory of relativity (GR) and its astronomical verification, modern cosmology was born. Until then, the best scientific theory of universal gravity had been proposed by Newton in the late 17th century, with the law of gravitational attraction. There are some approaches that derive cosmology using Newtonian gravity without resorting to Einstein's theory of relativity, for example, see [114]. GR provides a description of space, time, gravity, and matter, at the macroscopic level, through differential geometry. Introduced by Einstein in 1915 [72], it successfully describes and accounts for a variety of gravitational phenomena [2, 6, 102, 170], assumes that spacetime is dynamical and that its curvature is induced by its energy-momentum content. Gravity is therefore considered a consequence of spacetime curvature and hence dictates the motion of energy/matter. This is often summarised in Wheeler's famous statement, "spacetime tells matter how to move; matter tells spacetime how to curve" [129]. The equation that describes the interplay between the geometry of spacetime and its energy-momentum content is the Einstein equation (in geometrised units)

$$G_{\mu\nu} - \Lambda g_{\mu\nu} = 8\pi T_{\mu\nu} \,, \tag{2.1}$$

where $G_{\mu\nu} = R_{\mu\nu} + \frac{1}{2}Rg_{\mu\nu}$ is the Einstein tensor, $R_{\mu\nu}$ is the Ricci tensor, R is the Ricci scalar, Λ is the cosmological constant, $g_{\mu\nu}$ is the metric tensor, and $T_{\mu\nu}$ the energy-momentum tensor. In the most general setting, the Einstein equation leads to a set of ten independent non-linear coupled partial differential equations (PDEs), known as the Einstein field equations. This set of PDEs is, in general, challenging to solve; however, imposing spacetime symmetries allows us to simplify the task. The simplifying assumption in cosmology is given by the cosmological principle, which states that the universe looks the same everywhere over large enough scales and thus is assumed to be homogeneous and isotropic; these terms will be defined rigorously after Proposition 2.14.

We begin by providing an overview of some key mathematical tools, namely, Killing vectors and Lie derivatives, which encapsulate the concept of symmetry. The symmetries stated by the cosmological principle allow us to build the Friedmann–Lemaître–Robertson–Walker metric. We conclude by considering the Friedmann equations. Following the tools introduced in Chapter 1, we first provide a qualitative analysis using dynamical systems, and then the exact solutions for universes with different curvatures (flat, open, and closed).

2.2 Flow

Before we begin to discuss spacetime symmetries, let us provide the following definition.

Definition 2.1 ([91, p. 169] Spacetime): A *spacetime* is a pair $(\mathscr{M}, g)$, where $\mathscr{M}$ is a four-dimensional smooth, connected manifold, with a given smooth Lorentzian metric g on $\mathscr{M}$ of signature $(-,+,+,+)$.

We can try to extend our intuition for symmetries in $\mathbb{R}^3$ to understand spacetime symmetries. If we consider a sphere S^2, it *looks the same* in all directions. However, if the sphere is deformed into a general ellipsoid, whose axes are of different lengths, then the rotational symmetry may cease to exist. We wish the metric to encapsulate the distinction between these two spaces and we seek a mathematical statement.

In Section 1.3, we encountered the concept of flow; see Definition 1.2. This immediately extends to a differentiable vector field on a manifold $\mathscr{M}$.

Definition 2.2 (Flow): A *flow* φ_t on a manifold $\mathscr{M}$ is a one-parameter family of diffeomorphisms[1] $\varphi_t : \mathbb{R} \times \mathscr{M} \to \mathscr{M}$, parametrised by $t \in \mathbb{R}$, such that, for each $s, t \in \mathbb{R}$, $\varphi_s \circ \varphi_t = \varphi_{s+t}$.

It follows that φ_0 is the identity map, and that $\varphi_{-t} = \varphi_t^{-1}$. Therefore, this is a one-parameter group. The flow φ_t gives rise to trajectories on the manifold, which are the smooth maps $\mathbb{R} \to \mathscr{M}$

[1] We call two sets M and N *diffeomorphic* if there exists a C^∞-map $\varphi : M \to N$ with a C^∞ inverse $\varphi^{-1} : N \to M$; the map φ is then called a *diffeomorphism*.

given by $t \mapsto \varphi_t(x_0)$ for some $x_0 \in \mathscr{M}$.

We have seen how one-parameter families of diffeomorphisms arise from vector fields. Conversely, any flow defines a vector field, as follows. Given a point $p \in \mathscr{M}$, $\varphi_t(p)$ traces out a curve in the manifold as t varies. Doing this for every point $p \in \mathscr{M}$ yields a collection of curves which fill the manifold. We can now define the vector field $\boldsymbol{\xi}(p)$ as the set of tangent vectors to each of these curves at any point. In other words, we have

$$\boldsymbol{\xi}\,(p) = \left.\frac{\mathrm{d}\varphi_t(p)}{\mathrm{d}t}\right|_{t=0}. \tag{2.2}$$

This vector field is said to be *generated by* φ_t. For more details, see, for example, [48, 51].

The flow, φ_t, of the vector field $\boldsymbol{\xi}$ is said to be an *isometry*, i.e. a distance-preserving transformation, if the metric *looks the same* at each point along a given flow line. To write this statement mathematically, we first introduce the Lie derivative.

2.3 Lie derivatives

Coordinate transformations which leave the metric invariant are of importance since they encode information about symmetries.

Definition 2.3 (Local isometry): A coordinate transformation $x^\mu \mapsto x'^\mu = x'^\mu(x^\nu)$ of a spacetime $(\mathscr{M}, g_{\mu\nu})$ is called a *local isometry* if

$$g'_{\mu\nu}(x) = g_{\mu\nu}(x)\,, \tag{2.3}$$

where $g'_{\mu\nu}$ is the metric written in terms of the transformed coordinates x'^μ.

In other words, the transformed metric $g'_{\mu\nu}(x')$ is the *same* function of its argument x'^α as the original metric $g_{\mu\nu}(x)$ is of its argument x^α.

Since the metric $g_{\mu\nu}$ is a covariant tensor, it transforms as

$$g_{\mu\nu}(x) = \frac{\partial x'^\alpha}{\partial x^\mu}\frac{\partial x'^\beta}{\partial x^\nu} g'_{\alpha\beta}(x'). \tag{2.4}$$

By using Eq. (2.3), we obtain the condition

$$g_{\mu\nu}(x) = \frac{\partial x'^\alpha}{\partial x^\mu}\frac{\partial x'^\beta}{\partial x^\nu} g_{\alpha\beta}(x')\,. \tag{2.5}$$

As we shall see later on in Section 2.5, some isometries, called *infinitesimal isometries*, give rise to invariant quantities via Noether's theorem. To identify such symmetries, we only need to consider a so-called *infinitesimal* coordinate transformation

$$x^\mu \mapsto x'^\mu = x^\mu + \varepsilon\,\xi^\mu(x)\,, \tag{2.6}$$

where $\varepsilon \ll 1$ and ξ^μ is a vector field. In this case, we say that ξ^μ *generates* the isometries.

To characterise the isometries of the metric, we introduce the Lie derivative. The Lie derivative is a connection-independent (i.e. it does not depend on the Christoffel symbol components) derivative operator acting on tensors, along a vector field ξ; it is a linear operator, denoted by $\mathscr{L}_\xi$, which satisfies the Leibniz rule, and maps tensors to tensors.

Definition 2.4 (Lie derivative of a function): Let f be a smooth function on $\mathscr{M}$ to $\mathbb{R}$, $f \in C^\infty(\mathscr{M})$, and let ξ^μ be a contravariant vector. Then, the Lie derivative of f along ξ is defined by

$$\mathscr{L}_\xi f = \xi^\mu \partial_\mu f \,. \tag{2.7}$$

Remark 2.5: Note that Definition 2.4 coincides with the definition of directional derivative of a function f along a vector ξ in vector calculus.

The definition of the Lie derivative can be extended to higher rank tensors, in particular the metric tensor, which we state as follows.

Definition 2.6 (Lie derivative of the metric): For a metric tensor $g_{\mu\nu}$ on some manifold $\mathscr{M}$, the Lie derivative of the metric along a vector ξ is given by

$$\left(\mathscr{L}_\xi g\right)_{\mu\nu} = \xi^\alpha \partial_\alpha g_{\mu\nu} + g_{\alpha\nu}\partial_\mu \xi^\alpha + g_{\mu\alpha}\partial_\nu \xi^\alpha \,. \tag{2.8}$$

The following theorem illustrates the relation between local isometries and the Lie derivative.

Theorem 2.7 ([59, Chapter 7, Section 7])

A smooth vector field ξ on a spacetime $(\mathscr{M}, g)$ generates a local isometry if $(\mathscr{L}_\xi g)_{\mu\nu} = 0$.

Proof. Let us begin by differentiating Eq. (2.6), which gives

$$\frac{\partial x'^\mu}{\partial x^\nu} = \delta^\mu_\nu + \varepsilon\, \partial_\nu \xi^\mu \,. \tag{2.9}$$

Substituting in Eq. (2.5) yields

$$g_{\mu\nu}(x) = \left(\delta^\mu_\alpha + \varepsilon\, \partial_\mu \xi^\alpha\right)\left(\delta^\nu_\beta + \varepsilon\, \partial_\nu \xi^\beta\right) g_{\alpha\beta}\left(x^\gamma + \varepsilon\, \xi^\gamma\right). \tag{2.10}$$

By Taylor's theorem, we write

$$g_{\alpha\beta}\left(x^\gamma + \varepsilon\, \xi^\gamma\right) = g_{\alpha\beta} + \varepsilon \xi^\gamma \partial_\gamma g_{\alpha\beta}(x) + \mathcal{O}\left(\varepsilon^2\right), \tag{2.11}$$

and, hence, obtain

$$g_{\mu\nu}(x) = g_{\mu\nu}(x) + \varepsilon \left[g_{\mu\beta}\partial_\nu \xi^\beta + g_{\nu\beta}\partial_\mu \xi^\beta + \xi^\gamma \partial_\gamma g_{\mu\nu} \right] + \mathcal{O}\left(\varepsilon^2\right) \tag{2.12}$$

$$= g_{\mu\nu}(x) + \varepsilon \left(\mathscr{L}_\xi g\right)_{\mu\nu} + \mathcal{O}\left(\varepsilon^2\right). \tag{2.13}$$

To first order in ε, it follows that $\left(\mathscr{L}_\xi g\right)_{\mu\nu} = 0$. □

2.4 Killing vectors

In order to find the vectors ξ such that $\left(\mathscr{L}_\xi g\right)_{\mu\nu} = 0$, we can re-write Eq. (2.8) in a more convenient form. In the following, we use the definitions given in Eqs. (0.1) and (0.2). In particular, the *metricity condition* allows us to determine a unique expression for the Christoffel symbols,

$$\nabla_\sigma g_{\mu\nu} = 0 \iff \partial_\sigma g_{\mu\nu} - \Gamma^\alpha_{\sigma\mu} g_{\alpha\nu} - \Gamma^\alpha_{\sigma\nu} g_{\mu\alpha} = 0 \tag{2.14}$$

$$\iff \partial_\sigma g_{\mu\nu} = \Gamma^\alpha_{\sigma\mu} g_{\alpha\nu} + \Gamma^\alpha_{\sigma\nu} g_{\mu\alpha}\,. \tag{2.15}$$

Substituting in Eq. (2.8) gives

$$\left(\mathscr{L}_\xi g\right)_{\mu\nu} = \xi^\sigma \left(\Gamma^\alpha_{\sigma\mu} g_{\alpha\nu} + \Gamma^\alpha_{\sigma\nu} g_{\mu\alpha}\right) + g_{\alpha\nu}\partial_\mu \xi^\alpha + g_{\mu\alpha}\partial_\nu \xi^\alpha \tag{2.16}$$

$$= \left(\partial_\mu \xi^\alpha + \Gamma^\alpha_{\sigma\mu}\xi^\sigma\right) g_{\alpha\nu} + \left(\partial_\nu \xi^\alpha + \Gamma^\alpha_{\sigma\nu}\xi^\sigma\right) g_{\mu\alpha} \tag{2.17}$$

$$= \nabla_\mu \xi^\alpha g_{\alpha\nu} + \nabla_\nu \xi^\alpha g_{\mu\alpha} \tag{2.18}$$

$$= \nabla_\mu \xi_\nu + \nabla_\nu \xi_\mu\,, \tag{2.19}$$

which therefore implies that the generators of isometries satisfy the equation

$$\nabla_\mu \xi_\nu + \nabla_\nu \xi_\mu = 0\,. \tag{2.20}$$

Equations (2.20) are called *Killing's equations*, after the mathematician Wilhelm Killing.

Definition 2.8 (Killing vector): A vector (field) ξ satisfying Eq. (2.20) is called a Killing vector (field) of the metric g.

Killing's equations, given in Eq. (2.20), are a general characterisation of Killing vectors in the sense that any solution corresponds to an isometry of the metric. Geometrically, the flow generated by Killing vector fields gives a one-parameter family of diffeomorphisms of the manifold that leaves the metric invariant, i.e. it *preserves* the metric.

2.5 Killing vectors and Noether's theorem

Killing vectors and isometries play an important role in the motion of test particles as described by the geodesic equations. Let us recall what we mean by an affinely parametrised geodesic.

Definition 2.9 (Geodesics): A curve $\mathcal{C}$ given by $x^\mu(\lambda)$ with affine parameter λ is called a *geodesic* if it satisfies the equation

$$\frac{\mathrm{d}^2 x^\mu}{\mathrm{d}\lambda^2} + \Gamma^\mu_{\nu\rho}\frac{\mathrm{d}x^\nu}{\mathrm{d}\lambda}\frac{\mathrm{d}x^\rho}{\mathrm{d}\lambda} = 0\,, \tag{2.21}$$

where the Christoffel symbols $\Gamma^\mu_{\nu\rho}$ are given by Eq. (0.1).

Geometrically, a geodesic is a locally length-minimising path, which turns out to be equivalent to Eq. (2.21). We can now state Noether's theorem, due to the mathematician Emmy Noether.

Theorem 2.10 (Noether's theorem [48, Chapter 3, Section 8])

Let $(\mathscr{M}, g)$ be a spacetime, let ξ^μ be a Killing vector field, and let $\mathrm{d}x^\mu/\mathrm{d}\lambda$ be tangent to an affinely parameterised geodesic. Then $\xi_\mu \mathrm{d}x^\mu/\mathrm{d}\lambda$ is constant along the geodesic.

Proof. We want to show that $Q \coloneqq \xi_\mu \mathrm{d}x^\mu/\mathrm{d}\lambda$ is constant along a geodesic and so we need to show that its derivative vanishes. We compute

$$\frac{\mathrm{d}Q}{\mathrm{d}\lambda} = \partial_\nu \xi_\mu \frac{\mathrm{d}x^\nu}{\mathrm{d}\lambda}\frac{\mathrm{d}x^\mu}{\mathrm{d}\lambda} + \xi_\mu \frac{\mathrm{d}^2 x^\mu}{\mathrm{d}\lambda^2}\,. \tag{2.22}$$

By the definition of affinely parametrised geodesic, we can re-write

$$\frac{\mathrm{d}Q}{\mathrm{d}\lambda} = \partial_\nu \xi_\mu \frac{\mathrm{d}x^\nu}{\mathrm{d}\lambda}\frac{\mathrm{d}x^\mu}{\mathrm{d}\lambda} - \xi_\mu \Gamma^\mu_{\alpha\beta}\frac{\mathrm{d}x^\alpha}{\mathrm{d}\lambda}\frac{\mathrm{d}x^\beta}{\mathrm{d}\lambda} = \nabla_\mu \xi_\mu \frac{\mathrm{d}x^\nu}{\mathrm{d}\lambda}\frac{\mathrm{d}x^\mu}{\mathrm{d}\lambda} = 0\,, \tag{2.23}$$

since $\nabla_\mu \xi_\nu$ is anti-symmetric by Killing's equations, Eq. (2.20). □

Remark 2.11: This is analogous to obtaining conserved quantities (first integrals) in Newtonian mechanics.

If our spacetime has a Killing vector field ξ, we can construct a *current* from a symmetric tensor, like the energy-momentum tensor. The name "current" is borrowed from electromagnetism to highlight that the conserved quantity satisfies a continuity equation $\nabla_\mu J^\mu = 0$, analogous to the current density in the conservation of electric charge law.

Theorem 2.12 ([48, Chapter 3, Section 8])

Let ξ^μ be a Killing vector field and let $T_{\mu\nu}$ be a symmetric tensor such that $\nabla_\mu T^{\mu\nu} = 0$. Then one can construct a conserved current *$J^\mu \coloneqq T^{\mu\nu}\xi_\nu$ such that $\nabla_\mu J^\mu = 0$.*

Proof. We can compute

$$\nabla_\mu J^\mu = \nabla_\mu \left(T^{\mu\nu}\xi_\nu\right) = \xi_\nu \nabla_\mu T^{\mu\nu} + T^{\mu\nu}\nabla_\mu \xi_\nu. \tag{2.24}$$

By assumption, $\nabla_\mu T^{\mu\nu} = 0$; and $T^{\mu\nu}\nabla_\mu \xi_\nu = 0$ because $T^{\mu\nu}$ is symmetric whilst $\nabla_\mu \xi_\nu$ is anti-symmetric by Killing's equations, Eq. (2.20). Hence, $\nabla_\mu J^\mu = 0$. □

Remark 2.13: Note that, for all Q^μ with $\nabla_\mu Q^\mu = 0$, we can write

$$\nabla_\mu Q^\mu = \frac{1}{\sqrt{-g}} \partial_\mu \left(\sqrt{-g} Q^\mu \right) , \tag{2.25}$$

which follows from the definition of covariant derivative and the identity

$$\Gamma^\mu_{\nu\mu} = \partial_\nu \left(\log \sqrt{-g} \right) . \tag{2.26}$$

Here $g = \det(g_{\mu\nu})$. It is now easier to see Q^μ satisfies a conservation equation which can be integrated over a volume, and, by applying the divergence theorem, we can define a conserved quantity.

2.6 Maximally symmetric manifolds

The following subsection follows the treatment of [51, 59]. The Killing equations, Eq. (2.20), can be differentiated to obtain a second order system of equations, as follows,

$$-\nabla_\gamma \nabla_\alpha \xi_\beta - \nabla_\gamma \nabla_\beta \xi_\alpha = 0 \tag{2.27}$$

$$\nabla_\alpha \nabla_\beta \xi_\gamma + \nabla_\alpha \nabla_\gamma \xi_\beta = 0 \tag{2.28}$$

$$\nabla_\beta \nabla_\gamma \xi_\alpha + \nabla_\beta \nabla_\alpha \xi_\gamma = 0 \, . \tag{2.29}$$

By adding these equations, we can re-arrange to obtain

$$\left(\nabla_\alpha \nabla_\gamma - \nabla_\gamma \nabla_\alpha \right) \xi_\beta + \left(\nabla_\beta \nabla_\gamma - \nabla_\gamma \nabla_\beta \right) \xi_\alpha + \left(\nabla_\alpha \nabla_\beta + \nabla_\beta \nabla_\alpha \right) \xi_\gamma = 0 \, . \tag{2.30}$$

The identity

$$\nabla_\sigma \nabla_\nu V_\mu - \nabla_\nu \nabla_\sigma V_\mu = R^\rho{}_{\mu\nu\sigma} V_\rho \tag{2.31}$$

yields

$$R^\sigma{}_{\beta\gamma\alpha} \xi_\sigma + R^\sigma{}_{\alpha\gamma\beta} \xi_\sigma + 2\nabla_\alpha \nabla_\beta \xi_\gamma + R^\sigma{}_{\gamma\alpha\beta} \xi_\sigma = 0 \tag{2.32}$$

$$\implies \left(R^\sigma{}_{\beta\gamma\alpha} + R^\sigma{}_{\alpha\gamma\beta} + R^\sigma{}_{\gamma\alpha\beta} \right) \xi_\sigma + 2\nabla_\alpha \nabla_\beta \xi_\gamma = 0 \, . \tag{2.33}$$

Since $R^\sigma{}_{\gamma\alpha\beta} = -R^\sigma{}_{\alpha\beta\gamma} - R^\sigma{}_{\beta\gamma\alpha}$ by the first Bianchi identity, and $R^\sigma{}_{\alpha\gamma\beta} = -R^\sigma{}_{\alpha\beta\gamma}$, we are left with

$$-2R^\sigma{}_{\alpha\beta\gamma} \xi_\sigma + 2\nabla_\alpha \nabla_\beta \xi_\gamma = 0 \, , \tag{2.34}$$

which can be re-arranged into

$$\nabla_\alpha \nabla_\beta \xi_\gamma = R^\sigma{}_{\alpha\beta\gamma} \xi_\sigma \,. \tag{2.35}$$

Given ξ_σ and $\nabla_\nu \xi_\sigma$ at some point $p \in \mathscr{M}$, we can determine the second derivatives of ξ_σ at p and find higher order derivatives via Eq. (2.35). As a result of Eq. (2.35), each Killing vector of a given metric is uniquely defined by its value at a point on the manifold and the value, at the same point, of the anti-symmetric tensor $\nabla_\nu \xi_\sigma$. For an n-dimensional spacetime, there are at most n linearly independent values of ξ_σ at a point and, since Killing's equations, in Eq. (2.20), imply that $\nabla_\mu \xi_\nu$ is anti-symmetric, there are at most $n(n-1)/2$ linearly independent possible values of $\nabla_\mu \xi_\nu$ at a point. All isometries of a given (pseudo-)Riemannian manifold $(\mathscr{M}, g)$ form a group denoted by $\mathrm{Iso}(\mathscr{M}, g)$. The dimension of the space of Killing vectors equals the dimension of the group of isometries. As a corollary, we obtain the following.

Proposition 2.14 ([51, Proposition 6.2.6])

The dimension of the group of isometries of an n-dimensional (pseudo-)Riemannian manifold $(\mathscr{M}, g)$ is less than or equal to $n(n+1)/2$.

A (pseudo-)Riemannian manifold $(\mathscr{M}, g)$ is called *maximally symmetric* if the dimension of $\mathrm{Iso}(\mathscr{M}, g)$ is equal to $n(n+1)/2$. A (pseudo-)Riemannian manifold $(\mathscr{M}, g)$ is called *homogeneous* if the action of $\mathrm{Iso}(\mathscr{M}, g)$ is transitive, i.e. for any two points $p, q \in \mathscr{M}$ there exists an isometry which maps p to q. This is the statement that there are no privileged points. This implies that the dimension of $\mathrm{Iso}(\mathscr{M}, g)$ is at least n. A (pseudo-)Riemannian manifold is called *isotropic* if the Riemann tensor of the metric is at each point x invariant under the group of rotations of the tangent space to $\mathscr{M}$ at x. This statement implies that the manifold has no privileged directions at a point.

When studying spacetime as a pseudo-Riemannian manifold $\mathscr{M}$, we will want to consider three-dimensional space-like slices corresponding to a fixed time, which are Riemannian submanifolds $\mathcal{M}^3$ of $\mathscr{M}$ with induced metric h, and on which we will use Roman indices (as opposed to Greek indices). It is on these slices that we will impose assumptions on the isometry group.

It is not immediately clear whether and how one can choose these space-like three-dimensional time slices. Indeed, in general, it cannot always be done, and when it can be done, the choice is in no sense unique; these questions are explored in detail in [62]. Under assumptions which certainly hold in the cosmological setting (e.g. that the spacetime manifold is time-orientable and simply-connected), a choice can be made. Consider a unit vector field u^α of future-pointing time-like vectors on the spacetime manifold. Such a vector field corresponds to taking the unit tangent

vectors to the worldlines of a family of freely-falling observers, one at every point in the manifold; this analogy is taken from [51, Section 6.3]. The space-like time slices at every point in the manifold are then characterised by being perpendicular to u^α at every point. In differential geometry terms, this gives rise to a *foliation* of $(\mathscr{M}, g)$ by Riemannian three-manifolds $(\mathcal{M}^3_\tau, h)$ parametrised by the proper time τ of any one of the freely falling observers.

Considering one of these time slices, we have the following proposition.

Proposition 2.15 ([51, Proposition 6.2.8])

Let $(\mathcal{M}^3, h)$ be a complete three-dimensional Riemannian manifold such that either $(\mathcal{M}^3, h)$ is homogeneous and isotropic at some point p; or $(\mathcal{M}^3, h)$ is isotropic at every point. Then $(\mathcal{M}^3, h)$ is maximally symmetric.

In several physically relevant cases (like our universe), the whole spacetime is not maximally symmetric, but it can be decomposed into maximally symmetric subspaces. The condition that that each slice is homogeneous and isotropic requires that the curvature of the spatial metric at any point is a constant; otherwise all points would not be geometrically identical. Such a space is called a space of *constant curvature*. For a space of constant curvature, we have

$$R_{\rho\sigma\mu\nu} = k\left(g_{\rho\mu}g_{\sigma\nu} - g_{\rho\nu}g_{\sigma\mu}\right), \tag{2.36}$$

where k is a constant, called the *curvature*. In differential geometry, spaces of constant curvature are known as Einstein spaces.

Definition 2.16 (Einstein space): A spacetime $(\mathscr{M}, g)$ is said to be an *Einstein space* if the Ricci tensor satisfies

$$R_{\mu\nu} = \lambda g_{\mu\nu}, \quad \text{for some constant } \lambda\,. \tag{2.37}$$

Proposition 2.17 ([59, Chapter 24, Section 7])

A (pseudo-)Riemannian manifold $(\mathscr{M}, g)$ that is isotropic at every point is an Einstein space.

Proof. Let us begin by considering the Einstein tensor $G_{\mu\nu}$ of a general n-dimensional metric $g_{\mu\nu}$ (of any signature)

$$G_{\mu\nu} = R_{\mu\nu} - \frac{1}{2}g_{\mu\nu}R\,. \tag{2.38}$$

If the space is isotropic, there is no distinguished choice of eigenvector. In other words, $g_{\mu\nu}$ has a single eigenvalue whose eigenspace is the full tangent space. This implies that $G^\mu{}_\nu$ is proportional

to the identity δ^μ_ν, for which every vector is an eigenvector. Thus,

$$G^\mu{}_\nu = -k\delta^\mu_\nu \iff G_{\mu\nu} = -kg_{\mu\nu}\,, \tag{2.39}$$

for some k. From the contracted Bianchi identity, $\nabla_\nu G^\mu{}_\nu = 0$, it follows immediately that k is a constant. Let us now consider the trace of Eq. (2.39), that is,

$$g^{\mu\nu}G_{\mu\nu} = -kg^{\mu\nu}g_{\mu\nu} \implies g^{\mu\nu}R_{\mu\nu} - \frac{1}{2}g^{\mu\nu}g_{\mu\nu}R = -kg^{\mu\nu}g_{\mu\nu} \tag{2.40}$$

$$\implies R - \frac{1}{2}nR = -kn \tag{2.41}$$

$$\implies \frac{2-n}{2}R = -kn \tag{2.42}$$

$$\implies R = \frac{2n}{n-2}k\,. \tag{2.43}$$

Substituting back into Eqs. (2.38) and (2.39), we have

$$R_{\mu\nu} - \frac{n}{n-2}kg_{\mu\nu} = -kg_{\mu\nu} \implies R_{\mu\nu} = \frac{2}{n-2}kg_{\mu\nu}\,, \tag{2.44}$$

which matches Definition 2.16. □

We can now show the following result.

Proposition 2.18 ([59, Chapter 24, Section 7])

For a space-like time slice $(\mathcal{M}^3, h)$ that is isotropic about every point, the Riemann curvature tensor is given by

$$R_{abcd} = k\left(h_{ac}h_{bd} - h_{ad}h_{bc}\right), \tag{2.45}$$

where k is a constant and h_{ab} is a three-dimensional metric.

Proof. The Riemann curvature tensor can be decomposed as

$$R_{abcd} = h_{ac}R_{bd} + h_{bd}R_{ac} - h_{ad}R_{bc} - h_{bc}R_{ad} + \frac{1}{2}\left(h_{ad}h_{bc} - h_{ac}h_{bd}\right)R, \tag{2.46}$$

i.e. in terms of the Ricci tensor R_{ab} and the Ricci scalar R. This is known as the *Ricci decomposition*; for more details, see [115, Proposition 7.28]. When $n = 3$, Eq. (2.44) and Eq. (2.43) then read $R_{ab} = 2kh_{ab}$ and $R = 6k$, respectively, for some constant k. Substituting these into Eq. (2.46) gives

$$R_{abcd} = 2kh_{ac}h_{bd} + 2kh_{bd}h_{ac} - 2kh_{ad}h_{bc} - 2kh_{bc}h_{ad} + 3k\left(h_{ad}h_{bc} - h_{ac}h_{bd}\right) \tag{2.47}$$

$$= k\left(h_{ac}h_{bd} - h_{ad}h_{bc}\right). \tag{2.48}$$

□

2.7 Cosmological principle and the FLRW metric

If we take a cubic box of side 100 Mpc (1 pc $\approx 3.09 \times 10^{16}$ m), and count the number of galaxies within such a box, the number in this volume is approximately the same independently of the box [30]. We say that, when averaged over sufficiently large scales, the universe is homogeneous. The Cosmic Microwave Background (CMB) radiation is the same in every direction, to roughly one part in 25,000 [9], supporting the assumption that the universe is isotropic on these scales. These observations are at the heart of the *cosmological principle*. Mathematically, there exists a time coordinate t such that, on each constant-time hypersurface (the submanifold $\mathcal{M}^3$), the universe looks the same at every point and in every direction [51]. In other words, our universe can be described through spacelike maximally symmetric hypersurfaces, which may evolve in time. This can be achieved by introducing a *scale factor* $a(t)$, which tells us how "large" the hypersurface is at time t, such that the spacetime metric is

$$\mathrm{d}s^2 = -\mathrm{d}t^2 + a^2(t)\mathrm{d}\sigma^2\,, \tag{2.49}$$

where $\mathrm{d}\sigma^2$ denotes the line element on $\mathcal{M}^3$. We can now employ the fact that the spatial part of the metric is isotropic about every point. This means it is convenient to use spherical polar coordinates that encode the spherical symmetry; maximal symmetry implies spherical symmetry. In a spherically symmetric spacetime, every point is on a two-surface which is a two-sphere $\mathbb{S}^2$, whose line element is given by $\mathrm{d}\Omega^2 = \mathrm{d}\theta^2 + \sin^2\theta\mathrm{d}\varphi^2$; for more details about spherically symmetric spacetimes, see for example [146]. Hence, one has

$$\mathrm{d}\sigma^2 = \mathrm{e}^{\lambda(r)}\mathrm{d}r^2 + r^2\left(\mathrm{d}\theta^2 + \sin^2\theta\mathrm{d}\varphi^2\right), \tag{2.50}$$

where λ is a function of r. The components of the Ricci tensor ${}^{(3)}R$, corresponding to the induced metric $\mathrm{d}\sigma^2$, are given by

$${}^{(3)}R_{11} = \frac{\lambda'(r)}{r}\,, \tag{2.51}$$

$${}^{(3)}R_{22} = 1 + \mathrm{e}^{-\lambda(r)}\left(\frac{1}{2}r\lambda'(r) - 1\right), \tag{2.52}$$

$${}^{(3)}R_{33} = \sin^2\theta\left[1 + \mathrm{e}^{-\lambda(r)}\left(\frac{1}{2}r\lambda'(r) - 1\right)\right]. \tag{2.53}$$

From Eq. (2.44), we have that, for $n = 3$, $R_{\mu\nu} = 2kg_{\mu\nu}$. Thus, Eqs. (2.51) and (2.52) yield

$$\frac{\lambda'(r)}{r} = 2k\mathrm{e}^{\lambda(r)} \tag{2.54}$$

$$1 + \mathrm{e}^{-\lambda(r)}\left(\frac{1}{2}r\lambda'(r) - 1\right) = 2kr^2\,, \tag{2.55}$$

and we note that Eq. (2.53) also leads to Eq. (2.55).

Solving Eqs. (2.54) and (2.55) simultaneously leads to

$$\mathrm{e}^{-\lambda(r)} = 1 - kr^2 \,. \tag{2.56}$$

We thus have

$$\mathrm{d}\sigma^2 = \frac{\mathrm{d}r^2}{1-kr^2} + r^2\left(\mathrm{d}\theta^2 + \sin^2\theta \mathrm{d}\varphi^2\right). \tag{2.57}$$

The *Friedmann–Lemaître–Robertson–Walker metric* is given by

$$\mathrm{d}s^2 = -\mathrm{d}t^2 + a^2(t)\left[\frac{\mathrm{d}r^2}{1-kr^2} + r^2\mathrm{d}\Omega^2\right], \tag{2.58}$$

where $\mathrm{d}\Omega^2 = \mathrm{d}\theta^2 + \sin^2\theta\mathrm{d}\varphi^2$. This metric was obtained independently by Friedmann [82], Lemaître [117], Robertson [140–142], and Walker [166].

Further, we can always apply a rescaling of distances by a positive constant so that the curvature k keeps its sign, but lies in the set $\{-1, 0, 1\}$, which correspond to the hyperbolic space ($\mathbb{H}^3$), the flat Euclidean space ($\mathbb{E}^3$), and the 3-sphere ($\mathbb{S}^3$), respectively. To this end, we introduce a third angle, χ, in addition to θ and φ, such that

$$r = \begin{cases} \sinh(\chi)\,, & 0 \le \chi \le \infty\,, \quad k = -1\,, \\ \chi\,, & 0 \le \chi \le \infty\,, \quad k = 0\,, \\ \sin(\chi)\,, & 0 \le \chi \le \pi\,, \quad k = +1\,. \end{cases} \tag{2.59}$$

Let us observe that, if $\chi \ll 1$, then $\sin(\chi) = \chi + \mathcal{O}(\chi^3)$ and $\sinh(\chi) = \chi + \mathcal{O}(\chi^3)$. This shows that, for small angles, the metrics in the three curvature regimes approximate one another. This allows us to re-write the metric in Eq. (2.58) as

$$\mathrm{d}s^2 = -\mathrm{d}t^2 + a(t)^2\left(\mathrm{d}\chi^2 + r^2\mathrm{d}\Omega^2\right). \tag{2.60}$$

Lastly, we remark that, in cosmology, the stress-energy, or energy-momentum, tensor $T_{\mu\nu}$, which is the matter part of the Einstein field equations, is taken to be

$$T_{\mu\nu} = \mathrm{diag}(-\rho, p, p, p),$$

where ρ describes the energy density and p the pressure of a perfect, barotropic fluid. In particular, p and ρ are related by an equation of the form $p = p(\rho)$.

2.8 Cosmological field equations

The maximal symmetry of the FLRW spacetime reduces the Einstein field equation, given in Eq. (2.1), from PDEs to the *Friedmann equations*, which are two ODEs,

$$\left(\frac{\dot{a}}{a}\right)^2 = \frac{8\pi}{3}\rho + \frac{\Lambda}{3} - \frac{k}{a^2}\,, \tag{2.61}$$

$$\frac{\ddot{a}}{a} = -\frac{4\pi}{3}(\rho + 3p) + \frac{\Lambda}{3}\,. \tag{2.62}$$

Recall that Λ denotes the cosmological constant and k denotes the curvature constant. By taking the time derivative of Eq. (2.61), and combining with Eqs. (2.61) and (2.62), we find the *energy-momentum conservation equation* (also known as the *continuity equation*) in cosmology, that is,

$$\dot{\rho} + 3\frac{\dot{a}}{a}(\rho + p) = 0\,, \tag{2.63}$$

which is satisfied by all matter.

The Friedmann equations, Eqs. (2.61) and (2.62), and the energy-momentum conservation equation, Eq. (2.63), are under-determined since we have two independent equations and three unknown functions, namely $a(t)$, $\rho(t)$, and $p(t)$. In order to close this system, we make the following modelling assumption: we assume a linear relation between ρ and p (the so-called *equation of state*), that is,

$$p = w\rho\,, \tag{2.64}$$

where $w \in [-1, 1]$ is a constant called the *equation of state parameter*. Note that this is the equation of a perfect *barotropic fluid*, i.e. a fluid in which the pressure is purely a function of density. A few commonly employed values for the equation of state parameter are shown in Table 2.1; for more details, see for example [130].

Table 2.1: Physical values for the equation of state parameter w.

Value of w	Matter-energy content
-1	cosmological constant or dark energy
$-1 < w < -1/3$	dynamical dark energy
$-1/3$	negative spatial curvature
0	dust (matter)
$1/3$	radiation
1	stiff matter (speed of sound equals the speed of light)

In the presence of a single perfect fluid, with a given value of w, we can relate the fluid's energy density ρ and pressure p to the speed of sound c_s in the fluid according to

$$c_s^2 = \frac{\partial p}{\partial \rho} = w\,. \tag{2.65}$$

For $w < 0$, the speed of sound c_s takes an imaginary value, which causes instabilities. When $w = 0$, the pressure vanishes and the perfect fluid models dust. For $w = 1/3$, there is radiation, which carries momentum, hence pressure is present. It is clear that, when $w = 1$, and reinserting the speed of light c in $p = wc^2\rho$, we have $c_s^2 = c^2$. We can now combine Eq. (2.63) with Eq. (2.64) to obtain

$$\frac{\dot{\rho}}{\rho} = -3(1+w)\frac{\dot{a}}{a} \implies \frac{\mathrm{d}}{\mathrm{d}t}(\log\rho) = -3(1+w)\frac{\mathrm{d}}{\mathrm{d}t}(\log a)$$
$$\implies \log\rho = -3(1+w)\log a + C\,, \tag{2.66}$$

where C is a constant of integration. This means

$$\rho = \rho_0 a^{-3(1+w)}\,, \tag{2.67}$$

for a constant ρ_0. This allows one to re-write Eq. (2.61) as

$$\left(\frac{\dot{a}}{a}\right)^2 = \frac{8\pi}{3}\rho_0 a^{-3(1+w)} + \frac{\Lambda}{3} - \frac{k}{a^2} \implies \dot{a}^2 = \frac{8\pi}{3}\rho_0 a^{-(1+3w)} + \frac{\Lambda}{3}a^2 - k\,. \tag{2.68}$$

At this stage, it becomes clearer that, if we take $w = -1$, the term containing $a^{-(1+3w)}$ becomes a^2, hence the fluid behaves like the term containing the cosmological constant. Similarly, if we set $w = -1/3$, the term $a^{-(1+3w)}$ becomes a^0, behaving like a negative spatial curvature term. Upon rescaling the density constant, the equation of state parameter, and the cosmological constant by

$$\beta \coloneqq \frac{8\pi}{3}\rho_0\,, \quad \gamma \coloneqq 1 + 3w\,, \quad \lambda \coloneqq \frac{\Lambda}{3}\,, \tag{2.69}$$

we can express Eq. (2.68) as

$$\dot{a}^2 = \beta a^{-\gamma} + \lambda a^2 - k\,, \tag{2.70}$$

and Eq. (2.62) as

$$\frac{\ddot{a}}{a} = -\frac{\gamma}{2}\beta a^{-2-\gamma} + \lambda\,. \tag{2.71}$$

Let us remark that: β, which is proportional to the initial energy density, is always a positive quantity; the effective equation of state parameter w is bounded between -1 and 1, which implies that $-2 \leq \gamma \leq 4$; the cosmological constant Λ is a real constant and so is λ; lastly, the curvature constant k can take values in the set $\{-1, 0, 1\}$.

Equation (2.70) can be solved by separating the variables and yields the following integrals

$$\int_{t_0}^{t} \mathrm{d}\tilde{t} = \int \frac{\mathrm{d}a}{\sqrt{\beta a^{-\gamma} + \lambda a^2 - k}} \tag{2.72}$$
$$\implies t - t_0 = \int \sqrt{\frac{a^\gamma}{\beta + \lambda a^{2+\gamma} - k a^\gamma}}\,\mathrm{d}a\,, \tag{2.73}$$

where t_0 is a constant of integration.

In Eq. (2.73), let us consider what happens for large values of a. In particular, for $\lambda > 0$, and $a \gg 1$, we have

$$\beta + \lambda a^{2+\gamma} - k a^{\gamma} \sim \lambda a^{2+\gamma}\,, \tag{2.74}$$

which implies

$$t - t_0 \sim \int_{a_0}^{a} \sqrt{\frac{\widetilde{a}^{\gamma}}{\lambda \widetilde{a}^{2+\gamma}}} \mathrm{d}\widetilde{a} = \int_{a_0}^{a} \frac{\mathrm{d}\widetilde{a}}{\sqrt{\lambda}\widetilde{a}} \tag{2.75}$$

$$= \frac{1}{\sqrt{\lambda}} \log(a) - \frac{1}{\sqrt{\lambda}} \log(a_0) = \frac{1}{\sqrt{\lambda}} \log\left(\frac{a}{a_0}\right), \tag{2.76}$$

where $a_0 = a(t_0)$. Therefore, for $a \gg 1$, one has

$$a \sim a_0 \exp\Big(\sqrt{\lambda}(t - t_0)\Big) = a_0 \exp\left(\sqrt{\frac{\Lambda}{3}}(t - t_0)\right), \tag{2.77}$$

which is the late-time exponential expansion.

2.9 Exact cosmological solutions

In this section, we discuss the solutions and mathematical properties of the Friedmann equation, Eq. (2.70). We are interested in the non-linear first-order ordinary differential equation, with varying parameters β, λ, and k. Standard GR and cosmology textbooks discuss the solutions in the case of a vanishing cosmological constant ($\Lambda = 0$), see for example [25, 30, 59], by separating the cases for matter and radiation, and looking at the different values of k. A solution for arbitrary w is derived in [17], in terms of the hypergeometric function. Subsequently, it was shown in [74] that the cosmological field equations can be rewritten as a Riccati differential equation, and this work was further extended in [120]. For a non-vanishing cosmological constant, a pedagogically more intuitive qualitative study is proposed in [148] by considering "effective potentials". Many of the sub-cases can be integrated directly using elementary functions and were reviewed in the context of multi-fluid cosmology [76]. The most general form of Eq. (2.70) can be solved by using elliptic functions. In [68, 69, 107, 118], an analytic solution for a non-vanishing cosmological constant in the cases of matter-domination (zero pressure) and radiation-domination is derived in terms of elliptic integrals. In [3, 57, 58, 60, 128], a solution in terms of the Weierstrass-$\wp$ function is found. In [10], analytic expressions are presented for all combinations of Λ and k in the presence and absence of radiation and non-relativistic matter, together with the most complete case referred to by the authors as the $\Lambda\gamma$CDM model, which assumes $\Lambda \neq 0$ and $k \neq 0$, to indicate the simultaneous presence of radiation and dust—hence, both γ and CDM (cold dark matter). Before looking at how to obtain the explicit solutions, let us now provide an overview of their qualitative features.

2.9.1 *A dynamical systems approach*

A classification of the solutions to the Friedmann equations using dynamical systems techniques is provided in [160], similar to those that will be used in Chapter 4.

Since the scale factor $a(t)$ represents a measure of the size of the universe at some time t, let us now introduce the *Hubble function*, which is the rate of expansion of the universe at some time t, and is defined as

$$H(t) \coloneqq \frac{\dot{a}(t)}{a(t)} \,. \tag{2.78}$$

This helps us re-write the Friedmann equations, Eqs. (2.61) and (2.62), as

$$3H^2 + 3\frac{k}{a^2} - \Lambda = \kappa\rho \,, \tag{2.79}$$

$$-2\dot{H} - 3H^2 - \frac{k}{a^2} + \Lambda = \kappa p \,, \tag{2.80}$$

where we set $\kappa = 8\pi$, which is the coupling constant in geometrised units, representing the strength of the gravitational force. By dividing Eq. (2.79) by $3H^2$, we obtain

$$1 = \frac{\kappa\rho}{3H^2} + \frac{\Lambda}{3H^2} - \frac{k}{a^2H^2} \,. \tag{2.81}$$

It is now convenient to introduce the following dimensionless variables

$$\Omega \coloneqq \frac{\kappa\rho}{3H^2} \,, \quad \Omega_\Lambda \coloneqq \frac{\Lambda}{3H^2} \,, \quad \Omega_k \coloneqq -\frac{k}{a^2H^2} \,, \tag{2.82}$$

which represent the density, cosmological constant, and curvature components. We can now write the Friedmann constraint in Eq. (2.81) as

$$1 = \Omega + \Omega_\Lambda + \Omega_k \,. \tag{2.83}$$

This means that we have two independent quantities, say, Ω_Λ and Ω_k, as the third quantity can be expressed in terms of the others. Let us remark that whilst $\Omega > 0$, in principle, there is no further constraint on Ω_k and Ω_Λ. Differentiating the variables in Eq. (2.82) with respect to $\log(a)$, and solving Eq. (2.62) for $\dot{H}$, we obtain the system

$$\Omega_\Lambda' = -\Omega_\Lambda(3w(\Omega_k + \Omega_\Lambda - 1) + \Omega_k + 3\Omega_\Lambda - 3) \,, \tag{2.84}$$

$$\Omega_k' = -\Omega_k(3w(\Omega_k + \Omega_\Lambda - 1) + \Omega_k + 3\Omega_\Lambda - 1) \,. \tag{2.85}$$

Here, differentiation with respect to $\log(a)$ is denoted by a prime. This system has three fixed points: $(\Omega_\Lambda^*, \Omega_k^*) \in \{(0,0), (1,0), (0,1)\}$. These fixed points correspond to three different types of universe: the Einstein–de Sitter space, i.e. a universe with flat spatial sections and no cosmological constant; a de Sitter space, i.e. a universe with positive cosmological constant and with flat spatial

sections; and the Milne universe, i.e. a universe with no cosmological constant and with hyperbolic ($k < 0$) spatial section. For $-1 < w \leq 1$, the eigenvalues and classification of the fixed points are given in Table 2.2. Note that, when $w = -1/3$, Point O and Point A have a zero eigenvalue and a positive one; the latter ensures that there is at least one unstable direction, so these fixed points are unstable.

Table 2.2: Stability of the critical points for the system given in Eqs. (2.84) and (2.85).

Point	Coordinates	q	Eigenvalues	Classification	Type of universe
Point O	$(0,0)$	$(1+3w)/2$	$3(1+w), \quad 1+3w$	saddle if $-1 < w < -1/3$ unstable if $-1/3 \leq w \leq 1$	Einstein–de Sitter
Point A	$(1,0)$	0	$2, \quad -1-3w$	unstable if $-1 < w < -1/3$ saddle if $-1/3 \leq w \leq 1$	de Sitter
Point B	$(0,1)$	-1	$-2, \quad -3(1+w)$	stable	Milne

To determine the regions of accelerated expansion, which are the subsets of the phase space in which $\ddot{a} > 0$, one can consider the deceleration parameter q defined by

$$1 + q = -\frac{\dot{H}}{H^2} = -\frac{H'}{H} = \frac{3}{2}(w+1) - \frac{1}{2}(3w+1)\Omega_k - \frac{3}{2}(w+1)\Omega_\Lambda \,, \tag{2.86}$$

using Eq. (2.80). The region of accelerated expansion, for which $q < 0$, is given by

$$q = -1 + \frac{3}{2}(w+1) - \frac{1}{2}(3w+1)\Omega_k - \frac{3}{2}(w+1)\Omega_\Lambda \tag{2.87}$$

$$= \frac{1}{2}(3w+1)(1-\Omega_k) - \frac{3}{2}(w+1)\Omega_\Lambda < 0 \,, \tag{2.88}$$

which implies

$$\Omega_k > 1 - \frac{3(w+1)}{3w+1}\Omega_\Lambda \,. \tag{2.89}$$

When $w = 0$, $\Omega_k > 1 - 3\Omega_\Lambda$, shown as a shaded region in Fig. 2.1, and, when $w = 1/3$, $\Omega_k > 1 - 2\Omega_\Lambda$. Equation (2.86) can be integrated to find $a(t)$ at any fixed point $(\Omega_\Lambda^*, \Omega_k^*)$. Note that, at a fixed point, the right-hand side of Eq. (2.86) is constant; if the constant is non-zero, then one has

$$a(t) \propto (t - t_0)^{2/[3(w+1) - (3w+1)\Omega_k^* - 3(w+1)\Omega_\Lambda^*]} \,. \tag{2.90}$$

When the right-hand side of Eq. (2.86) is zero, then H is a constant and a evolves exponentially in t, which corresponds to the universe undergoing a de Sitter expansion. One can see that at Point O, corresponding to the case $\Lambda = 0$ and $k = 0$, we have

$$a \propto (t - t_0)^{2/[3(w+1)]}. \tag{2.91}$$

A straightforward computation shows that $\Omega_\Lambda = 0$, $\Omega_k = 0$, and $\Omega_\Lambda + \Omega_k = 1$ are invariant lines,

that is, any trajectory that starts on these lines stays on them forever. No solution curve can cross these lines. Crossing $\Omega_k = 0$ would yield a change of topology since k would go from positive to negative; it can be seen as the line which separates open from closed universes. Moreover, the region $\Omega_\Lambda + \Omega_k > 1$ is unphysical as it corresponds to values for which $\Omega < 0$. Recent observations [6] suggest that our universe has a small positive cosmological constant and, whilst the ΛCDM models predicts vanishing curvature, there is some evidence that supports the possibility for negative values of k. This corresponds to the triangle bounded by the invariant lines.

We remark that when $w = -1$ (cosmological constant) and $w = -1/3$ (curvature term), Ω_Λ or Ω_k can be redefined, respectively, so as to include Ω. In Fig. 2.1, we plot the dynamics in the case $w = 0$ (dust). For $w = 1/3$, that is, a radiation-dominated universe, the system exhibits a qualitatively similar behaviour. In this example, we can see how, as we approach Point A, the cosmological constant dominates the late-time accelerated expansion, and curvature will never dominate. In particular, the scale factor is exponential in t, as given in Eq. (2.77).

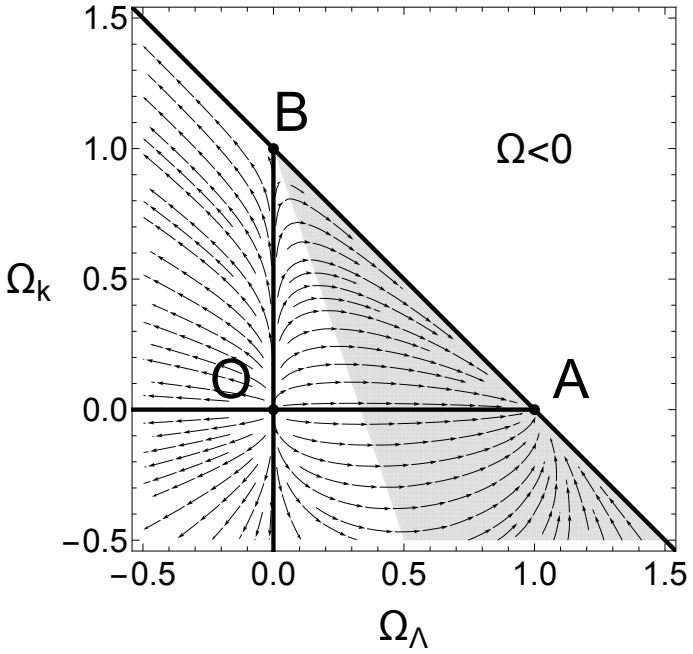

Fig. 2.1: Phase portrait of the dynamical system given in Eqs. (2.84) and (2.85) for $w = 0$. The shaded region, $\Omega_k > 1 - 3\Omega_\Lambda$, represents accelerated expansion. The invariant lines are shown.

2.9.2 *Classification of the solutions*

To visualise the behaviour of the universe in different cases, it is helpful to employ the *dynamic classification*, introduced by Harrison in [96] and discussed in [59, 97, 114]. According to each of the three values of the curvature constant, the different behaviour of the cosmological constant dictates the type of universe we are in, as shown in Fig. 2.3, and we differentiate between *oscillating*

universes and *continuously expanding* models.

In particular, $\Lambda < 0$ yields an oscillating universe for all values of k. This can be understood by considering the cosmological constant as an attractive force which eventually leads the universe to collapse, ending in the so-called *big crunch*. This is what typically happens in universes with a closed topology ($k = +1$). One way to see this is to follow a similar approach to the one outlined in [148]. Recall that the equation of motion for a particle with unit mass, moving in one dimension, and subject to a potential $V(x)$, is

$$\ddot{x} = -\frac{\mathrm{d}V}{\mathrm{d}x}\,, \tag{2.92}$$

which integrates to the energy equation

$$\frac{1}{2}\dot{x}^2 + V(x) = E\,, \tag{2.93}$$

where E is a constant. Let us consider Eq. (2.68) and note that we can write

$$\frac{1}{2}\dot{a}^2 - \frac{4\pi}{3}\rho_0 a^{-(1+3w)} - \frac{\Lambda}{6}a^2 + \frac{k}{2} = 0\,. \tag{2.94}$$

Upon defining

$$V(a) \coloneqq -\frac{4\pi}{3}\rho_0 a^{-(1+3w)} - \frac{\Lambda}{6}a^2 + \frac{k}{2}\,, \tag{2.95}$$

Eq. (2.94) reads

$$\frac{1}{2}\dot{a}^2 + V(a) = 0\,. \tag{2.96}$$

By comparing Eqs. (2.93) and (2.94), we note that the total energy in this case is zero. Since $\dot{a}^2 \geq 0$, we must have $V(a) < 0$ for possible motion. Assuming that $w \geq 0$, and that, at the big bang, i.e. near $a = 0$, $\dot{a} > 0$, then we can make the following considerations. For $k = 1$ and $\Lambda = 0$, the potential vanishes at

$$a_{\max} = \left(\frac{8\pi}{3}\rho_0\right)^{1/(1+3w)}\,. \tag{2.97}$$

The universe can only access the region where the potential is negative, that is, near $a = 0$ and for $a \leq a_{\max}$. At $a_{\max}$, the dynamics must turn around and the universe ends in a big crunch, see Fig. 2.2.

The dynamics is analogous for $\Lambda < 0$ and $k \in \{-1, 0, 1\}$. To see this, consider Eqs. (2.70) and (2.71), namely,

$$\dot{a}^2 = \beta a^{-\gamma} + \lambda a^2 - k\,, \tag{2.98}$$

$$\frac{\ddot{a}}{a} = -\frac{\gamma}{2}\beta a^{-2-\gamma} + \lambda\,. \tag{2.99}$$

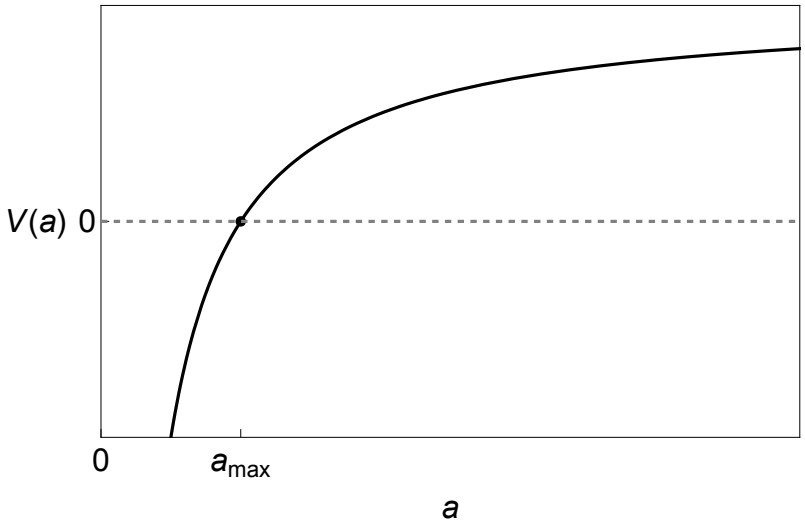

Fig. 2.2: Sketch of the effective potential for $k = +1$ and $\Lambda = 0$.

Now, let $a_{\max}$ be the value of a solution a at the maximum scale of the universe, that is, $a_{\max} = a(t_{\max})$. We seek the condition on $a_{\max}$ in order for it to be a maximum, that is, at $a_{\max}$ we require $\dot{a} = 0$ and $\ddot{a} < 0$. From Eq. (2.98),

$$\beta a_{\max}^{-\gamma} = k - \lambda a_{\max}^2 \,, \tag{2.100}$$

and, from Eq. (2.99), substituting in Eq. (2.100), we obtain

$$\begin{aligned} a_{\max}\ddot{a}(t_{\max}) &= -\frac{\gamma}{2}\beta a_{\max}^{-\gamma} + \lambda a_{\max}^2 = -\frac{\gamma}{2}(k - \lambda a_{\max}^2) + \lambda a_{\max}^2 \\ &= -\frac{\gamma}{2}k + \left(1 + \frac{\gamma}{2}\right)\lambda a_{\max}^2 < 0 \,. \end{aligned} \tag{2.101}$$

It follows that

$$a_{\max}^2 < \frac{\gamma k}{(2+\gamma)\lambda} \,. \tag{2.102}$$

For $\lambda > 0$, there exists such an $a_{\max} \in \mathbb{R}$ provided that $k = +1$. When $\lambda \to 0$, then $k > 0$, which is consistent with associating a closed topology to an oscillating universe. Lastly, for $\lambda < 0$, there is no condition on k, that is, we always have oscillating solutions. As shown by Fig. 2.3, some care is needed for the case $k = 1$ and $\lambda > 0$ since there exists a critical value of the cosmological constant from which the solutions start being oscillatory. This will be discussed in more detail in Chapter 3 since γ needs to be fixed so as to make concrete statements.

2.9.3 *Flat models*

Let us begin by considering flat models, that is, $k = 0$. In a way, these are the easiest cases and we can obtain formulae which hold for all the physical values of γ (or equivalently w). To simplify

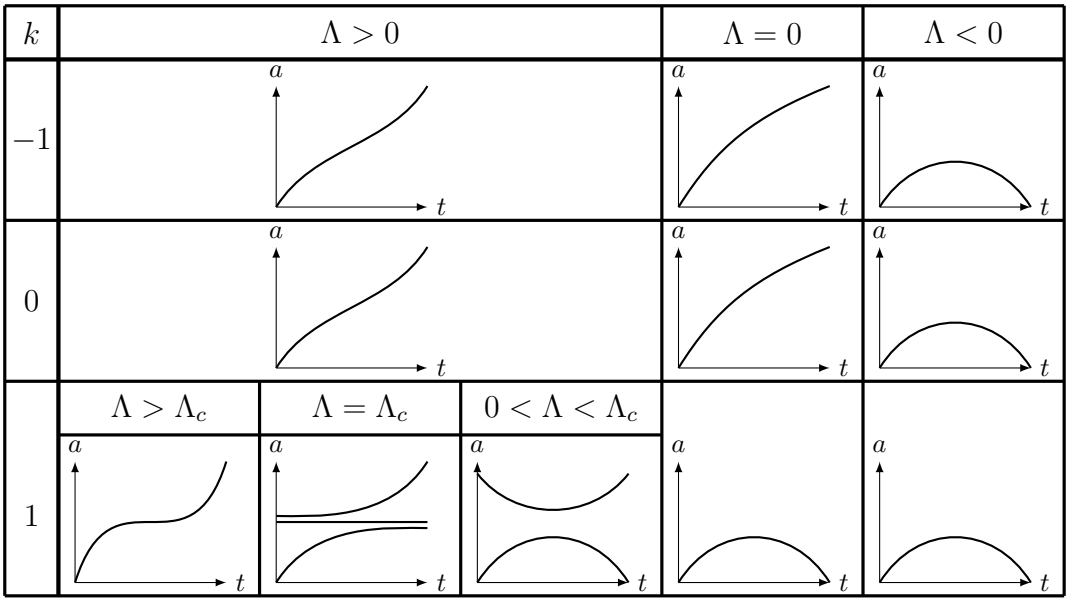

Fig. 2.3: Dynamic classification of Friedmann models according to curvature k and cosmological constant Λ, adapted from [59, Fig. 25.1]. Note that here Λ_c denotes a positive critical value of the cosmological constant $\Lambda_c = 4/(9\beta^2)$.

the notation in the following, we introduce

$$\widetilde{\gamma} \coloneqq \frac{\gamma}{2} + 1 = \frac{3}{2}(1+w)\,. \tag{2.103}$$

When $k = 0$, Eq. (2.73) reduces to

$$t - t_0 = \int \sqrt{\frac{a^\gamma}{\beta + \lambda a^{2+\gamma}}}\mathrm{d}a = \int a^{\gamma/2}(\beta + \lambda a^{2+\gamma})^{-1/2}\mathrm{d}a\,. \tag{2.104}$$

By Theorem 1.10, the integral in Eq. (2.104) is elementary if and only if at least one of following quantities is an integer:

$$\frac{\gamma/2+1}{2+\gamma}\,, \quad -\frac{1}{2}\,, \quad \frac{\gamma/2+1}{2+\gamma} - \frac{1}{2}\,, \tag{2.105}$$

which simplify to the triplet $1/2$, $-1/2$, and 0. Therefore, since 0 is an integer, this integral is elementary for all γ. When $\lambda = 0$, this gives

$$t - t_0 = \frac{a^{\widetilde{\gamma}}}{\sqrt{\beta}\widetilde{\gamma}} \Leftrightarrow a(t) = \left(\sqrt{\beta}\widetilde{\gamma}(t-t_0)\right)^{1/\widetilde{\gamma}}\,, \tag{2.106}$$

which is the Einstein–de Sitter model, and matches Eq. (2.91). When $\lambda > 0$, then

$$t - t_0 = \frac{1}{\widetilde{\gamma}\sqrt{\lambda}}\operatorname{arsinh}\left(\sqrt{\frac{\lambda}{\beta}}a^{\widetilde{\gamma}}\right) \Leftrightarrow a = \left(\sqrt{\frac{\beta}{\lambda}}\sinh\left(\widetilde{\gamma}\sqrt{\lambda}(t-t_0)\right)\right)^{1/\widetilde{\gamma}}\,. \tag{2.107}$$

Lastly, when $\lambda < 0$, we have

$$t - t_0 = \frac{1}{\widetilde{\gamma}\sqrt{|\lambda|}}\arcsin\left(\sqrt{\frac{|\lambda|}{\beta}}a^{\widetilde{\gamma}}\right) \Leftrightarrow a = \left(\sqrt{\frac{\beta}{|\lambda|}}\sin\left(\widetilde{\gamma}\sqrt{|\lambda|}(t-t_0)\right)\right)^{1/\widetilde{\gamma}}\,. \tag{2.108}$$

2.9.4 *Vanishing cosmological constant and non-zero curvature*

Models with a vanishing cosmological constant and positive or negative curvature admit a solution for arbitrary values of γ (or w). Here, Eq. (2.73) reads

$$t - t_0 = \int \sqrt{\frac{a^\gamma}{\beta - ka^\gamma}} \mathrm{d}a = \int a^{\gamma/2} (\beta - ka^\gamma)^{-1/2} \mathrm{d}a \,, \tag{2.109}$$

which integrates to

$$t - t_0 = \frac{2a^{\frac{\gamma}{2}+1}}{\sqrt{\beta}(\gamma+2)} \, {}_2F_1\left(\frac{1}{2}, \frac{1}{2} + \frac{1}{\gamma}; \frac{3}{2} + \frac{1}{\gamma}; \frac{a^\gamma k}{\beta}\right), \tag{2.110}$$

for $k = \pm 1$, where ${}_2F_1$ denotes the ordinary hypergeometric function introduced in Section 1.5.3. It is helpful to note that this solution can, in principle, be given in an explicit form by using the inverse hypergeometric function, but that would add no further insight. By Theorem 1.10, the integral in Eq. (2.109) is elementary if and only if at least one of the following is an integer:

$$\frac{\gamma/2+1}{\gamma} \,, \quad -\frac{1}{2} \,, \quad \frac{\gamma/2+1}{\gamma} - \frac{1}{2} \,, \tag{2.111}$$

that is,

$$\frac{1}{2} + \frac{1}{\gamma} \quad \text{or} \quad \frac{1}{\gamma} \,. \tag{2.112}$$

Explicitly, this means that γ satisfies one of the following conditions

$$\gamma = \frac{2}{2m-1} \,, \quad \text{for } m \in \mathbb{Z} \,, \tag{2.113}$$

$$\text{or} \quad \gamma = \frac{1}{n} \,, \quad \text{for } n \in \mathbb{Z} \setminus \{0\} \,. \tag{2.114}$$

This is achievable for $\gamma = 1$ or $\gamma = 2$, which correspond to dust ($w = 0$) and radiation ($w = 1/3$), respectively. As an example, we can see that Eq. (2.110) reduces to the well-known expressions for in the matter-dominated ($\gamma = 1$) and radiation-dominated ($\gamma = 2$) cases, which are given by

- for $k = 1$, matter-dominated:

$$t - t_0 = 2\beta \operatorname{arctan}\left(\frac{\sqrt{a}}{\sqrt{\beta - a} - \sqrt{\beta}}\right) - \sqrt{a}\sqrt{\beta - a} \,, \tag{2.115}$$

  and radiation-dominated:

$$t - t_0 = -\sqrt{\beta - a^2} \Leftrightarrow a = \sqrt{\beta - (t - t_0)^2} \,, \tag{2.116}$$

- for $k = -1$, for matter-dominated:

$$t - t_0 = \sqrt{a}\sqrt{a + \beta} - 2\beta \operatorname{artanh}\left(\frac{\sqrt{a}}{\sqrt{a + \beta} - \sqrt{\beta}}\right), \tag{2.117}$$

and for radiation-dominated:

$$t - t_0 = \sqrt{a^2 + \beta} \Leftrightarrow a = \sqrt{(t - t_0)^2 - \beta}\,. \tag{2.118}$$

More details regarding cosmological solutions and applications of Theorem 1.10 can be found in [50].

2.9.5 *Non-vanishing cosmological constant and non-zero curvature*

We finally turn our attention to integrals of the most general form

$$t - t_0 = \int \sqrt{\frac{a^\gamma}{\beta + \lambda a^{2+\gamma} - k a^\gamma}}\,\mathrm{d}a\,. \tag{2.119}$$

This type of integral does not admit a closed-form solution for an arbitrary (physical) value of γ (or w). However, we can restrict our focus to dust and radiation cases.

Matter-dominated solutions. We take $\gamma = 1$, which corresponds to $w = 0$. So, we are concerned with

$$t - t_0 = \int \sqrt{\frac{a}{\beta + \lambda a^3 - k a}}\mathrm{d}a\,. \tag{2.120}$$

If we denote the three roots of the polynomial $\lambda a^3 - ka + \beta$ by r_1, r_2, and r_3, this integrates to

$$t - t_0 = \frac{2r_1}{\sqrt{r_2}\sqrt{r_3 - r_1}} \left(\Pi\left(\frac{r_3}{r_3 - r_1}; \arcsin\left(\frac{\sqrt{a}\sqrt{r_3 - r_1}}{\sqrt{a - r_1}\sqrt{r_3}} \right), \frac{(r_1 - r_2)\, r_3}{r_2\,(r_1 - r_3)} \right) \right.$$
$$\left. - F\left(\arcsin\left(\frac{\sqrt{a}\sqrt{r_3 - r_1}}{\sqrt{a - r_1}\sqrt{r_3}} \right), \frac{(r_1 - r_2)\, r_3}{r_2\,(r_1 - r_3)} \right) \right), \tag{2.121}$$

that is a combination of elliptic integrals of the first and third kind, given in Definition 1.15.

Radiation-dominated solutions. We take $\gamma = 2$, corresponding to $w = 1/3$. We are left with

$$t - t_0 = \int \frac{a}{\sqrt{\beta + \lambda a^4 - k a^2}}\mathrm{d}a\,. \tag{2.122}$$

This integrates to

$$t - t_0 = -\frac{1}{2\sqrt{\lambda}} \log\left| -2a^2\lambda + 2\sqrt{\lambda}\sqrt{a^4\lambda - a^2 k + \beta} + k \right|, \tag{2.123}$$

for $k = \pm 1$.

We remark that so far we have provided analytic solutions to the case of a single barotropic fluid in the presence of a cosmological constant and curvature. In theory, one could look at the cases of two barotropic fluids, matter and radiation, say. This work was carried out in [10] and further results for multi-fluid cosmologies are discussed in [76], where Theorem 1.10 is used to classify which cases yield analytic solutions in terms of elementary functions.

2.10 Inflation and scalar fields in cosmology

In 1998, large collaborations led by Perlmutter, Riess, and Schmidt discovered, through the observation of distant Type Ia supernovae which were moving away from us, that the universe is not only expanding, but also accelerating [137, 138]; this discovery earned them the Nobel Prize in physics in 2011. A cosmological epoch of accelerated expansion is referred to as *inflation*[2]. This can be formulated through the following condition on the scale factor: $\ddot{a} > 0$. This can be written in terms of the Hubble parameter as

$$\frac{\mathrm{d}}{\mathrm{d}t}\left(aH\right)^{-1} < 0\,. \tag{2.124}$$

If we introduce the so-called *slow-roll parameter*

$$\varepsilon \coloneqq -\frac{\dot{H}}{H^2} = -\frac{\mathrm{d}\ln H}{\mathrm{d}N}\,, \tag{2.125}$$

and $\mathrm{d}N = \mathrm{d}\log(a) = H\mathrm{d}t$, as defined in Section 2.9.1, we can re-write Eq. (2.124) as

$$\frac{\mathrm{d}}{\mathrm{d}t}\left(aH\right)^{-1} = -\frac{1}{a}(1-\varepsilon) < 0 \implies \varepsilon < 1. \tag{2.126}$$

Note that as $\varepsilon \to 0$, H is constant and the spacetime is *de Sitter space*. Comparing Eq. (2.125) with Eq. (2.86), we see that $\varepsilon = 1 + q$, where q is the deceleration parameter. The terminology "slow roll" comes from the fact that the equations of motion reduce to those of a harmonic oscillator with damping, which are analogous to those of a ball rolling slowly in a shallow potential well [95].

By considering Eq. (2.62), with $\Lambda = 0$, we note that another way of stating inflation is to say that $\rho + 3p < 0$, which, with the assumption of a linear equation of state, corresponds to $w < -1/3$.

One way to model inflation in cosmology is by introducing a scalar field into the Lagrangian formulation of GR, which will be briefly discussed below. Scalar fields are a popular toy model in physics and turn out to be a very helpful tool in general relativity and cosmology because, despite being reasonably easy to handle, they yield non-trivial results. Any model of this type is referred to as *quintessence* [157], named after the fifth element in ancient and medieval philosophy, which was believed to be the fundamental substance of the universe and the source of all life and motion. When the field rolls very slowly compared to the expansion of the universe, inflation occurs: the kinetic energy is smaller than the potential energy.

As we will see, we can introduce a scalar field ϕ, called the *inflaton*, which behaves like a dynamical cosmological constant. The associated energy density component to this scalar field is what is sometimes called *dark energy*. In short, not only are scalar fields employed to charac-

[2]Here, when we refer to inflation, we mean the term broadly to include late-time cosmic acceleration, and not just early-time accelerated expansion.

terise inflation [30], but also dark matter (a hypothetical form of matter thought to account for approximately 85% of the matter content in the universe) [125, 158], and unified descriptions of dark matter and dark energy [26]. By modelling the behaviour of scalar fields, one can further understand the underlying mechanisms driving the expansion and the evolution of the universe.

In general, physical theories can be formulated using a variational approach. In GR, the concepts of kinetic and potential energies are not defined and, hence, it is not immediately clear what the action leading to the equations of motion should look like. In 1915, Hilbert [100] and Einstein determined independently that the Lagrangian for such an action should be

$$\mathcal{L}_{\mathrm{EH}} = R\sqrt{-g}, \tag{2.127}$$

where $g = \det(g_{\mu\nu})$; the corresponding action is called the *Einstein–Hilbert action* and is given by

$$S_{\mathrm{EH}} = \frac{1}{2\kappa}\int R\sqrt{-g}\,\mathrm{d}^4x = \frac{1}{2\kappa}\int g^{\mu\nu}R_{\mu\nu}\sqrt{-g}\,\mathrm{d}^4x\,. \tag{2.128}$$

The factor $\sqrt{-g}\,\mathrm{d}^4x$ is the invariant volume element of curved space-time. The minus sign under the square root is present because we are working in a Lorentzian space-time. The factor $\kappa = 8\pi G/c^4$ allows the action to have the dimensions of energy multiplied by time (in geometrised units, $G = c = 1$). The Ricci scalar, $R = g^{\mu\nu}R_{\mu\nu}$, is the simplest non-trivial quantity that can be constructed from the metric and its derivatives. In the presence of matter modelled as a relativistic perfect fluid, the Einstein field equations arising from the variation of the action S_{EH} with respect to the (inverse) metric, $g^{\mu\nu} \mapsto g^{\mu\nu} + \delta g^{\mu\nu}$, are

$$G_{\mu\nu} \coloneqq R_{\mu\nu} - \tfrac{1}{2}Rg_{\mu\nu} = \kappa T_{\mu\nu}\,, \tag{2.129}$$

where $T_{\mu\nu}$ is the energy momentum tensor.

For a scalar field, the Lagrangian (density) is given by

$$\mathcal{L}_\phi \coloneqq -\sqrt{-g}\left(\tfrac{1}{2}\partial_\mu\phi\partial^\mu\phi + V(\phi)\right), \tag{2.130}$$

where V is a general potential for the scalar field ϕ, see for example [30]. To determine the equation of motion for the scalar field, we consider the variation of the action

$$S_\phi = \int \mathcal{L}_\phi\,\mathrm{d}^4x \tag{2.131}$$

with respect to the scalar field, that is, $\phi \mapsto \phi + \delta\phi$. This yields the Klein–Gordon equation

$$\Box\phi - V'(\phi) = 0, \tag{2.132}$$

where $\Box \coloneqq \partial^\mu\partial_\mu$. The Klein–Gordon equation is a relativistic wave equation, related to the Schrödinger equation.

Under a variation of the action, Eq. (2.131), with respect to the (inverse) metric, that is, $g^{\mu\nu} \mapsto g^{\mu\nu} + \delta g^{\mu\nu}$, we obtain the energy momentum tensor for the scalar field

$$T^{(\phi)}_{\mu\nu} \coloneqq \partial_\mu\phi\partial_\nu\phi - g_{\mu\nu}\left(\tfrac{1}{2}\partial_\alpha\phi\partial^\alpha\phi + V(\phi)\right). \tag{2.133}$$

The cosmological Einstein field equations for a spatially flat, $k = 0$, FLRW metric read

$$3H^2 = \kappa^2\left(\rho + \tfrac{1}{2}\dot{\phi}^2 + V\right), \tag{2.134}$$

$$3H^2 + 2\dot{H} = -\kappa^2\left(p + \tfrac{1}{2}\dot{\phi}^2 - V\right), \tag{2.135}$$

and the Klein–Gordon equation becomes

$$\ddot{\phi} + 3H\dot{\phi} + \frac{\mathrm{d}V}{\mathrm{d}\phi} = 0\,. \tag{2.136}$$

As we mentioned in Eq. (2.63), the energy-momentum conservation $\dot{\rho} + 3H(\rho + p) = 0$ holds. Let us define the energy density and the pressure of a homogeneous scalar field respectively as

$$\rho_\phi = \tfrac{1}{2}\dot{\phi}^2 + V(\phi)\,, \tag{2.137}$$

$$p_\phi = \tfrac{1}{2}\dot{\phi}^2 - V(\phi)\,. \tag{2.138}$$

By imposing $p_\phi = w_\phi\rho_\phi$, we can define an effective equation of state for the scalar field, with a time-dependent w_ϕ, given by

$$w_\phi = \frac{p_\phi}{\rho_\phi} = \frac{\frac{1}{2}\dot{\phi}^2 - V(\phi)}{\frac{1}{2}\dot{\phi}^2 + V(\phi)}\,. \tag{2.139}$$

When $\dot{\phi}^2 \ll V$, which is true for slow-roll inflation, we recover $w_\phi \approx -1$, which coincides with a cosmological constant equation of state, responsible for the universe's acceleration. By using the approach outlined in Section 2.9.1, that is, by dividing Eq. (2.134) by $3H^2$, and upon defining the dimensionless variables

$$x^2 = \frac{\kappa^2\dot{\phi}^2}{6H^2}\,, \quad y^2 = \frac{\kappa^2 V}{3H^2}\,, \quad \Omega^2 = \frac{\kappa^2\rho}{3H^2}\,, \tag{2.140}$$

and setting $V = V_0\exp(-\lambda\kappa\phi)$, Copeland et al. [54] obtained

$$1 = x^2 + y^2 + \Omega^2 \implies 1 \geq 1 - x^2 - y^2 = \Omega^2 \geq 0\,, \tag{2.141}$$

which yields the constraint for the physical space given by the unit circle

$$0 \leq x^2 + y^2 \leq 1\,. \tag{2.142}$$

Moreover, since $V \geq 0$, we can restrict our analysis to $y \geq 0$. The lower half disc would correspond to a contracting universe because $H < 0$ in this region. By differentiating x and y, defined in Eq. (2.140) with respect to time, and substituting for $\ddot{\phi}$ from Eq. (2.136) and for $\dot{H}$ from

Eq. (2.135), they obtained the equations

$$x' = \sqrt{\frac{3}{2}}\lambda y^2 - \frac{3}{2}x\left((w-1)x^2 + (w+1)y^2 - w + 1\right), \tag{2.143}$$

$$y' = -\frac{3}{2}y\left((w-1)x^2 + (w+1)\left(y^2-1\right)\right) - \sqrt{\frac{3}{2}}\lambda xy, \tag{2.144}$$

where the prime denotes differentiation with respect to $\log(a)$, which is equivalent to dividing the equations for $\dot{x}$ and $\dot{y}$ through by H. The equations are invariant under the transformation $y \to -y$ and symmetric under time reversal $t \to -t$. Depending on the values of w and λ, there are up to five fixed points (critical points), as shown in Table 2.3.

Table 2.3: Stability of the critical points for system in Eqs. (2.143) and (2.144).
Here $\delta = \sqrt{(w-1)\left[(9w+7)\lambda^2 - 24(w+1)^2\right]}$.

Point	Coordinates	Existence	Eigenvalues	Classification
Point O	$(0,0)$	$\forall\lambda, w$	$\frac{3}{2}(w \pm 1)$	saddle
Point A_+	$(1,0)$	$\forall\lambda, w$	$3-3w\,,\quad 3-\sqrt{\frac{3}{2}}\lambda$	unstable if $\lambda \le \sqrt{6}$ saddle if $\lambda > \sqrt{6}$
Point A_-	$(-1,0)$	$\forall\lambda, w$	$3-3w\,,\quad 3+\sqrt{\frac{3}{2}}\lambda$	unstable if $\lambda \ge -\sqrt{6}$ saddle if $\lambda < -\sqrt{6}$
Point B	$\left(\sqrt{\frac{3}{2}}\frac{1+w}{\lambda}, \sqrt{\frac{3(1-w^2)}{2\lambda^2}}\right)$	$\lambda^2 \ge 3(1+w)$	$\frac{3}{4\lambda}\left[\lambda(w-1) \pm \delta\right]$	stable node if $3(1+w) < \lambda^2 < \frac{24(w+1)^2}{9w+7}$ stable spiral if $\lambda^2 \ge \frac{24(w+1)^2}{9w+7}$
Point C	$\left(\frac{\lambda}{\sqrt{6}}, \sqrt{1-\frac{\lambda^2}{6}}\right)$	$\lambda^2 < 6$	$\frac{\lambda^2}{2}-3\,,\quad \lambda^2 - 3(w+1)$	stable if $\lambda^2 < 3(1+w)$ saddle if $3(1+w) \ge \lambda^2 < 6$

From Eq. (2.135), we obtain the deceleration parameter

$$1 + q = -\frac{\dot{H}}{H^2} = -\frac{3}{2}\left[(w-1)x^2 + (w+1)(y^2-1)\right], \tag{2.145}$$

and at any fixed point (x^*, y^*) of the phase space, it can be integrated to give

$$a \propto (t-t_0)^{2/\left(3\left((w+1)(1-x_*^2-y_*^2)+2x_*^2\right)\right)}, \tag{2.146}$$

for some constant t_0. At all critical points, the universe expands according to a power-law, consistently with Eq. (2.106). When the right-hand side of Eq. (2.145) is zero, this corresponds to a constant H, and the scale factor evolves exponentially (de Sitter expansion).

To visualise some features of this model, we provide two examples. In Fig. 2.4, the only attractor is Point C, which represents an inflationary solution. In Fig. 2.5, Point B is the attractor, and the universe expands as if it were completely matter dominated (*scaling solution*), while Point C is a saddle point. Late-time accelerated solutions can be used to model dark energy. In [54], it was shown that scaling solutions, that is, when the energy density of the scalar field ρ_ϕ remains proportional to that of the barotropic fluid, are the unique late-time attractors whenever they exist.

In general, inflation ($\varepsilon \ll 1$) occurs if the kinetic energy density only makes a small contribution to ρ_ϕ, $\dot{\phi}^2 \ll V$. This is the *slow-roll inflation*. More examples can be found in [18, 28]. This model will provide the basis against which we will compare our results in Chapter 4.

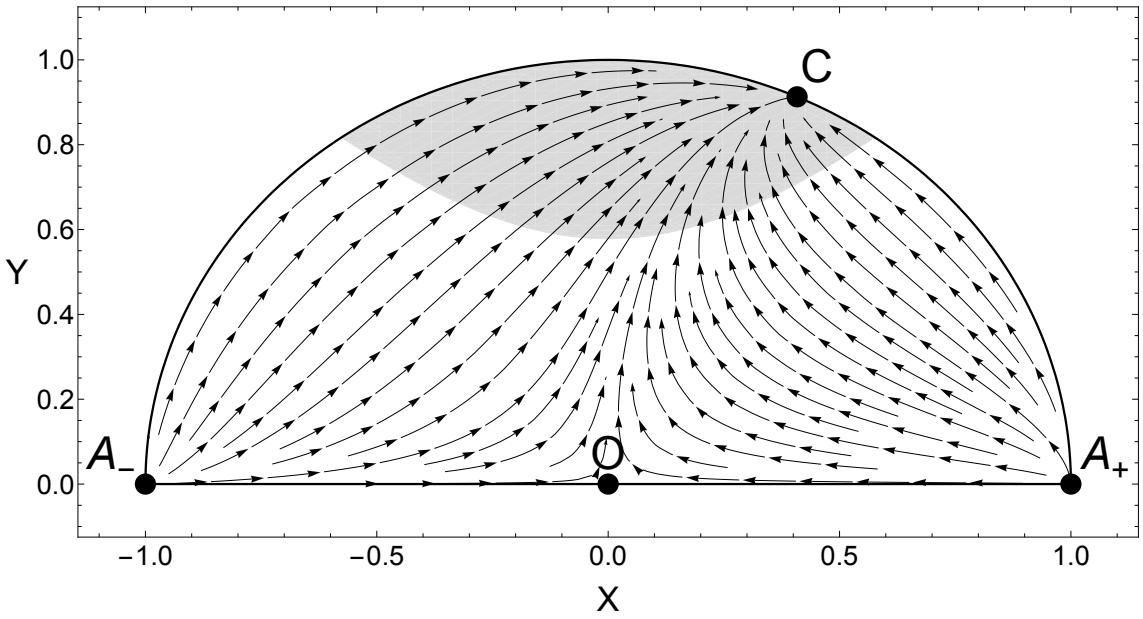

Fig. 2.4: Phase portrait of the dynamical system in Eqs. (2.143) and (2.144) for $w = 0$ and $\lambda = 1$. The shaded region represents accelerated expansion. Point C represents an inflationary solution.

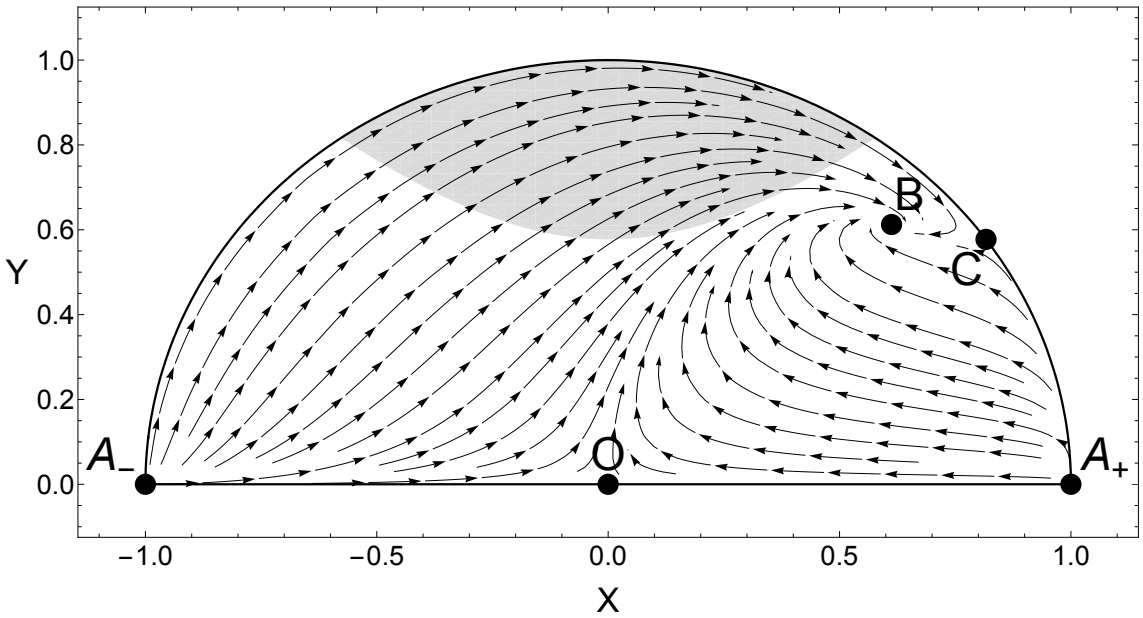

Fig. 2.5: Phase portrait of the dynamical system in Eqs. (2.143) and (2.144) for $w = 0$ and $\lambda = 2$. The shaded region represents accelerated expansion. Point B represents a scaling solution.

3

Azimuthal geodesics for closed FLRW cosmologies

3.1 Introduction

In GR, freely falling particles move along *geodesics*, which can be thought of as the "(locally) shortest distance between two points". The study of geodesics plays a fundamental role in cosmology since all electromagnetic signals (massless particles, or photons) propagate along null geodesics; these, therefore, are crucial for defining cosmological distances and deriving relationships such as the distance-redshift relations. On the other hand, massive particles move along timelike geodesics, and help us understand how gravity manifests as curved spacetime in the presence of cosmological objects like galaxies or galaxy clusters.

The main questions we try to address in this chapter can be summarised as follows:

- How do particles or rays of light move in the FLRW spacetime?
- How far can a photon travel in a closed universe from the big bang to the big crunch?

The work contained in this chapter expands on [33, 34].

3.2 Geodesics for FLRW

In Chapter 2, we obtained the metric of an expanding universe. We now want to determine how particles move in this spacetime. Most cosmological measurements involve detecting photons originating from various epochs and sources throughout the universe's evolution which eventually reach the Earth. As previously discussed, these photons can be treated as particles travelling along null geodesics. Therefore, we now apply the geodesic equation to describe a particle's motion through an expanding universe.

Definition 2.9 presented us with the geodesic equations. For the metric given in Eq. (2.58), we have the Lagrangian

$$\mathcal{L} = -t'^2 + a^2(t)\left[\frac{r'^2}{1-kr^2} + r^2\theta'^2 + r^2\sin^2\theta\varphi'^2\right], \tag{3.1}$$

with the prime denoting derivatives with respect to an affine parameter λ. The non-vanishing

Christoffel symbols $\Gamma^{\mu}_{\alpha\beta}$ associated to Eq. (2.58) are given in Appendix B. The four components of the geodesic equation Eq. (2.21) are

$$t'' + a\dot{a}\left(\frac{r'^2}{1-kr^2} + r^2\theta'^2 + r^2\sin^2\theta\varphi'^2\right) = 0\,, \tag{3.2}$$

$$r'' + 2\frac{\dot{a}}{a}t'r' + \frac{kr}{1-kr^2}r'^2 - r\left(1-kr^2\right)\left(\theta'^2 + \sin^2\theta\varphi'^2\right) = 0\,, \tag{3.3}$$

$$\theta'' + 2\frac{\dot{a}}{a}t'\theta' + \frac{2}{r}r'\theta' - \cos\theta\sin\theta\varphi'^2 = 0\,, \tag{3.4}$$

$$\varphi'' + 2\frac{\dot{a}}{a}t'\varphi' + \frac{2}{r}r'\varphi' + 2\frac{\cos\theta}{\sin\theta}\varphi'\theta' = 0\,. \tag{3.5}$$

From Section 2.6, we know that there exist six Killing vectors for the metric Eq. (2.58) that satisfy the Killing equations $\nabla_\mu\xi_\nu + \nabla_\nu\xi_\mu = 0$. Explicitly, these are given by

$$\xi_{(1)\mu} = a^2\left(0, \frac{1}{\sqrt{1-kr^2}}\sin\theta\cos\varphi, r\sqrt{1-kr^2}\cos\theta\cos\varphi, -r\sqrt{1-kr^2}\sin\theta\sin\varphi\right), \tag{3.6}$$

$$\xi_{(2)\mu} = a^2\left(0, \frac{1}{\sqrt{1-kr^2}}\sin\theta\sin\varphi, r\sqrt{1-kr^2}\cos\theta\sin\varphi, r\sqrt{1-kr^2}\sin\theta\cos\varphi\right), \tag{3.7}$$

$$\xi_{(3)\mu} = a^2\left(0, \frac{1}{\sqrt{1-kr^2}}\cos\theta, -r\sqrt{1-kr^2}\sin\theta, 0\right), \tag{3.8}$$

$$\xi_{(4)\mu} = a^2\left(0, 0, r^2\sin\varphi, r^2\cos\theta\sin\theta\cos\varphi\right), \tag{3.9}$$

$$\xi_{(5)\mu} = a^2\left(0, 0, -r^2\cos\varphi, r^2\cos\theta\sin\theta\sin\varphi\right), \tag{3.10}$$

$$\xi_{(6)\mu} = a^2\left(0, 0, 0, -r^2\sin^2\theta\right). \tag{3.11}$$

In Euclidean space, Eqs. (3.6)–(3.8) correspond to translations and Eqs. (3.9)–(3.11) to rotations, connected to the conservation of linear and angular momentum, respectively. Killing vectors imply the existence of conserved quantities along the geodesics, via Theorem 2.10, and here are given by

$$\frac{a^2}{\sqrt{1-kr^2}}\sin\theta\cos\varphi r' + a^2 r\sqrt{1-kr^2}\cos\theta\cos\varphi\theta' - a^2 r\sqrt{1-kr^2}\sin\theta\sin\varphi\varphi' =: p_x\,, \tag{3.12}$$

$$\frac{a^2}{\sqrt{1-kr^2}}\sin\theta\sin\varphi r' + a^2 r\sqrt{1-kr^2}\cos\theta\sin\varphi\theta' + a^2 r\sqrt{1-kr^2}\sin\theta\cos\varphi\varphi' =: p_y\,, \tag{3.13}$$

$$\frac{a^2}{\sqrt{1-kr^2}}\cos\theta r' - a^2 r\sqrt{1-kr^2}\sin\theta\theta' =: p_z\,, \tag{3.14}$$

$$a^2 r^2\sin\varphi\theta' + a^2 r^2\sin^2\theta\cot\theta\cos\varphi\varphi' =: L_x\,, \tag{3.15}$$

$$-a^2 r^2\cos\varphi\theta' + a^2 r^2\sin^2\theta\cot\theta\sin\varphi\varphi' =: L_y\,, \tag{3.16}$$

$$-a^2 r^2\sin^2\theta\varphi' =: L_z\,. \tag{3.17}$$

However, these are not all (functionally) independent, only p_z, L_z, p^2, and L^2 are independent, where

$$p^2 = p_x^2 + p_y^2 + p_z^2\,, \tag{3.18}$$

$$L^2 = L_x^2 + L_y^2 + L_z^2\,. \tag{3.19}$$

A direct calculation shows that L^2 and p^2 take the forms

$$L^2 = a^4 r^4 \left(\theta'\right)^2 + \csc^2\theta L_z^2 \,, \tag{3.20}$$

$$p^2 = \frac{a^4\left(r^2\left(1-kr^2\right)^2\left(\left(\theta'\right)^2 + \sin^2(\theta)\left(\varphi'\right)^2\right) + \left(r'\right)^2\right)}{1-kr^2} \,. \tag{3.21}$$

It is convenient to rewrite these equations as follows

$$(\theta')^2 = \frac{L^2}{a^4 r^4} - \frac{L_z^2}{a^4 r^4 \sin^2\theta} \,, \tag{3.22}$$

$$(r')^2 = \frac{1-kr^2}{a^4}\left(p^2 + kL^2 - \frac{L^2}{r^2}\right) , \tag{3.23}$$

which are two coupled first-order differential equations. Note that, from the θ-equation (3.22), we obtain a restriction for the θ-motion, that is,

$$\frac{L^2}{a^4 r^4} - \frac{L_z^2}{a^4 r^4 \sin^2\theta} \geq 0 \,. \tag{3.24}$$

Since $a^4 r^4 \geq 0$, then $L^2 - L_z^2/\sin^2\theta \geq 0$, which yields

$$\arcsin\left(\frac{L_z}{L}\right) \leq \theta \leq \pi - \arcsin\left(\frac{L_z}{L}\right) . \tag{3.25}$$

When $L_z = L$, the motion is confined to the equatorial plane, $\theta = \pi/2$.

Finally, the t-component of the geodesic equation becomes

$$t'' + (kL^2 + p^2)\frac{\dot{a}}{a^3} = 0 \implies (t')^2 - \frac{(kL^2+p^2)}{a^2} = \text{constant} \,. \tag{3.26}$$

Since the Lagrangian, $\mathcal{L}$, is a conserved quantity along a geodesic, and upon substitution of Eqs. (3.17), (3.22), and (3.23) in the Lagrangian given in Eq. (3.1), we find that such a constant is indeed $\mathcal{L}$. The value of $\mathcal{L}$ is zero for massless test particles, which move along null paths, and $\mathcal{L} = -1$ for massive test particles, which move along time-like paths. Therefore, we can write

$$(t')^2 - \frac{(kL^2+p^2)}{a^2} = \mathcal{L} \,. \tag{3.27}$$

The set of geodesic equations, therefore, simplifies to Eqs. (3.17), (3.22), (3.23) and (3.27), that is,

$$(t')^2 = \frac{(kL^2+p^2)}{a^2} + \mathcal{L} \,, \tag{3.28}$$

$$(r')^2 = \frac{1-kr^2}{a^4}\left(p^2 + kL^2 - \frac{L^2}{r^2}\right) , \tag{3.29}$$

$$(\theta')^2 = \frac{L^2}{a^4 r^4} - \frac{L_z^2}{a^4 r^4 \sin^2\theta} \,, \tag{3.30}$$

$$(\varphi')^2 = \frac{L_z^2}{a^4 r^4 \sin^4\theta} \,, \tag{3.31}$$

3.2.1 *Radial geodesics*

Radial geodesics are well studied and feature in most GR and cosmology textbooks; see, for example, [25, 48]. These describe the paths followed by particles (massless or massive) that move without any angular momentum (measured about the coordinate origin), since no motion is assumed in the angular directions. Let us first focus on radial null geodesics. For these, we can set $\theta = \varphi = \text{constant}$, which reduces Eq. (3.1) to

$$-(t')^2 + \left(\frac{a^2}{1-kr^2}\right) r'^2 = 0\,. \tag{3.32}$$

Consider the four-momentum of a photon

$$P^\mu \coloneqq \frac{\mathrm{d}x^\mu}{\mathrm{d}\lambda}\,, \tag{3.33}$$

which decomposes into the energy, $E = P^0 = \mathrm{d}t/\mathrm{d}\lambda$, and the three momenta P^i, for $i \in \{1,2,3\}$. From Eq. (3.32), it follows that

$$E^2 - \frac{a^2}{1-kr^2}(P^1)^2 = 0\,. \tag{3.34}$$

Moreover, observe that we can re-write Eq. (3.2) as

$$t'' + \left(\frac{a\dot{a}}{1-kr^2}\right) r'^2 = 0\,, \tag{3.35}$$

which can be written as

$$\frac{\mathrm{d}E}{\mathrm{d}\lambda} + \left(\frac{a\dot{a}}{1-kr^2}\right)(P^1)^2 = 0\,. \tag{3.36}$$

By substituting Eq. (3.34), we obtain

$$\frac{\mathrm{d}E}{\mathrm{d}\lambda} + \frac{\dot{a}}{a}E^2 = 0 \implies \frac{1}{E}\frac{\mathrm{d}E}{\mathrm{d}\lambda} + \frac{\dot{a}}{a}E = 0\,. \tag{3.37}$$

Noting that

$$\frac{1}{E} = \frac{\mathrm{d}\lambda}{\mathrm{d}t}\,, \tag{3.38}$$

Eq. (3.37) can be re-written as

$$\frac{\mathrm{d}E}{\mathrm{d}t} + \frac{\dot{a}}{a}E = 0\,, \tag{3.39}$$

which, after integrating, allows us to deduce

$$E \propto \frac{1}{a}\,. \tag{3.40}$$

This means that the energy, E, of a photon decays with the scale factor. From quantum mechanics, we know that the energy of a photon obeys the Planck–Einstein relation $E = hf$, where h is the

Planck constant and f is the emitted frequency. As the universe expands, the energy decreases and so does the frequency f. Light shifts towards redder colours and, therefore, objects seen at large distances will appear "redshifted". This is crucial for observations, as it allows one to infer the relative scale factor of the universe at the time of emission. In other words, the wavelength of light scales proportionally to the scale factor. The light emitted at time $t_{\rm e}$ with wavelength $\lambda_{\rm e}$ will be observed at a later time $t_{\rm obs}$ with a larger wavelength $\lambda_{\rm obs}$ given by

$$\lambda_{\rm obs} = \frac{a(t_{\rm obs})}{a(t_{\rm e})}\lambda_{\rm e}\,. \tag{3.41}$$

The fractional shift in wavelength

$$z \coloneqq \frac{\lambda_{\rm obs} - \lambda_{\rm e}}{\lambda_{\rm e}} = \frac{\lambda_{\rm obs}}{\lambda_{\rm e}} - 1 = \frac{a(t_{\rm obs})}{a(t_{\rm e})} - 1 \tag{3.42}$$

is called *redshift*.

Let us now turn our attention to the case of massive particles. Observe that, for a particle with four-momentum $P^\mu = (E, P^i)$, Eq. (2.21) can be rewritten as

$$\frac{{\rm d}P^\mu}{{\rm d}\lambda} + \Gamma^\mu_{\nu\rho}P^\nu P^\rho = 0\,, \tag{3.43}$$

where the $\mu = 0$ components reads

$$\frac{{\rm d}E}{{\rm d}\lambda} + \Gamma^0_{ij}P^i P^j = 0\,. \tag{3.44}$$

Using $P^0 = E$ and that, from Appendix B, $\Gamma^0_{rr} = (\dot{a}/a)g_{ij}$, one has

$$\frac{{\rm d}E}{{\rm d}\lambda} + \frac{\dot{a}}{a}g_{ij}P^iP^j = 0 \implies E\frac{{\rm d}E}{{\rm d}t} + \frac{\dot{a}}{a}p^2 = 0\,, \tag{3.45}$$

where we set $p^2 = g_{ij}P^iP^j$. Moreover, Eq. (3.1) yields

$$\mathcal{L} = g_{\mu\nu}P^\mu P^\nu = -E^2 + p^2 = -1 \implies -E^2 + p^2 = -1. \tag{3.46}$$

Differentiating Eq. (3.46) with respect to time, we have

$$E\frac{{\rm d}E}{{\rm d}t} = p\frac{{\rm d}p}{{\rm d}t}\,. \tag{3.47}$$

Combining Eqs. (3.45) and (3.47) leads to

$$\frac{{\rm d}p}{{\rm d}t} + \frac{\dot{a}}{a}p = 0\,, \tag{3.48}$$

which, upon integrating, allows us to deduce

$$p \propto \frac{1}{a}\,. \tag{3.49}$$

Therefore, as the universe expands, the physical three-momentum of a massive particle decays as

$1/a$. This is consistent with our previous result, in the case of light, where $p = E = hf$. Lastly, let us remark that for a non-relativistic particle, $p \approx mv$, as p decreases with the expansion of the universe, so will the velocity v, decaying as $1/a$.

3.2.2 *Angular motion: great circles*

So far, we have discussed the energy and momentum of particles moving along radial geodesics in FLRW. We now attempt to solve and provide an intepretation for Eqs.(3.28)–(3.31) to understand the shape of the orbits of particles.

Let us begin by considering Eqs. (3.30) and (3.31). By dividing the equations, we note that one can eliminate the radial coordinate and the time coordinate to arrive at

$$\frac{\mathrm{d}\theta}{\mathrm{d}\varphi} = \sin\theta\sqrt{\frac{L^2}{L_z^2}\sin^2\theta - 1}\,. \tag{3.50}$$

By separating the variables, we obtain

$$\varphi - \varphi_0 = \int \frac{\mathrm{d}\theta}{\sin\theta\sqrt{\frac{L^2}{L_z^2}\sin^2\theta - 1}} = \int \frac{\mathrm{d}\theta}{\sin^2\theta\sqrt{\frac{L^2}{L_z^2} - \csc^2(\theta)}} = \int \frac{\csc^2(\theta)\mathrm{d}\theta}{\sqrt{\frac{L^2}{L_z^2} - \csc^2(\theta)}}\,, \tag{3.51}$$

where φ_0 is a constant of integration, fixed by the initial conditions.
By noting that $\csc^2(\theta) = 1 + \cot^2(\theta)$, we can write

$$\varphi - \varphi_0 = \int \frac{\csc^2(\theta)\mathrm{d}\theta}{\sqrt{\frac{L^2}{L_z^2} - \left(1 + \cot^2(\theta)\right)}} = \int \frac{\csc^2(\theta)\mathrm{d}\theta}{\sqrt{\left(\frac{L^2}{L_z^2} - 1\right) - \cot^2(\theta)}}\,. \tag{3.52}$$

Let us now employ the substitution $u = \cot\theta$, so that $\mathrm{d}u = -\csc^2(\theta)\mathrm{d}\theta$, to obtain

$$\varphi - \varphi_0 = -\int \frac{\mathrm{d}u}{\sqrt{\left(\frac{L^2}{L_z^2} - 1\right) - u^2}} = -\arcsin\left(\frac{u}{\frac{L^2}{L_z^2} - 1}\right). \tag{3.53}$$

Taking sine of both sides and squaring yields

$$\cot^2\theta = \left(\frac{L^2}{L_z^2} - 1\right)\sin^2(\varphi - \varphi_0)\,. \tag{3.54}$$

Equation (3.54) describes arbitrary *great circles*. Recall that the geodesics on a two-sphere, $\mathbb{S}^2$, are indeed great circles. We also note that, for $L = L_z$, we find $\theta = \pi/2$. For all $L \neq L_z$, the geodesic motion lies in a tilted plane.

This result is true for any spherically symmetric, i.e. isotropic, metric in GR. As an example, consider the inhomogeneous and spherically symmetric Lemaître–Tolman–Bondi (LTB) line element is given by [40, 118, 156]

$$\mathrm{d}s^2 = -\mathrm{d}t^2 + A^2(t,r)\mathrm{d}r^2 + B^2(t,r)\left(\mathrm{d}\theta^2 + \sin^2\theta\mathrm{d}\varphi^2\right), \tag{3.55}$$

where $A(t,r)$ and $B(t,r)$ have both temporal and spatial dependence. Without prescribing A and

B, this metric possesses three contravariant Killing vector fields

$$\xi^{(1)}_\mu = (0, 0, \sin(\varphi), \cot(\theta)\cos(\varphi))\,, \tag{3.56}$$

$$\xi^{(2)}_\mu = (0, 0, -\cos(\varphi), \cot(\theta)\sin(\varphi))\,, \tag{3.57}$$

$$\xi^{(3)}_\mu = (0, 0, 0, -1)\,. \tag{3.58}$$

The corresponding conserved quantities along geodesics are

$$B(t,r)^2\left(\sin(\varphi)\theta' + \sin(\theta)\cos(\theta)\cos(\varphi)\varphi'\right) =: L_x\,, \tag{3.59}$$

$$B(t,r)^2\left(-\cos(\varphi)\theta' + \sin(\theta)\cos(\theta)\sin(\varphi)\varphi'\right) =: L_y\,, \tag{3.60}$$

$$-B(t,r)^2\sin^2(\theta)\varphi' =: L_z\,, \tag{3.61}$$

where L_x, L_y, and L_z are constants of motion, and, further, we note that

$$L^2 = L_x^2 + L_y^2 + L_z^2 = L_z^2\csc^2(\theta) + B(t,r)^4\left(\theta'\right)^2\,. \tag{3.62}$$

Let us now re-arrange Eq. (3.61) to obtain

$$\varphi' = -\frac{L_z}{B(t,r)^2\sin^2(\theta)}\,. \tag{3.63}$$

Similarly, Eq. (3.62) yields

$$(\theta')^2 = \frac{L^2}{B(t,r)^4} - \frac{L_z^2}{B(t,r)^4\sin^2(\theta)}\,. \tag{3.64}$$

Therefore,

$$\frac{\mathrm{d}\theta}{\mathrm{d}\varphi} = \sin(\theta)\sqrt{\frac{L^2}{L_z^2}\sin^2(\theta) - 1}\,, \tag{3.65}$$

which can be integrated to give

$$\cot^2(\theta) = \left(\frac{L^2}{L_z^2} - 1\right)\sin^2(\varphi - \varphi_0)\,, \tag{3.66}$$

for some constant φ_0, fixed by the initial conditions. These are, once again, great circles.

3.2.3 *Radial motion in polar angle form*

In Section 3.2.1, we discussed the known results related to radial geodesics. In the previous section, Section 3.2.2, we found that the (θ, φ)-motion happens in a tilted plane. In what follows, we further elaborate on the shape of the radial trajectories followed by the particles, *without* any assumptions on θ or φ. We also provide a coordinate representation of the orbits.

Let us begin by noting that, from Eq. (3.66), we know that any φ-dependence can be in fact related to a θ-dependence, except when $\theta = \pi/2$ (the case when the motion lies in the equatorial plane). Therefore, in principle, it suffices to look at the polar angle form of the radial equation of

motion, that is, to find an expression for $r(\theta)$.

Similarly to Section 3.2.2, we divide Eq. (3.23) by Eq. (3.22), which allows us to remove any dependence on the affine parameter and $a(t)$. By doing so, we find

$$\left(\frac{\mathrm{d}r}{\mathrm{d}\theta}\right)^2 = -\frac{r^2\left(kr^2-1\right)\left(L^2\left(kr^2-1\right)+p^2r^2\right)}{L^2-L_z^2\csc^2(\theta)}\,, \tag{3.67}$$

which can be re-written as

$$\left(\frac{\mathrm{d}r}{\mathrm{d}\theta}\right)^2 = -r^2\left[\left(k^2L^2+kp^2\right)r^4+\left(-2kL^2-p^2\right)r^2+L^2\right]\frac{1}{L^2}\left(1-\frac{1}{\left(L/L_z\right)^2\sin^2(\theta)}\right)^{-1}. \tag{3.68}$$

Now, Eq. (3.68) can be solved by separation of variables, which gives

$$\operatorname{artanh}\left(\sqrt{\frac{p^2}{L^2}\frac{r^2}{\left(kr^2-1\right)}+1}\right) = \arcsin\left(\frac{\cos\theta}{\sqrt{1-\left(L_z/L\right)^2}}\right)-\arcsin\left(\frac{\cos\theta_0}{\sqrt{1-\left(L_z/L\right)^2}}\right), \tag{3.69}$$

where θ_0 is fixed by the initial conditions and depends, in fact, on the orbit's radius.

If the orbit has a finite maximal radius (which is, for example, always true for $k=1$), it is convenient to choose $\theta_0=\pi-\arcsin(L/L_z)$ so that Eq. (3.69) reads

$$\operatorname{artanh}\left(\sqrt{\frac{p^2}{L^2}\frac{r^2}{\left(kr^2-1\right)}+1}\right) = \arcsin\left(\frac{\cos\theta}{\sqrt{1-\left(L_z/L\right)^2}}\right)+\frac{\pi}{2}\,. \tag{3.70}$$

If the orbit's radius extends to infinity (which is possible, for example, when $k=0$ or $k=-1$), we choose $\theta_0=\pi/2$ such that Eq. (3.69) becomes

$$\operatorname{artanh}\left(\sqrt{\frac{p^2}{L^2}\frac{r^2}{\left(kr^2-1\right)}+1}\right) = \arcsin\left(\frac{\cos\theta}{\sqrt{1-\left(L_z/L\right)^2}}\right). \tag{3.71}$$

By applying isometries and uniqueness of geodesics, we can bring our geodesics down to the equatorial plane. Therefore, without loss of generality, we can fix our initial conditions such that our geodesics are restricted to the plane $\theta=\pi/2$. However, we recall that the equations we have just computed do not hold, and we need to consider $r(\varphi)$. By dividing Eq. (3.29) by Eq. (3.31), and recalling that, when $\theta=\pi/2$, we have $L=L_z$ and $\sin(\theta)=1$, we obtain

$$\left(\frac{\mathrm{d}r}{\mathrm{d}\varphi}\right)^2 = \frac{r^2\left(1-kr^2\right)\left(kL^2r^2-L^2+p^2r^2\right)}{L^2}\,, \tag{3.72}$$

which integrates to

$$\varphi-\varphi_0 = \arctan\left(\sqrt{\frac{p^2}{L^2}\frac{r^2}{\left(1-kr^2\right)}-1}\right), \tag{3.73}$$

for some constant φ_0. Equation (3.73) can also be written as

$$\sqrt{\frac{p^2}{L^2}\frac{r^2}{\left(1-kr^2\right)}-1} = \tan(\varphi-\varphi_0)\,. \tag{3.74}$$

Let $\mathcal{M} \coloneqq p/L$ and note that we have the following conditions on r:

- if $k = -1$,

$$\mathcal{M} > 1 \quad \text{and} \quad r > \sqrt{\frac{1}{\mathcal{M}^2 - 1}}\,, \tag{3.75}$$

- if $k = 0$,

$$r > \frac{1}{\mathcal{M}}\,, \tag{3.76}$$

- if $k = 1$,

$$\sqrt{\frac{1}{\mathcal{M}^2 + 1}} < r < 1\,. \tag{3.77}$$

We now set $\varphi_0 = 0$, which yields

$$\tan^2(\varphi) = \frac{(\mathcal{M}^2 + k)r^2 - 1}{1 - kr^2}\,, \tag{3.78}$$

which can be re-arranged as

$$r^2 = \frac{\tan^2(\varphi) + 1}{\mathcal{M}^2 + k + k\tan^2(\varphi)} = \frac{\sec^2(\varphi)}{\mathcal{M}^2 + k\sec^2(\varphi)} = \frac{1}{k + \mathcal{M}^2\cos^2(\varphi)}\,. \tag{3.79}$$

Re-arranging gives

$$\left(k + \mathcal{M}^2\cos^2(\varphi)\right) r^2 = 1 \iff k(x^2 + y^2) + \mathcal{M}^2 x^2 = 1, \tag{3.80}$$

where we used that $r^2 = x^2 + y^2$ and $x^2 = r^2\cos^2(\varphi)$. We now consider the cases $k = -1$, $k = 0$, and $k = 1$.

- When $k = -1$, Eq. (3.80) reads

$$(\mathcal{M}^2 - 1)x^2 - y^2 = 1\,, \tag{3.81}$$

  which is the equation of a hyperbola.

- When $k = 0$, Eq. (3.80) reads

$$x = \pm\sqrt{\frac{1}{\mathcal{M}}}\,, \tag{3.82}$$

  which are two straight lines parallel to the y-axis.

- When $k = 1$, Eq. (3.80) reads

$$(\mathcal{M}^2 + 1)x^2 + y^2 = 1\,, \tag{3.83}$$

  which is the equation of an ellipse. Note that as $\mathcal{M} \to 0$, that is when $p \gg L$, the ellipse approaches a circle.

These are shown in Fig. 3.1.

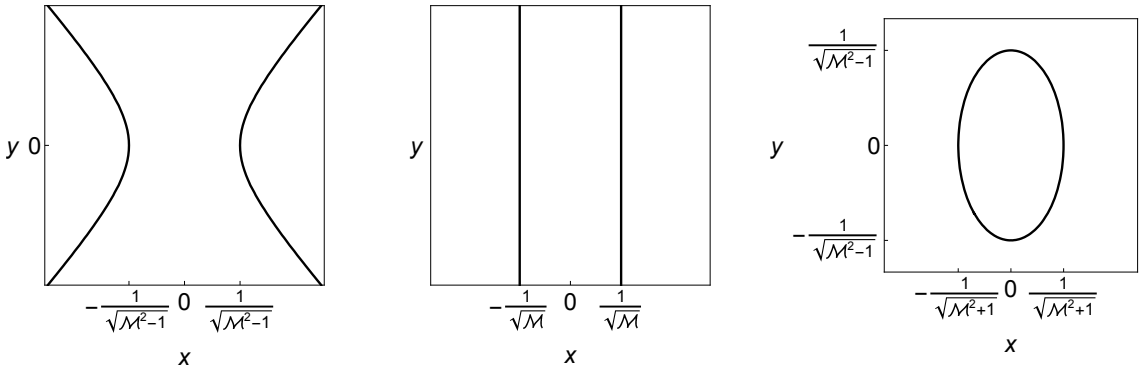

Fig. 3.1: Cartesian form of Eq. (3.73) for $k = -1$, $k = 0$, and $k = 1$, respectively. Here $x = r\cos\varphi$, $y = r\sin\varphi$, and $\mathcal{M} = p/L$.

3.3 Closed FLRW universes

Philosophically, the idea of a universe that cyclically begins and ends precedes modern physical cosmology. In ancient Greece, this was referred to as the *eternal return* (or eternal recurrence), and is associated to Stoic philosophers, approximately 300 BCE. The concept was also more recently revived by Nietzsche. In the realm of physical cosmology, the concept of oscillating universes has also been a subject of theoretical exploration. In [96], Harrison provided a classification for FLRW models, including oscillatory universes. These models of a universe undergoing cycles of expansion and contraction were also further explored in [21, 23, 24, 41]. In particular, in [22], the closed-universe recollapse conjecture—which states that, under certain conditions, the expanding universe could eventually reverse its course, contracting back to a highly dense state, and initiating a new cycle of expansion and contraction—was proposed as a potential solution to cosmological issues, such as the *singularity problem*. Cyclic models have also been considered as alternatives to cosmic inflation [121]. In this section, we restrict our attention to the closed universe solutions with a single barotropic fluid and a vanishing cosmological constant as these provide a good starting point for our discussion.

Let us examine the geometry of the hypersurfaces when $k = 1$. We observe that as $\rho \to 1$, Eq. (2.58) has a singularity. We now introduce a third angle χ such that

$$r = \sin(\chi)\,, \tag{3.84}$$

and Eq. (2.57) reads

$$\mathrm{d}\sigma^2 = \mathrm{d}\chi^2 + \sin^2(\chi)\left(\mathrm{d}\theta^2 + \sin^2(\theta)\mathrm{d}\varphi^2\right), \tag{3.85}$$

which is the line element of $\mathbb{S}^3$, the three-sphere. By suppressing one dimension, or considering a

hypersurface, we have a two-sphere, as shown in Fig. 3.2. This is similar to obtaining circles as a result of taking a section of a sphere.

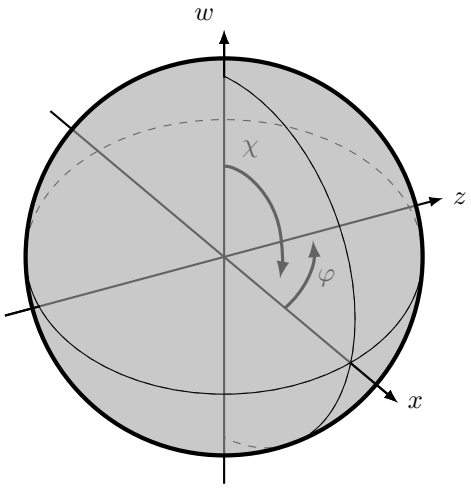

Fig. 3.2: Coordinates on the two-sphere obtained by fixing t and $\theta = \pi/2$.

As a result, the geometry of a closed universe, which is spatially a sphere, allows for a scenario in which the universe expands up to a maximum size, before recollapsing during the so-called *big crunch*. This oscillatory behaviour was first observed by Friedmann [82].

Let us recall the solution obtained in Eq. (2.110), which, for $k = 1$, is given by

$$t - t_0 = \frac{2a^{\frac{\gamma}{2}+1}}{\sqrt{\beta}(\gamma+2)}\, {}_2F_1\left(\frac{1}{2}, \frac{1}{2} + \frac{1}{\gamma}; \frac{3}{2} + \frac{1}{\gamma}; \frac{a^\gamma k}{\beta}\right). \tag{3.86}$$

First, we note that, by setting the left-hand side of Eq. (2.98) to zero, with $\lambda = 0$ and $k = 1$, we obtain the maximal value of $a(t)$, that is,

$$a_{\max} = \beta^{1/\gamma}. \tag{3.87}$$

From Eq. (3.86), we can therefore find the time $t_{\max}$ corresponding to $a_{\max}$, assuming that $t_0 = 0$, which is given by

$$t_{\max} = \frac{2\sqrt{\pi}\beta^{\frac{1}{\gamma}}\Gamma\left(\frac{3}{2} + \frac{1}{\gamma}\right)}{(\gamma+2)\Gamma\left(1 + \frac{1}{\gamma}\right)}, \tag{3.88}$$

where Γ is the Gamma function, given in Eq. (1.90). Here, we used the identity in Eq. (1.91).

We shall now study various special values of w. The time at which the big crunch occurs is denoted by t_{end}; in Section 3.4.1, we show that $t_{\text{end}} = 2t_{\max}$.

Case $w = 0$. For $w = 0$, which corresponds to a matter-dominated universe, Eq. (3.86) reduces to

$$t = \beta \arctan\left(\frac{\sqrt{a}}{\sqrt{\beta - a}}\right) - \sqrt{a}\sqrt{\beta - a}\,. \tag{3.89}$$

Whilst it is not possible to solve this equation explicitly for $a(t)$, we can derive a solution in parametrised form. Let us begin by defining

$$\sqrt{\frac{a}{\beta - a}} = \frac{1}{\sqrt{(\beta/a) - 1}} = \tan(u) \iff a = \beta \sin^2(u)\,. \tag{3.90}$$

Hence, Eq. (3.89) can be written as

$$t = \beta\,(u - \sin(u)\cos(u))\,. \tag{3.91}$$

Recalling that

$$\sin^2(u) = \frac{1}{2}(1 - 2\cos(2u))\,, \tag{3.92}$$

$$\sin(u)\cos(u) = \frac{1}{2}\sin(2u)\,, \tag{3.93}$$

and, upon setting $\widetilde{u} \coloneqq 2u$, Eq. (3.90) and Eq. (3.91) can be written as

$$a = \frac{\beta}{2}(1 - \cos(\widetilde{u}))\,, \tag{3.94}$$

$$t = \frac{\beta}{2}(\widetilde{u} - \sin(\widetilde{u}))\,, \tag{3.95}$$

respectively, which is the standard parametrisation of a cycloid, i.e. the curve traced by a point on the rim of a circle rolling along a straight line, first studied and named by Galileo in 1599. We can see that at $t = 0$, i.e. $u = 0$, we have $a(0) = 0$. The universe expands up to

$$a_{\max} = \beta\,, \tag{3.96}$$

at $t_{\max} = \pi\beta/2$, that is when $\widetilde{u} = \pi$, after which the universe contracts again until it reaches $a = 0$ at $t_{\text{end}} = \pi\beta$, when $\widetilde{u} = 2\pi$ which is the so-called big crunch.

Case $w = 1/3$. A closed universe filled with radiation corresponds to $w = 1/3$, and, in this case, Eq. (2.110) yields

$$t = \sqrt{\beta} - \sqrt{\beta - a^2}\,. \tag{3.97}$$

We can solve Eq. (3.97) explicitly for the scale factor $a(t)$,

$$a(t) = \sqrt{t\left(2\sqrt{\beta} - t\right)}\,. \tag{3.98}$$

The universe achieves a maximum size at

$$a_{\max} = \sqrt{\beta} \quad \text{at} \quad t_{\max} = \sqrt{\beta}\,. \tag{3.99}$$

Note that the universe reaches an end at $t_{\text{end}} = 2\sqrt{\beta}$.

A method for implicit solutions. We can obtain some other implicit solutions by considering the following integration method. Consider Eq. (2.98) with $\lambda = 0$ and $k = 1$, that is,

$$\dot{a}^2 = \beta a^{-\gamma} - 1 \implies \frac{\mathrm{d}a}{\mathrm{d}t} = \sqrt{\beta a^{-\gamma} - 1} \implies \int \sqrt{\frac{a^\gamma}{\beta - a^\gamma}}\mathrm{d}a = \int \mathrm{d}t = t - \tau\,, \tag{3.100}$$

for some constant τ. As we shall see, unlike in the previous cases, the constant of integration does not correspond to the start of the universe's expansion cycle. Let $a = \beta^{1/\gamma}\sin^{2/\gamma}(u)$, which implies

$$\frac{\mathrm{d}a}{\mathrm{d}u} = \frac{2\beta^{1/\gamma}}{\gamma}\cos(u)\sin^{(2/\gamma)-1}(u)\,, \tag{3.101}$$

whence Eq. (3.100) reads

$$t - \tau = \frac{2\beta^{1/\gamma}}{\gamma}\int \sqrt{\frac{\beta\sin^2(u)}{\beta - \beta\sin^2(u)}}\cos(u)\sin^{(2/\gamma)-1}(u)\mathrm{d}u = \frac{2\beta^{1/\gamma}}{\gamma}\int \sin^{2/\gamma}(u)\,\mathrm{d}u\,. \tag{3.102}$$

We obtained an integral of the form $\int \sin^n(x)\,\mathrm{d}x$, for $n \neq 0$, which has a recurrence relation

$$\int \sin^{2/\gamma}(u)\mathrm{d}u = -\frac{\gamma}{2}\sin^{(2/\gamma)-1}(u)\cos(u) + \left(1 - \frac{\gamma}{2}\right)\int \sin^{(2/\gamma)-2}(u)\mathrm{d}u\,. \tag{3.103}$$

Therefore, we have a parametrisation of the form

$$t - \tau = \frac{2\beta^{1/\gamma}}{\gamma}\left[-\frac{\gamma}{2}\sin^{(2/\gamma)-1}(u)\cos(u) + \left(1 - \frac{\gamma}{2}\right)\int \sin^{(2/\gamma)-2}(u)\mathrm{d}u\right], \tag{3.104}$$

$$a = \beta^{1/\gamma}\sin^{2/\gamma}(u)\,. \tag{3.105}$$

Case $w = -1/9$. This allows us, for example, to consider the case $\gamma = 2/3$, that is, $w = -1/9$. Physically, this may be associated to some exotic form of dark energy, with slightly negative pressure, which does not drive an accelerated expansion of the universe as this would require $w < -1/3$. In this instance, we have that

$$t - \tau = \beta^{3/2}\left[-\sin^2(u)\cos(u) - 2\cos(u)\right], \tag{3.106}$$

$$a = \beta^{3/2}\sin^3(u)\,. \tag{3.107}$$

Since $a = 0$ when $u = 0$, we can set $\tau = 2\beta^{3/2}$ so that $t(u = 0) = 0$. Once again, we can see that the maximal value $a_{\max}$ is achieved at $u = \pi/2$, and $a_{\max} = \beta^{3/2}$. This occurs at time $t_{\max} = 2\beta^{3/2}$, which is half of the time elapsed between the beginning and the big crunch.

Case $w = 1$. Lastly, consider the case $w = 1$, which corresponds to a universe filled with a stiff fluid. In this case, we are not able to obtain a simplification of Eq. (2.110); however, we can obtain a parametrised solution instead. If we consider $\gamma = 4$, then Eqs. (3.104) and (3.105) read

$$t - \tau = \frac{\beta^{1/4}}{2}\left[-2\sin^{-1/2}(u)\cos(u) - \int \sin^{-3/2}(u)\mathrm{d}u\right], \tag{3.108}$$

$$a = \beta^{1/4}\sin^{1/2}(u)\,. \tag{3.109}$$

However, this parametrisation is not in terms of elementary functions. To see this, let us recall the reduction formula for $\int \sin^n(x)\,\mathrm{d}x$ for $n \neq 0$, that is,

$$\int \sin^n(x)\,\mathrm{d}x = -\frac{1}{n}\sin^{n-1}(x)\cos(x) + \frac{n-1}{n}\int \sin^{n-2}(x)\mathrm{d}x\,. \tag{3.110}$$

By setting $n = 1/2$ and re-arranging, we have

$$\int \sin^{-3/2}(x)\mathrm{d}x = -2\sin^{-1/2}(x)\cos(x) - \int \sin^{1/2}(x)\mathrm{d}x\,. \tag{3.111}$$

Using the double angle formula for $\sin(x)$, we have

$$\int \sqrt{\sin(x)}\mathrm{d}x = \int \sqrt{1 - 2\sin^2\left(\frac{\pi}{4} - \frac{x}{2}\right)}\mathrm{d}x\,. \tag{3.112}$$

By making the substitution

$$v = \frac{\pi}{4} - \frac{x}{2} \implies \frac{\mathrm{d}v}{\mathrm{d}x} = -\frac{1}{2}\,, \tag{3.113}$$

we can re-write the integral in Eq. (3.112) as

$$\int \sqrt{\sin(x)}\mathrm{d}x = -2\int \sqrt{1 - 2\sin^2(v)}\mathrm{d}v\,, \tag{3.114}$$

which matches the elliptic integral of the second kind, introduced in Eq. (1.79), resulting in

$$\begin{aligned}\int \sqrt{\sin(x)}\mathrm{d}x &= -2E(v, 2) + C \\ &= -2E\left(\frac{\pi}{4} - \frac{x}{2}, 2\right) + C\,,\end{aligned} \tag{3.115}$$

where C is a constant of integration. Putting everything together, we have therefore shown that

$$t - \tau = -\beta^{1/4}E\left(\frac{\pi}{4} - \frac{u}{2}, 2\right), \tag{3.116}$$

$$a = \beta^{1/4}\sin^{1/2}(u)\,. \tag{3.117}$$

Once again, $a = 0$ at $u = 0$, thus, we can set $\tau = E(\pi/4, 2)$ so that $t(u = 0) = 0$. The maximum size $a_{\max} = \beta^{1/4}$ is attained at $t_{\max} = E(\pi/4, 2)$, which is halfway through the lifetime of the universe, which ends at $t_{\mathrm{end}} = 2E(\pi/4, 2)$.

The essential information about the evolution of these universes is encapsulated in the values of

$a_{\max}$ and $t_{\max}$, see Eqs. (3.87)–(3.88), which give the maximum size of the universe and the total lifetime of the universe, $2t_{\max}$. In turn, these depend on just two parameters: the initial density of the universe, $\beta = 8\pi\rho_0/3$, and the equation of state coefficient, $\gamma = 1 + 3w$.

In Fig. 3.3, we show how the position of the maximum, $(t_{\max}, a_{\max})$, varies according to β and w. In particular, the dotted lines show the curve traced out by the maximum as w varies and β is held constant; conversely, the solid lines represent points of constant w and varying β. We show only the values of w considered in this section along with the case $w = -1/3$, which corresponds to the lowest physically meaningful value possible, and some representative values for $\beta \in [0.2, 1.4]$.

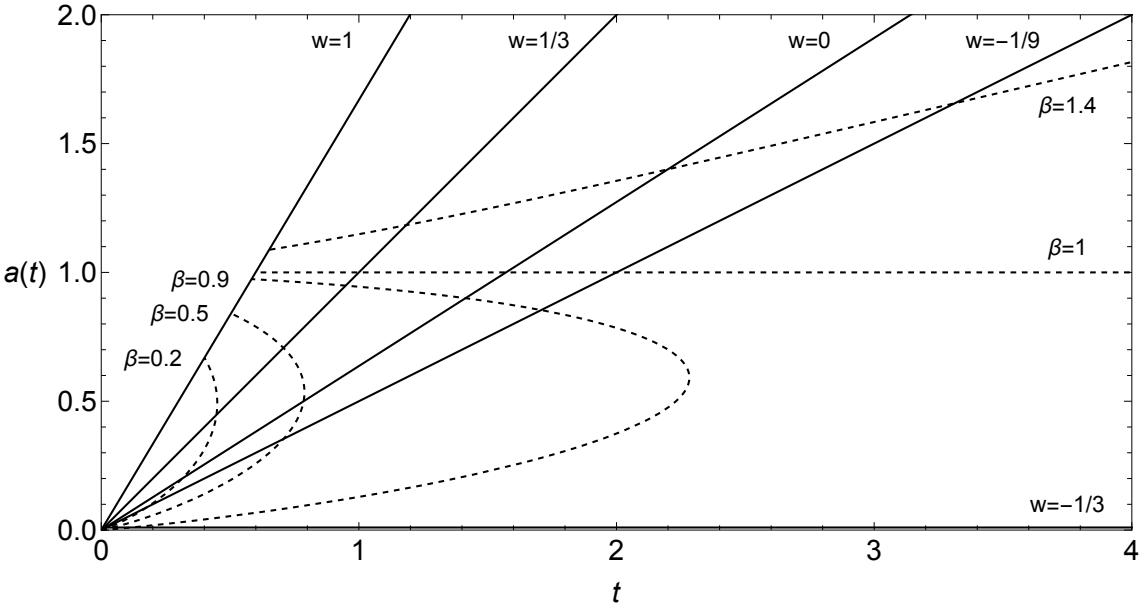

Fig. 3.3: The curves traced out by $(t_{\max}, a_{\max})$ for constant values of w (solid) and for constant values of β (dashed).

To further illustrate what the curves in Fig. 3.3 represent, consider universes with $w = 0$ (dust) and different initial densities. The evolutions of the scale factor for these universes are shown in Fig. 3.4a, and the maximum point for each evolution lies on the solid black line. Similarly, Fig. 3.4b and Fig. 3.4c show evolutions of the scale factor for fixed initial densities, $\beta = 0.5$ and $\beta = 1.4$ respectively, as the parameter w changes.

The curves traced out for fixed w, or, equivalently, fixed γ, are lines through the origin given by

$$a_{\max}(t_{\max}) = \frac{(\gamma+2)\Gamma\left(1+\frac{1}{\gamma}\right)}{2\sqrt{\pi}\Gamma\left(\frac{3}{2}+\frac{1}{\gamma}\right)} t_{\max}\,. \tag{3.118}$$

Instead, for fixed β, there is the critical value $\beta = 1$, where the universes' maximal size $a_{\max}$ is the same for all w, but their lifetime varies. For subcritical initial densities, $0 < \beta < 1$, there is a global bound on both the maximum size and the lifetime of the universe over all values of w, the

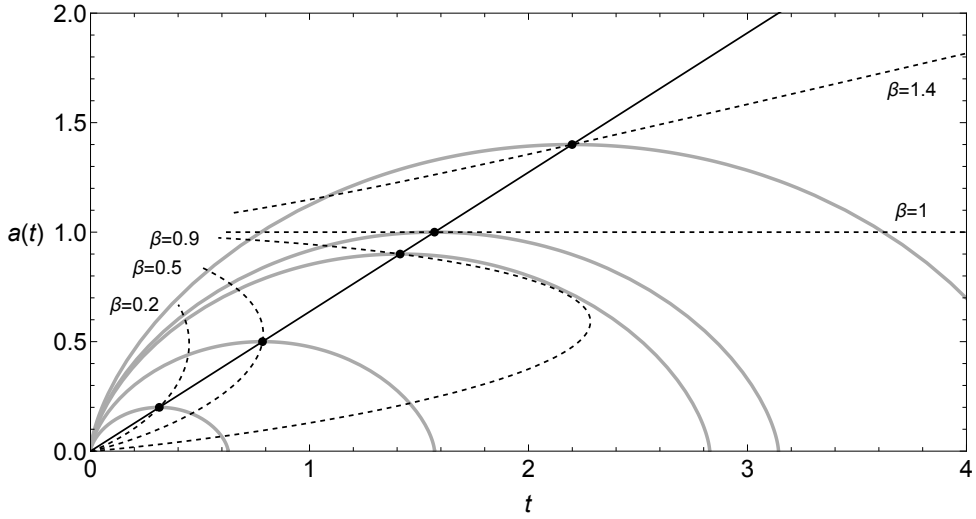

(a) $w = 0$ and $\beta \in \{0.2, 0.5, 0.9, 1, 1.4\}$.

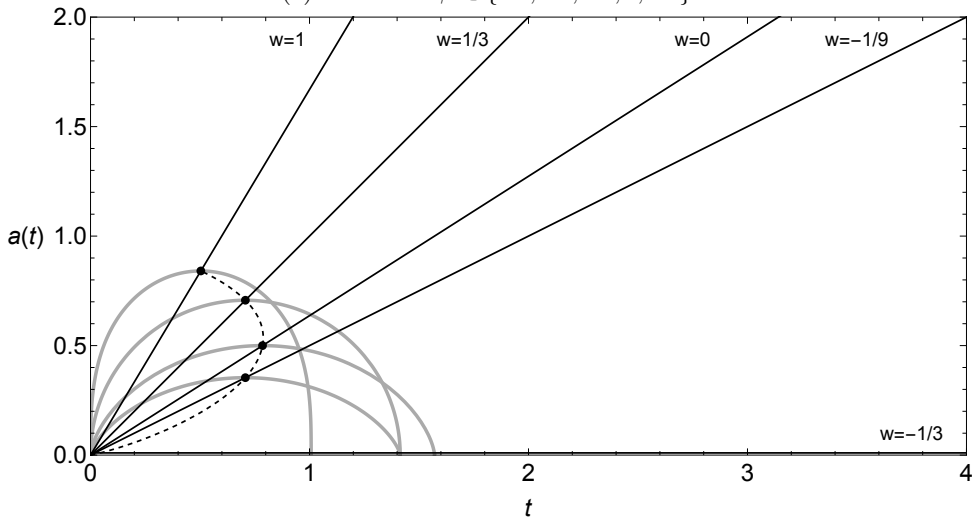

(b) $\beta = 0.5$ and $w \in \{-1/9, 0, 1/3, 1\}$.

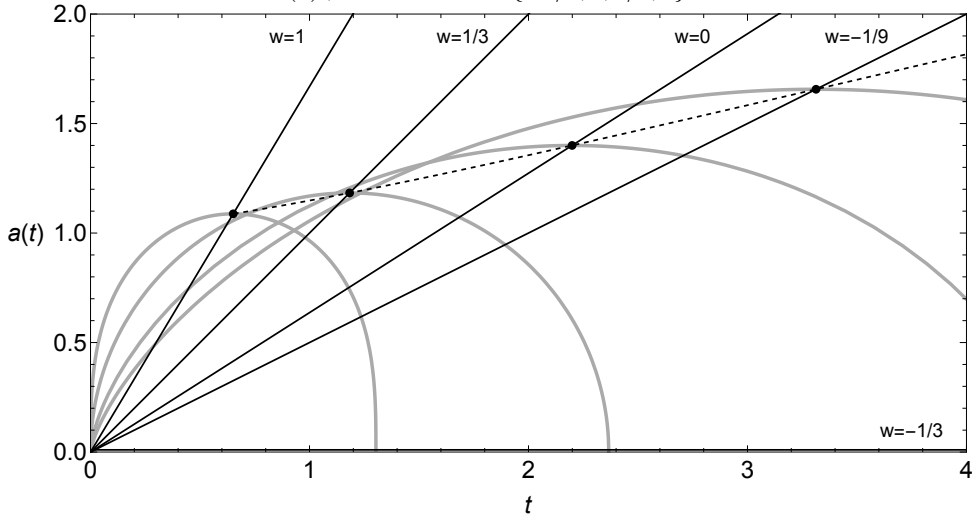

(c) $\beta = 1.4$ and $w \in \{-1/9, 0, 1/3, 1\}$.

Fig. 3.4: Evolution of $a(t)$ (in grey) for various parameter values. These are overlaid on the curves traced out by $(t_{\max}, a_{\max})$ for constant values of w (solid) and for constant values of β (dashed).

largest universe is not the longest lived and viceversa. In the supercritical case, $\beta > 1$, there is no bound on $a_{\max}$ and t_{end} as w varies. Inside the physical region of Fig. 3.3, which excludes the origin $(0, 0)$, the family of lines for constant w do not intersect each other and neither do the family of curves for constant β. This means that for any, physically possible, value for $(t_{\max}, a_{\max})$, there is a unique choice of parameters w and β giving rise to such a universe.

Although the dominant observational evidence has strongly supported the idea of a spatially flat universe rather than a closed one, recent observations have raised the possibility that the universe might actually have a closed geometry [6, 13, 63–65, 84, 92, 147, 161, 162]. In this spacetime, as we shall see, if a photon is emitted at the beginning of the universe, and we wait long enough, it will return to where it begins, circling the universe, motivating us to study azimuthal geodesics.

3.4 Azimuthal geodesics

In GR, azimuthal geodesics have been extensively studied in the context of rotating systems and settings involving spherical symmetry, for example the movement around massive objects such as black holes, e.g. [49], where special functions arise [52, 113].

Many textbooks, for example [25, 30, 119, 165], set the following problem as an exercise:

> **Problem 3.1:** Consider the spatially spherical universe, without cosmological constant. Consider a light signal travelling along the azimuth (so that $\mathrm{d}r/\mathrm{d}\lambda = \mathrm{d}\theta/\mathrm{d}\lambda = 0$).
>
> (i) Show that, in a dust filled universe, a light ray emitted at the big bang travels precisely once around the universe by the time of the big crunch.
>
> (i) Show that, in a radiation filled universe, a light ray emitted at the big bang travels precisely halfway around the universe by the time of the big crunch.

In other words, the problem asks us to compute the distance travelled along an azimuthal null geodesic during the evolution of a closed universe. However, this is restricted to two special cases: the matter-dominated universe (dust, pressureless matter) and the radiation-dominated universe, since in these cases one can find simple closed-form solutions to the field equations. It turns out that the angles computed in these two settings differ by a factor of two. Before proceeding, let us first review the conditions necessary for azimuthal geodesics.

Conditions for azimuthal geodesics. As we are primarily interested in the study of azimuthal geodesics in a closed universe ($k = 1$), let us investigate the full geodesic equations assuming $r = r_0 = \text{constant}$. This means

$$\frac{\mathrm{d}r}{\mathrm{d}\lambda} = \frac{\mathrm{d}^2 r}{\mathrm{d}\lambda^2} = 0\,. \tag{3.119}$$

Thus, Eq. (3.3) implies

$$-r_0\left(1-r_0^2\right)\left(\theta'^2+\sin^2(\theta)\varphi'^2\right)=0 \implies r_0\left(1-r_0^2\right)=0\,, \tag{3.120}$$

since having both θ and φ constant is of no interest to us. The solutions are $r_0=\pm 1$ and $r_0=0$. We take $r_0=1$, since it is the only physically meaningful solution. Let us remark that technically $r_0\to 1$, since, as $r\to 1$, Eq. (2.58) has a singularity. However, this is fine since, as we saw in Section 3.3, we can compactify the metric by introducing the third angle χ such that $r=\sin(\chi)$, and taking $r_0=1$ would correspond to setting $\chi=\pi/2$.

In Eqs. (3.12)–(3.14), this yields $p_x=p_y=p_z=0$, which in turn implies $p=0$. Consequently, Eq. (3.23) is also identically satisfied.

Next, we assume $\theta=\theta_0=$ constant. Substituting into Eq. (3.4), one immediately arrives at

$$\cos(\theta_0)\sin(\theta_0)\varphi'^2=0\,. \tag{3.121}$$

Since solutions with constant φ are not of interest to us, we are left with $\theta_0=\pi/2$. We neglect the solution $\theta_0=0$ as it corresponds to a pole. This yields $L_x=L_y=0$ by Eqs. (3.15)–(3.16). Putting everything together, Eq. (3.17) reads $L=L_z=-a^2\varphi'$, or equivalently, one can incorporate the minus sign into the constants L and L_z to have

$$L=L_z=a^2\varphi'\,, \tag{3.122}$$

since L and L_z are constants. This final relation is the starting point for the study of azimuthal geodesics. Without loss of generality, we can therefore set

$$r_0=1 \quad \text{and} \quad \theta_0=\frac{\pi}{2}\,. \tag{3.123}$$

Solution to Problem 3.1. Consider the line element give in Eq. (2.58) with $r=r_0$ and $\theta=\theta_0$, both constants. These can be set according to Eq. (3.123). Along an azimuthal geodesic, the line element becomes

$$\mathrm{d}s^2=0 \implies -\mathrm{d}t^2+a^2(t)\mathrm{d}\varphi^2=0\,, \tag{3.124}$$

which we can solve for $\mathrm{d}\varphi$ and integrate. We are told to assume that the massless test particle, e.g. a photon, is released at $t=0$, the big bang. We are interested in the total angular distance $\Delta\varphi$ travelled during the evolution of the universe up to the big crunch when $t=t_{\mathrm{end}}$, which is given by

$$\Delta\varphi=\int_{\varphi(0)}^{\varphi(t_{\mathrm{end}})}\mathrm{d}\varphi=\int_0^{t_{\mathrm{end}}}\frac{\mathrm{d}t}{a(t)}\,, \tag{3.125}$$

where $a(t)$ is the solution to Eq. (2.70) which satisfies $a(0) = 0$.

(i) In the case of a dust-filled universe, we can use Eqs. (3.94)–(3.95). In particular, we can express Eq. (3.125) as an integral in terms of the variable $\widetilde{u}$, that is,

$$\begin{aligned}\Delta\varphi &= \int_{u(t=0)=0}^{u(t_{\rm end})=2\pi} \frac{\beta/2(1-\cos(\widetilde{u}))}{\beta/2(1-\cos(\widetilde{u}))}\mathrm{d}\widetilde{u} \\ &= \int_0^{2\pi} \mathrm{d}\widetilde{u} = 2\pi\,. \end{aligned} \tag{3.126}$$

(ii) In the radiation dominated universe, we use Eq. (3.98) in Eq. (3.125) to obtain

$$\begin{aligned}\Delta\varphi &= \int_{t=0}^{t_{\rm end}=2\sqrt{\beta}} \frac{\mathrm{d}t}{\sqrt{t\left(2\sqrt{\beta}-t\right)}} = \int_{t=0}^{t_{\rm end}=2\sqrt{\beta}} \frac{\mathrm{d}t}{\beta-\left(t-\sqrt{\beta}\right)^2} \\ &= \left[\arcsin\left(\frac{t-\sqrt{\beta}}{\sqrt{\beta}}\right)\right]_{t=0}^{t=2\sqrt{\beta}} = \arcsin(1)-\arcsin(-1) = \pi\,. \end{aligned} \tag{3.127}$$

In what follows, we will show that this angular distance can be found for all cosmological models with linear equation of state $p = w\rho$ without solving explicitly for $a(t)$. Moreover, we will broaden the scope to encompass several other cases.

3.4.1 *Vanishing cosmological constant and single fluid*

We first consider an extension of Problem 3.1 to the case of a vanishing cosmological constant and a single barotropic fluid with equation of state $p = w\rho$. As we can observe from Fig. 3.4 and the results obtained in Section 3.3, the solutions exhibit symmetry around the time $t_{\rm max}$ corresponding to the maximal value $a_{\rm max}$. This can be shown more generally by considering the properties of the solutions to the Friedmann equations, Eqs. (2.98) and (2.99).

Recall that, in Eq. (3.87), we stated $a_{\rm max} = \beta^{1/\gamma}$, and said this corresponds to some time $t_{\rm max}$. The value of this time depends on the chosen initial conditions and we will not need that value for what follows. To see that $a_{\rm max}$ is indeed a local maximum, we consider Eq. (2.62) and evaluate $\ddot{a}$ at $t_{\rm max}$, which gives

$$\begin{aligned}\ddot{a}_{\rm max} &= -\frac{4\pi}{3}(1+3w)\rho_{\rm max}a_{\rm max} = -\frac{4\pi}{3}\rho_0(1+3w)(a_{\rm max})^{-3(1+w)}a_{\rm max} \\ &= -\frac{4\pi}{3}(1+3w)\rho_0(a_{\rm max})^{-2-3w} < 0 \end{aligned} \tag{3.128}$$

provided $(1+3w) > 0$ or $w > -1/3$, as stated above. Note that, in the second step, we used the conservation equation, Eq. (2.67). Having established the existence of a maximum value, we now show that the solution is symmetric relative to that maximum. To do so, we show that the part of the solution for t less than $t_{\rm max}$ satisfies the same differential equation as the part for t greater

than $t_{\max}$ with time reversed. Let us set

$$L(t) = a\left(t_{\max} - t\right) =: a\left(\tau_-\right), \quad 0 \le t \le t_{\max}\,; \tag{3.129}$$

$$R(t) = a\left(t_{\max} + t\right) =: a\left(\tau_+\right), \quad 0 \le t\,; \tag{3.130}$$

which satisfy $a_{\max} = a(t_{\max}) = L(0) = R(0)$, this means they coincide at $t = 0$. We can view $L(t)$ as the 'left' part of the solution and $R(t)$ as its 'right' part. Thus, we have $\dot{L} = -\dot{a}$, $\dot{R} = \dot{a}$, and $-\mathrm{d}t = \mathrm{d}\tau_-$, $\mathrm{d}t = \mathrm{d}\tau_+$. Now, we go back to Eq. (2.98) and note

$$\left(\frac{\mathrm{d}a}{\mathrm{d}t}\right)^2 = \beta a(t)^{-\gamma} - 1 \iff \left(\frac{\mathrm{d}a}{\mathrm{d}\tau_-}\right)^2 = \beta a(\tau_-)^{-\gamma} - 1 \tag{3.131}$$

$$\iff \left(-\frac{\mathrm{d}L}{\mathrm{d}t}\right)^2 = \beta L(t)^{-\gamma} - 1 \tag{3.132}$$

$$\iff \left(\frac{\mathrm{d}L}{\mathrm{d}t}\right)^2 = \beta L(t)^{-\gamma} - 1 \tag{3.133}$$

and similarly for R. Hence, both the 'left' part and the 'right' part satisfy the same differential equation and satisfy the same initial condition at $t = 0$: $L(0) = a_{\max} = R(0)$.

In general, the differential equation $(\dot{y})^2 = \beta y^{-\gamma} - 1$ does not have a unique solution, for a given initial condition; however, we can rewrite it as $\dot{y} = \pm\sqrt{\beta y^{-\gamma} - 1}$. Except for initial conditions of the form $y(t_0) = 0$, both of these equations satisfy the Picard–Lindelöf theorem, Theorem 1.1. In our case, the initial condition is $y(0) = a_{\max}$ and $a_{\max} \neq 0$, so we can conclude that there are exactly two solutions to the original differential equation.

In order to conclude that $L(t) \equiv R(t)$, we can use the fact that $a_{\max}$ is a local maximum, so in a neighbourhood of $t = 0$, $L(t)$ and $R(t)$ should both be decreasing functions (away from the maximum). Therefore, they both satisfy $\dot{y} = -\sqrt{\beta y^{-\gamma} - 1}$ with the same initial condition, and hence are equal by Theorem 1.1. This proves that the solutions are symmetric with respect to $t_{\max}$, and it also implies that $L(t_{\max}) = R(t_{\max}) = a(0)$. We now assume $a(0) = 0$, which means the complete solution $a(t)$ vanishes for different times, namely at $t = 0$ and at $t = 2t_{\max} =: t_{\mathrm{end}}$.

This means our cosmological model has the following generic behaviour: the scale factor $a(t)$ vanishes at $t = 0$, then sharply increases ($\dot{a} \to \infty$ as $t \to 0$) up to a maximum value $a_{\max}$. Respectively, these correspond to the big bang and the subsequent expansion of the universe. After reaching $a_{\max}$, the universe collapses with its evolution ending in the big crunch, where $a \to 0$ as $t \to t_{\mathrm{end}}$. Since this model has a finite lifetime, it is meaningful to consider the total distance travelled by a massless test particle (e.g. a photon) released at the beginning of the universe.

Therefore, it is convenient to use the symmetry of the solution about its maximum and write

$$\Delta\varphi = 2 \int_0^{t_{\max}} \frac{\mathrm{d}t}{a(t)}\,. \tag{3.134}$$

Going back to Eq. (2.98), for $0 \leq t \leq t_{\max}$, we have that

$$\frac{\mathrm{d}a}{\mathrm{d}t} = \sqrt{\beta a^{-\gamma} - 1} \quad \Longrightarrow \quad \mathrm{d}t = \frac{\mathrm{d}a}{\sqrt{\beta a^{-\gamma} - 1}} \,. \tag{3.135}$$

The negative root corresponds to the contraction phase $t_{\max} \leq t \leq t_{\mathrm{end}}$. Therefore we arrive at

$$\Delta\varphi = 2 \int_0^{t_{\max}} \frac{\mathrm{d}t}{a(t)} = 2 \int_0^{a_{\max}} \frac{\mathrm{d}a}{a\sqrt{\beta a^{-\gamma} - 1}} \,. \tag{3.136}$$

We shall employ the substitution $y = \sqrt{\beta a^{-\gamma} - 1}$ or $a^{-\gamma} = \frac{1}{\beta}\left(1 + y^2\right)$. Thus

$$\frac{\mathrm{d}y}{\mathrm{d}a} = -\frac{\beta\gamma a^{-\gamma-1}}{2\sqrt{\beta a^{-\gamma} - 1}} \quad \Longrightarrow \quad \mathrm{d}a = -\frac{2y}{\beta\gamma a^{-\gamma-1}}\mathrm{d}y \,. \tag{3.137}$$

This reduces the integral in Eq. (3.136) to a standard integration problem

$$\int \frac{\mathrm{d}a}{a\sqrt{\beta a^{-\gamma} - 1}} = -\frac{2}{\gamma}\int \frac{\mathrm{d}y}{1 + y^2} = -\frac{2}{\gamma}\arctan(y) + C = -\frac{2}{\gamma}\arctan\left(\sqrt{\beta a^{-\gamma} - 1}\right) + C \,, \tag{3.138}$$

with some constant of integration C. It is now straightforward to evaluate the angular distance

$$\Delta\varphi = 2 \int_0^{a_{\max}} \frac{\mathrm{d}a}{a\sqrt{\beta a^{-\gamma} - 1}} = -\frac{4}{\gamma}\left[\arctan\left(\sqrt{\beta a^{-\gamma} - 1}\right)\right]_0^{a_{\max}} \,. \tag{3.139}$$

As $a \to a_{\max} = \beta^{1/\gamma}$, due to Eq. (3.87), we find $\arctan\left(\sqrt{\beta a^{-\gamma} - 1}\right) \to 0$. On the other hand, the lower limit, $a \to 0$, gives $\arctan\left(\sqrt{\beta a^{-\gamma} - 1}\right) \to \pi/2$. Recalling $\gamma = 1 + 3w$, we obtain

$$\Delta\varphi = \frac{2\pi}{1 + 3w} \,, \tag{3.140}$$

valid for all $w > -1/3$, shown in Fig. 3.5. Interestingly, this angle can also be computed in the unphysical region where $w > 1$. For such cosmological fluids, the speed of sound exceeds the speed of light. Therefore, the region $w > 1$ must be considered unphysical. The other region, $w \leq -1/3$ where our formula does not apply, is due to the acceleration equation, Eq. (2.71). For such negative values, the universe's expansion dominates the gravitational attraction so that the universe never recollapses. Consequently, the effective angle tends to infinity as the universe expands.

3.4.2 *Two-fluid cosmologies*

In the instance of two fluid cosmologies (for a review, see e.g. [76]), the Friedmann equations for a closed universe ($k = 1$) read

$$\left(\frac{\dot{a}}{a}\right)^2 = \frac{8\pi}{3}\left(\rho_1 + \rho_2\right) - \frac{1}{a^2} \,, \tag{3.141}$$

$$\frac{\ddot{a}}{a} = -\frac{4\pi}{3}\left[\left(\rho_1 + 3p_1\right) + \left(\rho_2 + 3p_2\right)\right] \,, \tag{3.142}$$

where the dot denotes the derivative with respect to cosmic time t. The evolution of $a(t)$ is determined by the energy-momentum content and we assume the universe to be filled with two

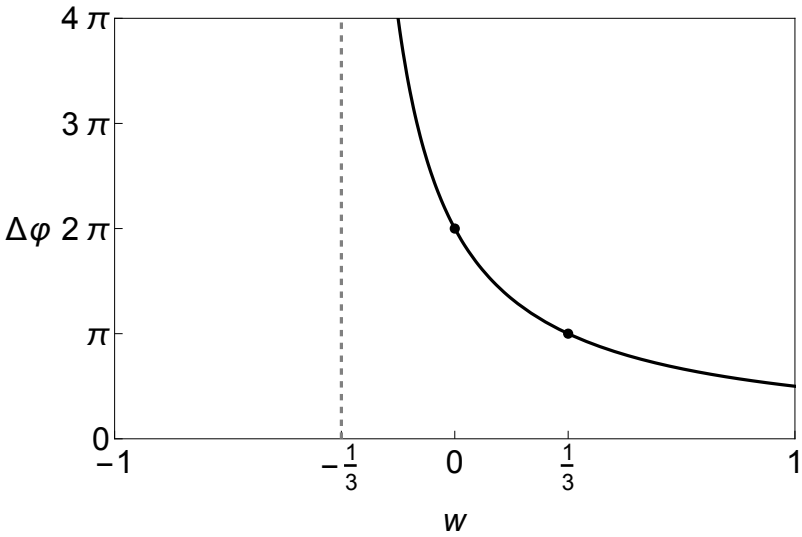

Fig. 3.5: Plot for $\Delta\varphi$ in terms of w, for $-1 \leq w \leq 1$. The dashed line shows the asymptotic behaviour at $w = -1/3$. The dots represent the previously known results for $w = 0$ and $w = 1/3$.

perfect barotropic fluids with equation of state $p_i(t) = w_i\rho_i(t)$, for $i \in \{1, 2\}$, where $\rho_i(t)$ is the energy density, $p_i(t)$ is the pressure, and w_i is the equation of state parameter. Equations (3.141) and (3.142) imply the energy-momentum conservation,

$$\dot{\rho}_i + 3\frac{\dot{a}}{a}(\rho_i + p_i) = 0\,, \quad \text{for } i \in \{1, 2\}\,, \tag{3.143}$$

which is satisfied by each fluid component, and yields

$$\rho_i = \rho_i^{(0)} a^{-3(1+w_i)}\,, \quad \text{for } i \in \{1, 2\}\,, \tag{3.144}$$

where $\rho_i^{(0)}$, for $i \in \{1, 2\}$, is a constant of integration.
We now define $\beta_i \coloneqq 8\pi\rho_i^{(0)}/3$, and $\gamma_i \coloneqq 1 + 3w_i$, for $i \in \{1, 2\}$, and re-write Eq. (3.141) as

$$(\dot{a})^2 = \beta_1 a^{-\gamma_1} + \beta_2 a^{-\gamma_2} - 1\,. \tag{3.145}$$

We can use Eq. (3.145) to derive the value of the angle travelled by a particle on an azimuthal geodesic during one cycle of expansion and re-collapse for a closed FLRW universe in terms of β_i, for $i \in \{1, 2\}$.

We now extend Problem 3.1 to the case of massive particles in a single barotropic fluid and two-fluid cosmologies. We are concerned with azimuthal geodesics, so, as stated in Eq. (3.123), we set $\theta = \pi/2$ and $r = 1$. This implies that the Lagrangian in Eq. (3.1) reads

$$\mathcal{L} = -t'^2 + a^2(t)\varphi'^2\,, \tag{3.146}$$

which, together with Eq. (3.122), $L_z = a^2\varphi'$, yields

$$\mathcal{L} = -t'^2 + \frac{L_z^2}{a^2}\,. \tag{3.147}$$

Noting that $\varphi' = \dot{\varphi} t'$, which can be written as

$$t' = \frac{\varphi'}{\dot{\varphi}} = \frac{L_z}{a^2} \frac{\mathrm{d}t}{\mathrm{d}\varphi} \,, \tag{3.148}$$

we find

$$\mathcal{L} = -\left(\frac{L_z}{a^2} \frac{\mathrm{d}t}{\mathrm{d}\varphi} \right)^2 + \frac{L_z^2}{a^2} \implies \frac{L_z}{a^2} \frac{\mathrm{d}t}{\mathrm{d}\varphi} = \sqrt{\frac{L_z^2}{a^2} - \mathcal{L}} = \frac{L_z}{a} \sqrt{1 - \frac{\mathcal{L}}{L_z^2} a^2} \,, \tag{3.149}$$

which gives

$$\frac{L_z}{a^2} = \frac{\mathrm{d}\varphi}{\mathrm{d}t} \left(\frac{L_z}{a} \sqrt{1 - \frac{\mathcal{L}}{{L_z}^2} a^2} \right) \implies \frac{\mathrm{d}\varphi}{\mathrm{d}t} = \frac{1}{a \sqrt{1 - (\mathcal{L}/L_z^2)\, a^2}} \,. \tag{3.150}$$

By separating the variables, we then obtain the expression for the angle travelled by a particle moving along an azimuthal geodesic during the expansion and subsequent re-collapse of the universe. Assuming $a(0) = 0$ and symmetry with respect to the value of the cosmic time $t = t_{\max}$ at which $a(t)$ attains its maximum value $a_{\max}$, which still holds in the general setting, we find

$$\Delta\varphi = 2 \int_0^{t_{\max}} \frac{\mathrm{d}t}{a \sqrt{1 - (\mathcal{L}/L_z^2)\, a^2}} \,. \tag{3.151}$$

By employing Eq. (3.145), this can be rewritten as

$$\Delta\varphi = 2 \int_0^{a_{\max}} \left[a^2 \left(1 - \frac{\mathcal{L}}{L_z^2} a^2 \right) \left(\beta_1 a^{-\gamma_1} + \beta_2 a^{-\gamma_2} - 1 \right) \right]^{-1/2} \mathrm{d}a \,, \tag{3.152}$$

where $a_{\max}$ satisfies $\dot{a} = 0$ in Eq. (3.141) and $\ddot{a} < 0$ in Eq. (3.142).

3.4.3 *Massless particles in two-fluid cosmologies*

As we can see from Eq. (3.144), the energy-momentum density evolves differently according to the equation of state parameter. In the case of a universe filled with two barotropic fluids, this means that one of the fluids may prevail for some time in the universe's evolution. This approach allows for a more comprehensive understanding of the dynamics of the universe.

Let us now return to the case of massless particles and extend the approach to the two-fluid case. For convenience, we use the rescaling

$$a \mapsto (\beta_1)^{1/\gamma_1}\, a \,, \quad \text{and} \quad t \mapsto (\beta_1)^{1/\gamma_1}\, t \,, \tag{3.153}$$

such that Eq. (3.145) can be re-written in terms of $\xi := \beta_2 / (\beta_1)^{\gamma_2/\gamma_1}$, and reads

$$(\dot{a})^2 = a^{-\gamma_1} + \xi a^{-\gamma_2} - 1 \,. \tag{3.154}$$

We again want to argue that the solution is symmetric about a maximum $a_{\max} = a(t_{\max})$ and so a single cycle of expansion recollapse passes in time $t_{\mathrm{end}} = 2t_{\max}$. This is true, and the proof follows

exactly the same reasoning presented at the start of Section 3.4.1. Moreover, since $\mathcal{L} = 0$ for null geodesics, Eq. (3.152) becomes

$$\Delta\varphi = 2 \int_0^{a_{\max}} \left[a^2 \left(a^{-\gamma_1} + \xi a^{-\gamma_2} - 1\right)\right]^{-1/2} \mathrm{d}a \,. \tag{3.155}$$

This integral does not admit a general closed-form solution for unspecified values of γ_1 and γ_2. We therefore consider some specific, physical, choices of γ_1 and γ_2.

3.4.3.1 *Dust and radiation*

For a universe filled with dust ($w_1 = 0$, i.e. $\gamma_1 = 1$) and radiation ($w_2 = 1/3$, i.e. $\gamma_2 = 2$), Eq. (3.155) yields

$$\Delta\varphi = 2 \int_0^{a_{\max}} \frac{\mathrm{d}a}{\sqrt{-a^2 + a + \xi}} = 2 \int_0^{a_{\max}} \frac{\mathrm{d}a}{\sqrt{\left(\frac{1}{4} + \xi\right) - \left(a - \frac{1}{2}\right)^2}} = 2 \left[\arcsin\left(\frac{a - \frac{1}{2}}{\sqrt{\frac{1}{4} + \xi}}\right)\right]_0^{a_{\max}} . \tag{3.156}$$

The maximum value of the scale factor can be found from Eq. (3.154) and satisfies

$$a^{-1} + \xi a^{-2} - 1 = 0 \iff -a^2 + a + \xi = 0 \,, \tag{3.157}$$

which yields $a = \frac{1}{2} \pm \sqrt{\frac{1}{4} + \xi}$. Since $\xi > 0$, we have $a_{\max} = \frac{1}{2} + \sqrt{\frac{1}{4} + \xi}$. Inserting this into Eq. (3.156) gives

$$\Delta\varphi = \pi + 2 \arcsin\left(\frac{1}{\sqrt{4\xi + 1}}\right) . \tag{3.158}$$

In Fig. 3.6a on p. 113, we show $\Delta\varphi$ as a function of $\xi = \beta_2/\beta_1^2$. The limit $\xi \to 0$ corresponds to a universe that contains only dust, for which we obtain $\Delta\varphi = 2\pi$, as expected. In the limit $\xi \to \infty$, which corresponds to a universe that contains only radiation, we find the known result $\Delta\varphi \to \pi$.

3.4.3.2 *Radiation and stiff matter*

For a universe filled with radiation ($w_1 = 1/3$, i.e. $\gamma_1 = 2$) and stiff matter ($w_2 = 1$, i.e. $\gamma_2 = 4$), from Eq. (3.155), we find that

$$\Delta\varphi = 2 \int_0^{a_{\max}} \frac{\mathrm{d}a}{\sqrt{1 + \xi a^{-2} - a^2}} = 2 \int_0^{a_{\max}} \frac{a \, \mathrm{d}a}{\sqrt{a^2 + \xi - a^4}} \tag{3.159}$$

$$= 2 \int_0^{a_{\max}} \frac{a \, \mathrm{d}a}{\sqrt{\left(\frac{1}{4} + \xi\right) - \left(a^2 - \frac{1}{2}\right)^2}} = \left[\arcsin\left(\frac{a^2 - \frac{1}{2}}{\sqrt{\frac{1}{4} + \xi}}\right)\right]_0^{a_{\max}} . \tag{3.160}$$

The maximum value of the scale factor can be found from Eq. (3.154), and satisfies

$$a^{-2} + \xi a^{-4} - 1 = 0 \implies -a^4 + a^2 + \xi = 0 \,, \tag{3.161}$$

which yields

$$a = \pm\sqrt{\frac{1}{2} \pm \sqrt{\frac{1}{4} + \xi}}\,. \tag{3.162}$$

Since $\xi > 0$ and $a_{\max} > 0$, we have

$$a_{\max} = \sqrt{\frac{1}{2} + \sqrt{\frac{1}{4} + \xi}}\,. \tag{3.163}$$

Inserting this into Eq. (3.160) gives

$$\Delta\varphi = \frac{\pi}{2} + \arcsin\left(\frac{1}{\sqrt{4\xi + 1}}\right). \tag{3.164}$$

In Fig. 3.6b, we show $\Delta\varphi$ in function of $\xi = \beta_2/\beta_1^2$. The limit $\xi \to 0$ corresponds to a universe that contains only radiation, for which $\Delta\varphi = \pi$. In the limit $\xi \to \infty$, i.e. the limit corresponding to a universe filled only with stiff matter, we obtain $\Delta\varphi \to \pi/2$.

Note that, mathematically, the case discussed here is similar to that for a dust and radiation filled universe, see Section 3.4.3.1. The reason is that the ratio $\gamma_2/\gamma_1 = 2$ in both cases.

3.4.3.3 *Dust and stiff matter*

Here, we consider a universe filled with dust ($w_1 = 0$, i.e. $\gamma_1 = 1$) and stiff matter ($w_2 = 1$, i.e. $\gamma_2 = 4$). Unlike the cases studied in Section 3.4.3.1 and Section 3.4.3.2, we now have $\gamma_2/\gamma_1 = 4$ and $\xi = \beta_2/\beta_1^4$. Equation (3.155) then becomes

$$\Delta\varphi = 2\int_0^{a_{\max}} \frac{a}{\sqrt{a^3 + \xi - a^4}}\mathrm{d}a\,, \tag{3.165}$$

and $a_{\max}$ is one of the roots of the polynomial

$$a^4 - a^3 - \xi = 0\,. \tag{3.166}$$

This is an integral which cannot be given in terms of elementary functions, but is elliptic. The analytic expression for $\Delta\varphi$, in this case, is quite complicated since it involves a combination of the incomplete elliptic integrals of the first kind $F(\phi, k)$ and of the third kind $\Pi(\phi, n, m)$, given in Definition 1.15, containing all the roots of $a^4 - a^3 - \xi = 0$. We remark that the discriminant of this polynomial is given by $\Delta = -\xi^2(256\xi + 27) < 0$, since $\xi > 0$, this means that the polynomial has two real roots (one positive and one negative), and two complex conjugate roots. We denote these roots by a_i, for $i \in \{1, 2, 3, 4\}$, and $a_{\max}$ is the positive real root, and find

$$\Delta\varphi = \left[\frac{2}{\sqrt{(a_1 - a_3)(a_2 - a_4)}}\left(a_2\, F(\phi, m) + (a_1 - a_2)\,\Pi(\phi, n, m)\right)\right]_0^{a_{\max}}, \tag{3.167}$$

where

$$\phi = \arcsin\left(\sqrt{\frac{(a-a_1)\,(a_2-a_4)}{(a-a_2)\,(a_1-a_4)}}\right), \quad n = \frac{a_1-a_4}{a_2-a_4}\,, \quad m = \frac{(a_2-a_3)\,(a_1-a_4)}{(a_1-a_3)\,(a_2-a_4)}\,. \tag{3.168}$$

Noting that, for $a_{\max} = a_4$, the upper integration boundary gives the complete elliptic integrals of the first and third kind. We provide a plot of $\Delta\varphi$ as a function of ξ in Fig. 3.6c. The behaviour of the function $\Delta\varphi$ for small and large values of ξ can be easily examined. As $\xi \to 0$, we have

$$\Delta\varphi = 2\int_0^{t_{\max}} \frac{\mathrm{d}t}{a(t)} = 2\int_0^{a_{\max}} \frac{\mathrm{d}a}{\sqrt{a-a^2}} \tag{3.169}$$

where we note that $a_{\max} \to 1$ in this limit. We thus find that for $\xi \to 0$,

$$\Delta\varphi = 2\int_0^1 \frac{\mathrm{d}a}{\sqrt{a-a^2}} = 2\pi\,, \tag{3.170}$$

which is indeed consistent with the fact that as $\xi \to 0$, we are in the limit $\beta_2 \to 0$. For large values of ξ, it is more helpful to return to the integral form containing β_1 and β_2, and note that as $\beta_1 \to 0$, the integral becomes

$$\Delta\varphi = 2\int_0^{\beta_2^{1/4}} \frac{a}{\sqrt{\beta_2-a^4}}\mathrm{d}a = \frac{\pi}{2}.$$

3.4.4 *Masless particle in a fluid with a cosmological constant*

We will now discuss the azimuthal geodesics of a massless particle in a universe filled by matter, radiation, or stiff matter, together with a cosmological constant. To this end, we note that, for a cosmological constant Λ, we can use Eq. (3.145) where we set $\beta_2 \equiv \Lambda/3$ and $\gamma_2 = -2$, or, equivalently, $w_2 = -1$, effectively treating the cosmological constant as a fluid with negative equation of state parameter. In the following, we also set $\beta_1 = \beta$, $\gamma_1 = \gamma$, and, thus, $\xi = \Lambda\beta^{2/\gamma}/3$. Observe that $\xi > 0$ when $\Lambda > 0$, and $\xi < 0$ when $\Lambda < 0$.

Before proceeding with our analysis, we seek the condition that the solution $a_{\max}$ has to satisfy in order for it to be a positive real maximum. Equations (3.145) and (3.142) read

$$\dot{a}^2 = a^{-\gamma} + \xi a^2 - 1\,, \tag{3.171}$$

$$a\ddot{a} = -\frac{1}{2}\gamma a^{-\gamma} + \xi a^2 = -\frac{1}{2}\gamma a^{-\gamma} + \xi a^2\,. \tag{3.172}$$

Positive cosmological constant. First we note that if a is a (positive) maximum, then from Eq. (3.171), we can write

$$a^{-\gamma} = 1 - \xi a^2\,, \tag{3.173}$$

whence Eq. (3.172) reads

$$a\ddot{a} = -\frac{1}{2}\gamma\left(1-\xi a^2\right)+\xi a^2 = -\frac{\gamma}{2}+\left(\frac{\gamma}{2}+1\right)\xi a^2. \tag{3.174}$$

To ensure the existence of a (positive) maximum we require $\ddot{a}<0$, which implies

$$-\frac{\gamma}{2}+\left(\frac{\gamma}{2}+1\right)\xi a^2<0 \iff 0<a<\frac{1}{\sqrt{\xi}}\sqrt{\frac{\gamma}{\gamma+2}} \equiv \frac{1}{\sqrt{\xi}}\sqrt{\frac{1+3w}{3(1+w)}}. \tag{3.175}$$

In order to be able to make some more concrete statements, we need to fix the value of w, or equivalently γ, and discuss the number of roots of Eq. (3.173).

Negative cosmological constant We note that Eq. (3.172) does not yield a constraint for a maximum as $a\ddot{a}<0$ for all a, γ, and ξ. However, as we will see, this does not constitute a problem as it will be straightforward to identify the maximum in the specific scenarios.

3.4.4.1 *Dust and cosmological constant*

We now discuss the case of a universe filled with dust ($w_1=0$, i.e. $\gamma_1=1$) and a cosmological constant ($w_2=-1$, i.e. $\gamma_2=-2$). Equation (3.155) then reads

$$\Delta\varphi = 2\int_0^{a_{\max}} \frac{\mathrm{d}a}{\sqrt{a+\xi a^4-a^2}}\,, \tag{3.176}$$

where $\xi=\Lambda\beta^2/3$. By letting

$$a=\frac{1}{x+1/3} \implies \frac{\mathrm{d}a}{\mathrm{d}x}=-\frac{1}{(x+1/3)^2}\,, \tag{3.177}$$

Eq. (3.176) becomes

$$\Delta\varphi = -2\int_{\infty}^{x_{\max}} \frac{\mathrm{d}x}{\sqrt{x^3-x/3+\xi-2/27}} = 4\int_{x_{\max}}^{\infty} \frac{\mathrm{d}x}{\sqrt{4x^3-4x/3+4\xi-8/27}}\,, \tag{3.178}$$

where $x_{\max}=a_{\max}^{-1}-1/3$. We have thus obtained an elliptic integral in Weierstrass form, introduced in Section 1.5.2. Hence,

$$\Delta\varphi = 4\wp^{-1}\left(\frac{1}{a_{\max}}-\frac{1}{3};\frac{4}{3};\frac{8}{27}-4\xi\right), \tag{3.179}$$

where $\wp^{-1}$ is the inverse Weierstrass $\wp$-function. The value of $a_{\max}$ can be found from Eq. (3.154) by determining the roots of the third-degree polynomial in the scale factor a, that is,

$$\xi a^3-a+1=0\,. \tag{3.180}$$

We will discuss the cases of the positive and the negative cosmological constant separately. The discriminant of the polynomial in Eq. (3.180) is given by $\Delta=(4-27\xi)\xi$.

Positive cosmological constant ($\xi > 0$) One can easily see that the depressed cubic polynomial in Eq. (3.180) has at least one negative real root and two complex conjugate roots if $\Delta < 0$, i.e. $\xi > 4/27$; and it has three real roots if $\Delta \geq 0$, i.e. $0 < \xi < 4/27$. We can therefore restrict our attention to the case $0 < \xi < 4/27$, as other values would not lead to a closed universe. In the present case, from Eq. (3.175), we have an additional constraint on the value of $a_{\max}$: $0 < a_{\max} < 1/\sqrt{3\xi}$. It can than be verified that the value of $a_{\max}$ is given by

$$a_{\max} = \frac{\sqrt[3]{-1}\left(2\sqrt[3]{-3}\xi - \sqrt[3]{2}\left(\xi^{3/2}\sqrt{81\xi - 12} - 9\xi^2\right)^{2/3}\right)}{6^{2/3}\xi\sqrt[3]{\xi^{3/2}\sqrt{81\xi - 12} - 9\xi^2}}\,. \tag{3.181}$$

Note that although, at first glance, Eq. (3.181) appears to be complex (due to the square roots of negative terms), it is indeed real. In Fig. 3.7a on p. 114, we show the value of $\Delta\varphi$ as a function of ξ. We note that as $\xi \to 0$, $\Delta\varphi \to 2\pi$, while for $\xi \to 4/27$, $\Delta\varphi \to \infty$. This can also be verified by setting $\xi = 4/27$ in the initial integral, Eq. (3.176). Physically, this means that, if the positive cosmological constant is dominant in the universe, closed universe solutions are no longer possible and, hence, the angular distance travelled by a massless particle on an azimuthal geodesic diverges.

Negative cosmological constant ($\xi < 0$) We note that the discriminant, Δ, is always negative in this case. This means that there is only one positive real root, which is our maximum, and two complex conjugate roots. In other words, for a negative cosmological constant, the universe always exhibits oscillatory behaviour. The value of $a_{\max}$ is thus given by

$$a_{\max} = \frac{\sqrt[3]{2}\left(\sqrt{3}\sqrt{\xi^3(27\xi - 4)} - 9\xi^2\right)^{2/3} + 2\sqrt[3]{3}\xi}{6^{2/3}\xi\sqrt[3]{\sqrt{3}\sqrt{\xi^3(27\xi - 4)} - 9\xi^2}}\,. \tag{3.182}$$

We remark that, as $\xi \to -\infty$, $\Delta\varphi \to 0$.

3.4.4.2 *Radiation and cosmological constant*

We now turn our attention to the case of a universe filled with radiation ($w_1 = 1/3$, i.e. $\gamma_1 = 2$) and a cosmological constant ($w_2 = -1$, i.e. $\gamma_2 = -2$). This gives

$$\Delta\varphi = 2\int_0^{a_{\max}} \frac{\mathrm{d}a}{\sqrt{1 + \xi a^4 - a^2}}\,, \tag{3.183}$$

where $\xi = \Lambda\beta/3$, and $a_{\max}$ is computed from

$$\xi a^4 - a^2 + 1 = 0. \tag{3.184}$$

Equation (3.184) is bi-quadratic in a, and

$$a = \pm\sqrt{\frac{2}{1 \pm \sqrt{1 - 4\xi}}}\,. \tag{3.185}$$

The maximum real root is given by

$$a_{\max} = \sqrt{\frac{2}{1+\sqrt{1-4\xi}}}\,, \tag{3.186}$$

for $\xi < 1/4$. To determine the value of $\Delta\varphi$, given in Eq. (3.183), let us make the following substitution

$$a = \frac{\sqrt{1-\sqrt{1-4\xi}}\sin(y)}{\sqrt{2}\sqrt{\xi}} \implies \frac{\mathrm{d}a}{\mathrm{d}y} = \frac{\sqrt{1-\sqrt{1-4\xi}}\cos(y)}{\sqrt{2}\sqrt{\xi}}\,, \tag{3.187}$$

and observing that

$$a = \frac{\sqrt{1-\sqrt{1-4\xi}}\sin(y)}{\sqrt{2}\sqrt{\xi}} \equiv \sqrt{\frac{2}{1+\sqrt{1-4\xi}}}\sin(y) = a_{\max}\sin(y), \tag{3.188}$$

which implies that $a = 0$ corresponds to $y = 0$ and $a_{\max} = \pi/2$. This allows us to write Eq. (3.183) as

$$\Delta\varphi = \frac{2\sqrt{2}}{\sqrt{1+\sqrt{1-4\xi}}}\int_0^{\pi/2} \frac{\mathrm{d}y}{\sqrt{1-\frac{\left(-2\xi-\sqrt{1-4\xi}+1\right)}{2\xi}\sin^2(y)}}\,. \tag{3.189}$$

Equation (3.189) is a complete elliptic integral of the first kind, that is, of the form $K(k)$, where the modulus k is given by

$$k^2 \coloneqq \frac{\left(-2\xi-\sqrt{1-4\xi}+1\right)}{2\xi} \tag{3.190}$$

$$= -\frac{\sqrt{1-4\xi}}{2\xi} + \frac{1}{2\xi} - 1 \equiv \frac{1-\sqrt{1-4\xi}}{1+\sqrt{1-4\xi}}\,. \tag{3.191}$$

We therefore conclude that the value of $\Delta\varphi$ is

$$\Delta\varphi = 2\sqrt{\frac{2}{1+\sqrt{1-4\xi}}}K\left(\frac{1-\sqrt{1-4\xi}}{1+\sqrt{1-4\xi}}\right). \tag{3.192}$$

Positive cosmological constant ($\xi > 0$) For the equations above to be meaningful, we require

$$1-4\xi > 0 \iff 0 < \xi < 1/4. \tag{3.193}$$

Note that the root $a_{\max}$ given in Eq. (3.186) satisfies the condition from Eq. (3.175),

$$0 < a < 1/\sqrt{2\xi}\,, \tag{3.194}$$

and hence is, indeed, a maximum. The dependence of $\Delta\varphi$ on ξ is shown in Fig. 3.7b. In the limit $\xi \to 0$, we see that $\Delta\varphi = \pi$ as expected. As $\xi \to 1/4$, $\Delta\varphi \to \infty$. The divergence again relates to the fact that, when the positive cosmological constant becomes too large, closed universe solutions cease to exist.

Negative cosmological constant ($\xi < 0$) In this case, we have again no restriction on ξ, and the universe always exhibits oscillatory behaviour. As $\xi \to -\infty$, then $\Delta\varphi$ decays to zero.

3.4.4.3 *Stiff matter and cosmological constant*

For stiff matter ($w_1 = 1$, i.e. $\gamma_1 = 4$) and a cosmological constant ($w_2 = -1$, i.e. $\gamma_2 = -2$), we get

$$\Delta\varphi = 2 \int_0^{a_{\max}} \frac{a}{\sqrt{1 + \xi a^6 - a^4}} \mathrm{d}a \,, \tag{3.195}$$

where $\xi = \Lambda\sqrt{\beta}/3$. The maximum value of a corresponds to one of the roots of

$$\xi a^6 - a^4 + 1 = 0 \,, \tag{3.196}$$

and we denote it by $a_{\max}$, as usual, to be determined below. Let us perform the substitution

$$y = 3\xi a^2 - 1 \iff \frac{\mathrm{d}y}{\mathrm{d}a} = 6\xi a \,, \tag{3.197}$$

which allows us to re-write Eq. (3.195) as

$$\Delta\varphi = \frac{2}{6\xi} \int_{-1}^{3\xi a_{\max}^2 - 1} \frac{\mathrm{d}y}{\sqrt{1 + \xi\left(\frac{y+1}{3\xi}\right)^3 - \left(\frac{y+1}{3\xi}\right)^2}} = \int_{-1}^{3\xi a_{\max}^2 - 1} \frac{\mathrm{sgn}(\xi) 2\sqrt{3}\, \mathrm{d}y}{\sqrt{4y^3 - 12y + 4(27\xi^2 - 2)}} \tag{3.198}$$

$$= \mathrm{sgn}(\xi) 2\sqrt{3} \left[\wp^{-1}\left(y; 12; -4\left(27\xi^2 - 2\right)\right)\right]_{-1}^{3\xi a_{\max}^2 - 1} \,. \tag{3.199}$$

If we take the limit $\xi \to 0$ in Eq. (3.195), we can easily find the value of $\Delta\varphi$ which corresponds to that of a universe without a cosmological constant. Indeed, from Eq. (3.196) as $\xi \to 0$, the maximum value of $a_{\max} = 1$, and we have

$$\Delta\varphi = \int_0^{a_{\max}} \frac{2a}{\sqrt{1 - a^4}} \mathrm{d}a = \frac{\pi}{2} \,.$$

Positive cosmological constant ($\xi > 0$) We need to find a condition on ξ which guarantees that the polynomial in Eq. (3.196) has a positive real root. This polynomial can be reduced to a cubic polynomial by letting $x = a^2$, which is

$$\xi x^3 - x^2 + 1 = 0 \,. \tag{3.200}$$

A positive real root of Eq. (3.196) can arise only as the positive square root of a positive real root x of $\xi x^3 - x^2 + 1 = 0$. It is easy to check that it has exactly one negative real root, and so it has a positive real root if and only if it has more than one real root, i.e. if and only if it has non-negative discriminant. Its discriminant is $\Delta = 4 - 27\xi^2$, which is non-negative only if $\xi \leq 2/\left(3\sqrt{3}\right)$.

Therefore, when $0 < \xi \leq 2/\left(3\sqrt{3}\right)$, the polynomial in Eq. (3.196) has two positive roots and two negative roots—these will be repeated roots when $\xi = 2/\left(3\sqrt{3}\right)$. Further, we have the constraint

from Eq. (3.175). It can be verified that the value of $a_{\max}$ is given by

$$a_{\max} = \frac{\sqrt{2^{2/3}\left(-1-\mathrm{i}\sqrt{3}\right)\delta^{2/3} + 4\sqrt[3]{\delta} + 2\mathrm{i}\sqrt[3]{2}\left(\sqrt{3}+\mathrm{i}\right)}}{2\sqrt{3}\sqrt[6]{\delta}\sqrt{\xi}}\,, \tag{3.201}$$

where $\delta = -27\xi^2 + 3\xi\sqrt{3}\sqrt{27\xi^2-4} + 2$. As in the case of Eq. (3.181), this is real-valued, despite appearing to be complex. Once again, this is a constraint on the positive cosmological constant. For larger values of ξ, and hence of the cosmological constant, we do not have re-collapsing universes. In Fig. 3.7c, we show $\Delta\varphi$ as a function of ξ.

Negative cosmological constant ($\xi < 0$) Again, there is no restriction on ξ and the only real positive root is given by

$$a_{\max} = \frac{\sqrt{(-2)^{2/3}\delta^{2/3} + 2\sqrt[3]{\delta} - 2\sqrt[3]{-2}}}{\sqrt{6}\sqrt[6]{\delta}\sqrt{\xi}}\,, \tag{3.202}$$

where δ is defined as above. Here $\sqrt[3]{-2}$ denotes the principal cubic root of -2, which is the non-real cube root with positive imaginary part. It is worth remarking once again that, despite appearing to be complex at first glance, $a_{\max}$ is real. As $\xi \to -\infty$, then $\Delta\varphi$ decays to zero.

3.4.5 *Massive particles in single-fluid cosmologies*

We shift our focus to the case of a massive particle in a closed FLRW universe, i.e. we choose $\mathcal{L} = -1$ in Eqs. (3.151) and (3.152). We restrict our attention to single-fluid cosmologies, i.e. we set $\beta_1 = \beta$, $w_1 = w$, and $\gamma_1 = \gamma$, while $\beta_2 = w_2 = \gamma_2 = 0$. In this context, we do not study the case of a cosmological constant, since the physically relevant case of a positive cosmological constant does not lead to closed universe solutions. Recall that for dust, radiation, and stiff matter, respectively, the maximum value of the scale factor $a(t)$ is given by $a_{\max} = \beta^{1/\gamma}$, as shown in Eq. (3.87).

3.4.5.1 *Dust*

Here $w = 0$, i.e. $\gamma = 1$, and consequently the integral to be evaluated reads

$$\Delta\varphi = 2\int_0^\beta \frac{\mathrm{d}a}{a\sqrt{\beta a^{-1}-1}\sqrt{1+L_z^{-2}a^2}} = 2\int_0^\beta \frac{\mathrm{d}a}{\sqrt{a\left(\beta-a\right)\left(1+L_z^{-2}a^2\right)}}. \tag{3.203}$$

Assume $L_z > 0$, for simplicity and since we assume an isotropic universe, and $\beta > 0$ as it is an energy density. Let us employ the following substitution

$$\cos(y) = \frac{(\beta-a)L_z - a\sqrt{\beta^2+L_z^2}}{(\beta-a)L_z + a\sqrt{\beta^2+L_z^2}} \tag{3.204}$$

$$\implies a = \frac{\beta L_z - \beta\cos(y)L_z}{\cos(y)\left(\sqrt{\beta^2+L_z^2}-L_z\right) + \sqrt{\beta^2+L_z^2}+L_z}\,, \tag{3.205}$$

which yields

$$\frac{\mathrm{d}a}{\mathrm{d}y} = \frac{2\beta\sin(y)L_z\sqrt{\beta^2+L_z^2}}{\left((\cos(y)-1)L_z-(\cos(y)+1)\sqrt{\beta^2+L_z^2}\right)^2}\,. \tag{3.206}$$

Furthermore, when $a=0$, $\cos(y)=1$, that is, $y=0$; whereas, when $a=\beta$, $\cos(y)=-1$, that is $y=\pi$. Hence, Eq. (3.203) reads

$$\Delta\varphi = \int_0^{\pi} \frac{4\sqrt{L_z}}{\sqrt{4\sqrt{\beta^2+L_z^2}-2\left(\sqrt{\beta^2+L_z^2}-L_z\right)\sin^2(y)}}\mathrm{d}y \tag{3.207}$$

$$= 4\sqrt{\frac{L_z}{\sqrt{L_z^2+\beta^2}}}\int_0^{\pi/2} \frac{\mathrm{d}y}{\sqrt{1-\left(\frac{1}{2}-\frac{L_z}{2\sqrt{\beta^2+L_z^2}}\right)\sin^2(y)}}\,, \tag{3.208}$$

where we used the symmetry of the integrand to rewrite the upper limit. This is now in the same form as the complete elliptic integral of the first kind given in Definition 1.15. We hence obtain

$$\Delta\varphi = 4\sqrt{\frac{L_z}{\sqrt{L_z^2+\beta^2}}}K\left(\frac{1}{2}-\frac{1}{2}\frac{L_z}{\sqrt{L_z^2+\beta^2}}\right). \tag{3.209}$$

In Fig. 3.8a on p. 115, we show $\Delta\varphi$ as a function of the ratio between angular momentum and energy density L_z/β. We find that as $L_z\to\infty$ then $\Delta\varphi\to 2\pi$. This is indeed consistent with the well-known result of Problem 3.1 as well as the more general result obtained in Section 3.4.1.

3.4.5.2 *Radiation*

In this case, $w=1/3$, i.e. $\gamma=2$, and hence

$$\Delta\varphi = 2\int_0^{\sqrt{\beta}} \frac{\mathrm{d}a}{a\sqrt{\beta a^{-2}-1}\sqrt{1+L_z^{-2}a^2}} = 2\int_0^{\sqrt{\beta}} \frac{\mathrm{d}a}{\sqrt{(\beta-a^2)\left(1+L_z^{-2}a^2\right)}}\,. \tag{3.210}$$

By making the substitution

$$a=\sqrt{\beta}\sin(y) \implies \frac{\mathrm{d}a}{\mathrm{d}y}=\sqrt{\beta}\cos(y)\,, \tag{3.211}$$

and noting that, for $a=0$, $y=0$, and, for $a=\sqrt{\beta}$, $y=\pi/2$, we have

$$\Delta\varphi = \int_0^{\pi/2} \frac{\sqrt{\beta}\cos(y)}{\sqrt{(\beta-\beta\sin^2(y))(1+\frac{\beta}{L_z^2}\sin^2(y))}}\mathrm{d}y = \int_0^{\pi/2} \frac{2}{\sqrt{1+\frac{\beta}{L_z^2}\sin^2(y)}}\mathrm{d}y\,, \tag{3.212}$$

which is in the same form as the complete elliptic integral of the first kind given in Definition 1.15. Therefore, provided that $\beta>0$, one obtains

$$\Delta\varphi = 2K\left(-\frac{\beta}{L_z^2}\right). \tag{3.213}$$

In Fig. 3.8b, we show $\Delta\varphi$ in terms of $L_z/\sqrt{\beta}$; as $L_z \to \infty$, $\Delta\varphi \to \pi$, as expected.

3.4.5.3 *Stiff matter*

For $w = 1$, i.e. $\gamma = 4$, we have

$$\Delta\varphi = 2\int_0^{\sqrt[4]{\beta}} \frac{\mathrm{d}a}{a\sqrt{\beta a^{-4}-1}\sqrt{1+L_z^{-2}a^2}} = 2\int_0^{\beta^{1/4}} \frac{a}{\sqrt{(\beta-a^4)\left(1+L_z^{-2}a^2\right)}}\mathrm{d}a\,. \tag{3.214}$$

Let us now consider the substitution

$$a = \sqrt{\sqrt{\beta}-2\sqrt{\beta}\sin^2(y)} \implies \frac{\mathrm{d}a}{\mathrm{d}y} = -\frac{2\sqrt{\beta}\sin(y)\cos(y)}{\sqrt{\sqrt{\beta}-2\sqrt{\beta}\sin^2(y)}}\,. \tag{3.215}$$

When $a = 0$, $y = \pi/4$, and, for $a = \sqrt[4]{\beta}$, $y = 0$. This allows us to re-write Eq. (3.214) as

$$\Delta\varphi = -\frac{2L_z}{\sqrt{\sqrt{\beta}+L_z^2}}\int_{\pi/4}^{0} \frac{\mathrm{d}y}{\sqrt{1-\frac{2\sqrt{\beta}}{\sqrt{\beta}+L_z^2}\sin^2(y)}} = \frac{2L_z}{\sqrt{\sqrt{\beta}+L_z^2}}\int_0^{\pi/4} \frac{\mathrm{d}y}{\sqrt{1-\frac{2\sqrt{\beta}}{\sqrt{\beta}+L_z^2}\sin^2(y)}}\,, \tag{3.216}$$

which is an incomplete elliptic integral of the first kind, given in Definition 1.15. Therefore,

$$\Delta\varphi = \frac{2L_z}{\sqrt{\sqrt{\beta}+L_z^2}}F\left(\frac{\pi}{4}, \frac{2\sqrt{\beta}}{L_z^2+\sqrt{\beta}}\right), \tag{3.217}$$

provided $\beta > 0$, where F denotes the incomplete elliptic integral of the first kind given in Eq. (1.78). An alternate form, which can be derived using computational softwares (e.g. Mathematica), is

$$\Delta\varphi = \frac{L_z}{\sqrt{\sqrt{\beta}+L_z^2}}K\left(\frac{2\sqrt{\beta}}{L_z^2+\sqrt{\beta}}\right) - \frac{1}{2}\frac{\sqrt{\beta}}{L_z^2}\,{}_3F_2\left(\frac{3}{4}, 1, \frac{5}{4}; \frac{3}{2}, \frac{3}{2}; \frac{\beta}{L_z^4}\right), \tag{3.218}$$

provided $\beta > 0$. Here ${}_3F_2$ is the generalised hypergeometric function, introduced in Section 1.5.3. While Eqs. (3.217) and (3.218) differ in form, they yield an identical plot. In Fig. 3.8c, we show $\Delta\varphi$ as a function of $L_z/\sqrt[4]{\beta}$. In the limit $L_z \to \infty$, this returns $\Delta\varphi \to \pi/2$, which is consistent with our previous results.

3.4.6 *Discussion*

We have presented the full set of solutions to the geodesic equation in FLRW spacetimes, and found a closed formula for the azimuthal distance travelled by a massless or massive test particle, respectively, in a closed universe during one cycle of expansion and re-collapse. We have extended Problem 3.1 to two-fluid cosmologies, which allow us to include a cosmological constant, Λ. This is possible as long as the cosmological constant does not dominate over the fluid in such a way as to render closed universe solutions impossible. In our computations, this is reflected by the angle $\Delta\varphi$ diverging at this limit.

In the case of massless test particles moving in two-fluid cosmologies, we find that the integrals

determining $\Delta\varphi$ can be solved in terms of elementary functions only for a universe filled with (a) dust and radiation or (b) radiation and stiff matter. All other cases lead to elliptic integrals. Extending these results to a massive test particle in a one-fluid model, we find that for dust, radiation, and stiff matter, the value of $\Delta\varphi$ is given in terms of the complete elliptic integral of the first kind with the elliptic modulus depending on the energy density of the fluid and the angular momentum of the particle. In principle, Problem 3.1 could be extended to other set-ups, e.g. to the motion of a massive test particle in two-fluid cosmologies. However, as suggested by the general expression for $\Delta\varphi$ given in Eq. (3.152), this would likely involve hyperelliptic integrals or would require numerical tools.

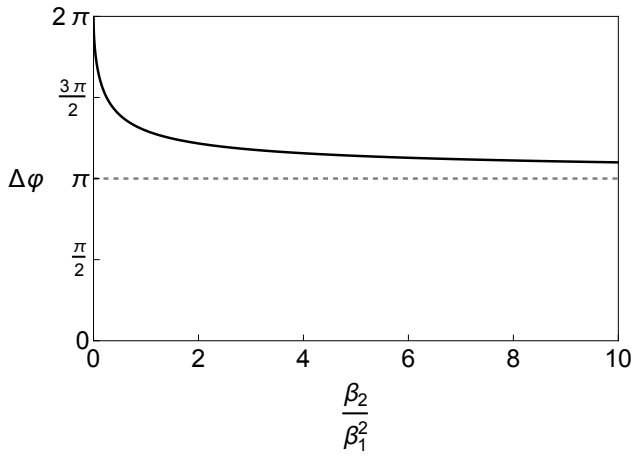

(a) Dust and radiation.

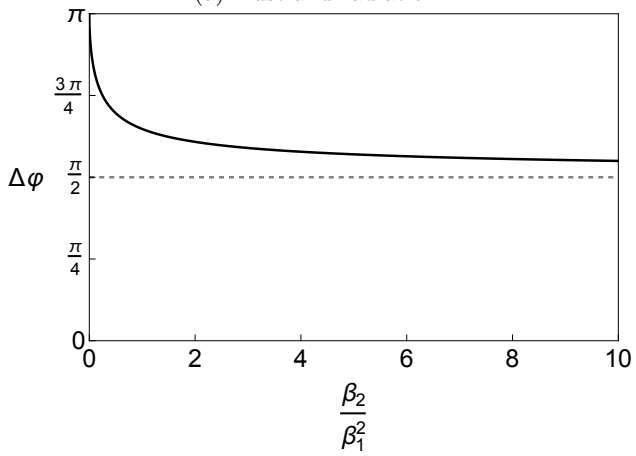

(b) Radiation and stiff matter.

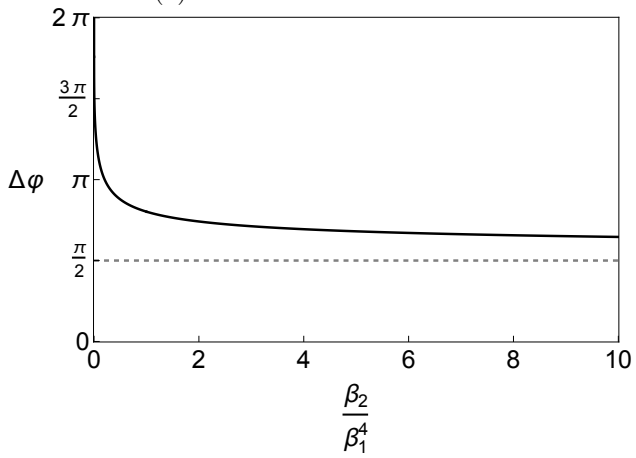

(c) Dust and stiff matter.

Fig. 3.6: Plot for the angular distance $\Delta\varphi$ in terms of $\xi = \beta_2/\beta_1^{\gamma_2/\gamma_1}$ for a massless particle moving in a universe filled with two fluids.

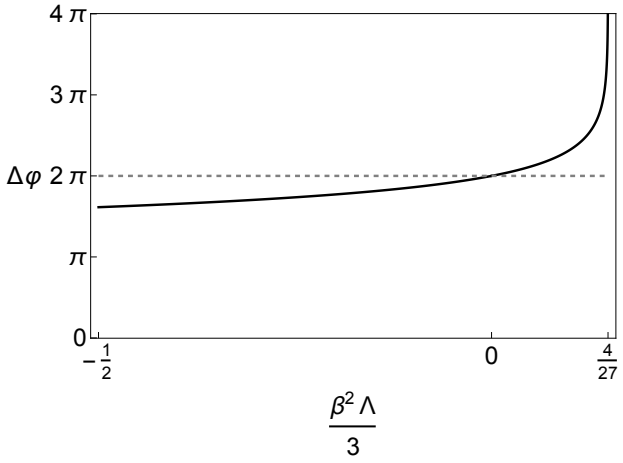

(a) Dust.

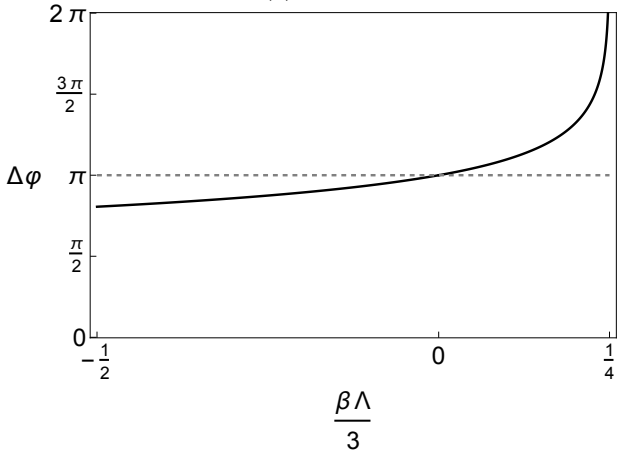

(b) Radiation.

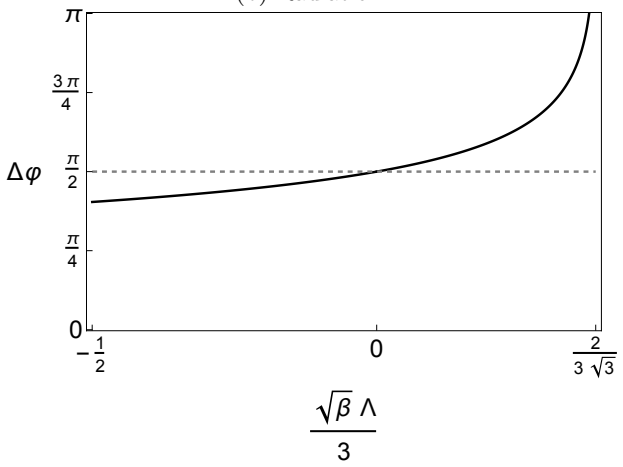

(c) Stiff matter.

Fig. 3.7: Plot for the angular distance $\Delta\varphi$ in terms of $\xi = \Lambda\beta^{2/\gamma}/3$ for a massless particle moving in a universe filled with cosmological constant and a second perfect, barotropic fluid.

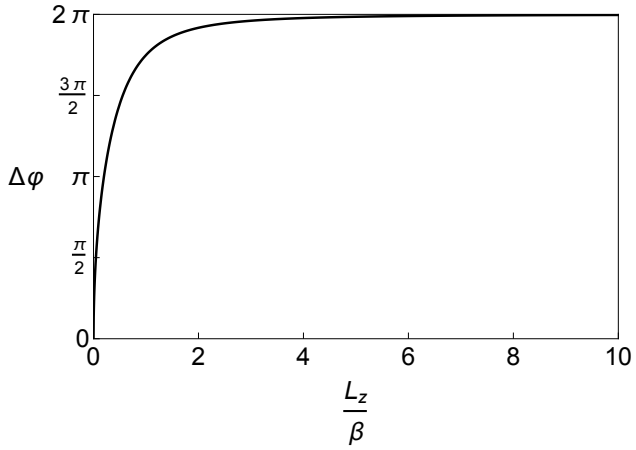

(a) Dust.

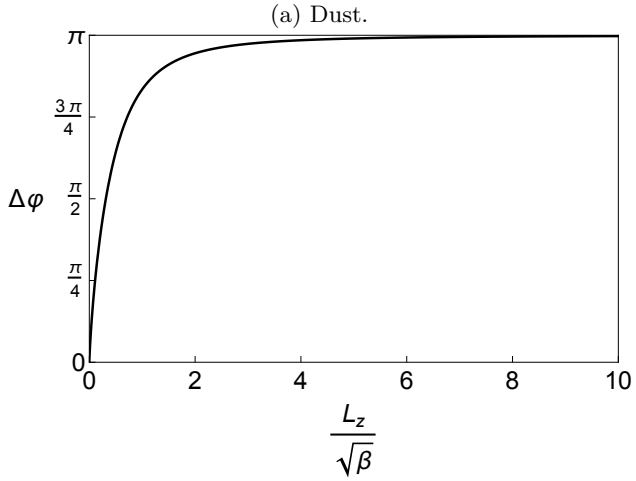

(b) Radiation.

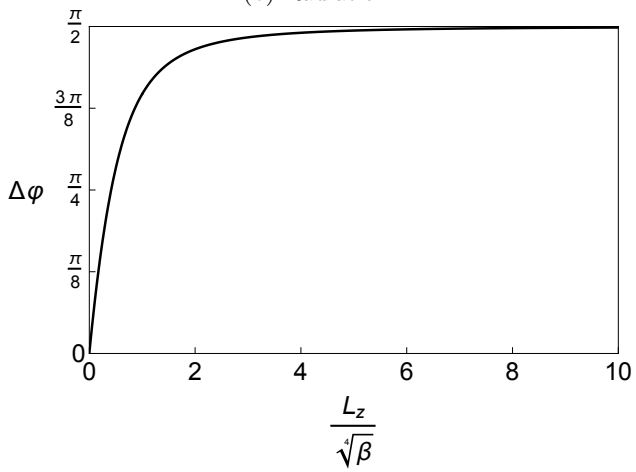

(c) Stiff matter.

Fig. 3.8: Plot for the angular distance $\Delta\varphi$ travelled by a massive test particle in a closed universe filled with a single perfect barotropic fluid. Here L_z is the angular momentum of the test particle.

4

Cosmological fluids with boundary and bulk term couplings

4.1 Introduction

Despite the great success of GR in its predictions, explanations, and observational verifications, modifications and extensions to GR have been put forth since its earliest days. These modified theories of gravity have been revived and gained interest in the last few decades, in light of the discovery of the accelerated expansion of the universe, particularly with the attempt to describe the 'dark sector' (i.e. dark matter and dark energy). One way to modify gravity is to introduce an interaction term (between dark matter and dark energy) at the level of the action.

In this chapter, we begin with a Lagrangian formulation of GR, where the dark matter fluid is described through the formalism introduced by Brown [43], and we examine couplings where the interaction term includes a boundary term, which comes from re-writing the Ricci scalar as a linear combination of a bulk and a boundary, i.e. $R = \mathbf{G} + \mathbf{B}$. The aim is to study the background cosmology within this framework through the lenses of the theory of dynamical systems.

The following expands on the work contained in [37].

4.2 Lagrangian formulation

Physical theories can be obtained through variational principles—that is, given a Lagrangian, or equivalently an action, one can obtain the Euler–Lagrange equations, which result in the governing equations for a physical theory; in classical mechanics, the Lagrangian is the difference between kinetic energy and potential energy. However, in GR, it is not immediately obvious what the action leading to the equations of motion should look like.

4.2.1 *The Einstein–Hilbert action*

As mentioned in Section 2.10, in 1915, Hilbert [100] and Einstein deduced that the Lagrangian for such action should be

$$\mathcal{L}_{\mathrm{EH}} = R\sqrt{-g}, \tag{4.1}$$

where $g = \det(g_{\mu\nu})$. Note that the Ricci scalar, $R = g^{\mu\nu}R_{\mu\nu}$, is the only independent scalar that may be obtained from the Riemann curvature tensor and the simplest non-trivial quantity that can be constructed from the metric and its derivatives. The action

$$S_{\rm EH} = \frac{1}{2\kappa}\int R\sqrt{-g}\,\mathrm{d}^4x = \frac{1}{2\kappa}\int g^{\mu\nu}R_{\mu\nu}\sqrt{-g}\,\mathrm{d}^4x \tag{4.2}$$

is often referred to as the Einstein–Hilbert action. The factor $\sqrt{-g}\,\mathrm{d}^4x$ is the invariant volume element of curved space-time. The minus sign under the square-root is present because we are working in a Lorentzian space-time. The factor $\kappa = 8\pi G/c^4$ allows the action to have the dimensions of energy times time. From the Ricci tensor, $R \sim \partial\Gamma + \Gamma\Gamma$, and the connection, $\Gamma \sim \partial g$, we deduce that the Einstein–Hilbert action is second order in its derivatives, so one would expect fourth order field equations; however, these higher-order terms feature in the action as a boundary term and, hence, they vanish and do not contribute to the field equations. The variation of Eq. (2.128) with respect to the (inverse) metric $g^{\mu\nu}$ leads to the Einstein field equations in absence of any matter, that is,

$$\delta g^{\mu\nu}: \quad G_{\mu\nu} \coloneqq R_{\mu\nu} - \frac{1}{2}Rg_{\mu\nu} = 0, \tag{4.3}$$

where $G_{\mu\nu}$ is the Einstein tensor. The details of this derivation can be found in standard GR textbooks, for example, [30, 59]. In order to get the equations with matter sources, one needs to add an action describing the matter fields so as to obtain the correct right-hand side of the equations of motion.

4.2.2 *Scalar-fluid theories*

In order to recover the non-vacuum Einstein field equations, see for example [48], it is customary to consider an action of the form $S_{\rm tot} = S_{\rm EH} + S_{\rm matter}$, where $S_{\rm matter}$ is the action for matter. This leads to an *ad hoc* definition of the energy-momentum tensor, that is,

$$T_{\mu\nu} := \frac{-2}{\sqrt{-g}}\frac{\delta S_{\rm matter}}{\delta g^{\mu\nu}}. \tag{4.4}$$

An alternative approach is provided by so-called *scalar-fluid theories*. In these, an action for a relativistic perfect fluid is defined and, by using the variational approach, one derives the energy-momentum tensor.

The term *scalar-fluid theories* was coined in [110] to refer to the class of theories in which the fluid and the scalar field describe the dark matter and dark energy sectors respectively, based on [38, 39]. The Lagrangian formalism for relativistic perfect fluids was introduced by Brown [43] and is outlined below.

Within Brown's framework, the Lagrangian (density) for the relativistic fluid may be written

as

$$\mathcal{L}_{\rm M} = -\sqrt{-g}\rho(n,s) + J^\mu \left(\varphi_{,\mu} + s\theta_{,\mu} + \beta_A \alpha^A{}_{,\mu}\right), \tag{4.5}$$

where ρ is the energy density of the matter fluid, prescribed to be a function of the particle number density n and the entropy density per particle s; the fields φ, θ, and β_A are all Lagrange multipliers, and α^A are the Lagrangian coordinates of the fluid, where A takes the values $1, 2, 3$; J^μ is the vector-density particle-number flux, which is related to n via

$$J^\mu = \sqrt{-g} n U^\mu\,, \quad |J| = \sqrt{-g_{\mu\nu} J^\mu J^\nu}\,, \quad n = \frac{|J|}{\sqrt{-g}}\,, \tag{4.6}$$

where U^μ is the fluid 4-velocity and satisfies $U_\mu U^\mu = -1$. The independent dynamical variables of the Lagrangian in Eq. (4.5) are $g^{\mu\nu}$, J^μ, s, φ, θ, β_A, and α^A. We note that, in this approach, the pressure of the fluid is defined as

$$p := n\frac{\partial \rho}{\partial n} - \rho\,, \tag{4.7}$$

which is consistent with the first law of thermodynamics. The variation of the action

$$S_{\rm M} = \int \left(-\sqrt{-g}\rho(n,s) + J^\mu \left(\varphi_{,\mu} + s\theta_{,\mu} + \beta_A \alpha^A{}_{,\mu}\right)\right) \mathrm{d}^4 x \tag{4.8}$$

with respect to the (inverse) metric $g^{\mu\nu}$ yields the energy-momentum tensor

$$\delta g^{\mu\nu}: \quad T_{\mu\nu} := \frac{-2}{\sqrt{-g}} \frac{\delta S_{\rm M}}{\delta g^{\mu\nu}} = p g_{\mu\nu} + (\rho + p) U_\mu U_\nu\,. \tag{4.9}$$

In the presence of matter modelled as a relativistic perfect fluid, the Einstein field equations arising from the action $S_{\rm EH}$ and $S_{\rm M}$ are

$$G_{\mu\nu} := R_{\mu\nu} - \frac{1}{2} R g_{\mu\nu} = 8\pi T_{\mu\nu}\,. \tag{4.10}$$

4.2.3 *Matter couplings*

We now introduce some *matter couplings*, in other words, terms in the Lagrangian that describe how matter couples to the spacetime metric and affects the spacetime dynamics, and derive the Einstein field equations for such couplings. By writing,

$$S_{\rm matter} = \int L_{\rm matter}(g, \psi, \nabla\psi)\sqrt{-g}\,\mathrm{d}^4 x, \tag{4.11}$$

one assumes the *principle of minimal gravitational coupling* [29]. The expression *minimal coupling* was first introduced by Gell-Mann [75, 83] in the context of the electromagnetic interaction. Given a Lagrangian with all electric charges switched off, the coupling with the electromagnetic interaction

is obtained via the substitution

$$\partial_\alpha \mapsto \partial_\alpha + \mathrm{i}eA_\alpha, \tag{4.12}$$

that is, the electromagnetic interaction is introduced by replacing every partial derivative with a "new" *covariant* derivative. Similarly, the gravitational interaction is switched on as follows. When the scalar (or spinor) field actions, formulated in Minkowski space, are defined on an arbitrary manifold, one replaces the Minkowski metric $\eta_{\mu\nu}$ with a Lorentzian metric $g_{\mu\nu}$. The partial derivatives ∂_α are replaced by the covariant derivatives ∇_α, and, hence, in the Lagrangian, one makes the substitution

$$\eta_{\mu\nu} \mapsto g_{\mu\nu}, \quad \partial_\alpha \mapsto \nabla_\alpha, \quad \sqrt{-\eta}\mathrm{d}^4x \mapsto \sqrt{-g}\mathrm{d}^4x. \tag{4.13}$$

Non-minimal couplings contain terms which directly connect the matter fields to geometrical quantities, e.g. the Riemann tensor, or the Ricci tensor. Any coupling term which involves curvature vanishes in the limit of special relativity; this does not occur in the presence of minimally coupled terms.

4.2.4 *Bulk and boundary couplings*

It is well known that a total derivative term can be isolated from the Ricci scalar, yielding the *Gamma squared action*. This was already noted by Einstein in 1916 [71]. By performing variations with respect to the metric, the Gamma squared action also gives rise to the Einstein field equations. However, the underlying Lagrangian is no longer a coordinate scalar as it differs from a true scalar by the total derivative term. The suffix 'pseudo' denotes quantities that resemble scalars or tensors but are not invariant under general coordinate transformations. As shown in [35], we can re-write the Einstein–Hilbert action as

$$S_{\mathrm{EH}} = \frac{1}{2\kappa}\int \mathcal{L}_{\mathrm{EH}}\,\mathrm{d}^4x = \frac{1}{2\kappa}\int R\sqrt{-g}\,\mathrm{d}^4x = \frac{1}{2\kappa}\int (\mathbf{G}+\mathbf{B})\sqrt{-g}\,\mathrm{d}^4x\,. \tag{4.14}$$

The *bulk term* $\mathbf{G}$ is defined as

$$\mathbf{G} := g^{\mu\nu}\left(\Gamma^\lambda_{\mu\sigma}\Gamma^\sigma_{\lambda\nu} - \Gamma^\sigma_{\mu\nu}\Gamma^\lambda_{\lambda\sigma}\right)\,, \tag{4.15}$$

and the *boundary term* $\mathbf{B}$ is given by

$$\mathbf{B} := \frac{1}{\sqrt{-g}}\partial_\sigma\left(\frac{\partial_\mu\left(gg^{\mu\sigma}\right)}{\sqrt{-g}}\right) = \frac{1}{\sqrt{-g}}\partial_\sigma\left(\sqrt{-g}B^\sigma\right), \tag{4.16}$$

where the boundary pseudovector B^σ is given by

$$B^\sigma = g^{\mu\nu}\Gamma^\sigma_{\mu\nu} - g^{\sigma\nu}\Gamma^\lambda_{\lambda\nu}\,. \tag{4.17}$$

Since **G** and **B** do not transform like scalars under diffeomorphisms, we refer to them as pseudo-scalars. Moreover, **B** takes the form of a total derivative, and hence it does not feature in the Euler–Lagrange equations.

By construction, the bulk term **G** is quadratic in the Christoffel symbols and hence the action

$$S_{\mathrm{E}} = \frac{1}{2\kappa}\int \mathbf{G}\sqrt{-g}\,\mathrm{d}^4x = \frac{1}{2\kappa}\int g^{\mu\nu}(\Gamma^{\lambda}_{\mu\sigma}\Gamma^{\sigma}_{\lambda\nu} - \Gamma^{\sigma}_{\mu\nu}\Gamma^{\lambda}_{\lambda\sigma})\sqrt{-g}\,\mathrm{d}^4x\,, \tag{4.18}$$

is called the *Gamma squared action* or, sometimes, the *Einstein action*, to distinguish it from the Einstein–Hilbert action. Recent progress was made in [35, 36] on constructing modified theories of gravity based on this decomposition. These models can be linked naturally to a variety of other modified gravity models, such as $f(T)$ and $f(Q)$ gravity, either within the context of GR or in the metric-affine framework; for details, see [103]. The Christoffel symbols are usually interpreted as the gravitational field strengths. We can motivate this by recalling that they contain the first partial derivatives of the metric, which represent the gravitational potentials. The bulk term is thus quadratic in the field strengths, similar to other field theories, like Yang-Mills theories or elasticity theory. This analogy provides the primary motivation for splitting the Ricci scalar as in Eq. (4.14). This split naturally yields a boundary term which could be coupled to other fields present in the model. Couplings of this type are interesting as they are purely geometrical and thus have no direct links with classical physics. This is similar to Brans–Dicke theories, where a scalar field is coupled to the curvature scalar [42]. By isolating the bulk and boundary terms, we can therefore consider more intricate couplings involving those two parts, which make up the curvature scalar.

4.2.5 *Total action and interaction terms*

We can now set up the total action which contains gravity (see Section 4.2.1), a fluid to describe matter (see Section 4.2.2), a scalar field ϕ to describe quintessence (see Section 2.10), and an interaction term to model the interaction between matter and quintessence. This means we consider

$$S_{\mathrm{tot}} = \int \left(\tfrac{1}{2\kappa}\mathcal{L}_{\mathrm{EH}} + \mathcal{L}_{\mathrm{fluid}} + \mathcal{L}_{\phi} + \mathcal{L}_{\mathrm{int}}\right)\mathrm{d}^4x\,, \tag{4.19}$$

where $\mathcal{L}_{\phi}$ is the scalar field Lagrangian (density) given by

$$\mathcal{L}_{\phi} = -\sqrt{-g}\Big(\tfrac{1}{2}g^{\mu\nu}\nabla_{\mu}\phi\nabla_{\nu}\phi + V(\phi)\Big), \tag{4.20}$$

with given scalar field potential V, as introduced in Eq. (2.130). The Lagrangian (density) $\mathcal{L}_{\mathrm{int}}$ is an interaction coupling term, which allows us to couple the fluid to the scalar field.

The various independent variables in Brown's approach allow one to propose some types of coupling terms which do not exist in other settings. In previous work [38, 39], Böhmer et al.

proposed interaction terms of the form $f(n, s, \phi)$ and $f(n, s, \phi)J^\mu\partial_\mu\phi$, whose corresponding cosmological models gave rise to some physically relevant dynamics, containing dark energy dominated late-time accelerating solutions and scaling solutions.

In particular, as we wish to take into account boundary terms, we chose the following terms as the suitable possibilities for $\mathcal{L}_{\rm int}$:

(i) algebraic scalar coupling: $\mathcal{L}_{\rm int} := -\sqrt{-g}f(n, s, \phi, \mathbf{B})$

(ii) algebraic vector coupling: $\mathcal{L}_{\rm int} := -\sqrt{-g}f(n, s, \phi)B^\mu J_\mu$

(iii) derivative coupling: $\mathcal{L}_{\rm int} := -\sqrt{-g}f(n, s, \phi)B^\mu\partial_\mu\phi$.

Depending on the specific interaction term chosen, one should also note that the physical dimensions of f differ for the different couplings.

Coupling (ii) is very restrictive in the context of cosmology. We find that the consistency of the cosmological equations implies that f is proportional to n, thereby eliminating the scalar field from the coupling, that is, $f(n, s, \phi) \equiv f(n) \propto n$. Consequently, we find equations which largely coincide with the standard cosmological equations, and the model does not exhibit novel behaviour. We postpone the discussion of term (i) and other related models to Chapter 5.

4.3 Boundary term derivative coupling

For the remainder of this chapter, we restrict our attention to the interaction term (iii) and henceforth $\mathcal{L}_{\rm int}$ denotes this interaction Lagrangian. We shall show that this term has behaviour relevant to cosmology, and gives rise to cosmological equations which are amenable to analysis.

4.3.1 *Variations and field equations*

We begin with the variations of the action in Eq. (4.19) with respect to the the fields φ, θ, β_A, and the Lagrangian coordinates α^A, respectively, that is,

$$\delta\varphi: \quad J^\mu_{,\mu} = 0\,, \tag{4.21}$$

$$\delta\theta: \quad (sJ^\mu)_{,\mu} = 0\,, \tag{4.22}$$

$$\delta\alpha^A: \quad (\beta_A J^\mu)_{,\mu} = 0\,, \tag{4.23}$$

$$\delta\beta^A: \quad \alpha^A_{,\mu}J^\mu = 0\,. \tag{4.24}$$

These equations are independent of the gravitational action and are also independent of the interaction term. Next, varying Eq. (4.19) with respect to the entropy density, s, gives

$$\delta s: \quad nU^\mu\theta_{,\mu} = \frac{\partial\rho}{\partial s} + \frac{\partial f}{\partial s}B^\mu\partial_\mu\phi\,, \tag{4.25}$$

where the final term depends on the choice of f. Varying with respect to J^μ yields

$$\delta J^\mu : \quad \varphi_{,\mu} + s\theta_{,\mu} + \beta_A \alpha^A_{,\mu} + \frac{\partial \rho}{\partial n} U_\mu + \frac{\partial f}{\partial n} U_\mu B^\sigma \partial_\sigma \phi = 0 \,; \tag{4.26}$$

again, we have one term which depends on the coupling.

The variation of Eq. (4.19) with respect to the scalar field ϕ yields a modified Klein–Gordon equation

$$\delta\phi : \quad \Box\phi - V'(\phi) - \frac{\partial f}{\partial \phi} B^\mu \partial_\mu \phi + \nabla_\mu (f B^\mu) = 0 \,, \tag{4.27}$$

where $\Box := \nabla^\mu \nabla_\mu$.

Finally, the variation of Eq. (4.19) with respect to the metric tensor yields the Einstein field equations

$$\delta g^{\mu\nu} : \quad G_{\mu\nu} = \kappa (T^{(\mathrm{fluid})}_{\mu\nu} + T^{(\phi)}_{\mu\nu} + T^{(\mathrm{int})}_{\mu\nu}) \,, \tag{4.28}$$

where $G_{\mu\nu}$ is the Einstein tensor and

$$T^{(\mathrm{fluid})}_{\mu\nu} = (\rho + p) U_\mu U_\nu + p g_{\mu\nu}, \tag{4.29}$$

$$T^{(\phi)}_{\mu\nu} = \partial_\mu \phi \partial_\nu \phi - g_{\mu\nu} \Big(\frac{1}{2} \partial_\mu \phi \partial^\mu \phi + V(\phi) \Big) \,. \tag{4.30}$$

Both are the standard forms of the energy-momentum tensors for a perfect fluid and a scalar field, respectively. The energy-momentum tensor related to the interaction term is more complicated and is given by

$$\begin{aligned} T^{(\mathrm{int})}_{\mu\nu} = {} & g_{\mu\nu} f(n,s,\phi) B^\sigma \partial_\sigma \phi + \frac{1}{2} n \frac{\partial f}{\partial n} \left(U_\mu U_\nu + g_{\mu\nu} \right) B^\sigma \partial_\sigma \phi \\ & - 2\sqrt{-g}\, g_{\mu\nu} g^{\alpha\beta} \partial_\alpha \left(\frac{1}{\sqrt{-g}} f(n,s,\phi) \partial_\beta \phi \right) + 2\sqrt{-g}\, \partial_{(\mu} \left(\frac{1}{\sqrt{-g}} f(n,s,\phi) \partial_{\nu)} \phi \right) . \end{aligned} \tag{4.31}$$

The second line of this tensor appears due to variations of the boundary pseudo-vector with respect to the metric. This involves the second derivative terms of the scalar field; we note that one could rewrite the partial derivatives of the metric determinants using the Christoffel symbols, however, for our purposes, this does not introduce additional insights.

4.3.2 *Cosmological field equations*

For a spatially flat FLRW metric, Eq. (4.28) yields the cosmological Einstein field equations given by

$$3H^2 = \kappa \Big(\rho + \frac{1}{2} \dot{\phi}^2 + V - 6 f H \dot{\phi} \Big) \,, \tag{4.32}$$

$$3H^2 + 2\dot{H} = -\kappa \Big(p + \frac{1}{2} \dot{\phi}^2 - V + 2 f \ddot{\phi} + 2 \dot{\phi}^2 \frac{\partial f}{\partial \phi} \Big) \,, \tag{4.33}$$

and Eq. (4.27) leads to the modified Klein–Gordon (KG) equation

$$\ddot{\phi} + 3H\dot{\phi} + \frac{\partial V}{\partial \phi} - 6f(3H^2 + \dot{H}) + 18nH^2\frac{\partial f}{\partial n} = 0\,; \tag{4.34}$$

cf. Section 2.10. Here the dot denotes differentiation with respect to cosmological time.

Taking the derivative of Eq. (4.32) with respect to time, and solving Eqs.(4.33)–(4.34) for $\dot{H}$ and $\ddot{\phi}$, and Eq. (4.32) for f shows that Eqs. (4.32)–(4.34) imply the fluid energy-momentum conservation equation $\dot{\rho} + 3H(\rho + p) = 0$. Let us also note that the only dependence on the scale factor $a(t)$ in the field equations is via the Hubble function and its derivative. These equations feature both first and second derivatives of the scalar field, ϕ. However, following the approach outlined in Section 2.10, one can introduce a new variable which depends on the first derivative of the scalar field, leading to field equations which are first order. In short, this is the key idea behind the dynamical systems formulation.

In line with previous studies, e.g. [54], we assume V has the exponential form

$$V(\phi) = V_0 \exp\left(-\kappa\lambda\phi\right)\,, \tag{4.35}$$

where $V_0 > 0$ is a constant and $\lambda \geq 0$ is a dimensionless parameter. We note that this form for V is invertible, which will allow us to view ϕ as a function of V. This potential is most convenient as the exponential form allows one to close the autonomous system of equations without the introduction of an additional variable.

Assuming a non-negative potential allows us to introduce the well-known variables

$$x = \frac{\sqrt{\kappa}\dot{\phi}}{\sqrt{6}H}\,, \quad y = \frac{\sqrt{\kappa V}}{\sqrt{3}H}\,, \quad \sigma = \frac{\sqrt{\kappa\rho}}{\sqrt{3}H}\,. \tag{4.36}$$

We restrict to the case that $H > 0$, i.e. that the universe is expanding (choosing $H < 0$ would correspond to a contracting universe). It follows that the variables y and σ are non-negative.

When the FLRW metric is considered in Eq. (4.21) and Eq. (4.22), one immediately finds that the entropy density $s = s_0$ is a constant. Consequently, the coupling function is of the form $f(n, s, \phi) \equiv f(n, \phi)$. Moreover, Eq. (4.21) and Eq. (4.22) also imply that the particle number density is $n = n_0 a^{-3}$, where n_0 is a constant, which is expected by conservation of matter.

Going back to Brown's formulation in Eq. (4.5), we have that the energy density is a function of n, since the fluid's entropy s is constant, thus $\rho = \rho(n)$. On the other hand, in standard cosmology, it is customary to assume a linear equation of state of the form $p = w\rho$. We will now show that, the definition of pressure in Eq. (4.7) is equivalent to the assumption that the density is a power of the particle number density. To see this, let us consider $\rho = n^{w+1}$, for some w, which implies

$$p = n\frac{\partial \rho}{\partial n} - \rho = n(w+1)n^w - n^{w+1} = (w+1)n^{w+1} - n^{w+1} = wn^{w+1} = w\rho. \tag{4.37}$$

For the matter dominated case, $w = 0$, this gives that $p = 0$. On the other hand, integrating Eq. (4.7) with the assumption that $p = w\rho$ implies $\rho = n^{w+1}$, as required.

As in Section 2.10, we are mainly interested in the dynamics within the physically meaningful portion of the phase space. By dividing Eq. (4.32) by $3H^2$ and using the variables given in Eq. (4.36), one obtains the Friedmann constraint equation, to which we will generally refer as the *constraint equation*,

$$x^2 + y^2 + \sigma^2 - 2\sqrt{6\kappa}\, x f(n, \phi) = 1\,. \tag{4.38}$$

We note that f must be chosen to have the same dimensions as $\kappa^{-1/2}$ to ensure that this equation is consistent. In addition, we remark that, from Eq. (4.36) and using the relation $\rho = n^{w+1}$, one can express n as a function of σ and H. Similarly, from Eqs. (4.35) and (4.36), one can write ϕ in terms of y and H. Moreover, Eq. (4.38) is an algebraic relation between all the variables, which implies that the variables are not all independent.

We finish this section by noting that, for $f(n, \phi) \equiv 0$, we recover the model studied in [54], which we can view as our baseline model. When interpreting our results, we draw analogies and highlight differences with this baseline model. In that work, the constraint equation, Eq. (4.38), is solved for the matter variable σ which is then eliminated from the other equations, reducing the system to two differential equations and we follow the same approach here.

4.4 Constant interaction

To begin our study of specific models, we consider perhaps the simplest non-trivial one, where the coupling function is a constant, which we normalise as

$$f(n, s, \phi) = \frac{k}{2\sqrt{6\kappa}}\,, \tag{4.39}$$

for some constant k. This model shares some similarities with [54] and is an ideal prelude to the analysis of more complicated models.

4.4.1 *General properties and dynamical systems formulation*

Let us start with the Klein–Gordon equation, Eq. (4.34), which simplifies to

$$\ddot{\phi} + 3H\dot{\phi} + \frac{\partial V}{\partial \phi} = \sqrt{\frac{3}{2}}\frac{k}{\sqrt{\kappa}}\left(3H^2 + \dot{H}\right) =: \frac{Q}{\dot{\phi}}, \tag{4.40}$$

where we introduce the quantity Q to match previous work on dark sector couplings [31]. The energy density and pressure of the scalar field are given by $\rho_\phi = \dot{\phi}^2/2 + V$ and $p_\phi = \dot{\phi}^2/2 - V$,

respectively. This allows us to re-write Eq. (4.40) in the well-known form

$$\dot{\rho}_\phi + 3H(\rho_\phi + p_\phi) = \sqrt{\frac{3}{2}}\frac{k}{\sqrt{\kappa}}\dot{\phi}(3H^2 + \dot{H}) = Q\,, \tag{4.41}$$

hence Q can be re-expressed as

$$Q = H^2\sqrt{\frac{3}{2}}\frac{k}{\sqrt{\kappa}}\dot{\phi}\left(3 + \frac{\dot{H}}{H^2}\right) = H^2\sqrt{\frac{3}{2}}\frac{k}{\sqrt{\kappa}}\dot{\phi}(2-q), \tag{4.42}$$

where $q = -1 - \dot{H}/H^2$ is the standard deceleration parameter. It is well known from dark sector coupling models [31, 153] that $Q > 0$ means an energy transfer from dark matter to dark energy and $Q < 0$ a transfer in the opposite direction. Let us rewrite Eq. (4.42) using the variable x, defined in Eq. (4.36), which gives

$$Q = \frac{3H^3}{\kappa}\,kx(2-q)\,. \tag{4.43}$$

This allows us to see that, for $k > 0$, Eq. (4.43) implies that an epoch of accelerated expansion, $q < 2$, gives a positive coupling when $x > 0$, leading to more energy going into the scalar field. In turn, this leads to an epoch of further acceleration and can be seen as a self-reinforcing effect. The above argument is reversed for $f < 0$ (i.e. $k < 0$). Given that the late-time universe is dark energy dominated while the early universe contains considerably more dark matter than dark energy, it is reasonable to consider $f > 0$ (i.e. $k > 0$) and it will turn out that such models indeed evolve into epochs of late-time accelerated expansion.

Next, we consider a fluid with equation of state $p = w\rho$, which, as discussed at the end of Section 4.3.2, is equivalent to setting $\rho = n^{1+w}$. The constraint equation, Eq. (4.38), then reads

$$x^2 - kx + y^2 + \sigma^2 = 1\,. \tag{4.44}$$

The quantity σ^2 is the relative energy density of matter, sometimes denoted by Ω_m when discussing explicit cosmological models. For a scalar field, it is helpful to introduce the effective equation of state

$$w_\phi = \frac{p_\phi}{\rho_\phi} = \frac{\frac{1}{2}\dot{\phi}^2 - V}{\frac{1}{2}\dot{\phi}^2 + V}\,. \tag{4.45}$$

Here, $w_\phi \in [-1, 1]$ and we get $w_\phi = -1$ when $\dot{\phi} = 0$, as is expected for dark energy. The energy density of the scalar field is given by

$$\Omega_\phi := x^2 + y^2\,. \tag{4.46}$$

Hence, Eq. (4.44) can also be written as

$$\Omega_\mathrm{m} + \Omega_\phi - kx = 1\,. \tag{4.47}$$

At this point, it is clear that one can introduce improved variables by completing the square of the x-term in Eq. (4.44). Namely, we write

$$\left(x - \frac{k}{2}\right)^2 + y^2 + \sigma^2 = 1 + \frac{k^2}{4}, \tag{4.48}$$

and divide by the new right-hand side so that we arrive at

$$X^2 + Y^2 + \Sigma^2 = 1\,, \tag{4.49}$$

where

$$X = \frac{x - k/2}{\sqrt{1 + k^2/4}}\,, \quad Y = \frac{y}{\sqrt{1 + k^2/4}}\,, \quad \Sigma = \frac{\sigma}{\sqrt{1 + k^2/4}}\,. \tag{4.50}$$

These variables will prove particularly useful for our subsequent qualitative analysis. By dividing Eq. (4.33) by H^2, and solving Eq. (4.34) for $\ddot{\phi}$ and the constraint equation for Σ, one can obtain the acceleration equation

$$1 + q = -\frac{\dot{H}}{H^2} = \frac{3}{2}\left[(1 + w) - (w - 1)X^2 - Y^2\left((1 + w) - \frac{\lambda k}{\sqrt{6}}\right)\right]\,, \tag{4.51}$$

which can be integrated to find $a(t)$ at any given fixed point (X_0, Y_0). The right-hand side, at a fixed point, is constant. If this constant is non-zero, the scale factor evolves as a power law in cosmological time, that is, $a \propto (t - t_0)^{\mu}$, where μ is that power and t_0 is an integration constant. We therefore have that μ is given by

$$\frac{1}{\mu} = \frac{3}{2}\left[(1 + w) - (w - 1)X_0^2 - Y_0^2\left((1 + w) - \frac{\lambda k}{\sqrt{6}}\right)\right] = 1 + q\,. \tag{4.52}$$

When the right-hand side of Eq. (4.51) vanishes at some fixed point, the scale factor $a(t)$ evolves exponentially. This corresponds to H being constant at this point, that is, a universe undergoing a de Sitter expansion.

It can be useful to define the total energy density and total pressure of the cosmological model

$$\widetilde{\rho} = \rho + \frac{1}{2}\dot{\phi}^2 + V + \rho_{\text{int}}\,, \tag{4.53}$$

$$\widetilde{p} = p + \frac{1}{2}\dot{\phi}^2 - V + p_{\text{int}}\,, \tag{4.54}$$

where we set $\rho_{\text{int}} = -kH\sqrt{6/\kappa} + \dot{\phi}$ and $p_{\text{int}} = k\ddot{\phi}/\sqrt{6\kappa}$, as suggested by Eq. (4.32) and Eq. (4.33). This naturally leads to the effective equation of state parameter $\widetilde{w} = \widetilde{p}/\widetilde{\rho}$. For power law models, this effective equation of state parameter is directly related to the power μ, and one has

$$\mu = \frac{2}{3(1 + \widetilde{w})}\,, \quad \text{or} \quad \widetilde{w} = \frac{2}{3\mu} - 1\,. \tag{4.55}$$

We note that the power μ, the effective equation of state parameter $\widetilde{w}$, and the deceleration parameter q, all encode the same physical information.

Similar to previously studied models, e.g. [54], the positivity of the matter variable and Eq. (4.49) imply that $0 \leq \Sigma \leq 1$, and hence $0 \leq X^2 + Y^2 \leq 1$. Together with the fact that $Y \geq 0$, since we are considering an expanding universe, this means that the phase space for the variables X and Y is a half disc of radius one. One can now find the maximum and minimum values of the deceleration parameter q (or alternatively $1/\mu$) from Eq. (4.52), subject to these constraints on X and Y. Assuming a physical equation of state parameter, $-1 < w < 1$, we find the upper bounds

$$q_{\max} = \begin{cases} 2 & \text{if} \quad \lambda k \leq 2\sqrt{6} \qquad \text{at } (\pm 1, 0)\,, \\ -1 + \sqrt{\frac{3}{8}}\lambda k & \text{if} \quad \lambda k > 2\sqrt{6} \qquad \text{at } (0, 1)\,, \end{cases} \tag{4.56}$$

and the lower bounds

$$q_{\min} = \begin{cases} \frac{1}{2}(1+3w) & \text{if} \quad \lambda k > \sqrt{6}(1+w) \qquad \text{at } (0, 0)\,, \\ -1 + \sqrt{\frac{3}{8}}\lambda k & \text{if} \quad \lambda k = \sqrt{6}(1+w) \qquad \text{at } (0, 1/2)\,, \\ -1 + \sqrt{\frac{3}{8}}\lambda k & \text{if} \quad \lambda k < \sqrt{6}(1+w) \qquad \text{at } (0, 1)\,. \end{cases} \tag{4.57}$$

These values allow us to make various general statements about the dynamical behaviour of the system, before looking at phase space plots or numerical solutions. The lower bounds on the deceleration parameter are of particular interest. Substituting the conditions on λk at the points $(0, 1/2)$ and $(0, 1)$ into the expression for $q_{\min}$ gives the bound $q_{\min} \leq (1 + 3w)/2$. Consequently, we find that when $w < -1/3$, we have acceleration for these models. However, at some of these critical points one can have acceleration for other values of w, for example $w = 0$, by choosing λk sufficiently small. This makes such models physically relevant for cosmology; recall the physical significance of different values of w summarised in Table 2.1.

We are now ready to state the dynamical equations of the system, using the variables defined in Eq. (4.50). This leads to two independent equations

$$X' = \frac{1}{4}\left[\sqrt{6}\lambda\sqrt{k^2+4}\,Y^2 + X\left(Y^2\left(\sqrt{6}\lambda k - 6w - 6\right) - 6(w-1)\left(X^2-1\right)\right)\right], \tag{4.58}$$

$$Y' = -\frac{1}{4}Y\left[\sqrt{6}\lambda\sqrt{k^2+4}\,X + \left(Y^2-1\right)\left(-\sqrt{6}\lambda k + 6w + 6\right) + 6(w-1)X^2\right]. \tag{4.59}$$

Here a prime denotes a derivative with respect to the logarithm of the scale factor, $\log(a)$. One can now follow the standard dynamical systems approach to study this system, outlined in Section 1.3. We begin with the fixed points of Eqs. (4.58)–(4.59). We note that these are two polynomial equations of degree three, meaning that one could find up to nine real distinct critical points, by Bézout's Theorem. If $Y = 0$, the second equation is automatically satisfied, and this leads to the solutions $X \in \{-1, 0, +1\}$. Next, excluding $Y = 0$, one notes that Y appears only as Y^2 in the

equations, meaning that there are up to four more solutions. Two of these are at negative values of Y, which we exclude, again because we are considering an expanding universe ($Y \geq 0$). Assuming $\lambda > 0$ and $-1 \leq w \leq 1$, we obtain a total of five critical points, shown in Table 4.1.

Table 4.1: Critical points of system given in Eqs. (4.58) and (4.59).

Point	Coordinates (X, Y)	Existence
Point O	$(0, 0)$	for all k
Point A_-	$(-1, 0)$	for all k
Point A_+	$(1, 0)$	for all k
Point B	$\left(\frac{\lambda\sqrt{k^2+4}}{2\sqrt{6}-\lambda k}, \frac{2\sqrt{6-\sqrt{6}k\lambda-\lambda^2}}{2\sqrt{6}-\lambda k}\right)$	for $k < \frac{6-\lambda^2}{\sqrt{6}\lambda}$; note $X^2+Y^2=1$
Point C	$\left(\frac{\sqrt{6}(1+w)-\lambda k}{\lambda\sqrt{k^2+4}}, \frac{\sqrt{\left(\sqrt{6}\lambda k-6(1+w)\right)(w-1)}}{\lambda\sqrt{k^2+4}}\right)$	for $-1 \leq w < 1$, $2\sqrt{\frac{2}{3}}\frac{3(1+w)-\lambda^2}{(3+w)\lambda} \leq k \leq \sqrt{6}\frac{1+w}{\lambda}$ for $w = 1$, $k \geq \frac{6-\lambda^2}{\sqrt{6}\lambda}$

Note that Point B is always located on the boundary of the phase space while Point C is generally inside the phase space, if it exists. For the special value

$$k = 2\sqrt{\frac{2}{3}}\frac{3(1+w)-\lambda^2}{(3+3)\lambda}\,, \tag{4.60}$$

the lower existence bound, Point C is also on the boundary. Next, one needs to study the eigenvalues of the stability matrix at each of the critical points. For the first four points, Point O, Point A_-, Point A_+, and Point B, these are given in Table 4.2. Note that we will discuss the occurrence of possible zero eigenvalues separately to keep the discussion more straightforward. For example, one may immediately note that the choice $w = 1$ implies at least one zero eigenvalue for the Point O, Point A_-, and Point A_+.

The final critical point, Point C, is more difficult to study as the eigenvalues are much more involved. They are the solutions of the characteristic polynomial in ξ

$$\begin{aligned} 0 = \xi^2 + \frac{3}{2}(1-w)\xi - \frac{3(1-w)}{2(k^2+4)\lambda^2} \\ \times \left(3\lambda^2k^2(w+3) + \sqrt{6}\lambda k(2\lambda^2 - 3(w+1)(w+5)) + 12(w+1)(-\lambda^2+3w+3)\right). \end{aligned} \tag{4.61}$$

Solving this quadratic equation is easy, however, the explicit solutions do not offer much insight given that they contain three free parameters. For concrete parameter choices, we discuss this point in more detail below. One easy result to extract is the sum of the eigenvalues ξ_1 and ξ_2 at this point, that is, $\xi_1 + \xi_2 = -3(1-w)/2$. As this number is negative for $w \neq 1$, this point cannot have two positive eigenvalues and therefore will have at least one stable direction. This implies that Point C is a saddle point, stable node, or stable spiral.

There are many parameter choices resulting in zero eigenvalues, $w = 1$ being the obvious one. However, the choice $k\lambda = \sqrt{6}(1+w)$ also gives a zero eigenvalue for Point O. The stability analysis of such points requires techniques beyond linear stability theory. These are well known and their applications in cosmology were discussed, for example, in [18, 28, 32]. However, in what follows, we consider the two most physically relevant cases, namely a matter-dominated universe ($w = 0$), and a radiation-dominated one ($w = 1/3$), and employ linear stability theory. As we shall see, these cases lead to qualitatively similar results.

4.4.2 *The matter dominated case*

Setting $w = 0$, Eqs. (4.58) and (4.59) read

$$X' = \frac{1}{4}\left[\sqrt{6}\sqrt{k^2+4}\lambda Y^2 + X\left(Y^2\left(\sqrt{6}k\lambda - 6\right) + 6\left(X^2-1\right)\right)\right], \tag{4.62}$$

$$Y' = -\frac{1}{4}Y\left[\sqrt{6}\sqrt{k^2+4}\lambda X + \left(Y^2-1\right)\left(6-\sqrt{6}k\lambda\right) - 6X^2\right]. \tag{4.63}$$

Point O, Point A_-, Point A_+, and Point B are independent of w and all results discussed above apply and coincide with those given in Table 4.1; their stability was outlined in Table 4.2. The location of Point C, when it exists, depends on w and so do its corresponding eigenvalues. For $w = 0$, the coordinates of Point C are given by

$$\left(\frac{\sqrt{6}-k\lambda}{\sqrt{k^2+4}\lambda}, \frac{\sqrt{6-\sqrt{6}k\lambda}}{\sqrt{k^2+4}\lambda}\right), \tag{4.64}$$

Table 4.2: Stability of the critical points, Point O, Point A_-, Point A_+ and Point B, for the system in Eqs. (4.58) and (4.59). The classification assumes that the eigenvalues are non-zero.

Point	Eigenvalues	Classification
Point O	$\frac{3}{2}(w-1)$, $\frac{3}{2}(1+w)-\frac{\sqrt{6}}{4}k\lambda$	saddle if $k\lambda < \sqrt{6}(1+w)$ stable if $k\lambda > \sqrt{6}(1+w)$
Point A_-	$3(1-w)$, $3-\sqrt{\frac{3}{8}}\lambda\left(k-\sqrt{k^4+4}\right)$	saddle for all λ
Point A_+	$3(1-w)$, $3-\sqrt{\frac{3}{8}}\lambda\left(k+\sqrt{k^4+4}\right)$	saddle if $k < \frac{6-\lambda^2}{\sqrt{6}\lambda}$ stable if $k > \frac{6-\lambda^2}{\sqrt{6}\lambda}$
Point B	$\frac{2\sqrt{6}\left(\lambda^2+6\right)}{2\sqrt{6}-\lambda k} - 3(w+3)$, $\frac{\sqrt{6}(6+\lambda^2)}{2\sqrt{6}-\lambda k} - 6$	unstable if $\frac{6-\lambda^2}{\sqrt{6}\lambda} < k < \frac{2\sqrt{6}}{\lambda}$ saddle if $2\sqrt{\frac{2}{3}}\frac{3(1+w)-\lambda^2}{(3+w)\lambda} < k < \frac{6-\lambda^2}{\sqrt{6}\lambda}$ stable if $k > \frac{2\sqrt{6}}{\lambda}$ or $k < 2\sqrt{\frac{2}{3}}\frac{3(1+w)-\lambda^2}{(3+w)\lambda}$

and its corresponding eigenvalues are given by

$$-\frac{3}{4} \pm \frac{\sqrt{3}\sqrt{75k^2\lambda^2 - 84\lambda^2 + 8\sqrt{6}k\left(2\lambda^2 - 15\right)\lambda + 288}}{4\sqrt{k^2+4}\lambda}\,. \tag{4.65}$$

We now outline some physical properties of the critical points of the system, with the values of effective equation of state parameter $\widetilde{w}$ and the deceleration parameter shown in Table 4.3.

Table 4.3: Physical properties of the fixed points for the matter dominated case, for the system in Eqs. (4.58) and (4.59).

Point	$\widetilde{w}$	q
Point O	0	1/2
Point A_-	1	2
Point A_+	1	2
Point B	$\frac{2\sqrt{6}\left(\lambda^2-3\right)+9k\lambda}{6\sqrt{6}-3k\lambda}$	$\frac{\sqrt{6}\left(\lambda^2-2\right)+4k\lambda}{2\sqrt{6}-k\lambda}$
Point C	0	1/2

In order to analyse the stability of the fixed points, we look at the different regions in the (k, λ)-plane, see Fig. 4.1, and we recall that $\lambda > 0$. The curves plotted come from the conditions in the right-hand column of Table 4.2 and those for the existence of the fixed points. First, we remark that the fixed points Point O, Point A_-, and Point A_+ exist for all values of λ and k. Moreover, there are four distinct regions of values of k and λ, which yield different stability properties of the critical points, and, hence, different cosmological phenomena. We discuss these four different cases and comment on their suitability as a cosmological model.

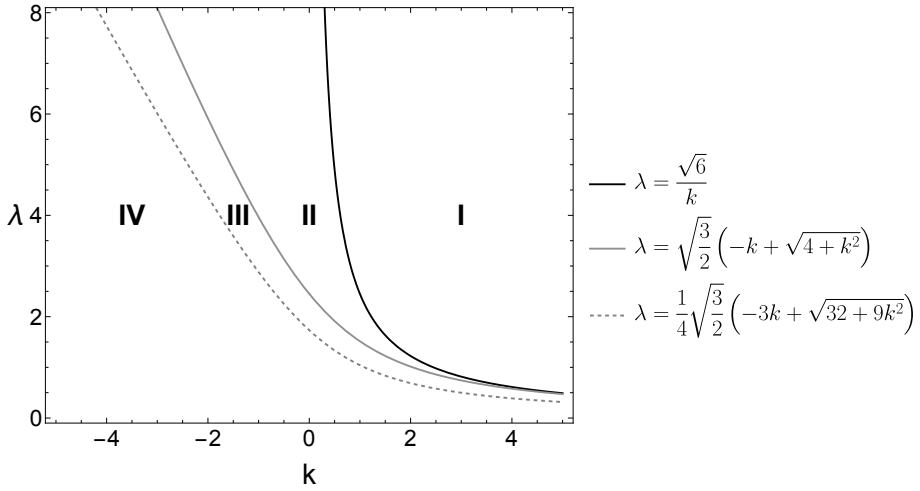

Fig. 4.1: Existence and stability regions in (k, λ)-plane for $w = 0$. The plotted curves follow from the stability criteria shown in Table 4.2.

Region I. For values within Region I, there are only three critical points. In particular, Point O is a stable node; Point A_- is an unstable node; and Point A_+ is a saddle. Since Point O is the

only attractor of the system, all trajectories will eventually approach it. Point A_- can be thought of as the past-time attractor, in the sense that all trajectories would start near it. Lastly, some trajectories are attracted towards Point A_+, but are eventually repelled and move towards Point O. This case is not of physical interest; the phase space is exemplified in Fig. 4.2, where we set $k = 2$ and $\lambda = 2$.

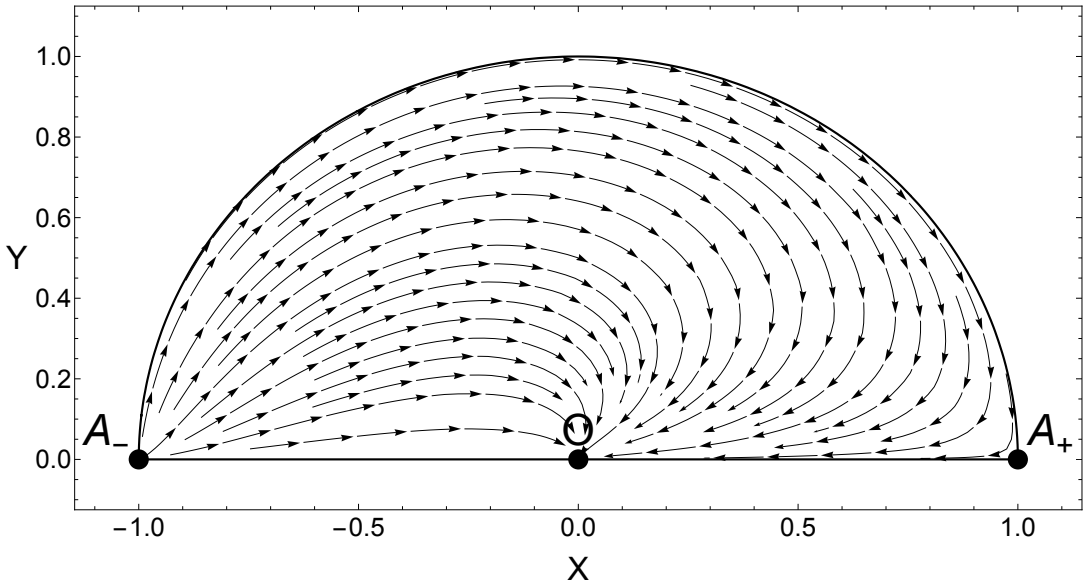

Fig. 4.2: Phase space with $k = 2$ and $\lambda = 2$. No acceleration region present.

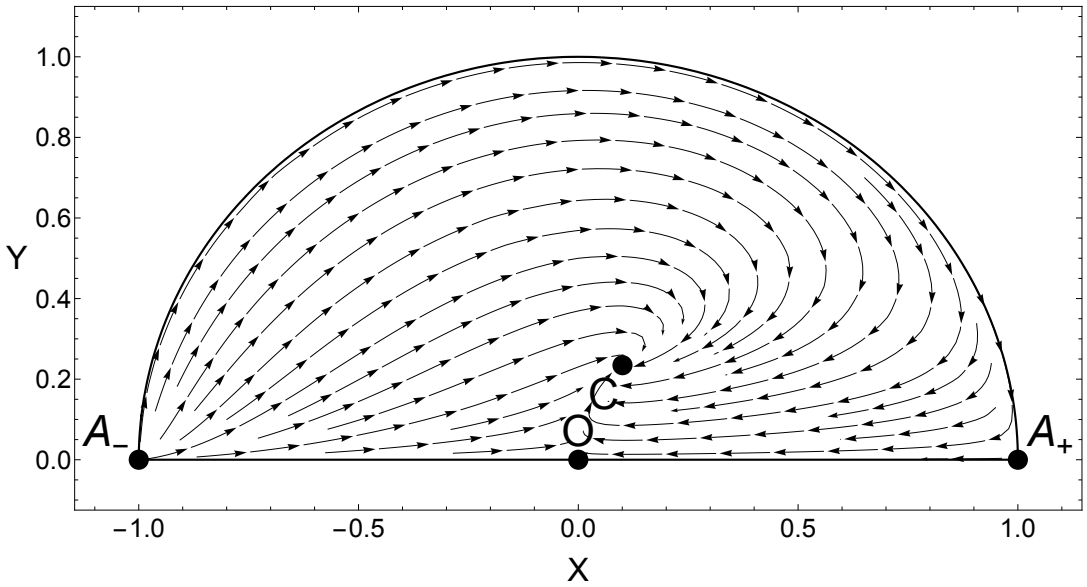

Fig. 4.3: Phase space with $k = 1$ and $\lambda = 2$. Point C is a stable node, that is, the only attractor describing a scaling solution with $\widetilde{w} = w = 0$. No acceleration region present.

Region II. In Region II, Point B does not exist. We therefore have four critical points: Point A_-, which is an unstable node; Point C, which is a stable node; and Point O and Point A_+, which

are both saddles. We note that here, Point C represents the *scaling solution* [11] as the effective equation of state parameter matches the matter one ($\widetilde{w} = w = 0$). Hence, the universe expands as if it was completely matter dominated despite the scalar field's influence, according to Eq. (4.52). The type of dynamics is illustrated by Fig. 4.3, where we set $k = 1$ and $\lambda = 2$. We remark the analogy with case III discussed in [54]. We note that there is no region of accelerated expansion, but this solution is of physical relevance for the so-called *cosmic coincidence problem* [81], which asks why the values of the energy densities of dark energy and dark matter are roughly the same order of magnitude at the present time; in particular, a way to address this is to assume the presence of a scalar field which hides its effects on cosmological scales.

Region III. In Region III, there are five critical points in the phase space. Point A_-, Point O, and Point C still behave as an unstable node, a saddle point, and a stable node, respectively. Point A_+ is now an unstable node. Point B exists and is a saddle point. This is shown in Fig. 4.4, where $k = 1/2$ and $\lambda = 3/2$. Point C always lies outside the acceleration region, so it does not represent a late-time inflationary solution; it is, again, a scaling solution. We highlight the analogy with case II discussed in [54]. All trajectories connect Point A_- or Point A_+ to Point C, with the exception of the orbits along the boundary.

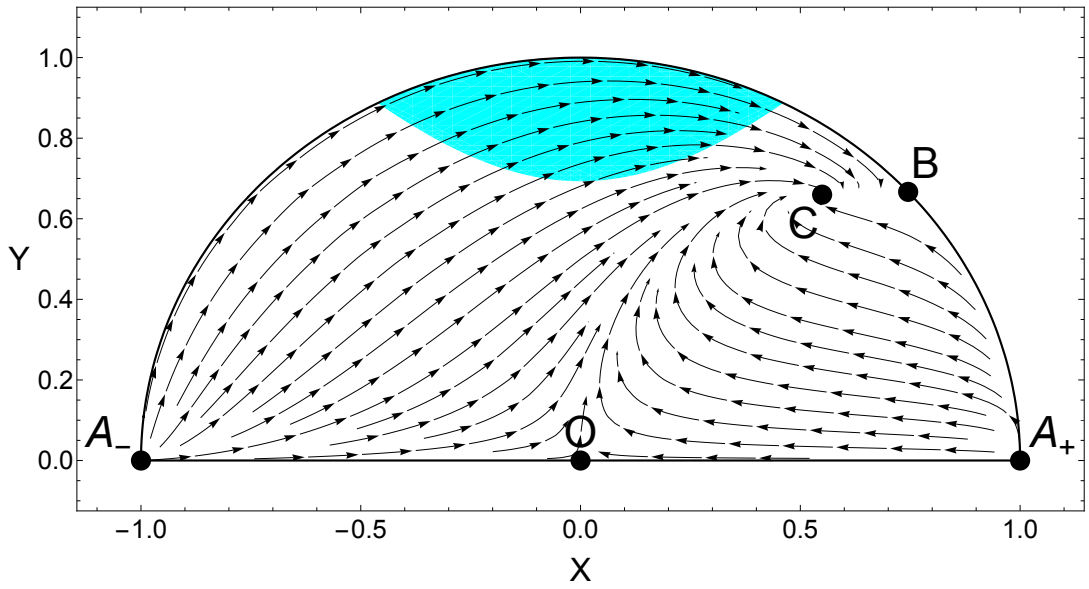

Fig. 4.4: Phase space with $k = 1/2$ and $\lambda = 3/2$. Here the only attractor is Point C where the universe expands as if it is completely matter dominated (scaling solution), while Point B is a saddle point. The shaded region represents the area of the phase space where there is accelerated expansion.

Region IV. In Region IV, there are again four fixed points since Point C lies outside the physical space. Here, Point A_- is always an unstable node and can be seen as the past attractor. Similar to

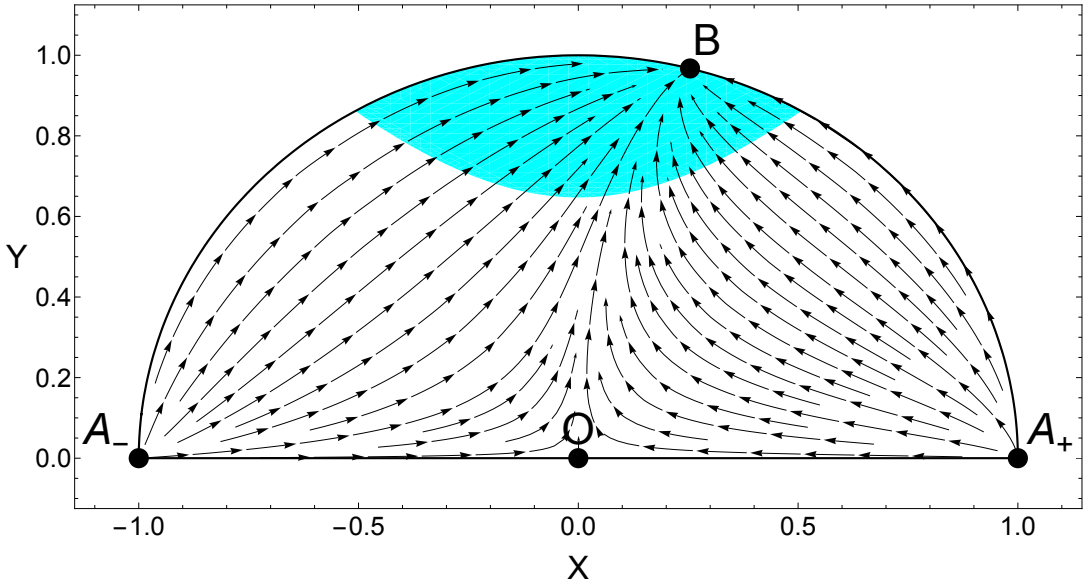

Fig. 4.5: Phase space with $k = 1$ and $\lambda = 1/2$. Here Point B is the only attractor and represents a late-time inflationary cosmological solution. The shaded area represents the part of the phase space where there is accelerated expansion.

Region III, A_+ is an unstable node. Point O is a saddle point whereas Point B is a stable node and therefore the late-time attractor. We note that here Point B lies within the region of accelerated expansion, hence we are in the presence of a cosmological solution with accelerated expansion. This is illustrated in Fig. 4.5. Once again, we emphasise the analogy with case I discussed in [54].

4.4.3 *The radiation dominated case*

In the case of a radiation-dominated universe, we set $w = 1/3$. Equations (4.58) and (4.59) now read

$$X' = \frac{1}{4}\left[\sqrt{6}\sqrt{k^2+4}\lambda Y^2 + X\left(Y^2\left(\sqrt{6}k\lambda - 8\right) + 4\left(X^2-1\right)\right)\right], \tag{4.66}$$

$$Y' = -\frac{1}{4}Y\left[\sqrt{6}\sqrt{k^2+4}\lambda X + \left(Y^2-1\right)\left(8-\sqrt{6}k\lambda\right) - 4X^2\right]. \tag{4.67}$$

As previously noted, the coordinates of Point O, Point A_-, Point A_+, and Point B are fixed for any w, and given in Table 4.1; their stability was presented in Table 4.2. For $w = 1/3$, Point C has coordinates

$$\left(\frac{4\sqrt{6}-3k\lambda}{3\sqrt{k^2+4}\lambda}, \sqrt{\frac{2}{3}}\frac{\sqrt{8-\sqrt{6}k\lambda}}{\sqrt{k^2+4}\lambda}\right), \tag{4.68}$$

which exists for $k > 4\sqrt{2}/(\lambda\sqrt{3})$, assuming $\lambda > 0$, and its corresponding eigenvalues are

$$-\frac{1}{2} \pm \frac{\sqrt{\lambda\left(123\lambda k^2 + 8\sqrt{6}\left(3\lambda^2-32\right)k - 180\lambda\right)+768}}{2\sqrt{3}\sqrt{k^2+4}\lambda}. \tag{4.69}$$

As shown in Fig. 4.6, the stability properties of the critical points exhibit analogous behaviour to that in the matter-dominated case. We note that, once again, we have four regions in the (k, λ)-plane (assuming $\lambda > 0$), which lead to four different main cases as before.

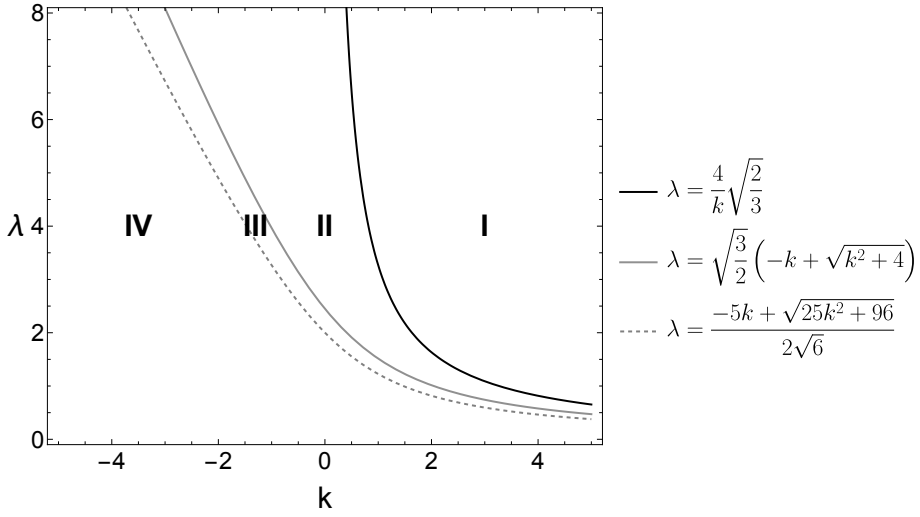

Fig. 4.6: Existence and stability regions in (k, λ)-plane for $w = 1/3$. The plotted curves follow from the stability criteria shown in Table 4.2.

Since the cases are very similar to those discussed in the previous section, we provide phase space diagrams to exemplify the dynamics of Region III and Region IV only. These are the more physically interesting regions as they allow for accelerated expansion to take place. In Region III, see Fig. 4.7, Point C, that is, the late time attractor, always lies outside the region of accelerated expansion. This also occurred for $w = 0$, since the value of the deceleration parameter q, at Point C, is positive. For values of λ and k within Region III, we find five critical points and a scaling solution as before. Moreover, as before, in Region IV, we have a solution to the cosmological field equations that lies within the region of accelerated expansion. This is illustrated in Fig. 4.8.

4.5 Non-constant interaction model $\alpha = 2$

4.5.1 *Equations of the model*

We are now considering a model with a non-constant interaction term. As we wish to exploit dynamical systems techniques without increasing the number of independent variables, we consider an interaction of the form

$$f(n, \phi) = \frac{k}{2\sqrt{6\kappa}} n^{\alpha(1+w)/2} V^{-\alpha/2}, \tag{4.70}$$

where α is a fixed power. Let us make the following observations to motivate this particular choice for f. In cosmology, $s = s_0$ and $n = n_0 a^{-3}$. Moreover, if we consider the linear equation of state $p = w\rho$ and the definition of p from Brown's fluid model, one has $\rho = n^{w+1}$. Therefore, this specific

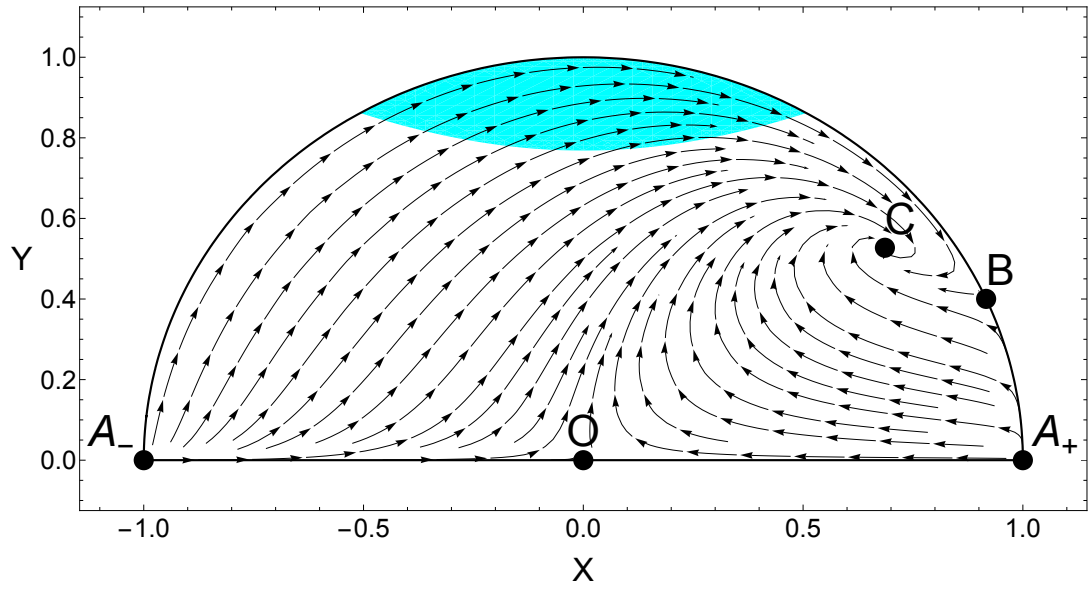

Fig. 4.7: Phase space with $k = 1/4$ and $\lambda = 2$. Here the only attractor is Point C where the universe expands as if it is completely matter dominated (scaling solution), while Point B is a saddle point. The shaded area represents the part of the phase space where there is accelerated expansion.

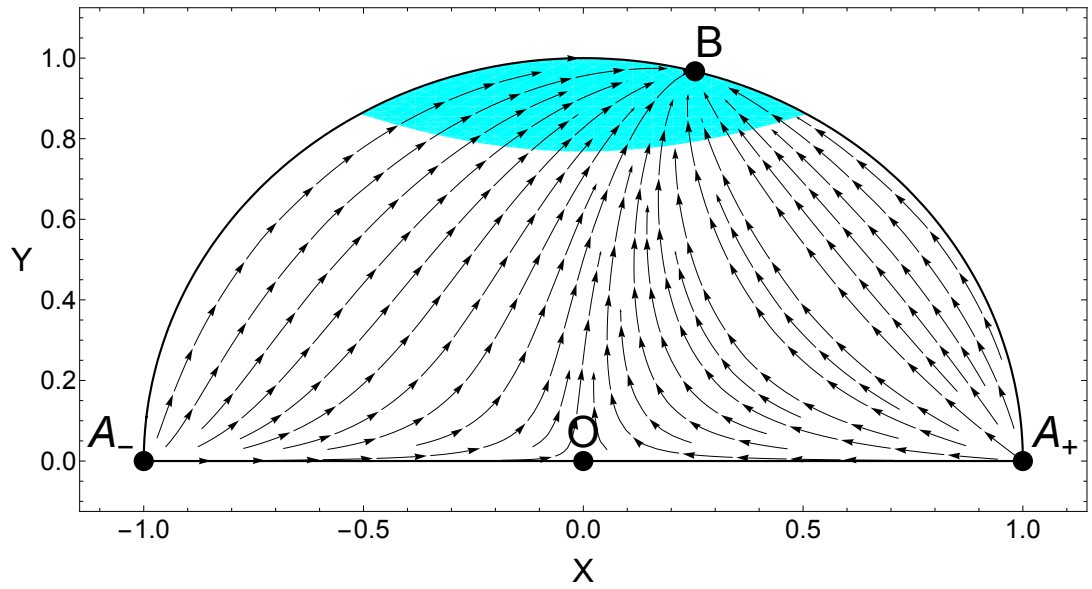

Fig. 4.8: Phase space with $k = 1$ and $\lambda = 1/2$. Here Point B is the only attractor and represents a late-time inflationary cosmological solution. The shaded area represents the part of the phase space where there is accelerated expansion.

form allows us to use the variables introduced in Eq. (4.36) directly, so Eq. (4.38) becomes

$$1 - x^2 - y^2 - \sigma^2 + k\, x \frac{\sigma^\alpha}{y^\alpha} = 0\,. \tag{4.71}$$

The dynamics of the system depends on the parameters w, λ, k, and α. We note that one could consider the limit $\alpha \to 0$ and recover Eq. (4.44).

It is clear that larger (integer) values of α can make the study of this system difficult, since the constraint equation, Eq. (4.71), would become a polynomial equation of high order. At the same time, even the values $\alpha = \pm 1$ introduce challenges as one has to deal with cubic equations. In fact, the two simplest cases that can be studied explicitly, without introducing further complications, are when $\alpha = \pm 2$.

For $\alpha = 2$, the constraint equation, Eq. (4.71), can be written as

$$\begin{aligned} y^2\left(1-x^2-y^2-\sigma^2\right)+k\,x\sigma^2=0 \quad &\Leftrightarrow \quad y^2\left(1-x^2-y^2\right)+\sigma^2\left(kx-y^2\right)=0\,, \\ &\Leftrightarrow \quad \sigma^2=\frac{y^2\left(1-x^2-y^2\right)}{y^2-kx}\,, \end{aligned} \tag{4.72}$$

allowing us to eliminate σ from the equations, so that the dynamical system remains two-dimensional. Moreover, as $\sigma^2 \geq 0$, we have

$$\frac{y^2(1-x^2-y^2)}{y^2-kx} \geq 0\,. \tag{4.73}$$

This gives rise to the physical regions of the phase space which is bounded by three curves: the line $y = 0$ (recall that $y \geq 0$ by Eq. (4.36), the unit circle $1 - x^2 - y^2 = 0$, and the parabola $y^2 - kx = 0$. This circle and parabola have a point of intersection in the half-plane $y \geq 0$ for all values of k, and when $k \neq 0$, they divide the half-plane into four regions. Exactly two of those regions are in the physical phase space, and are defined by the inequalities

$$1-x^2-y^2 \geq 0 \quad \text{and} \quad y^2-kx>0\,, \tag{4.74}$$

$$\text{or} \quad 1-x^2-y^2 \leq 0 \quad \text{and} \quad y^2-kx<0\,. \tag{4.75}$$

One of these regions is bounded (it lies within the unit semi-circle), while the other is unbounded. These two regions meet at the point of intersection between the circle and the parabola, given by

$$\left(\frac{1}{2}\left(\sqrt{k^2+4}-k\right), \sqrt{\frac{k}{2}(\sqrt{k^2+4}-k)}\right) \quad \text{for } k>0\,, \tag{4.76}$$

$$\left(-\frac{1}{2}\left(\sqrt{k^2+4}+k\right), \sqrt{-\frac{k}{2}\left(\sqrt{k^2+4}+k\right)}\right) \quad \text{for } k<0\,. \tag{4.77}$$

It is easy to check that if we take the limit as x and y approach this intersection point of the expression in Eq. (4.73), we get a strictly positive value. Hence, the intersection point also lies in the physical phase space, and, in principle, trajectories may pass from one region into the other. The geometry of the physical phase space is illustrated in subsequent figures; for example, Fig. 4.10.

The dynamical system in its full generality reads

$$x' = \frac{2y^6\left(\sqrt{6}\lambda-3(w+1)x\right)-6(w-1)x\left(x^2-1\right)y^4+k\mathcal{A}+k^2\mathcal{B}}{4y^4-8kxy^2+k^2\left(2x^2y^2+\left(x^2+1\right)^2+y^4-2y^2\right)}\,, \tag{4.78}$$

where

$$\begin{aligned}\mathcal{A} =&3y^4\left(4w-\sqrt{6}\lambda\left(x^2+1\right)x+6x^2+2\right)+\left(x^2-1\right)y^2\left(x^2\left(3w-2\sqrt{6}\lambda x-3\right)+9w+3\right)\\&-\left(y^6\left(3w+\sqrt{6}\lambda x+3\right)\right),\end{aligned}\tag{4.79}$$

$$\begin{aligned}\mathcal{B} =&x\left(-3(w+1)x^4-6(w+2)x^2y^2-3(w-1)y^4\right.\\&\left.+3\left(w-2y^2+1\right)+\sqrt{6}\lambda x\left(x^4+\left(x^2+3\right)y^2-1\right)\right),\end{aligned}\tag{4.80}$$

and

$$y'=\frac{-4y^5\left(3w\left(x^2+y^2-1\right)-3x^2+\sqrt{6}\lambda x+3y^2-3\right)+k\mathcal{C}+k^2\mathcal{D}}{2\left(4y^4-8kxy^2+k^2\left(2x^2y^2+\left(x^2+1\right)^2+y^4-2y^2\right)\right)},\tag{4.81}$$

where

$$\begin{aligned}\mathcal{C} =&2y^3\left(6(w-1)x^3+6(w+3)x\left(y^2-1\right)\right.\\&\left.-2\sqrt{6}\lambda x^4-3\sqrt{6}\lambda x^2\left(y^2-2\right)-\sqrt{6}\lambda y^2\left(y^2-1\right)\right),\end{aligned}\tag{4.82}$$

$$\begin{aligned}\mathcal{D} =&y\left(-6wx^4-12(w+2)x^2\left(y^2-1\right)-6wy^2\left(y^2-2\right)-6w\right.\\&\left.+\sqrt{6}\lambda x\left(3x^4+x^2\left(4y^2-6\right)+y^4-1\right)\right).\end{aligned}\tag{4.83}$$

Let us remark that isolating the terms in powers of k allows us to consider the limit $k\to 0$ easily, where these equations reduce to those of [54]. These equations are quite cumbersome to deal with, and, in particular, finding the fixed points and their respective eigenvalues is quite a difficult task analytically since it involves very long expressions. However, there are some simple ones to find, which we outline in Table 4.4 below, and we remark that these do not constitute the full analysis of the model. In the next sections, we will provide a complete analysis for $w=0$.

Table 4.4: Some of the critical points for the non-constant interaction model, assuming $\lambda>0$.

Point	Coordinates (x,y)	Eigenvalues
Point O	$(0,0)$	$-3w,\quad 3(1+w)$
Point A_-	$(-1,0)$	$-3(1+w)-\sqrt{6}\lambda,\quad 3+\sqrt{\frac{3}{2}}\lambda$
Point A_+	$(1,0)$	$-3(1+w)+\sqrt{6}\lambda,\quad 3-\sqrt{\frac{3}{2}}\lambda$
Point B	$\left(\frac{\lambda}{\sqrt{6}},\frac{\sqrt{6-\lambda^2}}{\sqrt{6}}\right)$	$\frac{1}{2}\left(\lambda^2-6\right),\quad \lambda^2-3(1+w)$
Point C	$\left(\frac{\sqrt{3}}{\sqrt{2}(1+w)\lambda},0\right)$	$\frac{9(w+1)^2(w+3)-6\lambda^2(3w+1)}{4\lambda^2+6(w+1)^2},\quad \frac{9(w+1)^3-6\lambda^2(w+1)}{2\lambda^2+3(w+1)^2}$

4.5.2 *The matter-dominated case*

Since the non-constant coupling leads to a considerably more complicated dynamical system, we restrict our study to the matter dominated case $w = 0$. The dynamical equation for x is given by

$$x' = \frac{2y^4\left(3x^3 - 3x\left(y^2+1\right) + \sqrt{6}\lambda y^2\right) - k\,\mathcal{A} + k^2\,\mathcal{B}}{4y^4 - 8kxy^2 + k^2\left(x^4 + 2x^2\left(y^2+1\right) + \left(y^2-1\right)^2\right)}\,, \tag{4.84}$$

where the functions $\mathcal{A}$ and $\mathcal{B}$ are defined by

$$\mathcal{A} = y^2(x^2-1)(x^2(2\sqrt{6}\lambda x + 3) - 3) + 3y^4(\sqrt{6}\lambda(x^3+x) - 6x^2 - 2) + y^6(\sqrt{6}\lambda x + 3)\,, \tag{4.85}$$

$$\mathcal{B} = x\left[\sqrt{6}\lambda x(x^4 + (x^2+3)y^2 - 1) - 3(x^4 + 4x^2y^2 - y^4) - 6y^2 + 3\right]. \tag{4.86}$$

Similarly, the y equation reads

$$y' = \frac{-4y^5(-3x^2 + \sqrt{6}\lambda x + 3y^2 - 3) - k\,\mathcal{C} + k^2\,\mathcal{D}}{2\left(4y^4 - 8kxy^2 + k^2\left(x^4 + 2x^2\left(y^2+1\right) + \left(y^2-1\right)^2\right)\right)}\,, \tag{4.87}$$

where

$$\mathcal{C} = 2y^3\left(2\sqrt{6}\lambda x^4 + 6x^3 + 3\sqrt{6}\lambda x^2\left(y^2-2\right) - 18x\left(y^2-1\right) + \sqrt{6}\lambda y^2\left(y^2-1\right)\right)\,, \tag{4.88}$$

$$\mathcal{D} = xy\left(\sqrt{6}\lambda\left(3x^4 + x^2\left(4y^2-6\right) + y^4 - 1\right) - 24x\left(y^2-1\right)\right)\,. \tag{4.89}$$

Here a prime denotes a derivative with respect to the logarithm of the scale factor $\log(a)$.

We remark that the acceleration equation, which follows from Eq. (4.32) and Eq. (4.34), is

$$\frac{\dot{H}}{H^2} = \frac{6y^4\left(-x^2 + y^2 - 1\right) + k\,\mathcal{E} + k^2\,\mathcal{F}}{4y^4 - 8kxy^2 + k^2\left(x^4 + 2x^2\left(y^2+1\right) + \left(y^2-1\right)^2\right)} \tag{4.90}$$

where the functions $\mathcal{E}$ and $\mathcal{F}$ are given by

$$\mathcal{E} = \frac{\mathcal{C}}{2y} + 4\sqrt{6}\lambda x^2 y^2\,, \tag{4.91}$$

$$\mathcal{F} = x\left(12x\left(y^2-1\right) - \sqrt{6}\lambda\left(x^2+y^2-1\right)\left(2x^2+y^2\right)\right)\,. \tag{4.92}$$

4.5.2.1 *Critical points and stability*

To find the critical points, we need to solve the equations $x' = 0$ and $y' = 0$ simultaneously, which is a non-trivial task since both numerators are polynomials of degree seven, giving up to 49 roots. Many of those will lie outside the physical phase space, while others will come in complex conjugate pairs which also have no physical significance. At this point, it is not clear how many physical critical points this system will have for arbitrary λ and k, and, hence, one has to investigate the system carefully to extract them.

One way to find the critical points is to draw inspiration from the previous model. For example,

setting $y = 0$ in Eq. (4.87) leads to $y' = 0$, while setting $y = 0$ in Eq. (4.84) means that $x' = 0$ simplifies to

$$\frac{x\left(x^2-1\right)\left(\sqrt{6}\lambda x-3\right)}{1+x^2}=0\,. \tag{4.93}$$

This yields the first set of critical points $(-1,0)$, $(0,0)$, $(1,0)$, and $(\sqrt{3/2}\,/\lambda,0)$.

Secondly, we investigate critical points on the unit circle. By substituting $x = \cos\theta$ and $y = \sin\theta$ into Eq. (4.84) and Eq. (4.87), at a critical point we obtain

$$\frac{1}{2}\left(\sqrt{6}\lambda-6\cos\theta\right)\sin^2\theta=0\,, \tag{4.94}$$

$$\frac{1}{2}\left(\sqrt{6}\lambda-6\cos\theta\right)\sin\theta\cos\theta=0\,. \tag{4.95}$$

This gives another critical point at $(\lambda/\sqrt{6},\sqrt{1-\lambda^2/6})$.

Lastly, one can verify that setting $x_0 = \sqrt{3}\,/(\sqrt{2}\lambda)$ in the dynamical equations gives four additional solutions, other than $y_0 = 0$, which are

$$\left(\widehat{y}_{\pm}\right)^2=\frac{6+\sqrt{6}k\lambda}{8\lambda^2}\pm\frac{1}{8\lambda^2}\sqrt{36+2k\lambda\left(3k\lambda+2\sqrt{6}\left(4\lambda^2-15\right)\right)}\,. \tag{4.96}$$

We are not able to find other critical points in the physical phase space, either analytically or numerically. The critical points discussed above are summarised in Table 4.5, together with the corresponding values of the effective equation of state parameter and of the deceleration parameter. Note that there will be parameter regions where the critical points with y-coordinate $\widehat{y}_{\pm}$, called Point D_- and Point D_+, may not exist or where only one of these exits, see Fig. 4.9.

Table 4.5: Critical points of the dynamical system given in Eqs. (4.84) and (4.87), for which an explicit expression could be found.

Point	Coordinates (x,y)	$\widetilde{w}$	q	Existence
Point O	$(0,0)$	-1	-1	for all λ, k
Point A_-	$(-1,0)$	1	2	for all λ, k
Point A_+	$(1,0)$	1	2	for all λ, k
Point B	$\left(\lambda/\sqrt{6},\sqrt{1-\lambda^2/6}\right)$	$-1+\lambda^2/3$	$-1+\lambda^2/2$	$\lambda\leq\sqrt{6}$
Point C	$\left(\sqrt{3}\,/(\sqrt{2}\lambda),0\right)$	$-1+12/(3+2\lambda^2)$	$-1+18/(3+2\lambda^2)$	$\lambda\neq 0$
Point D_+	$\left(\sqrt{3}\,/(\sqrt{2}\lambda),\widehat{y}_+\right)$	0	$1/2$	see Fig. 4.9
Point D_-	$\left(\sqrt{3}\,/(\sqrt{2}\lambda),\widehat{y}_-\right)$	0	$1/2$	see Fig. 4.9

The stability properties of the critical points Point O, Point A_-, Point A_+, Point B, and Point C are straightforward to investigate and are collected in Table 4.6.

However, for Point D_- and Point D_+, the closed form expressions for the eigenvalues are very long and do not offer physical insight. However, when presenting specific cases, we give numerical

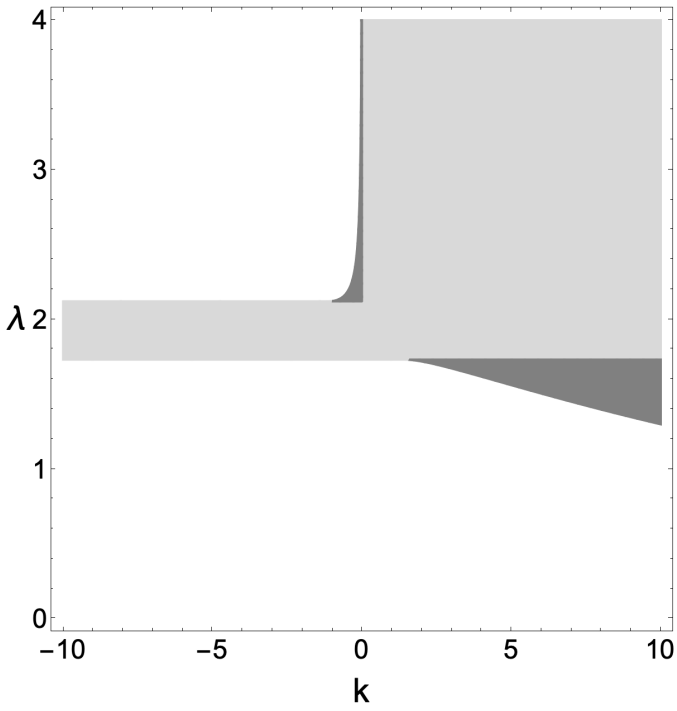

Fig. 4.9: Existence of Point D_+ and Point D_-: Point D_+ exists in the whole shaded region; Point D_- exists only in the dark grey region.

Table 4.6: Stability properties of the critical points for the non-constant interaction model, assuming $\lambda > 0$.

Point	Eigenvalues	Classification
Point O	$3, \quad 0$	unstable
Point A_-	$-\sqrt{6}\lambda - 3, \quad \sqrt{\frac{3}{2}}\lambda + 3$	saddle point ($\lambda > 0$)
Point A_+	$3 - \sqrt{\frac{3}{2}}\lambda, \quad \sqrt{6}\lambda - 3$	unstable node if $\sqrt{3/2} < \lambda < \sqrt{6}$ saddle if $\lambda < \sqrt{3/2}$ or $\lambda > \sqrt{6}$
Point B	$\frac{1}{2}\left(\lambda^2 - 6\right), \quad \lambda^2 - 3$	stable if $\lambda < \sqrt{3}$ saddle if $\sqrt{3} < \lambda < \sqrt{6}$ unstable if $\lambda > \sqrt{6}$
Point C	$\frac{18}{2\lambda^2+3} - \frac{3}{2}, \quad \frac{18}{2\lambda^2+3} - 3$	unstable if $\lambda < \sqrt{3/2}$ saddle if $\sqrt{3/2} < \lambda < 3/\sqrt{2}$ stable if $\lambda > 3/\sqrt{2}$

values for the eigenvalues and discuss the various critical points in more detail.

From Table 4.5, we observe that Point C has an effective equation of state parameter $\widetilde{w} < -1/3$ if $\lambda < \sqrt{15/2}$, and it is not located on the boundary of the phase space. For such a choice of λ, we note $\sqrt{15/2} > 3/\sqrt{2}$, which means that this point will be an attractor of the dynamical system. In turn, such a model will naturally give rise to a period of late-time accelerated expansion. Moreover, since $\sqrt{15/2} > \sqrt{6}$, Point B does not exist in this case.

The point where the two parts of the physical phase space meet (recall Eqs. (4.76) and (4.77)) is not, in general, a critical point. It is, however, a removable singularity for the dynamical system given in Eqs. (4.84) and (4.87), since both the denominators and numerators vanish, but in the limit, x' and y' have finite values. This point is mathematically interesting as it is a point in the phase space where trajectories can cross, in fact multiple trajectories accumulate at this point because the assumptions of the Picard–Lindelöf theorem for existence and uniqueness of solutions do not hold; see discussion in Section 1.3. Physically, it is always a point of accelerated expansion (since $q = -1$) and it is dark energy-dominated (since $\widetilde{w} = -1$); hence, it is a de Sitter point.

4.5.2.2 *Phase space diagrams and physical interpretation.*

Different choices of λ and k result in rather different cosmological models, since the number of critical points and their location vary significantly. Below we consider several cases which illustrate the diversity of the dynamical behaviour exhibited by the model. We select values of λ and k systematically, but do not necessarily include every possible scenario which could arise in these models.

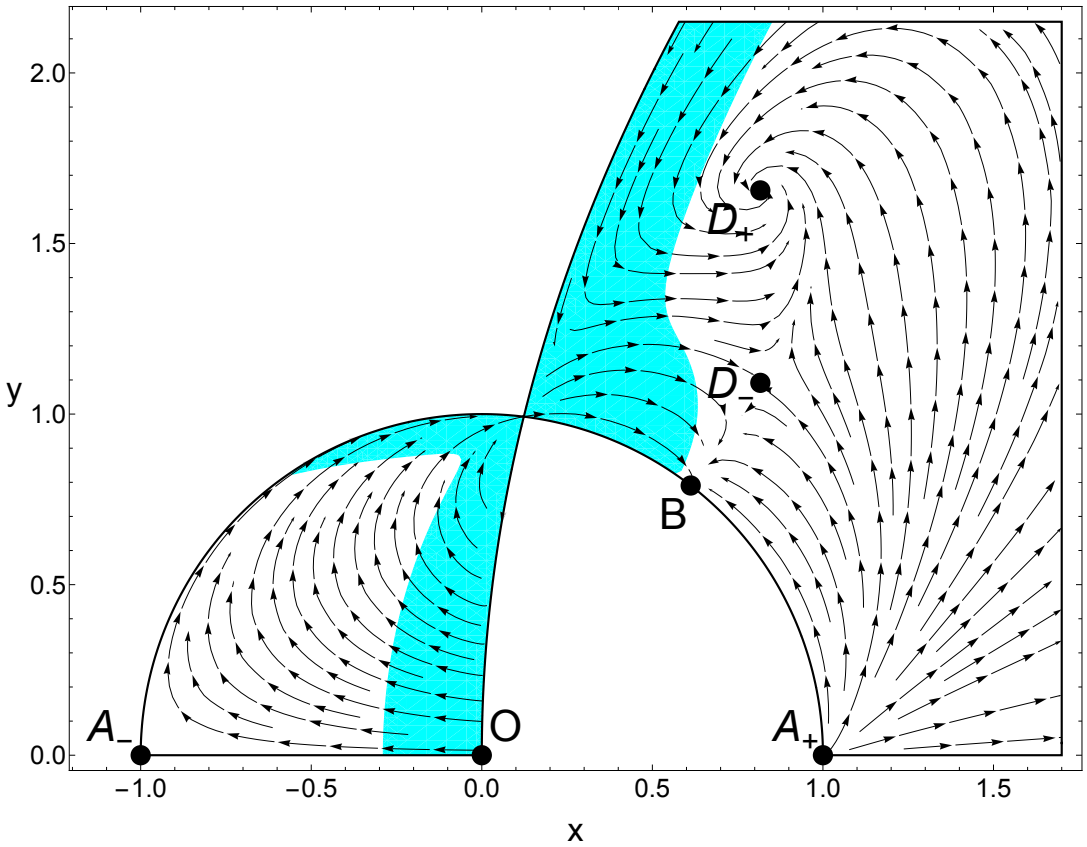

Fig. 4.10: The parameter values are $\lambda = 3/2$ and $k = 8$. The eigenvalues corresponding to Point D_+ are $-0.75 \pm 1.3713\mathrm{i}$ and the eigenvalues corresponding to Point D_- are -2.1570 and 0.6570. The shaded area represents the part of the phase space where there is accelerated expansion.

Case (i). We begin with $\lambda = 3/2$ and $k = 8$, as shown in Fig. 4.10. In this case, Point C does not exist, however, the other six critical points do exist. The phase space contains a region of accelerated expansion and we note that only Point O is in this region. Point O is an early-time attractor of the phase space, hence, this point could correspond to an early-time universe undergoing accelerated expansion. The other early-time attractor is Point A_+ which has an effective equation of state parameter $\widetilde{w} = 1$, and corresponds to the scalar field's kinetic energy being dominant. Trajectories starting at O will eventually reach the stable point, Point B, where the effective equation of state parameter is $\widetilde{w} = -1/4$. We note that this is negative but not less than $-1/3$, and therefore, not accelerating. Depending on the initial conditions chosen, some trajectories will approach Point D_- with $\widetilde{w} = 0$, which is matter dominated. On the other hand, trajectories starting in the proximity of Point A_+ will either also terminate at Point B, or reach Point D_+. This latter point is a stable spiral with $\widetilde{w} = 0$, and hence corresponds to a matter dominated universe. It is interesting to note that trajectories in this case can briefly go through a region of accelerated expansion before reaching Point D_+. While these parameter values yield an interesting phase space with a rich structure, this specific model has limited applicability for modern cosmology, since the stable fixed points do not lie within the accelerated region of the phase space.

Case (ii). Next, we consider the case $\lambda = \sqrt{3}$ and $k = \sqrt{8}$, see Fig. 4.11. In this particular case, Point D_- coincides with Point B for all k. As in the previous case, Point C does not exist in the physical phase plane. Point O, as before, is an unstable node and acts as an early-time attractor. Point A_- is a saddle and Point A_+ corresponds to the to other possible early-time attractor. According to Table 4.6, we note that Point B has eigenvalues 0 and $-3/2$, which means that we are dealing with a non-hyperbolic point. This point is a centre and one can verify that it is unstable. While this can be shown rigorously, it essentially follows from the fact that trajectories near Point B move towards the attractor, Point D_+, which is a stable spiral. It has eigenvalues $-3/4 \pm \mathrm{i}\sqrt{15}/4$. Similar to the previous case, Point O is an early-time attractor corresponding to an early-time universe undergoing accelerated expansion. There is no late-time attractor within the acceleration region.

Case (iii). We will briefly comment on the case where $\lambda = 3/\sqrt{2}$ and $k = 2/\sqrt{3}$, shown in Fig. 4.12. For this particular choice, Point C and Point D_- do not exist, while Point D_+ is located at the intersection of the two regions of the phase space. This case is mathematically quite interesting, however, less so from a physical point of view. Of mathematical interest are the following facts: Point D_+ is a point of discontinuity of the system. The stability matrix is singular

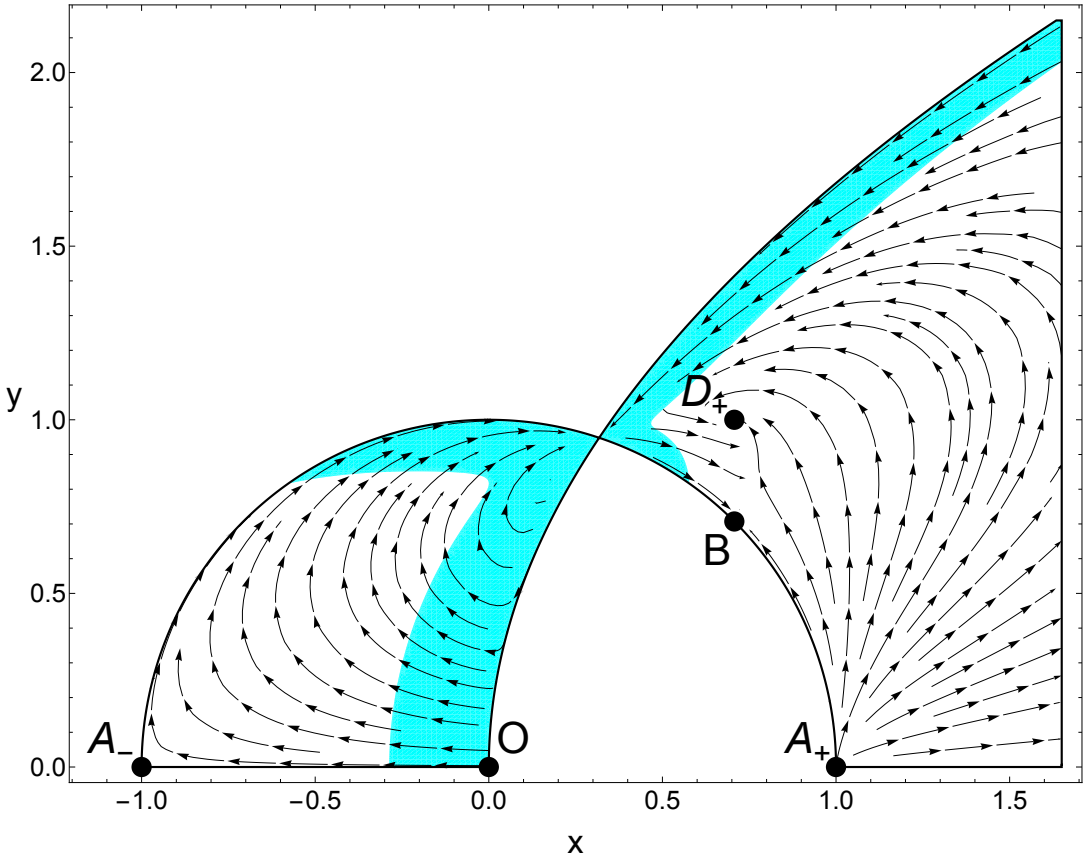

Fig. 4.11: The parameter values are $\lambda = \sqrt{3}$ and $k = \sqrt{8}$. Point B is an unstable centre and Point D_+ is a stable spiral. The shaded region represents the part where the phase space is accelerating.

at this point, meaning that linear stability theory cannot be used. We will not discuss this case further since it does not represent a physically meaningful scenario.

Case (iv). Next, we consider the case $\lambda = k = 1$, which turns out to be physically interesting as a cosmological model, see Fig. 4.13. There are two unstable nodes, Point O and Point C, which act as early-time attractors. As in the previous cases, Point O corresponds to an early-time universe undergoing accelerated expansion. Trajectories starting near Point O will eventually leave the acceleration region and be partially attracted to the saddle, Point A_-, after which they will reach the late-time attractor, the stable node at Point B. This point is also in the accelerated region, which means that this model not only allows for early-time acceleration (inflation) but also for late-time accelerated expansion. The effective equation of state parameter at Point B is $\widetilde{w} = -2/3$, as can be seen from Table 4.5. All trajectories starting out in the right part of the phase space will also be attracted to Point B, making this the global attractor of the system. We remark that, in this sense, the dynamical behaviour is similar to that shown in Fig. 4.5.

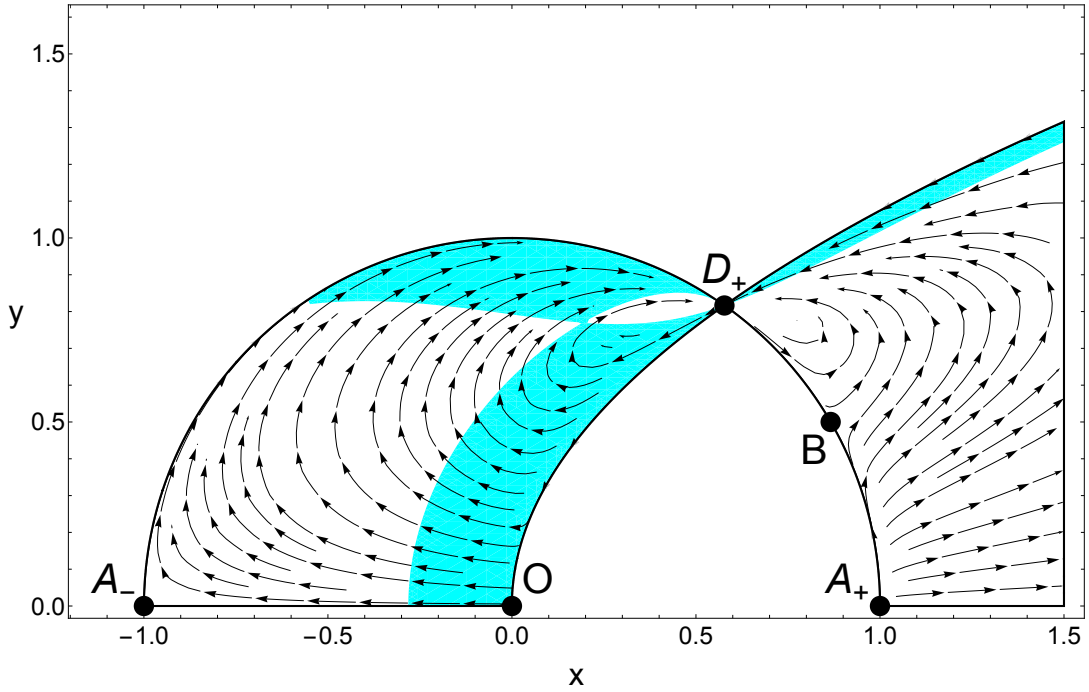

Fig. 4.12: The parameter values are $\lambda = 3/\sqrt{2}$ and $k = 2/\sqrt{3}$. The shaded region represents the part where the phase space is accelerating.

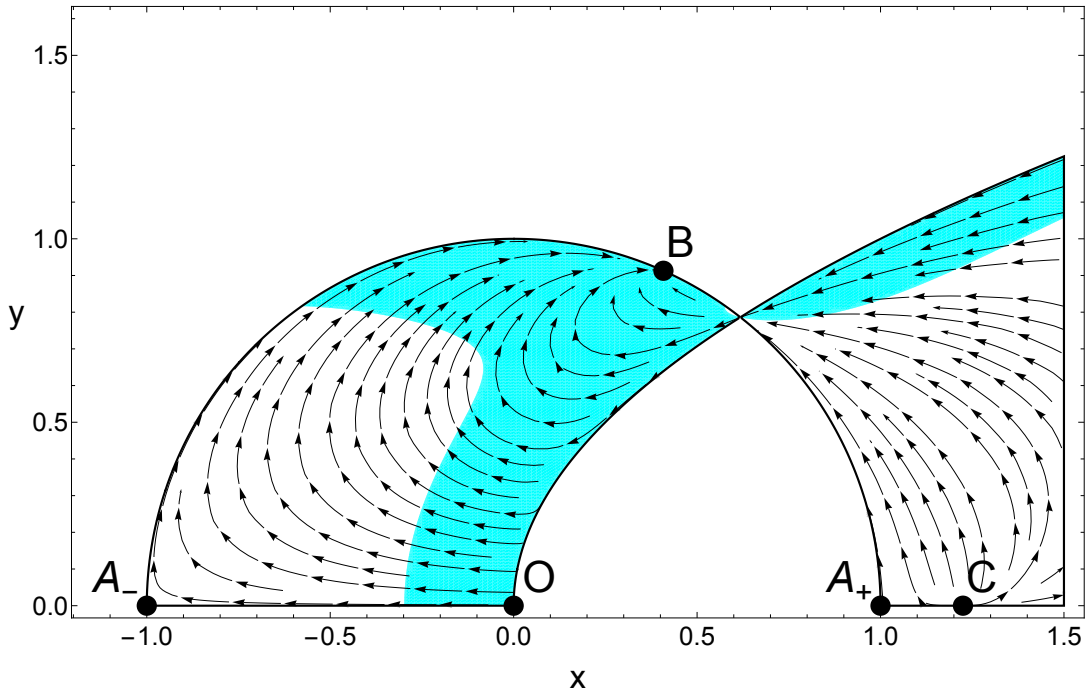

Fig. 4.13: The parameter values are $\lambda = 1$ and $k = 1$. The shaded region represents the part where the phase space is accelerating.

Case (v). We now present the case $\lambda = 1$ and $k = 20$, see Fig. 4.14. Here all the fixed points we found analytically exist within the physical phase space. This model not only has a rich dynamical structure, but is also of physical relevance. We have two early-time attractors, Point O in the

acceleration region, similar to the previous models, and Point C. Notice that Point C always satisfies $\widetilde{w} > 1$, and so is not of physical interest. We are therefore most interested in trajectories starting near Point O. These will initially move towards Point A_-, before leaving the left part of the phase space. By doing so, they will enter the acceleration region and move towards Point B where $\widetilde{w} = -2/3$. Other than the various complications introduced by the other critical points, and the more complicated phase space structure, the physical situation is again somewhat similar to those shown in Fig. 4.5 and Fig. 4.13. Let us also mention that Point D_+ represents scaling solutions as the effective equation of state parameter is zero, and the universe evolves as if it were only matter dominated while also containing the scalar field.

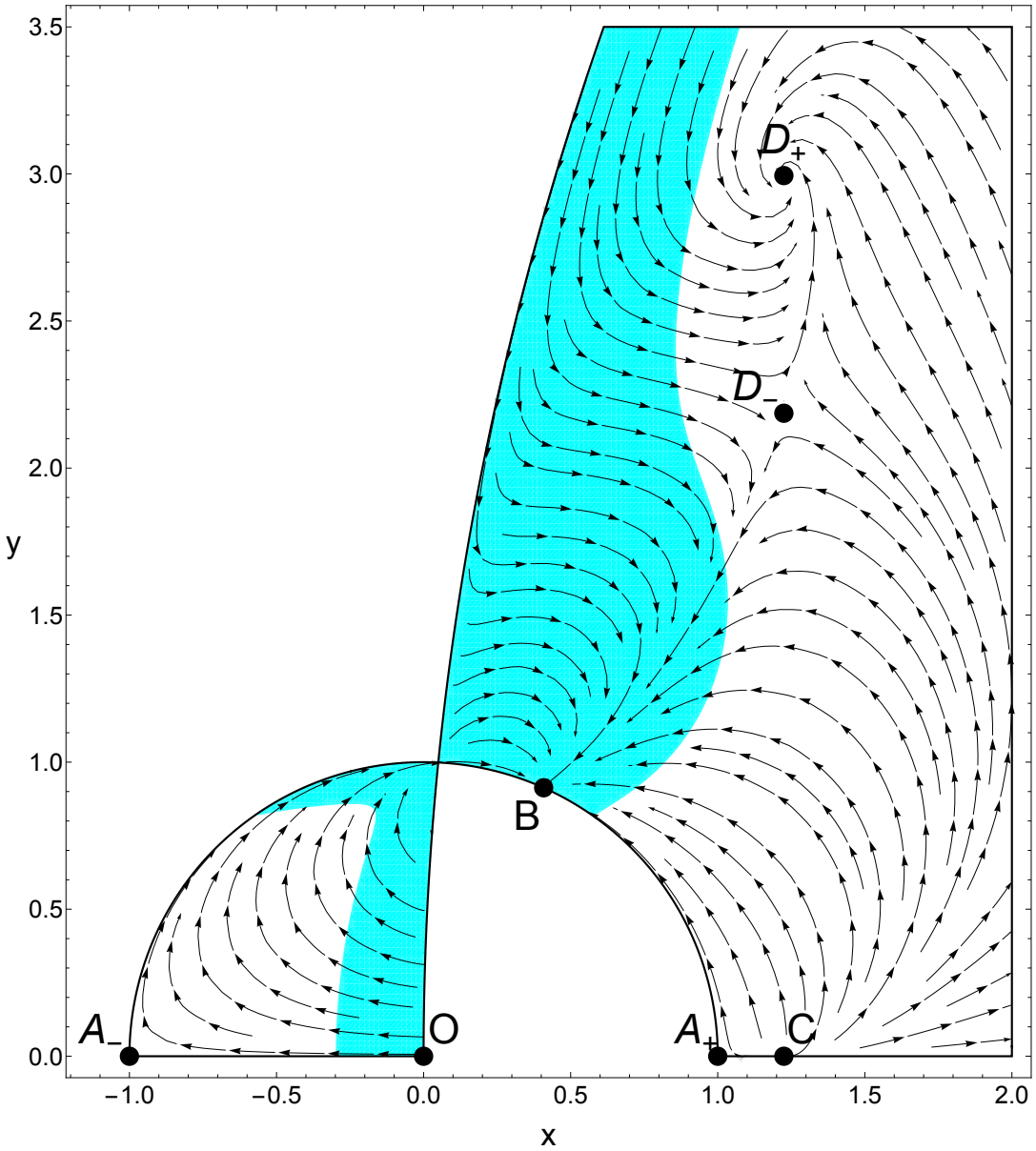

Fig. 4.14: The parameter values are $\lambda = 1$ and $k = 20$. The eigenvalues corresponding to Point D_+ are -0.75 ± 1.1119i and the eigenvalues corresponding to Point D_- are -2.3406 and 0.8406. The shaded area represents the part of the phase space where there is accelerated expansion.

Case (vi). To complete this section, we consider a case where the sign of the coupling is negative. We set $k = -1/4 < 0$ and $\lambda = \sqrt{5}$, and the phase plane is shown in Fig. 4.15. This model displays significantly different features than the cases where the coupling is positive. Point O can still be seen as an early-time attractor in the acceleration region. Depending on the chosen initial condition, trajectories will either terminate at Point D_+ or Point C. Such trajectories can come close to the saddle Point D_-, where $\widetilde{w} = 1/2$. However, the effective equation of state parameter is also quite large at the other two points, meaning that one cannot have a model with a late-time behaviour close to a matter dominated universe. None of the late-time attractors appear in the acceleration region. While this model displays many interesting mathematical features, it appears to be of more limited physical relevance.

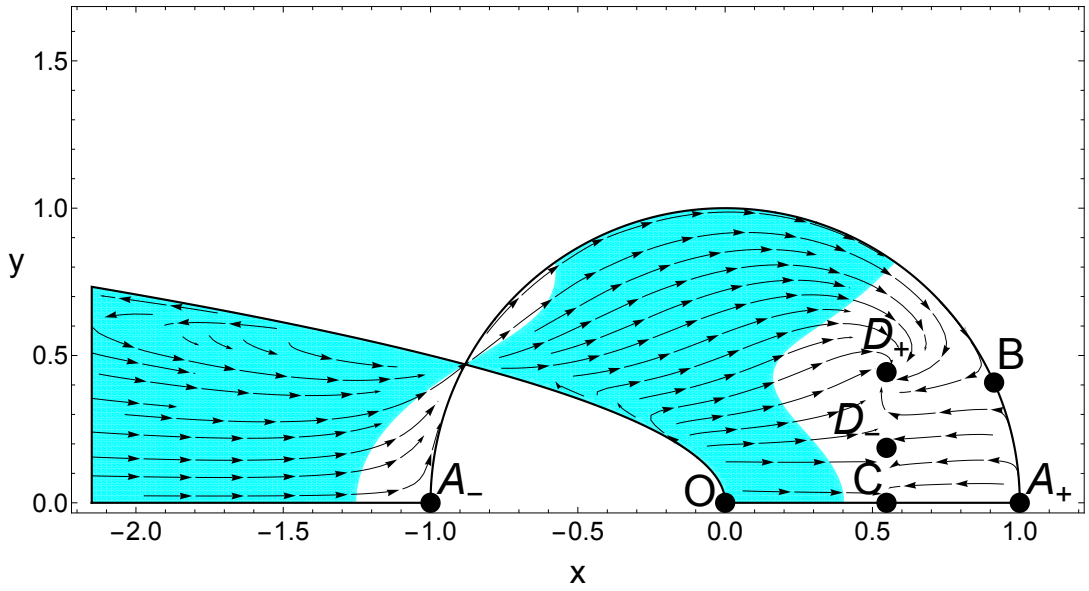

Fig. 4.15: The parameter values are $\lambda = \sqrt{5}$ and $k = -1/4$. The eigenvalues corresponding to Point D_+ are -0.75 ± 0.3654i and to Point D_- are -1.6598 and 0.1598. The shaded area represents the part of the phase space where there is accelerated expansion.

4.6 Quintessence with exponential potential in (x, σ)-coordinates

The model we will present in Section 4.7 is more simply investigated if we eliminate the variable y, and hence study it in the (x, σ)-plane. In order to have a baseline model with which we can compare our results, we now look at the quintessence model with exponential potential studied in [54], and summarised in Section 2.10, but solve the Friedmann constraint for y, as opposed to σ. We remark that, in Section 2.10, the dynamical variable σ^2 is denoted by Ω^2. Here we use the variables we defined in Eq. (4.36) and, therefore, Eq. (2.141) reads

$$1 = x^2 + y^2 + \sigma^2 \,. \tag{4.97}$$

Since, in the case of an exponential potential, we have that $V \geq 0$, the constraint yields

$$1 \geq 1 - x^2 - \sigma^2 = y^2 \geq 0\,, \tag{4.98}$$

whence we can deduce that the physical phase space is contained in the unit circle

$$0 \leq x^2 + \sigma^2 \leq 1\,. \tag{4.99}$$

Furthermore, since $\rho \geq 0$, that is, $\sigma \geq 0$, we can restrict our analysis to the upper half disc. Solving for y yields the following dynamical equations for x' and σ'

$$x' = \frac{3}{2}x\left(\sigma^2(w+1) + 2x^2 - 2\right) - \sqrt{\frac{3}{2}}\lambda\left(\sigma^2 + x^2 - 1\right), \tag{4.100}$$

$$\sigma' = \frac{3}{2}\sigma\left(\left(\sigma^2 - 1\right)(w+1) + 2x^2\right). \tag{4.101}$$

We recall that the prime denotes differentiation with respect to $\log(a)$. We also note that the system is invariant under the transformation $\sigma \mapsto -\sigma$. The properties of the dynamical system depend on the values of the constants λ and w. The acceleration equation in terms of x and σ reads

$$\frac{\dot{H}}{H^2} = -\frac{3}{2}\left((w+1)\sigma^2 + 2x^2\right), \tag{4.102}$$

and the deceleration parameter q reads

$$q = -1 - \frac{\dot{H}}{H^2} = \frac{3}{2}(w+1)\sigma^2 + 3x^2 - 1. \tag{4.103}$$

From Eq. (4.102), one can find a at any fixed point (x^*, σ^*) of the phase space, that is,

$$a \propto (t - t_0)^{2/\left(6x_0^2 + 3(1+w)\sigma_0^2\right)}. \tag{4.104}$$

By noticing that we can define the effective (or total) energy density and pressure of the system as

$$\widetilde{\rho} = \rho + \tfrac{1}{2}\dot{\phi}^2 + V, \tag{4.105}$$

$$\widetilde{p} = p + \tfrac{1}{2}\dot{\phi}^2 - V, \tag{4.106}$$

and hence, an effective equation of state parameter, $\widetilde{w}$, in terms of the dimensionless variables and using the acceleration equation, Eq. (4.102),

$$\widetilde{w} = \frac{\widetilde{p}}{\widetilde{\rho}} = -1 + 2x_0^2 + (1+w)\sigma_0^2. \tag{4.107}$$

This allows us to re-write Eq. (4.104) as

$$a \propto (t - t_0)^{2/(3(1+\widetilde{w}))}\,. \tag{4.108}$$

The critical points of the dynamical system, Eqs. (4.100) and (4.101), are given in Table 4.7. We

Table 4.7: Critical points for Eqs. (4.100) and (4.101).

Point	Coordinates (x, σ)	Existence	$\widetilde{w}$	q
Point A_-	$(-1, 0)$	for all λ, w	1	2
Point A_+	$(1, 0)$	for all λ, w	1	2
Point B	$\left(\sqrt{\frac{3}{2}}\frac{w+1}{\lambda}, \frac{\sqrt{\lambda^2-3w-3}}{\lambda}\right)$	$\lambda^2 \geq 3(1+w)$	w	$\frac{1}{2}(3w+1)$
Point C	$\left(\lambda/\sqrt{6}, 0\right)$	for all λ, w	$\frac{\lambda^2}{3} - 1$	$\frac{\lambda^2}{2} - 1$
Point D	$(0, 1)$	for all w	w	$\frac{1}{2}(3w+1)$

notice the following features. At Point A_+ and Point A_-, the universe is dominated by the scalar field kinetic energy (i.e. $x^2 = 1$). The effective equation of state is that of a stiff fluid (i.e. $\widetilde{w} = 1$) and there is no acceleration as we can see from the value of the deceleration parameter, that is, $q = 2$. Moreover, as we can see from Eq. (4.108), the universe expands according to $a \propto t^{1/3}$. The existence of these fixed points is always guaranteed for all values of λ and w. Point B represents the *scaling solution*, where the effective equation of state reduces to the matter component equation of state. For physical values of w, we have $q < 0$, which means that there is acceleration only when $-1 \leq w < -1/3$; otherwise, there is no acceleration. Point C. The universe is completely dominated by the scalar field. However, unlike the case of (x, y)-coordinates, this point does not always lie within the unit circle, but only when $\lambda < \sqrt{6}$. We also notice that the effective equation of state parameter implies an accelerating universe for $\lambda^2 < 2$, that is, a power-law inflationary expansion ($\ddot{a} > 0$). When $\lambda \to 0$, we restore a de Sitter expansion solution dominated by a cosmological constant. Point D. This point behaves like the origin in the (x, y)-coordinates, and correspond to a matter dominated universe as $\sigma^2 = 1$. Its existence is guaranteed for all values of λ and w. Here, the effective equation of state parameter reduces to the matter equation of state parameter, and the universe expansion is dominated by the matter component (as opposed to the scalar field component). Similarly to Point B, there is acceleration only when $-1 \leq w < -1/3$.

We outline the stability analysis in Table 4.8.

We now consider how the different values of the parameters λ and σ yield different dynamics. In particular, for $\lambda > 0$, we can identify the following five regions in the (w, λ)-plane, as shown in Figure 4.16.

We briefly comment on the dynamics for each region as well as its cosmological implications.

Region I. In this region, all fixed points exist except Point B. In particular, we have that Point A_- and Point A_+ are both unstable, Point D is a saddle, and Point C is the attractor (stable node), which lies in the region of accelerated expansion. This is illustrated, for the case $w = 0$ (matter-domination), in Fig. 4.17.

Table 4.8: Stability of the critical points for system given in Eqs. (4.100) and (4.101). Here $\delta = \sqrt{(w-1)\left[(9w+7)\lambda^2 - 24(w+1)^2\right]}$.

Point	Eigenvalues	Classification
Point A_-	$-\frac{3}{2}(w-1)\,, \quad 6+\sqrt{6}\lambda$	unstable if $\lambda \geq -\sqrt{6}$ saddle if $\lambda < -\sqrt{6}$
Point A_+	$-\frac{3}{2}(w-1)\,, \quad 6-\sqrt{6}\lambda$	unstable if $\lambda \leq \sqrt{6}$ saddle if $\lambda > \sqrt{6}$
Point B	$\frac{3}{4\lambda}\left[\lambda(w-1) \pm \delta\right]$	stable node if $3(1+w) < \lambda^2 < \frac{24(w+1)^2}{9w+7}$ stable spiral if $\lambda^2 \geq \frac{24(w+1)^2}{9w+7}$
Point C	$\frac{1}{2}\left(\lambda^2-6\right), \quad \frac{1}{2}\left(\lambda^2-3w-3\right)$	stable if $\lambda^2 < 3(1+w)$ saddle if $3(1+w) \leq \lambda^2 < 6$
Point D	$\frac{3}{2}(w-1)\,, \quad 3(w+1)$	saddle

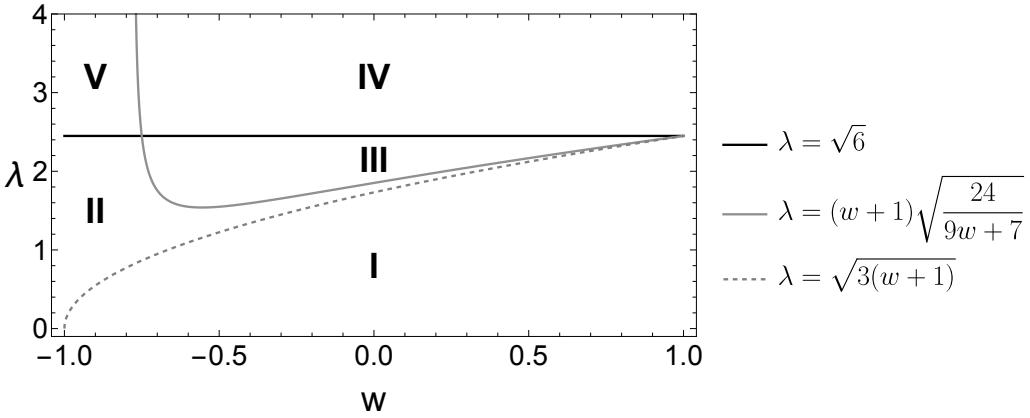

Fig. 4.16: Existence and stability regions in (w, λ)-plane. The plotted curves follow from the stability criteria shown in Table 4.8.

Region II and Region III. Here all fixed points exist. Point A_+ and Point A_- are both unstable, Point C and Point D are both saddle points. In Region II, Point B is a stable node, whereas, in Region III, Point B is a stable spiral. Hence, the main difference with Region I is that Point B is now the late-time attractor, but it lies outside the region of accelerated expansion. This means that Point B does not describe an inflationary solution. This is illustrated in Fig. 4.18, where we set, for the sake of example, $w = 0$ and $\lambda = 2$ (Region III).

Region IV and Region V. In this region, there are only four fixed points within the physical phase space. Point C exists but does not lie within it. More specifically, Point A_- is unstable, Point A_+ is a saddle, and Point D is a saddle. In Region IV, Point B is a stable spiral, whilst, in Region V, Point B is a stable node. Let us remark, however, that Region V is not wholly physically relevant as it emerges for negative values of w, close to $w = -1$. We show an example of Region IV in Fig. 4.19, where we fixed $w = 0$ and $\lambda = 3$.

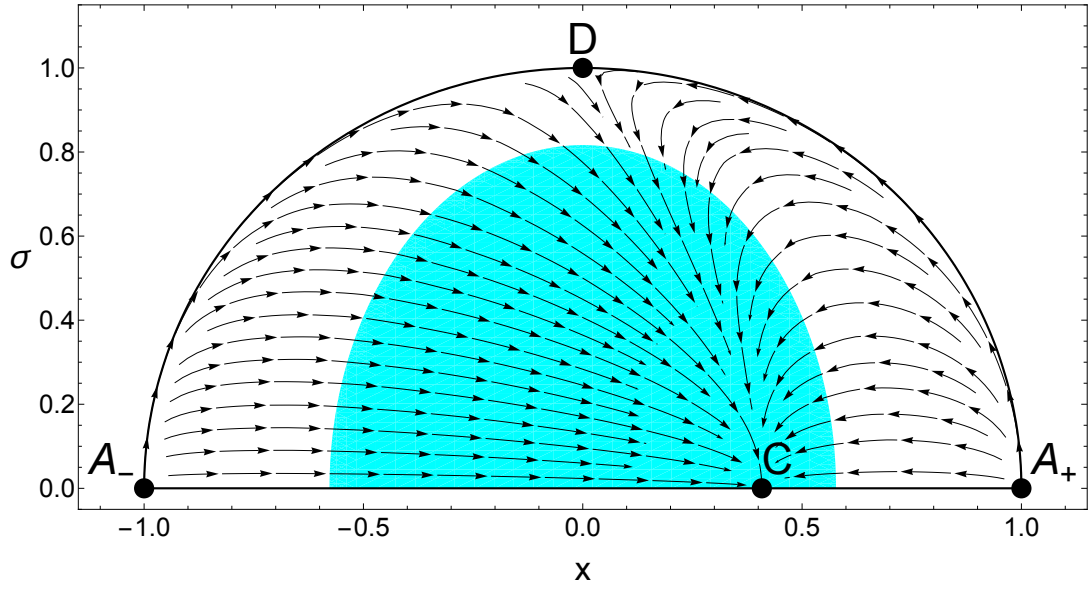

Fig. 4.17: Phase space with $w = 0$ and $\lambda = 1$. The shaded region represents the part where the phase space is accelerating.

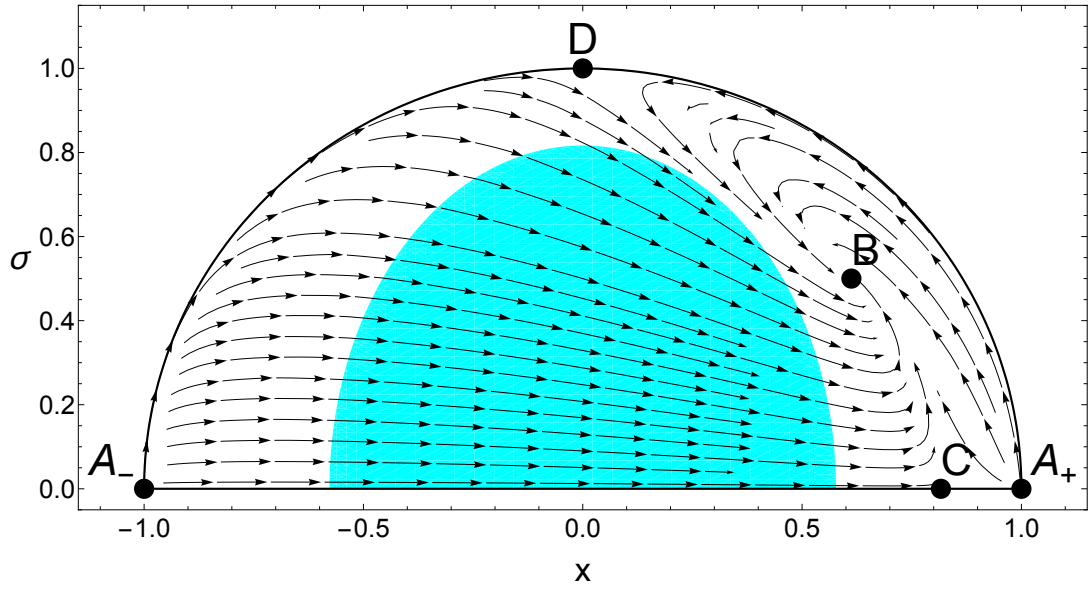

Fig. 4.18: Phase space with $w = 0$ and $\lambda = 2$. The shaded region represents the part where the phase space is accelerating.

As we can notice, the dynamics in the (x, σ)-coordinates is similar to that in the (x, y)-plane provided in [54]. Both encapsulate the same type of dynamics from a slightly different perspective.

We are now ready to use this approach to study another example of a non-constant interaction model. As we shall see, solving the Friedmann constraint for y yields a simpler system of differential equations to study.

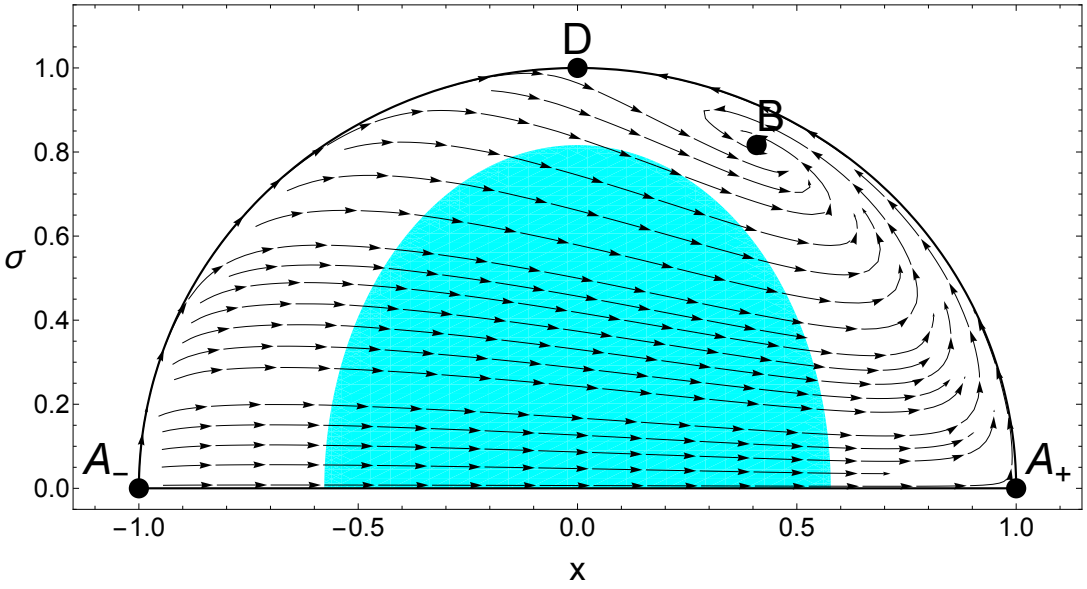

Fig. 4.19: Phase space with $w = 0$ and $\lambda = 3$. The shaded region represents the part where the phase space is accelerating.

4.7 Non-constant interaction model $\alpha = -2$

Consider the interaction term introduced in Eq. (4.70) and set $\alpha = -2$; then Eq. (4.71) reads

$$1 - x^2 - y^2 - \sigma^2 + k\,x\frac{y^2}{\sigma^2} = 0 \iff \sigma^2\left(1 - x^2 - y^2 - \sigma^2\right) + kxy^2 = 0, \tag{4.109}$$

$$\iff \sigma^2\left(1 - x^2 - \sigma^2\right) + y^2\left(kx - \sigma^2\right) = 0 \tag{4.110}$$

$$\iff y^2 = \frac{\sigma^2\left(1 - x^2 - \sigma^2\right)}{\sigma^2 - kx}\,, \tag{4.111}$$

which indicates one may eliminate y from the equations to keep the dynamical system two-dimensional. Moreover, since our potential is positive definite, $y \geq 0$, and $y^2 \geq 0$. Hence,

$$\frac{\sigma^2\left(1 - x^2 - \sigma^2\right)}{\sigma^2 - kx} \geq 0\,. \tag{4.112}$$

In the same way as we had for Eq. (4.73), this yields a physical phase space bounded by a line, a circle, and a parabola, consisting of a bounded and an unbounded region given by

$$1 - x^2 - \sigma^2 \geq 0 \quad \text{and} \quad \sigma^2 - kx > 0\,, \tag{4.113}$$

$$\text{or} \quad 1 - x^2 - \sigma^2 \leq 0 \quad \text{and} \quad \sigma^2 - kx < 0\,, \tag{4.114}$$

together with a single point where these meet, with (x, σ) coordinates

$$\left(\frac{1}{2}\left(\sqrt{k^2+4} - k\right), \sqrt{\frac{k}{2}(\sqrt{k^2+4} - k)}\right) \quad \text{for } k > 0\,, \tag{4.115}$$

$$\left(-\frac{1}{2}\left(\sqrt{k^2+4} + k\right), \sqrt{-\frac{k}{2}\left(\sqrt{k^2+4} + k\right)}\right) \quad \text{for } k < 0\,. \tag{4.116}$$

Again, trajectories may traverse this point to pass from one part of the region to the other.

For $\alpha = -2$, the dynamical system then reads

$$x' = \frac{2\sigma^4\left(3x\left(\sigma^2(w+1)+2x^2-2\right)-\sqrt{6}\lambda\left(\sigma^2+x^2-1\right)\right)+k\mathcal{A}+k^2\mathcal{B}}{4\sigma^4-8k\sigma^2x+k^2\left(\sigma^4-2\sigma^2+2\sigma^2x^2+\left(x^2+1\right)^2\right)}, \tag{4.117}$$

where $\mathcal{A}$ and $\mathcal{B}$ are given by

$$\begin{aligned}\mathcal{A} =& \sigma^6\left(3w+\sqrt{6}\lambda x+3\right)+\sigma^4\left(x^2\left(-9w+4\sqrt{6}\lambda x+9\right)-3(3w+5)\right)\\ &+\sigma^2\left(x^2-1\right)\left(x\left(\sqrt{6}\lambda\left(3x^2+1\right)-6x\right)-6(w+2)\right),\end{aligned} \tag{4.118}$$

$$\begin{aligned}\mathcal{B} =& x\left(6\sigma^4-3\left(\sigma^2+w+1\right)+3(w+1)x^4+3\sigma^2\left((3w+1)x^2+w\right)\right.\\ &\left.+\sqrt{6}\lambda x\left(\sigma^4-2\sigma^2-x^4+1\right)\right),\end{aligned} \tag{4.119}$$

and

$$\sigma' = \frac{12\sigma^5\left(\left(\sigma^2-1\right)(w+1)+2x^2\right)+k\mathcal{C}+k^2\mathcal{D}}{2\left(4\sigma^4-8k\sigma^2x+k^2\left(\sigma^4-2\sigma^2+2\sigma^2x^2+\left(x^2+1\right)^2\right)\right)}, \tag{4.120}$$

where $\mathcal{C}$ and $\mathcal{D}$ are given by

$$\begin{aligned}\mathcal{C} =& 2\sigma^3\left(\sqrt{6}\lambda\left(\sigma^2-1\right)^2-12\left(\sigma^2-1\right)wx+3\sqrt{6}\lambda x^4\right.\\ &\left.-12x^3+4\sqrt{6}\lambda\left(\sigma^2-1\right)x^2\right),\end{aligned} \tag{4.121}$$

$$\begin{aligned}\mathcal{D} =& \sigma\left(3(w+3)\left(\left(\sigma^2-1\right)^2+x^4\right)+6\left(\sigma^2-1\right)(3w+1)x^2\right.\\ &\left.-4\sqrt{6}\lambda\left(x^5+\left(\sigma^2-1\right)x^3\right)\right).\end{aligned} \tag{4.122}$$

Similarly to the case $\alpha = 2$, the equations of the dynamical system for arbitrary w are quite lengthy and hard to manage analytically, and they also have the property that, as $k \to 0$, we retrieve the model studied in [54], but in (x, σ)-coordinates, as illustrated in Section 4.6.

4.7.1 *The matter-dominated case*

To make more concrete statements about this model, let us consider when we fix w to zero, that is, in the case of matter-dominated universe. In this case, Eqs. (4.117) and (4.120) become

$$x' = \frac{2\sigma^4\left(x^2-1\right)\left(6x-\sqrt{6}\lambda\right)+2\sigma^6\left(3x-\sqrt{6}\lambda\right)+k\mathcal{A}+k^2\mathcal{B}}{4\sigma^4-8k\sigma^2x+k^2\left(\left(\sigma^2-1\right)^2+x^4+2\left(\sigma^2+1\right)x^2\right)}, \tag{4.123}$$

where

$$\begin{aligned}\mathcal{A} =& \sigma^2\left(\left(x^2-1\right)\left(x\left(\sqrt{6}\lambda\left(3x^2+1\right)-6x\right)-12\right)\right.\\ &\left.+\sigma^2\left(x^2\left(4\sqrt{6}\lambda x+9\right)-15\right)+\sigma^4\left(\sqrt{6}\lambda x+3\right)\right),\end{aligned} \tag{4.124}$$

$$\mathcal{B} = x\left(6\sigma^4-3\sigma^2-\sqrt{6}\lambda x^5+3x^4+3\sigma^2x^2+\sqrt{6}\lambda\left(\sigma^2-1\right)^2x-3\right), \tag{4.125}$$

and

$$\sigma' = \frac{12\sigma^5\left(\sigma^2+2x^2-1\right)+k\mathcal{C}+k^2\mathcal{D}}{2\left(4\sigma^4-8k\sigma^2x+k^2\left(\left(\sigma^2-1\right)^2+x^4+2\left(\sigma^2+1\right)x^2\right)\right)} \tag{4.126}$$

where

$$\mathcal{C} = 2\sigma^3\left(\sqrt{6}\lambda\left(\sigma^2-1\right)^2+3\sqrt{6}\lambda x^4-12x^3+4\sqrt{6}\lambda\left(\sigma^2-1\right)x^2\right), \tag{4.127}$$

$$\mathcal{D} = \sigma\left(9\left(\sigma^2-1\right)^2-4\sqrt{6}\lambda x^5+9x^4-4\sqrt{6}\lambda\left(\sigma^2-1\right)x^3+6\left(\sigma^2-1\right)x^2\right), \tag{4.128}$$

respectively. The acceleration equation is given by

$$\frac{\dot{H}}{H^2} = \frac{-6\left(\sigma^6+2\sigma^4x^2\right)+k\mathcal{E}+k^2\mathcal{F}}{4\sigma^4-8k\sigma^2x+k^2\left(\left(\sigma^2-1\right)^2+x^4+2\left(\sigma^2+1\right)x^2\right)}, \tag{4.129}$$

where

$$\mathcal{E} = \sigma^2\left(-\sqrt{6}\lambda\left(\sigma^2-1\right)^2-3\sqrt{6}\lambda x^4+12x^3-4\sqrt{6}\lambda\left(\sigma^2-1\right)x^2+12x\right) = -\frac{\mathcal{C}}{2\sigma}+12x\sigma^2, \tag{4.130}$$

$$\mathcal{F} = 2\left(-3\sigma^4+\sigma^2\left(x^2\left(\sqrt{6}\lambda x-3\right)+6\right)+x^3\left(\sqrt{6}\lambda\left(x^2-1\right)-3x\right)-3\right); \tag{4.131}$$

whereas, the effective equation of state parameter $\widetilde{w}$ is given by

$$\widetilde{w} = \frac{k^2(\mathcal{D}/\sigma)+k(\mathcal{C}/\sigma)+12\sigma^4\left(\sigma^2+2x^2-1\right)}{12\sigma^4-24k\sigma^2x+3k^2\left(\sigma^4+2\sigma^2\left(x^2-1\right)+\left(x^2+1\right)^2\right)}, \tag{4.132}$$

which as $k \to 0$ matches Eq. (4.107).

To determine the fixed points of the system, we follow a similar procedure to the case $\alpha = 2$. This yields the critical points in Table 4.9 and their stability in Table 4.10, which present the following properties. We first notice that Point O does not feature in the analysis presented in Section 4.6. The value of the deceleration parameter q at this point implies a universe where the expansion is decelerating very rapidly. As we shall see, if one demands that $\widetilde{w} \in (-1, 1]$, then this point always lies outside the physically relevant phase space. Point A_- and Point A_+ are again the scalar field kinetic energy dominated solutions, which exist for all values of λ and k. At these points the effective equation of state parameter $\widetilde{w} = 1$, which means the universe behaves like stiff matter, and we also note that there is no acceleration. For Point B to represent an inflationary solution, one requires $q < 0$, which implies $0 < \lambda < \sqrt{3/10}$. Morever, the value of the effective equation of state parameter $\widetilde{w}$ at this point is bounded between -1 and 1 only when $0 < \lambda \leq \sqrt{3}/2$. Point C_+ exists when

$$\frac{1}{\sqrt{2}} < \lambda \leq \sqrt{3} \quad \text{and} \quad k > 0$$
$$\text{or} \quad \lambda > \sqrt{3} \quad \text{and} \quad 2\sqrt{6}\lambda^2 - 2\sqrt{30}\sqrt{2\lambda^2-1} + 9\lambda k + 4\sqrt{6} > 0\,.$$

It represents a scaling solution since the effective equation of state matches the matter equation of state, $\widetilde{w} = w = 0$. As we can see from the deceleration parameter, at this point, there cannot be accelerated expansion. Note that when $\lambda = 1/\sqrt{2}$, Point C degenerates into Point B since $\widehat{\sigma}_+$ vanishes. Point C_- exists when

$$\lambda > \sqrt{3} \quad \text{and} \quad \frac{2\sqrt{60\lambda^2 - 30}}{9\lambda} - \frac{2\left(\sqrt{6}\lambda^2 + 2\sqrt{6}\right)}{9\lambda} \leq k < 0 \tag{4.133}$$

and is always a saddle point. Point D corresponds to a matter dominated universe $\sigma^2 = 1$ and is a critical point for all values of λ and k. It is always a saddle and, as previously noted in Section 4.6, it behaves like Point O in (x, y)-coordinates. At this point, there is no presence of the scalar field as both its kinetic and potential energies vanish. Moreover, this points lies at the intersection of the two regions of the phase space for $k = \sqrt{\frac{2}{3}}\lambda - \frac{1}{\lambda}\sqrt{\frac{3}{2}}$, or, equivalently, $\lambda = \frac{1}{2}\sqrt{\frac{3}{2}}\left(k \pm \sqrt{k^2 + 4}\right)$. Point E exists only when $k < 0$ and $\lambda > 0$, and is a stable node.

Table 4.9: Critical points for Eqs. (4.123) and (4.126). The existence conditions indicate the conditions for each critical point to exist within the physical phase space.
Here $\widehat{\sigma}_\pm = \dfrac{\sqrt{4\lambda^2 - 3\sqrt{6}k\lambda - 12 \pm \sqrt{54k^2\lambda^2 + 16\left(\lambda^2 - 3\right)^2 + 24\sqrt{6}k\left(\lambda^2 + 2\right)\lambda}}}{2\sqrt{2}\lambda}$.

Point	Coordinates (x, σ)	Existence	$\widetilde{w}$	q
Point O	$(0, 0)$	for all λ, k	3	5
Point A_-	$(-1, 0)$	for all λ, k	1	2
Point A_+	$(1, 0)$	for all λ, k	1	2
Point B	$\left(\sqrt{\frac{3}{2}}\frac{1}{\lambda}, 0\right)$	for $k > 0$, $0 < \lambda \leq \sqrt{3/2}$ for $k < 0$, $\lambda \geq \sqrt{3/2}$	$3 - \frac{12}{2\lambda^2 + 3}$	$5 - \frac{18}{2\lambda^2 + 3}$
Point C_+	$\left(\sqrt{\frac{3}{2}}\frac{1}{\lambda}, \widehat{\sigma}_+\right)$	see Fig. 4.20	0	1/2
Point C_-	$\left(\sqrt{\frac{3}{2}}\frac{1}{\lambda}, \widehat{\sigma}_-\right)$	see Fig. 4.20	0	1/2
Point D	$(0, 1)$	for all λ, k	0	1/2
Point E	$\left(-\frac{3}{2}\sqrt{\frac{3}{2}}\frac{1}{\lambda}, \sqrt{-\frac{3}{2}\sqrt{\frac{3}{2}}\frac{k}{\lambda}}\right)$	for $k < 0$, $\lambda > 0$	0	1/2

Before moving on to the analysis of the critical points, let us remark that, similarly to the case discussed in Section 4.5, the point in the physical phase space connecting the two main regions (recall Eqs. (4.115) and (4.116)) is a removable singularity for the dynamical system given in Eqs. (4.117) and (4.120). It is not possible to assign a single value of q or $\widetilde{w}$ to the system at this point, because q and $\widetilde{w}$ do not have well-defined limits as x and σ approach the intersection. Nevertheless, along any given trajectory through this point, the limit of q or $\widetilde{w}$ does exist; in particular, a trajectory in the physical phase space for which $-1 < \widetilde{w} \leq 1$ holds, and which

Table 4.10: Stability of the critical points for system given in Eqs. (4.123) and (4.126). Here λ is assumed to be nonnegative. For properties of Point C, see Fig. 4.20.

Point	Eigenvalues	Classification
Point O	$9/2\,,\quad -3$	saddle
Point A_-	$3/2\,,\quad 3+\sqrt{6}\lambda$	unstable node
Point A_+	$3/2\,,\quad 3-\sqrt{6}\lambda$	unstable if $0<\lambda<\sqrt{3/2}$ saddle if $\lambda>\sqrt{3/2}$
Point B	$3-\frac{18}{2\lambda^2+3}\,,\quad \frac{9}{2}-\frac{18}{2\lambda^2+3}$	stable node if $0<\lambda<1/\sqrt{2}$ saddle if $1/\sqrt{2}<\lambda<\sqrt{3/2}$ unstable node if $\lambda>\sqrt{3/2}$
Point D	$3\,,\quad -3/2$	saddle
Point E	$-15/2\,,\quad -9$	stable node

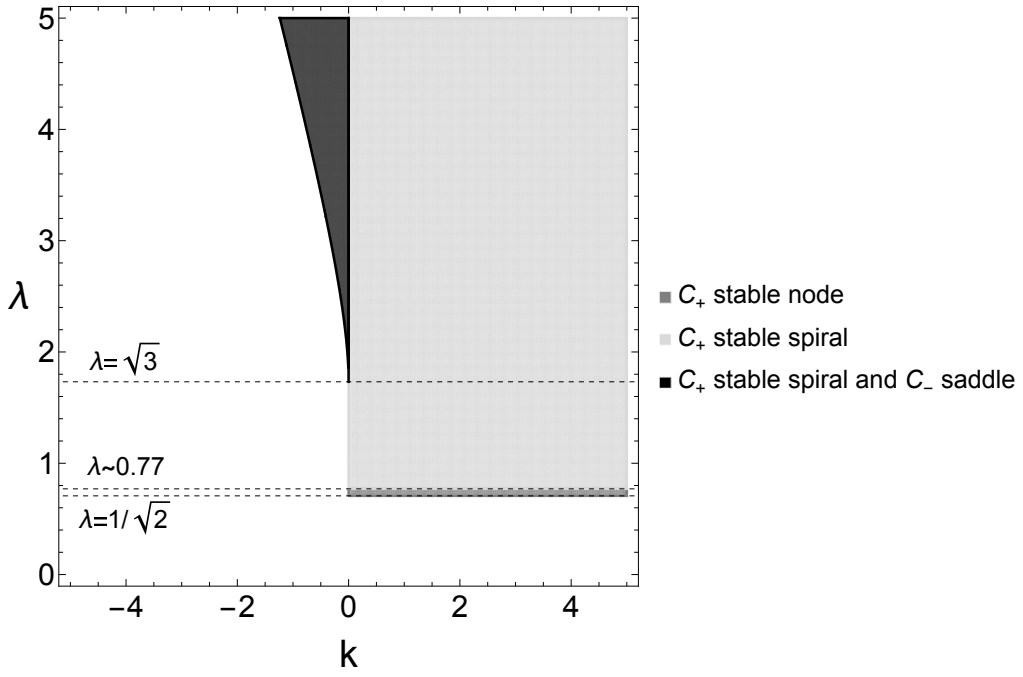

Fig. 4.20: The shaded regions are those where Point C_+ exists within the physical phase space. For values of k and λ within the dark gray region, Point C_+ is a stable node; for values of k and λ within the light gray region, Point C_+ is a stable spiral. Point C_- exists in the physical phase space only for values of k and λ within the black region and is a saddle point whereas Point C_+ is a stable spiral.

traverses the intersection point, will have $-1<\widetilde{w}\leq 1$ at the intersection point too.

4.7.2 *Phase space diagrams and physical interpretation*

For varying values of λ and k, we obtain different models, as shown in Fig. 4.21. Here we present some of the different cases and illustrate their cosmological meaning.

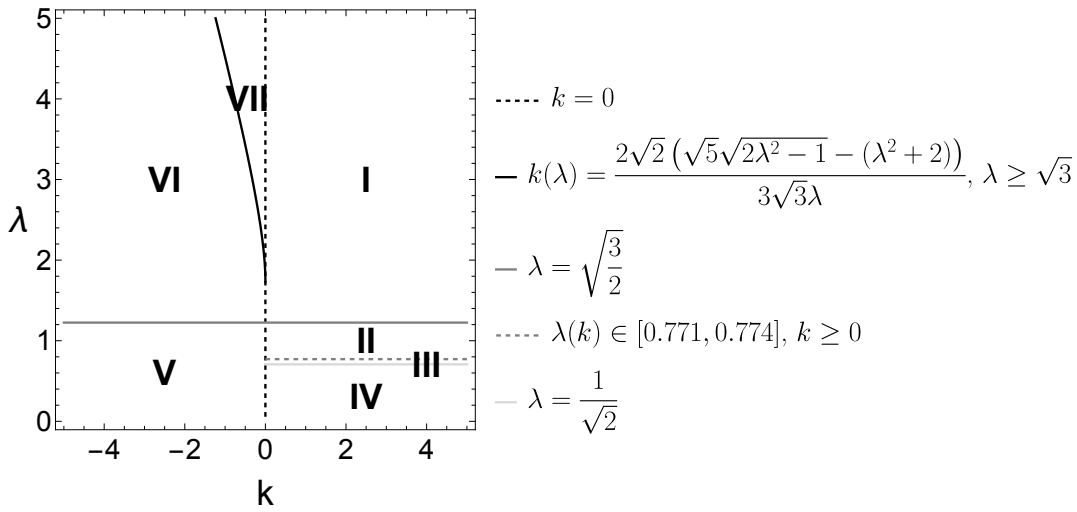

Fig. 4.21: Existence and stability regions in (k, λ)-plane for $w = 0$. The plotted curves follow from the stability criteria given in Table 4.10.

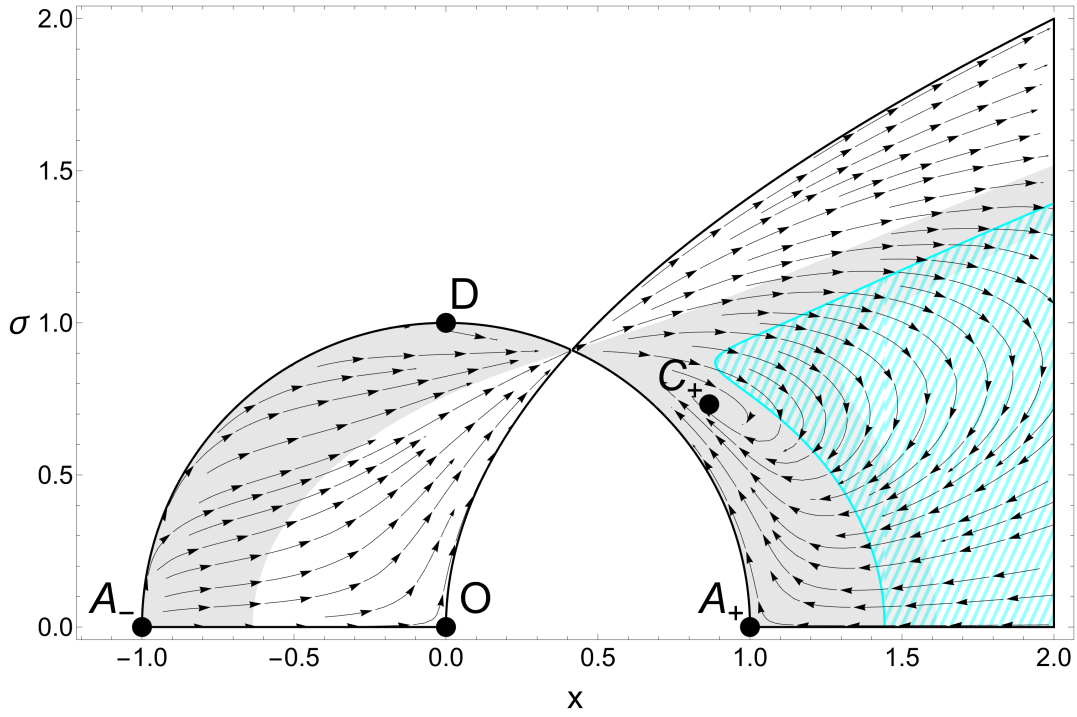

Fig. 4.22: The parameter values are $\lambda = \sqrt{2}$ and $k = 2$. Point C is a stable node. The shaded grey region represents the part where $-1 < \widetilde{w} \leq 1$. The hatched cyan region represents the part where the phase space is accelerating.

Region I. In this region, there are five fixed points within the physical phase space, as constrained by the Friedmann constraint. More specifically, we have Point O, which is a saddle; Point A_-, which is an unstable node; Point A_+, which is a saddle; Point C_+, which is a stable spiral; and Point D, which is a saddle. Firstly, let us note that the values taken by the effective equation of state parameter $\widetilde{w}$ are not physical at all fixed points (e.g. at Point O, $\widetilde{w} = 3$). Therefore,

apart from the Friedmann constraint, a further restriction of $\widetilde{w}$ is needed to obtain the physical phase space. As we shall see in specific examples, this condition limits the candidate trajectories remarkably. As shown in Fig. 4.22, consider the case $\lambda = \sqrt{2}$ and $k = 2$. The trajectories on the right-hand-side of the phase space cannot get too close to Point O. Therefore, a trajectory starting at A_- would reach the saddle point, Point D, and traverse the phase space before being attracted to Point C_+. For a trajectory to approach Point A_+, it would have to go through the region where $\widetilde{w} < -1$. We remark that Point C_+ is once again a scaling solution, but it is not inflationary. Since this case presents only a source (stable node), there is only one possible evolution, unlike in the case $\alpha = 2$, where we had two possible alternatives depending on the side of the phase space from which the trajectory begins.

Regions II and III. In these regions, there are six fixed points within the physical phase space, as constrained by the Friedmann constraint. In particular, Point O is a saddle; Point A_- is an unstable node; Point A_+ is unstable; Point B is a saddle; Point C_+ is a stable spiral in Region II and a stable node in Region III; and Point D is a saddle. The boundary between Region II and Region III is approximately at $\lambda \approx 0.77$. Whilst, from Fig. 4.21, the boundary may appear to be a line, it is, in fact, a non-constant function $\lambda(k)$ for $k > 0$, which takes values in the interval $[0.771, 0.774]$. The value of $\lambda(k)$ may be described as the root of a certain polynomial over the integers of degree 68 in λ and 32 in k; however, there is no benefit to studying this explicitly. We can, however, extract from this the limiting values as $k \to 0^+$ and $k \to \infty$. In particular, as $k \to 0^+$, $\lambda \to \frac{1}{22}\sqrt{3(259 - 5\sqrt{1057})} \approx 0.773164$, whereas as $k \to \infty$, $\lambda \to \frac{5}{\sqrt{42}} \approx 0.771517$. As an example for Region II, consider Fig. 4.23 in which $\lambda = k = 1$. A physically meaningful trajectory then starts near Point A_- and gets closer to the saddle, Point D, but never close to Point O. Then, it crosses to the left-hand side of the phase space, to the region of accelerated expansion, and spirals into Point C. In Fig. 4.23, we have plotted two numerical trajectories. The dashed blue trajectory always stays within $-1 < \widetilde{w} \leq 1$. However, the solid red trajectory, in the region of accelerated expansion, leaves the region $-1 < \widetilde{w} \leq 1$, landing in a region of phantom dark energy ($\widetilde{w} < -1$, in particular here $\widetilde{w} \approx -1.17$). The evolution of $x(t)$ and $\sigma(t)$ along with physical parameters $\widetilde{w}$ and q for this trajectory is displayed in Fig. 4.24. As we can see from the values of q, this solution features early-time inflation as well as late-time accelerated expansion. The effective equation of state parameter crosses the phantom divide at the present, i.e. $\log(a) = 0$; whereas, at late times, the trajectory approaches the Point C_+, which is matter-dominated, as can also be seen from the value of the equation of state parameter tending to zero. As one would expect, the longest time is spent in the vicinity of the fixed points. On the other hand, a trajectory which starts at Point A_+ would then move towards the saddle point, Point B, and spiral into Point C, after a small phase

of accelerated expansion. Point C is a scaling solution because the value of the effective equation of state parameter at this point reduces to that of the matter component.

Region IV. In this region, we have only five fixed points. In particular, Point O is a saddle; Point A_- is an unstable node; Point A_+ is unstable; Point B is a stable node; and Point D is a saddle. As an example, consider $\lambda = \sqrt{1/5}$ and $k = 2$, shown in Fig. 4.25. The limited physical phase space does not allow for many possible trajectories, but only yields two possibilities: a trajectory starting near Point A_- then moves towards the saddle, Point D, crosses the phase space to then ends up at Point B, which lies in the region of accelerated expansion and, hence, represents an inflationary solution; alternatively, there is a trivial universe evolution that starts in the vicinity of Point A_+ and ends at Point B. We remark that physically meaningful streamlines that give rise to phantom dark energy are also possible for this model.

Regions V. In this region, we have only five fixed points. In particular, Point O is a saddle; Point A_- is an unstable node; Point A_+ is unstable; Point D is a saddle; and Point E is a stable node. This case is analogous to that discussed in Region I. A trajectory starting near Point A_+ would be attracted to the saddle, Point D, before entering on the other side of the phases space, which in this case appears on the left-hand side, and would then be attracted to Point E, that is, the scaling solution. We remark that, like for Region I, Point E is not an inflationary solution since the region of accelerated expansion is for $x < -2$, which is not traversed by the physically relevant trajectories, and hence does not feature elsewhere. This also means that this specific model is not physically relevant.

Region VI and VII. In Region VI, we have six fixed points, whereas in Region VII we have all the fixed points. In particular, the fixed points which are common to both regions are: Point O which is a saddle; Point A_- which is an unstable node; Point A_+ which is a saddle; Point B which is an unstable node; Point D which is a saddle; and Point E which is a stable node. In Region VII, we also have Point C_-, which is a saddle, and Point C_+ is a stable spiral. Despite the apparently rich dynamics given by the presence of all these fixed points, a closer look reveals that, from a physical point of view, we obtain uninteresting behaviour. As an example, consider the case $\lambda = 5$ and $k = -1$, as shown in Fig. 4.26. Given the fact that we are interested in a limited phase space (the shaded grey region), a potentially viable trajectory is one that starts near Point A_-, follows the boundary, and then ends at Point E. However, the initial conditions for such trajectories would have to be very finely tuned since most trajectories that start very close to the boundary, near Point A_-, quickly move out of the physical region, as illustrated by the dashed blue trajectory in Fig. 4.26.

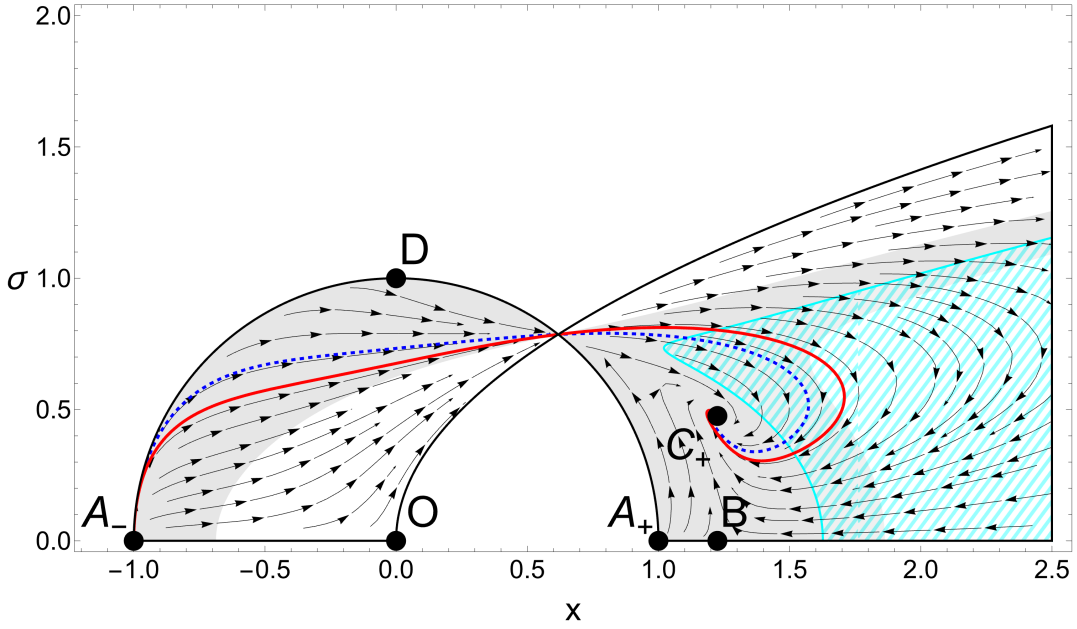

Fig. 4.23: The parameter values are $\lambda = 1$ and $k = 1$. Point B is a saddle and Point C is a stable spiral. The shaded grey region represents the part where $-1 < \widetilde{w} \leq 1$. The hatched cyan region represents the part where the phase space is accelerating. The dashed blue (initial condition $x(0) = -0.99$ and $\sigma(0) = 0.1399$) and solid red (initial condition $x(0) = -0.99$ and $\sigma(0) = 0.033$) curves represent two numerical trajectories.

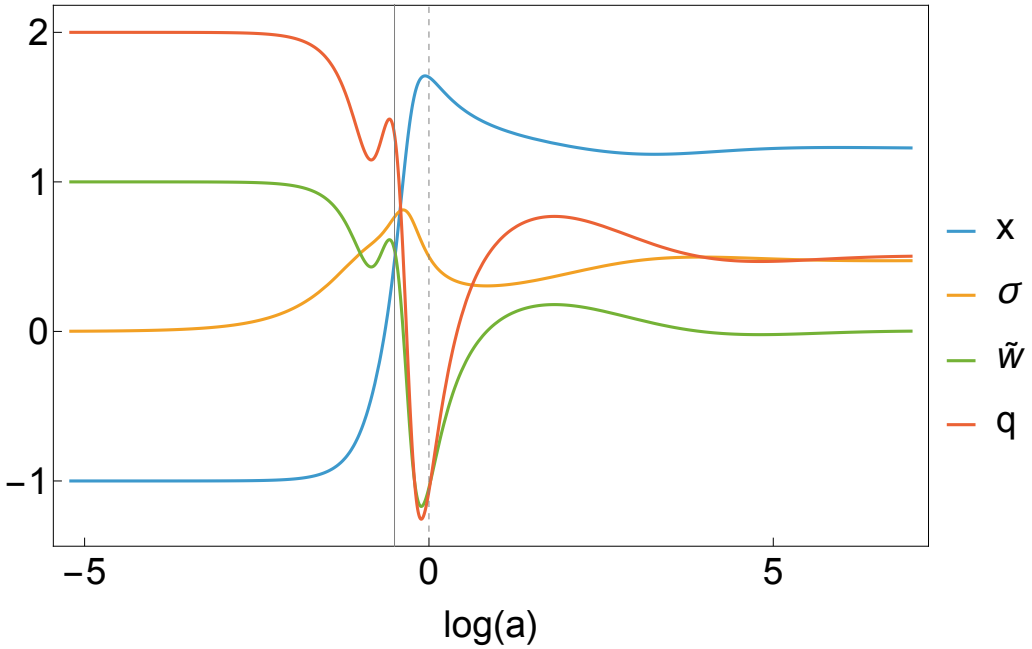

Fig. 4.24: Evolution of the solutions and physical parameters. The parameter values are $\lambda = 1$ and $k = 1$. The initial conditions are $x(0) = -0.99$ and $\sigma(0) = 0.033$), see solid red trajectory in Fig. 4.23. The solid grey line represents when the trajectory traverses the intersection between the two regions of the physical phase space; the dashed grey line represents the present time.

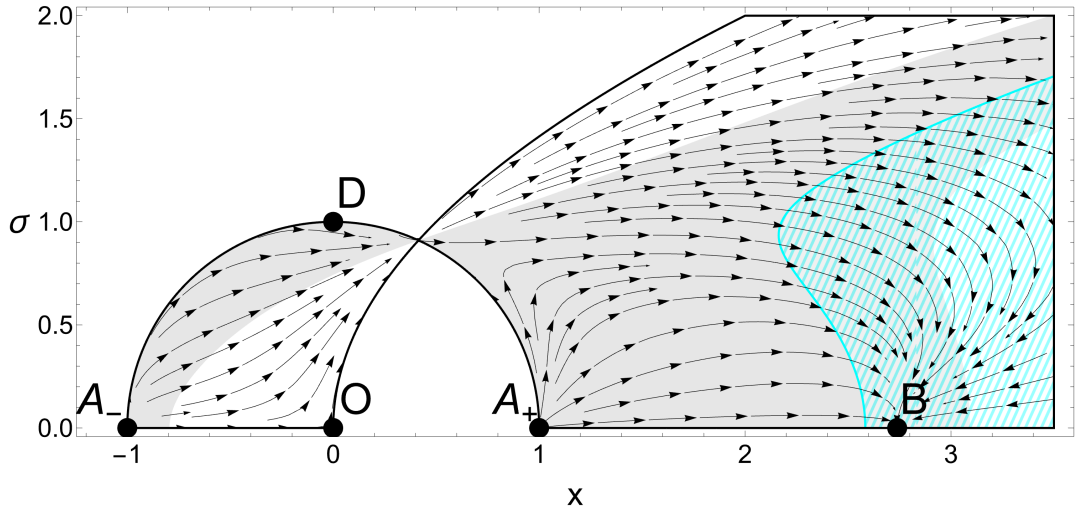

Fig. 4.25: The parameter values are $\lambda = \sqrt{1/5}$ and $k = 2$. Point B is a stable node. The shaded grey region represents the part where $-1 < \widetilde{w} \leq 1$. The hatched cyan region represents the part where the phase space is accelerating.

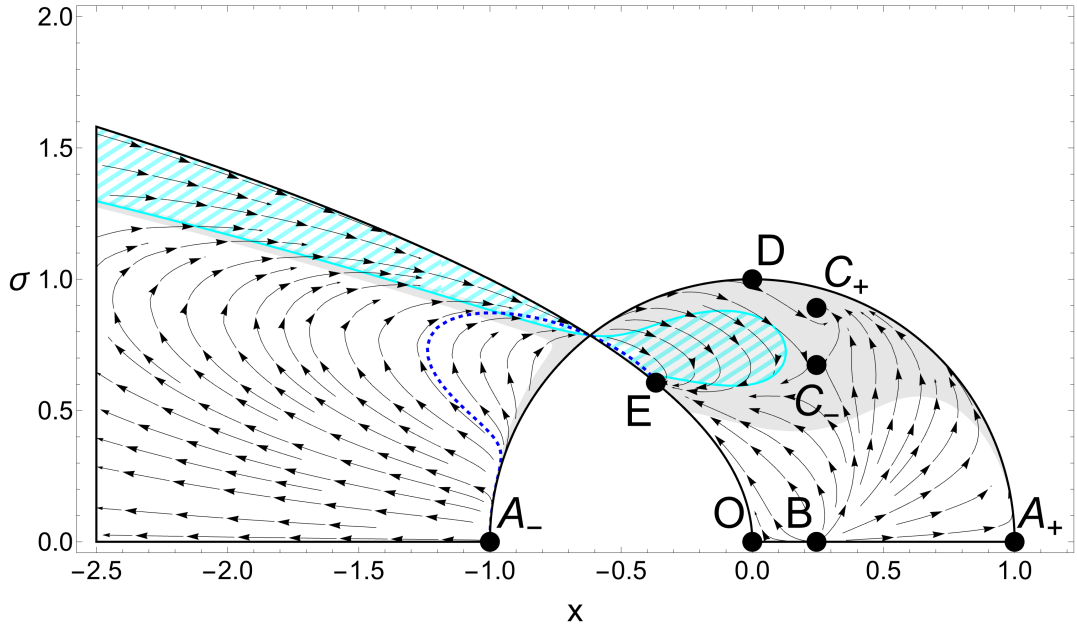

Fig. 4.26: The parameter values are $\lambda = 5$ and $k = -1$. The shaded grey region represents the part where $-1 < \widetilde{w} \leq 1$. The harched cyan region represents the part where the phase space is accelerating. The dashed blue curve (initial condition $x(0) = -0.99$ and $\sigma(0) = 0.0447102$) is a numerical trajectory.

5

Discussion and outlook

In this thesis, we studied two main problems. In Chapter 3, we looked at particle's motion for closed FLRW universes. In general, the study of geodesics is central to cosmology, as all electromagnetic signals travel along them as well as massive particles falling under gravity. Consequently, they are important in the definition of cosmological distances and yield, for example, the distance-redshift relations. We first obtained a formula for the azimuthal angle travelled by a photon within a cycle of recollapse and expansion of a closed universe, $\Delta\varphi = 2\pi/(1+3w)$. Upon setting $w = 0$ (matter-domination) and $w = 1/3$ (radiation-domination), we retrieved the well-known values of 2π and π respectively, which are discussed in cosmology textbooks. We then moved on to find a closed formula for the azimuthal distance travelled by a massless or massive test particle, respectively, in a closed universe during one cycle of expansion and re-collapse. While an FLRW model does not allow closed universe solutions for a universe solely filled with a positive cosmological constant $\Lambda > 0$, two-fluid cosmologies allow us to include Λ. This is, of course, possible as long as the positive cosmological constant does not dominate over the second fluid in such a way as to render closed universe solutions impossible. In our computations, we find that, as expected, $\Delta\varphi$ diverges when we reach this limit. When considering a massless test particle moving in two-fluid cosmologies, we find that the integrals determining $\Delta\varphi$ can be solved in terms of elementary functions only for a universe filled with (a) dust and radiation or (b) radiation and stiff matter; all other cases lead to elliptic integrals. Extending these results to a massive test particle in a one-fluid model, we find that for dust and radiation the value of $\Delta\varphi$ is given in terms of the complete elliptic integral of the first kind with the elliptic modulus depending on the energy density of the fluid and the angular momentum of the particle.

In principle, this could be extended to other set-ups, e.g. to the motion of a massive test particle in two-fluid cosmologies. As suggested by the general expression for $\Delta\varphi$ that we obtained, this would likely involve hyperelliptic integrals or would require numerical tools. Another potential avenue for exploration would be to see whether the geometrical optics approximation [129], which assumes that electromagnetic waves propagating in a source-free region of spacetime are locally plane-fronted and monochromatic, provides a good approximation to the motion of high frequency

gravitational waves through the universe using our solutions for the null geodesics. In [79], the geometrical optics approximation was recently used to describe gravitational waves produced by some astrophysical sources (in the primordial universe) and propagating through a non-empty universe.

In Chapter 4, we employed dynamical system techniques to study the background behaviour of cosmological models. These techniques offer a systematic approach to understanding the underlying dynamics, which allowed us to investigate the suitability of such models as realistic approximations of the universe. Our analysis involved mapping the cosmological equations onto a phase space, a step which relies heavily on the choice of suitable variables. This is rather non-trivial as various different variables could be employed and there is no particular reason to prefer one set of variables over any other. We therefore work with those variables which are known to be well suited for our task, see the review [18].

One of the main motivations of this work was to study models derived from a variational principle, in particular, we used Brown's approach for the formulation of the perfect fluid Langrangian for the cosmological matter. This approach, previously used by [38, 39] to study interaction functions of the form $f(n, s, \phi)$ and $f(n, s, \phi)J^\mu\partial_\mu\phi$, allowed us to introduce new coupling terms, including boundary term couplings, which have not been studied before in this context using fluids. Let us remark that models presenting non-minimal couplings to boundary terms have been studied, for example, in [19, 88, 105]; in particular, in [19, 105], a dynamical system analysis to teleparallel quintessence with a non-minimal coupling to a boundary term was performed. In this thesis, we have considered an algebraic vector coupling of the form $f(n, s, \phi)B^\mu J_\mu$, that is, coupling (ii) in Section 4.2.5, and noted that, in cosmology, one obtains the highly restrictive condition that f is proportional to n. Therefore, such a coupling does not yield interesting phenomena. We therefore focused on a derivative type coupling, $f(n, s, \phi)B^\mu\partial_\mu\phi$, motivated by previous work [39]. To gain an initial understanding of the resulting cosmological model, we began by studying the constant interaction model. This displayed similar behaviour to the well-known exponential potential quintessence model [54], where no interacting term is present. In fact, through a carefully chosen change of variables, we were able to arrive at a phase space which mirrors the one studied by those authors. These results demonstrate that our model can be seen as a natural extension of previous work.

We then proceeded to consider an interaction of the form $n^{\alpha(1+w)/2}V^{-\alpha/2}$. This choice was motivated by the fact that couplings of this form will not increase the dimension of the phase space: it will remain two-dimensional. The key advantage of this assumption is that one can directly compare results with many previously studied models. In particular, we focused on the matter dominated case, $w = 0$, and chose $\alpha = 2$. This choice leads to a rich dynamical structure

with several distinct scenarios that can be of physical relevance. We were able to obtain solutions with early-time inflationary attractors, as well as late-time acceleration. Our models also included scaling solutions, which have received recent attention, see [55], as they may help to resolve the *Hubble tension*, that is, the discrepancy between the value of the Hubble constant inferred from measurements of the early universe and those derived from more recent observations [66, 171]. We then looked at the case $\alpha = -2$. To be able to study this case, it was necessary to eliminate y from the equation instead of the matter variable σ. This prompted re-analysing the exponential potential quintessence model [54] in these other variables so that we could obtain a benchmark for our discussions.

Our approach to constructing coupled models lends itself to a significant amount of further study. First of all, one can study the constant coupling model in the radiation dominated universe. The results should, in principle, be qualitatively similar to the matter dominated case. One could attempt to present a comprehensive study for all w, however, this would not be without challenge. Regarding the non-constant coupling model we proposed, there are two obvious extensions to our work, namely the cases $\alpha \in \{-1, 1\}$. For integer values of α, the phase space will remain two-dimensional. However, one encounters other challenges which can be seen in Eq. (4.71). For large values of α, on the other hand, one is dealing with a polynomial of a high degree, which is difficult to handle. In such cases, the best way forward would be to eliminate the variable x. This is unusual, and has also not been considered in the past. On top of all of this, one could, of course, drop the assumption of working with an exponential potential in favour of power-law potentials, for example. Most of what has been done here would have to be re-investigated.

Moreover, our analysis can be repeated for the algebraic scalar coupling of the form $f(n, s, \phi, \mathbf{B})$, that is, coupling (i) in Section 4.2.5. For example, one could consider an algebraic coupled model that leaves the equations of motion second-order in metric derivatives, and set $f(n, s, \phi, \mathbf{B}) = \widetilde{f}(n, s, \phi)\mathbf{B}$. For a constant function $\widetilde{f}$, one would obtain the standard coupled scalar field dynamics, due to the interaction term taking the form of a total derivative. Considering $\widetilde{f} \propto \mathcal{F}(n^{\alpha(1+w)/2}V^{-\alpha/2})$, with some function $\mathcal{F}$ which is at least twice continuously differentiable, also allows one to close the system without increasing dimension. One may note that, upon rescaling the constant factors, for a model in which $\mathcal{F}$ is logarithmic, we obtain a model which is equivalent to the derivative coupling we considered in Section 4.5.

Lastly, we remark that other interesting models could include interaction functions which contain an explicit dependence on $\mathbf{G}$, or the Ricci scalar, or there could be higher order couplings containing terms, for example, $(B^\mu J_\mu)(B^\nu \partial_\nu \phi)$. Couplings to the bulk term would provide a different set of models, due to the inherent differences between $\mathbf{G}$ and $\mathbf{B}$; the theoretical implications of including nonminimal couplings to non-covariant objects is also a potential avenue for explo-

ration. The work in this thesis has been concerned with the background evolution of the universe, for which the FLRW metric is a good approximation. To connect our results with key cosmological observations (such as the CMB, structure formation, and other early-time probes), cosmological perturbation theory is necessary. This is a non-trivial task, but the dynamical systems work presented provides a good foundation for understanding the background equations and identifying viable models for future study.

Appendix A

Proof of Proposition 1.8

The proof of Proposition 1.8 can be found in [139]. Here, we provide a pedagogical exposition aimed at clarifying some key ideas which are stated without proof in [139]. To this end, we first introduce the following lemmata.

Lemma A.1

Let $u(z)$ be an algebraic function which has no zeros in $\widehat{\mathbb{C}}$. Then, it is a union of non-zero constant functions.

The following proof is based on a sketch of proof provided in [131, Section 8, Theorem 1].

Proof. Assume that $u(z)$ satisfies $P(u(z), z) = 0$, where

$$P(w, z) = a_n(z)w^n + \cdots + a_0(z) \tag{A.1}$$

is an irreducible polynomial with $a_n(z)$ not the zero polynomial. Our aim is to show that, if $u(z)$ has no zeros in $\widehat{\mathbb{C}}$, then each $a_i(z)$ is a constant. From this, it follows immediately that $u(z)$ is a union of constant functions, the roots of $P(w) = a_n w^n + \cdots + a_0$.

Suppose that $a_0(z)$ has a root $z_0 \in \mathbb{C}$, then we have $P(u(z_0), z_0) = 0$, that is,

$$a_n(z_0)u(z_0)^n + \cdots + a_1(z_0)u(z_0) = 0\,, \tag{A.2}$$

which has $u(z_0) = 0$ as a solution, contradicting the assumption that u has no zeros. Hence, $a_0(z)$ is a polynomial with no roots in $\mathbb{C}$, so it must be a non-zero constant.

Now we will consider $u(z)$ at $z = \infty$, and show that the assumption that this is non-zero implies that the remaining a_i's are constant. Let d be the maximum degree of the a_i's, and assume, for a contradiction, that $d \geq 1$. The condition that $P(u(z), z) = 0$ at $z \mapsto 1/z$ yields, after multiplying by z^d, the equation

$$z^d a_n(1/z)u(1/z)^n + \cdots z^d a_1(1/z)u(1/z) + a_0 z^d = 0\,. \tag{A.3}$$

Taking the limit as $z \to 0$, at least one of the first n terms on the left-hand side of Eq. (A.3),

i.e. any such term where $\deg(a_i) = d$, and the final term vanishes since $d \geq 1$. This equation has $u(\infty) = 0$ as a solution, a contradiction. Hence,

$$d = \max_{1 \leq i \leq n} \deg(a_i) = 0\,, \tag{A.4}$$

and these polynomials are all constant. □

Corollary A.2

Any non-constant algebraic function has at least one zero and one pole in $\widehat{\mathbb{C}}$.

Proof. By Lemma A.1, every non-constant algebraic function has a zero in $\widehat{\mathbb{C}}$. We will show that an algebraic function has a zero *if and only if* it has a pole, from which the claim follows.

Fix an algebraic function $u(z)$ which satisfies $P(u(z), z) = 0$, where

$$P(w, z) = a_n(z)u(z)^n + \cdots + a_0(z)\,. \tag{A.5}$$

Let $v(z) = 1/u(z)$, then $v(z)$ satisfies $Q(v(z), z) = 0$ where

$$Q(w, z) = a_0(z)v(z)^n + \cdots + a_n(z)\,. \tag{A.6}$$

Therefore, $v(z)$ is algebraic and, hence, has a zero $z_0 \in \widehat{\mathbb{C}}$ by Lemma A.1. This implies that $u(z)$ has a pole at z_0. □

Lemma A.3

If $u(z)$ *is algebraic, then the residues of* $u'(z)$ *are all zero.*

Proof. Fix $z_0 \in \mathbb{C}$, then we can write $u(z)$ near z_0 as a convergent power series on some neighbourhood of z_0

$$u(z) = \sum_{i=-p}^{\infty} a_i (z - z_0)^{i/m}\,, \tag{A.7}$$

(for a proof of this see e.g. [7, Chapter 8, Section 2.2]) for $m \in \mathbb{Z}_{\geq 0}$ and and $p \in \mathbb{Z}$. We can write

$$u(z) = \sum_{i=-p}^{-1} a_i (z - z_0)^{i/m} + a_0 + \sum_{i=1}^{\infty} a_i (z - z_0)^{i/m} \tag{A.8}$$

$$=: P + a_0 + Q\,. \tag{A.9}$$

We can compute u' by differentiating term by term. When we differentiate $P(z)$ we get terms of the form $b(z - z_0)^r$ where $r \leq -m^{-1} - 1 < -1$, so these terms do not contribute to the residue. Similarly, differentiating $Q(z)$ gives terms of the form $b(z - z_0)^r$, where $r \geq m^{-1} - 1 > -1$. So, again, Q does not contribute to the residue. Differentiating a_0 gives zero, so overall, $u(z)$ has no

residue.

If $z_0 = \infty$, we can perform an almost identical calculation to arrive at the same conclusion. □

Lemma A.4

If $u(z)$ is algebraic, then u'/u has rational residue at all $z_0 \in \widehat{\mathbb{C}}$, and if z_0 is a zero of u, then the residue is non-zero.

Proof. Fix $z_0 \in \mathbb{C}$ and write $u(z)$ near z_0 as a convergent power series on some neighbourhood of z_0

$$u(z) = \sum_{i=p}^{\infty} a_i (z - z_0)^{i/m}, \tag{A.10}$$

for $m \in \mathbb{Z}_{\geq 0}$ and and $p \in \mathbb{Z}$. We can write

$$u(z) = (z - z_0)^{p/m} \sum_{i=0}^{\infty} a_{i+p} (z - z_0)^{i/m} = a_p (z - z_0)^{p/m} \left(1 + \mathcal{O}\left((z - z_0)^{1/m}\right)\right). \tag{A.11}$$

Then,

$$u'(z) = a_p \frac{p}{q} (z - z_0)^{p/m - 1} \left(1 + \mathcal{O}\left((z - z_0)^{1/m}\right)\right). \tag{A.12}$$

So,

$$\frac{u'(z)}{u(z)} = \frac{p}{m} \frac{1}{z - z_0} \left(1 + \mathcal{O}\left((z - z_0)^{1/m}\right)\right). \tag{A.13}$$

Hence, u'/u has residue $p/m \in \mathbb{Q} \setminus \{0\}$. On the other hand, if $p = 0$,

$$u(z) = a_0 + a_1 (z - z_0)^{1/m} + \mathcal{O}\left((z - z_0)^{2/m}\right), \tag{A.14}$$

$$\implies u'(z) = \frac{a_1}{m} (z - z_0)^{1/m - 1} + a_2 (z - z_0)^{2/m - 1} \left(1 + \mathcal{O}\left((z - z_0)^{1/m}\right)\right). \tag{A.15}$$

So,

$$\frac{u'(z)}{u(z)} = \frac{(z - z_0)^{1/m - 1} \left(a_1/m + \mathcal{O}\left((z - z_0)^{1/m}\right)\right)}{a_0 + \mathcal{O}\left((z - z_0)^{1/m}\right)} \tag{A.16}$$

$$= (z - z_0)^{1/m - 1} \left(\frac{a_1}{m a_0} + \mathcal{O}\left((z - z_0)^{1/m}\right)\right). \tag{A.17}$$

Hence, u'/u has residue $0 \in \mathbb{Q}$. □

We are now ready to prove Proposition 1.8.

Proposition ([139, §II.12])

Let $f(z)$ be an algebraic function and assume $\int f(z)\,\mathrm{d}z$ is elementary, but not algebraic. Then, there is a point in $\widehat{\mathbb{C}}$ at which a branch of f has non-zero residue.

Proof. By Liouville's theorem, Theorem 1.6, we have

$$I = \int f(z)\mathrm{d}z = u_0(z) + c_1 \ln(u_1(z)) + \cdots + c_r \ln(u_r(z))\,, \tag{A.18}$$

where $u_i(z)$ algebraic, and non-constant for $i > 0$. Without loss of generality, we can assume $r \geq 1$, since otherwise $\int f(z)\,\mathrm{d}z = u_0(z)$ would be algebraic, contradicting the hypothesis. Note that it is not possible, in general, to rewrite

$$c_1 \ln(u_1(z)) + \cdots + c_r \ln(u_r(z)) = \ln\left(u_1(z)_1^c u_2(z)_2^c \cdots u_r(z)_r^c\right), \tag{A.19}$$

since, unless all c_i's are in $\mathbb{Q}$, neither $u_i(z)^{c_i}$ nor the product of such terms will be algebraic. Furthermore, we can assume that r is minimal; and this implies that the c_i's, which are complex constants, are linearly independent over $\mathbb{Q}$. That is because, if we could find $s_2, \ldots, s_r \in \mathbb{Q}$ such that

$$c_1 = s_2 c_2 + \cdots + s_r c_r\,, \tag{A.20}$$

then we could rewrite Eq. (A.18) as

$$I = \int f(z)\,\mathrm{d}z = u_0(z) + (s_2 c_2 + \cdots + s_r c_r)\ln u_1(z) + c_2 \ln u_2(z) + \cdots c_r \ln u_r(z) \tag{A.21}$$

$$= u_0(z) + c_2 \ln(u_1(z)^{s_2} u_2(z)) + c_3 \ln(u_1(z)^{s_3} u_3(z)) + \cdots + c_r \ln(u_1(z)^{s_r} u_r(z)), \tag{A.22}$$

which contains fewer logarithmic terms, contradicting the minimality of r.

Now, take, for instance, u_1, which is a non-constant algebraic function. By Corollary A.2, u_1 has a zero at $z_0 \in \widehat{\mathbb{C}}$. If we assume, for now, that $z_0 \in \mathbb{C}$, then u_1'/u_1 will have a nonzero residue at z_0 by Lemma A.4. Write each u_i'/u_i as a (rational) Laurent series at z_0 and define $q_i \in \mathbb{Q}$ to be the coefficient of $(z - z_0)$ in the expansion of u_i'/u_i, and $q_1 \neq 0$. Considering the residue at z_0 of

$$I' = u_0' + c_1 \frac{u_1'}{u_1} + \cdots + c_r \frac{u_r'}{u_r}\,, \tag{A.23}$$

and using the fact that the residue of u_0' is 0 (by Lemma A.3), we have

$$\mathrm{Res}(I', z_0) = 0 + c_1 q_1 + \cdots + c_r q_r \neq 0\,, \tag{A.24}$$

since $q_1 \neq 0$ and the c_i's are linearly independent over $\mathbb{Q}$. A similar argument can be made if u_1 has a zero at $z_0 = \infty$. Either way, we have shown that f has a non-zero residue at some point in $\widehat{\mathbb{C}}$. □

Appendix B

Christoffel symbols for FLRW metric

For the FLRW metric

$$\mathrm{d}s^2 = -\mathrm{d}t^2 + a^2(t)\left(\frac{\mathrm{d}r^2}{1-kr^2} + r^2\left(\mathrm{d}\theta^2 + \sin^2\theta \mathrm{d}\varphi^2\right)\right),$$

the Christoffel symbols are

$$\begin{aligned}
&\Gamma^t_{rr} = \frac{a\dot{a}}{1-kr^2}, && \Gamma^t_{\theta\theta} = a\dot{a}r^2, && \Gamma^t_{\varphi\varphi} = a\dot{a}r^2\sin^2\theta\,,\\
&\Gamma^r_{tr} = \Gamma^r_{rt} = \frac{\dot{a}}{a}, && \Gamma^r_{rr} = \frac{kr}{1-kr^2}, && \Gamma^r_{\theta\theta} = -r\left(1-kr^2\right),\\
&\Gamma^r_{\varphi\varphi} = -r\left(1-kr^2\right)\sin^2\theta, && \Gamma^\theta_{t\theta} = \Gamma^\theta_{\theta t} = \frac{\dot{a}}{a}, && \Gamma^\theta_{\theta r} = \frac{1}{r}\,,\\
&\Gamma^\theta_{\varphi\varphi} = -\cos\theta\sin\theta, && \Gamma^\varphi_{t\varphi} = \Gamma^\varphi_{\varphi t} = \frac{\dot{a}}{a}, && \Gamma^\varphi_{r\varphi} = \Gamma^\varphi_{\varphi r} = \frac{1}{r},\\
&\Gamma^\varphi_{\theta\varphi} = \Gamma^\varphi_{\varphi\theta} = \frac{\cos\theta}{\sin\theta}\,. &&&&
\end{aligned}$$

Bibliography

1. Aad G et al. Evidence for the spin-0 nature of the Higgs boson using ATLAS data. Phys. Lett. B 2013; 726:120–44. DOI: 10.1016/j.physletb.2013.08.026. arXiv: 1307.1432 [hep-ex]
2. Abbott BP et al. Observation of Gravitational Waves from a Binary Black Hole Merger. Phys. Rev. Lett. 2016; 116:061102. DOI: 10.1103/PhysRevLett.116.061102. arXiv: 1602.03837 [gr-qc]
3. Abdalla E and Correa-Borbonet LA. The Elliptic solutions to the Friedmann equation and the Verlinde's maps. 2002 Dec. arXiv: hep-th/0212205
4. Abramowitz M and Stegun IA. Handbook of mathematical functions with formulas, graphs, and mathematical tables. Vol. 55. US Government printing office, 1948
5. Adame AG et al. DESI 2024 VI: Cosmological Constraints from the Measurements of Baryon Acoustic Oscillations. 2024 Apr. arXiv: 2404.03002 [astro-ph.CO]
6. Aghanim N et al. Planck 2018 results. VI. Cosmological parameters. Astron. Astrophys. 2020; 641. [Erratum: Astron.Astrophys. 652, C4 (2021)]:A6. DOI: 10.1051/0004-6361/201833910. arXiv: 1807.06209 [astro-ph.CO]
7. Ahlfors LV et al. Complex analysis: an introduction to the theory of analytic functions of one complex variable. New York: McGraw-Hill, 1966
8. Akhiezer NI. Elements of the theory of elliptic functions. Vol. 79. American Mathematical Soc., 1990
9. Akrami Y et al. Planck 2018 results. VII. Isotropy and Statistics of the CMB. Astron. Astrophys. 2020; 641:A7. DOI: 10.1051/0004-6361/201935201. arXiv: 1906.02552 [astro-ph.CO]
10. Aldrovandi R, Cuzinatto R, and Medeiros L. Analytic solutions for the Λ-FRW model. Foundations of Physics 2006; 36:1736–52
11. Amendola L. Scaling solutions in general nonminimal coupling theories. Phys. Rev. D 1999; 60:043501. DOI: 10.1103/PhysRevD.60.043501. arXiv: astro-ph/9904120
12. Andrews GE, Askey R, and Roy R. Special functions. Vol. 71. Cambridge University Press, 1999
13. Anselmi S, Carney MF, Giblin JT, Kumar S, Mertens JB, O'Dwyer M, Starkman GD, and Tian C. What is flat ΛCDM, and may we choose it? JCAP 2023; 02:049. DOI: 10.1088/1475-7516/2023/02/049. arXiv: 2207.06547 [astro-ph.CO]
14. Armitage JV and Eberlein WF. Elliptic functions. Vol. 67. Cambridge University Press, 2006
15. Arnold VI. Ordinary differential equations. Springer Science & Business Media, 1992
16. Arrowsmith D and Place CM. Dynamical systems: differential equations, maps, and chaotic behaviour. Vol. 5. CRC Press, 1992
17. Assad MJD and Ademir Sales de Lima J. General and Unified Solution for Perfect Fluid Homogeneous and Isotropic Cosmological Models. Gen. Rel. Grav. 1988; 20:527. DOI: 10.1007/BF00758908

18. Bahamonde S, Böhmer CG, Carloni S, Copeland EJ, Fang W, and Tamanini N. Dynamical systems applied to cosmology: dark energy and modified gravity. Phys. Rept. 2018; 775-777:1–122. DOI: 10.1016/j.physrep.2018.09.001. arXiv: 1712.03107 [gr-qc]
19. Bahamonde S and Wright M. Teleparallel quintessence with a nonminimal coupling to a boundary term. Phys. Rev. D 2015; 92. [Erratum: Phys.Rev.D 93, 109901 (2016)]:084034. DOI: 10.1103/PhysRevD.92.084034. arXiv: 1508.06580 [gr-qc]
20. Bamba K, Capozziello S, Nojiri S, and Odintsov SD. Dark energy cosmology: the equivalent description via different theoretical models and cosmography tests. Astrophys. Space Sci. 2012; 342:155–228. DOI: 10.1007/s10509-012-1181-8. arXiv: 1205.3421 [gr-qc]
21. Barrow JD and Dabrowski MP. Oscillating Universes. Mon. Not. Roy. Astron. Soc. 1995; 275:850–62
22. Barrow JD, Galloway GJ, and Tipler FJ. The closed-universe recollapse conjecture. Mon. Not. Roy. Astron. Soc. 1986 Dec; 223:835–44. DOI: 10.1093/mnras/223.4.835
23. Barrow JD and Ganguly C. The Shape of Bouncing Universes. Int. J. Mod. Phys. D 2017; 26:1743016. DOI: 10.1142/S0218271817430167. arXiv: 1705.06647 [gr-qc]
24. Barrow JD, Kimberly D, and Magueijo J. Bouncing universes with varying constants. Class. Quant. Grav. 2004; 21:4289–96. DOI: 10.1088/0264-9381/21/18/001. arXiv: astro-ph/0406369
25. Baumann D. Cosmology. Cambridge University Press, 2022 Jul. DOI: 10.1017/9781108937092
26. Bertacca D, Bartolo N, and Matarrese S. Unified Dark Matter Scalar Field Models. Advances in Astronomy 2010; 2010:1–29. DOI: 10.1155/2010/904379
27. Billyard AP and Coley AA. Interactions in scalar field cosmology. Phys. Rev. D 2000; 61:083503. DOI: 10.1103/PhysRevD.61.083503. arXiv: astro-ph/9908224
28. Böhmer CG and Chan N. Dynamical systems in cosmology. *Dynamical and Complex Systems*. World Scientific, 2017 :121–56
29. Böhmer CG. Foundations of Gravity—Modifications and Extensions. *Modified Gravity and Cosmology: An Update by the CANTATA Network*. Cham: Springer International Publishing, 2021 :27–38. DOI: 10.1007/978-3-030-83715-0_3
30. Böhmer CG. Introduction to General Relativity and Cosmology. Essential Textbooks in Physics. World Scientific, 2016 Dec. DOI: 10.1142/q0034
31. Böhmer CG, Caldera-Cabral G, Lazkoz R, and Maartens R. Dynamics of dark energy with a coupling to dark matter. Phys. Rev. D 2008; 78:023505. DOI: 10.1103/PhysRevD.78.023505. arXiv: 0801.1565 [gr-qc]
32. Böhmer CG, Chan N, and Lazkoz R. Dynamics of dark energy models and centre manifolds. Phys. Lett. B 2012; 714:11–7. DOI: 10.1016/j.physletb.2012.06.064. arXiv: 1111.6247 [gr-qc]
33. Böhmer CG, d'Alfonso del Sordo A, and Hartmann B. Azimuthal geodesics in closed FLRW cosmologies. 2024 Jan. arXiv: 2401.04597 [gr-qc]
34. Böhmer CG, d'Alfonso del Sordo A, Hartmann B, and Münch LE. Azimuthal geodesics in closed FLRW cosmological models. Phys. Rev. D 2024; 110:083504. DOI: 10.1103/PhysRevD.110.083504. arXiv: 2404.18119 [gr-qc]
35. Böhmer CG and Jensko E. Modified gravity: A unified approach. Phys. Rev. D 2021; 104:024010. DOI: 10.1103/PhysRevD.104.024010. arXiv: 2103.15906 [gr-qc]
36. Böhmer CG and Jensko E. Modified gravity: A unified approach to metric-affine models. J. Math. Phys. 2023; 64:082505. DOI: 10.1063/5.0150038. arXiv: 2301.11051 [gr-qc]
37. Böhmer CG and Sordo A d'Alfonso del. Cosmological fluids with boundary term couplings. Gen. Rel. Grav. 2024; 56:75. DOI: 10.1007/s10714-024-03260-6. arXiv: 2404.05301 [gr-qc]
38. Böhmer CG, Tamanini N, and Wright M. Interacting quintessence from a variational approach Part I: algebraic couplings. Phys. Rev. D 2015; 91:123002. DOI: 10.1103/PhysRevD.91.123002. arXiv: 1501.06540 [gr-qc]

39. Böhmer CG, Tamanini N, and Wright M. Interacting quintessence from a variational approach Part II: derivative couplings. Phys. Rev. D 2015; 91:123003. DOI: 10.1103/PhysRevD.91.123003. arXiv: 1502.04030 [gr-qc]
40. Bondi H. Spherically symmetrical models in general relativity. Mon. Not. Roy. Astron. Soc. 1947; 107:410–25. DOI: 10.1093/mnras/107.5-6.410
41. Brandenberger R and Peter P. Bouncing Cosmologies: Progress and Problems. Found. Phys. 2017; 47:797–850. DOI: 10.1007/s10701-016-0057-0. arXiv: 1603.05834 [hep-th]
42. Brans C and Dicke RH. Mach's principle and a relativistic theory of gravitation. Phys. Rev. 1961; 124. Ed. by Hsu JP and Fine D:925–35. DOI: 10.1103/PhysRev.124.925
43. Brown JD. Action functionals for relativistic perfect fluids. Class. Quant. Grav. 1993; 10:1579–606. DOI: 10.1088/0264-9381/10/8/017. arXiv: gr-qc/9304026
44. Byrd PF and Friedman MD. Handbook of Elliptic Integrals for Engineers and Scientists. Vol. 67. Grundlehren der mathematischen Wissenschaften. Springer, 1971. DOI: 10.1007/978-3-642-65138-0
45. Caldera-Cabral G, Maartens R, and Urena-Lopez LA. Dynamics of interacting dark energy. Phys. Rev. D 2009; 79:063518. DOI: 10.1103/PhysRevD.79.063518. arXiv: 0812.1827 [gr-qc]
46. Capozziello S. Curvature quintessence. Int. J. Mod. Phys. D 2002; 11:483–92. DOI: 10.1142/S0218271802002025. arXiv: gr-qc/0201033
47. Capozziello S and Francaviglia M. Extended Theories of Gravity and their Cosmological and Astrophysical Applications. Gen. Rel. Grav. 2008; 40:357–420. DOI: 10.1007/s10714-007-0551-y. arXiv: 0706.1146 [astro-ph]
48. Carroll SM. Spacetime and Geometry: An Introduction to General Relativity. Cambridge University Press, 2019. DOI: 10.1017/9781108770385
49. Chandrasekhar S. The mathematical theory of black holes. Oxford University Press, 1985
50. Chen S, Gibbons GW, Li Y, and Yang Y. Friedmann's equations in all dimensions and Chebyshev's theorem. JCAP 2014; 12:035. DOI: 10.1088/1475-7516/2014/12/035. arXiv: 1409.3352 [astro-ph.CO]
51. Chruściel PT. Elements of general relativity. Springer Nature, 2020
52. Cieślik A and Mach P. Revisiting timelike and null geodesics in the Schwarzschild spacetime: general expressions in terms of Weierstrass elliptic functions. Class. Quant. Grav. 2022; 39:225003. DOI: 10.1088/1361-6382/ac95f2. arXiv: 2203.12401 [gr-qc]
53. Clifton T, Ferreira PG, Padilla A, and Skordis C. Modified Gravity and Cosmology. Phys. Rept. 2012; 513:1–189. DOI: 10.1016/j.physrep.2012.01.001. arXiv: 1106.2476 [astro-ph.CO]
54. Copeland EJ, Liddle AR, and Wands D. Exponential potentials and cosmological scaling solutions. Phys. Rev. D 1998; 57:4686–90. DOI: 10.1103/PhysRevD.57.4686. arXiv: gr-qc/9711068
55. Copeland EJ, Moss A, Sevillano Muñoz S, and White JMM. Scaling solutions as Early Dark Energy resolutions to the Hubble tension. 2023 Sep. arXiv: 2309.15295 [astro-ph.CO]
56. Copeland EJ, Sami M, and Tsujikawa S. Dynamics of dark energy. Int. J. Mod. Phys. D 2006; 15:1753–936. DOI: 10.1142/S021827180600942X. arXiv: hep-th/0603057
57. Coquereaux R and Grossmann A. Analytic Discussion of Spatially Closed Friedmann Universes With Cosmological Constant and Radiation Pressure. Annals Phys. 1982; 143:296. DOI: 10.1016/0003-4916(82)90030-6
58. D'Ambroise J. Applications of Elliptic and Theta Functions to Friedmann-Robertson-Lemaître-Walker Cosmology with Cosmological Constant. *MSRI summer graduate workshop: A Window into Zeta and Modular Physics*. 2009 Aug. arXiv: 0908.2481 [gr-qc]
59. d'Inverno R and Vickers J. Introducing Einstein's relativity: a deeper understanding. Oxford University Press, 2022

60. Dabrowski M and Stelmach J. Analytic solutions of Friedman equation for spatially opened universes with cosmological constant and radiation pressure. Annals of Physics 1986; 166:422–42
61. De Felice A and Tsujikawa S. f(R) theories. Living Rev. Rel. 2010; 13:3. DOI: 10.12942/lrr-2010-3. arXiv: 1002.4928 [gr-qc]
62. Delphenich DH. Proper Time Foliations of Lorentz Manifolds. 2002. arXiv: gr-qc/0211066 [gr-qc]
63. Dhawan S, Alsing J, and Vagnozzi S. Non-parametric spatial curvature inference using late-Universe cosmological probes. Mon. Not. Roy. Astron. Soc. 2021; 506:L1–L5. DOI: 10.1093/mnrasl/slab058. arXiv: 2104.02485 [astro-ph.CO]
64. Di Valentino E, Melchiorri A, and Silk J. Investigating Cosmic Discordance. Astrophys. J. Lett. 2021; 908:L9. DOI: 10.3847/2041-8213/abe1c4. arXiv: 2003.04935 [astro-ph.CO]
65. Di Valentino E, Melchiorri A, and Silk J. Planck evidence for a closed Universe and a possible crisis for cosmology. Nature Astron. 2019; 4:196–203. DOI: 10.1038/s41550-019-0906-9. arXiv: 1911.02087 [astro-ph.CO]
66. Di Valentino E, Mena O, Pan S, Visinelli L, Yang W, Melchiorri A, Mota DF, Riess AG, and Silk J. In the realm of the Hubble tension—a review of solutions. Class. Quant. Grav. 2021; 38:153001. DOI: 10.1088/1361-6382/ac086d. arXiv: 2103.01183 [astro-ph.CO]
67. *NIST Digital Library of Mathematical Functions*. https://dlmf.nist.gov/, Release 1.2.1 of 2024-06-15
68. Edwards D. Exact expressions for the properties of the zero-pressureFriedmann models. Mon. Not. Roy. Astron. Soc. 1972 Jan; 159:51. DOI: 10.1093/mnras/159.1.51
69. Edwards D. Exact Solutions for Friedmann Models with Radiation. Astrophys. Space Sci. 1973 Oct; 24:563–75. DOI: 10.1007/BF02637173
70. Einstein A. Cosmological Considerations in the General Theory of Relativity. Sitzungsber. Preuss. Akad. Wiss. Berlin (Math. Phys.) 1917; 1917:142–52
71. Einstein A. Hamilton's principle and the general theory of relativity. Sitzungsber. Preuss. Akad. Wiss. Berlin (Math. Phys.) 1916; 1916:1111–6
72. Einstein A. The foundation of the general theory of relativity. Annalen Phys. 1916; 49. Ed. by Hsu JP and Fine D:769–822. DOI: 10.1002/andp.19163540702
73. Euler L. Introduction to analysis of the infinite: Book I. Springer Science & Business Media, 2012
74. Faraoni V. Solving for the dynamics of the universe. Am. J. Phys. 1999; 67:732. DOI: 10.1119/1.19361. arXiv: physics/9901006
75. Faraoni V and Capozziello S. Beyond Einstein Gravity: A Survey of Gravitational Theories for Cosmology and Astrophysics. Dordrecht: Springer, 2011. DOI: 10.1007/978-94-007-0165-6
76. Faraoni V, Jose S, and Dussault S. Multi-fluid cosmology in Einstein gravity: analytical solutions. Gen. Rel. Grav. 2021; 53:109. DOI: 10.1007/s10714-021-02879-z. arXiv: 2107.12488 [gr-qc]
77. Farrar GR and Peebles PJE. Interacting dark matter and dark energy. Astrophys. J. 2004; 604:1–11. DOI: 10.1086/381728. arXiv: astro-ph/0307316
78. Ferraro R and Fiorini F. Modified teleparallel gravity: Inflation without inflaton. Phys. Rev. D 2007; 75:084031. DOI: 10.1103/PhysRevD.75.084031. arXiv: gr-qc/0610067
79. Fier J, Fang X, Li B, Mukohyama S, Wang A, and Zhu T. Gravitational wave cosmology: High frequency approximation. Phys. Rev. D 2021; 103:123021. DOI: 10.1103/PhysRevD.103.123021. arXiv: 2102.08968 [astro-ph.CO]
80. Filippov AF. Differential equations with discontinuous righthand sides: control systems. Vol. 18. Springer Science & Business Media, 2013
81. Fitch VL, Marlow DR, and Dementi MA. Critical problems in physics. Princeton University Press, 1998

82. Friedman A. On the Curvature of space. Z. Phys. 1922; 10:377–86. DOI: 10.1007/BF01332580
83. Gell-Mann M. The interpretation of the new particles as displaced charge multiplets. Nuovo Cim. 1956; 4:848–66. DOI: 10.1007/bf02748000
84. Glanville A, Howlett C, and Davis TM. Full-shape galaxy power spectra and the curvature tension. Mon. Not. Roy. Astron. Soc. 2022; 517:3087–100. DOI: 10.1093/mnras/stac2891. arXiv: 2205.05892 [astro-ph.CO]
85. Glendinning P. Stability, Instability and Chaos: An Introduction to the Theory of Nonlinear Differential Equations. Cambridge Texts in Applied Mathematics. Cambridge University Press, 1994 :i–vi
86. Granda LN and Jimenez DF. Dark Energy from Gauss-Bonnet and non-minimal couplings. Phys. Rev. D 2014; 90:123512. DOI: 10.1103/PhysRevD.90.123512. arXiv: 1411.4203 [gr-qc]
87. Griffiths Jerry B. and Podolsky J. Exact Space-Times in Einstein's General Relativity. Cambridge Monographs on Mathematical Physics. Cambridge: Cambridge University Press, 2009. DOI: 10.1017/CBO9780511635397
88. Guarnizo A, Castaneda L, and Tejeiro JM. Boundary Term in Metric f(R) Gravity: Field Equations in the Metric Formalism. Gen. Rel. Grav. 2010; 42:2713–28. DOI: 10.1007/s10714-010-1012-6. arXiv: 1002.0617 [gr-qc]
89. Guo ZK, Ohta N, and Tsujikawa S. Probing the Coupling between Dark Components of the Universe. Phys. Rev. D 2007; 76:023508. DOI: 10.1103/PhysRevD.76.023508. arXiv: astro-ph/0702015
90. Halburd R. Special Functions. *LTCC Advanced Mathematics Series: Volume 6 Analysis and Mathematical Physics*. World Scientific, 2017. Chap. 4:109–38. DOI: 10.1142/9781786341006_0004
91. Hall G. Symmetries and Curvature Structure in General Relativity. World Scientific Lecture Notes in Physics 2004; 46
92. Handley W. Curvature tension: evidence for a closed universe. Phys. Rev. D 2021; 103:L041301. DOI: 10.1103/PhysRevD.103.L041301. arXiv: 1908.09139 [astro-ph.CO]
93. Hardy GH. The integration of functions of a single variable. 2. University Press, 1916
94. Harko T, Lobo FSN, Nojiri S, and Odintsov SD. $f(R,T)$ gravity. Phys. Rev. D 2011; 84:024020. DOI: 10.1103/PhysRevD.84.024020. arXiv: 1104.2669 [gr-qc]
95. Haro J de and Elizalde E. Topics in Cosmology—Clearly Explained by Means of Simple Examples. Universe 2022; 8:166. DOI: 10.3390/universe8030166. arXiv: 2201.06097 [gr-qc]
96. Harrison ER. Classification of Uniform Cosmological Models. Mon. Not. Roy. Astron. Soc. 1967; 137:69–79
97. Harrison E. Cosmology: The Science of the Universe. 2nd ed. Cambridge University Press, 2000. DOI: 10.1017/CBO9780511804540
98. Hawking Stephen W. and Ellis GFR. The Large Scale Structure of Space-Time. Cambridge Monographs on Mathematical Physics. Cambridge University Press, 2023 Feb. DOI: 10.1017/9781009253161
99. He JH and Wang B. Effects of the interaction between dark energy and dark matter on cosmological parameters. JCAP 2008; 06:010. DOI: 10.1088/1475-7516/2008/06/010. arXiv: 0801.4233 [astro-ph]
100. Hilbert D. Die Grundlagen der Physik . (Erste Mitteilung.) Nachrichten von der Gesellschaft der Wissenschaften zu Göttingen, Mathematisch-Physikalische Klasse 1915; 1915:395–408
101. Horowitz W. Mesopotamian cosmic geography. Vol. 8. Eisenbrauns, 1998
102. Ishak M. Testing General Relativity in Cosmology. Living Rev. Rel. 2019; 22:1. DOI: 10.1007/s41114-018-0017-4. arXiv: 1806.10122 [astro-ph.CO]
103. Jensko E. A unified approach to geometric modifications of gravity. PhD thesis. U. Coll. London, 2023. arXiv: 2401.12567 [gr-qc]

104. Joyce A, Jain B, Khoury J, and Trodden M. Beyond the Cosmological Standard Model. Phys. Rept. 2015; 568:1–98. DOI: 10.1016/j.physrep.2014.12.002. arXiv: 1407.0059 [astro-ph.CO]
105. Kadam SA, Thakkar NP, and Mishra B. Dynamical system analysis in teleparallel gravity with boundary term. Eur. Phys. J. C 2023; 83:809. DOI: 10.1140/epjc/s10052-023-11937-6. arXiv: 2306.06677 [gr-qc]
106. Kasper T. Integration in finite terms: the Liouville theory. ACM Sigsam Bulletin 1980; 14:2–8
107. Kharbediya LI. Some exact solutions of the Friedmann equations with the cosmological term. Soviet Astronomy 1976 Dec; 20:647
108. Kiselman CO. Generalized elementary functions. Complex Variables and Elliptic Equations 2023; 68:918–31
109. Knill O. Weierstrass elliptic functions for the pendulum. 2023. arXiv: 2306.10653
110. Koivisto TS, Saridakis EN, and Tamanini N. Scalar-fluid theories: cosmological perturbations and large-scale structure. Journal of Cosmology and Astroparticle Physics 2015 Sep; 2015:47–47. DOI: 10.1088/1475-7516/2015/09/047
111. Koyama K. Gravity beyond general relativity. Int. J. Mod. Phys. D 2018; 27:1848001. DOI: 10.1142/S0218271818480012
112. Lachieze-Rey M and Luminet JP. Cosmic topology. Phys. Rept. 1995; 254:135–214. DOI: 10.1016/0370-1573(94)00085-H. arXiv: gr-qc/9605010
113. Lämmerzahl C and Hackmann E. Analytical Solutions for Geodesic Equation in Black Hole Spacetimes. Springer Proc. Phys. 2016; 170. Ed. by Nicolini P, Kaminski M, Mureika J, and Bleicher M:43–51. DOI: 10.1007/978-3-319-20046-0_5. arXiv: 1506.01572 [gr-qc]
114. Landsberg PT and Evans DA. Mathematical cosmology. An introduction. 1977
115. Lee JM. Introduction to Riemannian manifolds. Vol. 2. Springer, 2018
116. Legendre A. Exercises de calcul integral sur diverses ordres de transcendentes. 1811
117. Lemaître G. A Homogeneous Universe of Constant Mass and Growing Radius Accounting for the Radial Velocity of Extragalactic Nebulae. Annales Soc. Sci. Bruxelles A 1927; 47:49–59. DOI: 10.1007/s10714-013-1548-3
118. Lemaître G. L'Univers en expansion. Annales de la Société Scientifique de Bruxelles 1933 Jan; 53:51
119. Lightman AP. Problem book in relativity and gravitation. Princeton University Press, 1975
120. Lima JAS. Note on solving for the dynamics of the universe. Am. J. Phys. 2001; 69:1245–7. DOI: 10.1119/1.1405506. arXiv: astro-ph/0109215
121. Linde AD. Inflationary theory versus ekpyrotic / cyclic scenario. *Workshop on Conference on the Future of Theoretical Physics and Cosmology in Honor of Steven Hawking's 60th Birthday.* 2002 May :801–38. arXiv: hep-th/0205259
122. Liouville J. Premier mémoire sur la détermination des intégrales dont la valeur est algébrique. Impr. Royale, 1833
123. Luo AC. Discontinuous dynamical systems. Springer, 2012
124. Lützen J. Joseph Liouville 1809–1882: Master of pure and applied mathematics. Vol. 15. Springer Science & Business Media, 2012
125. Magana J and Matos T. A brief Review of the Scalar Field Dark Matter model. J. Phys. Conf. Ser. 2012; 378. Ed. by Barranco J, Contreras G, Delepine D, and Napsuciale M:012012. DOI: 10.1088/1742-6596/378/1/012012. arXiv: 1201.6107 [astro-ph.CO]
126. Magnano G, Ferraris M, and Francaviglia M. Nonlinear gravitational Lagrangians. Gen. Rel. Grav. 1987; 19:465. DOI: 10.1007/BF00760651
127. Marchisotto EA and Zakeri GA. An invitation to integration in finite terms. The College Mathematics Journal 1994; 25:295–308
128. McIntosh CBG. Relativistic cosmological models with both radiation and matter. Monthly Notices of the RAS 1968 Jan; 140:461. DOI: 10.1093/mnras/140.4.461
129. Misner CW, Thorne KS, and Wheeler JA. Gravitation. San Francisco: W. H. Freeman, 1973

130. Nemiroff RJ and Patla B. Adventures in Friedmann Cosmology: An Educationally Detailed Expansion of the Cosmological Friedmann Equations. Am. J. Phys. 2008; 76:265–76. DOI: 10.1119/1.2830536. arXiv: astro-ph/0703739
131. Nixon J. Theory of algebraic functions on the Riemann Sphere. Mathematica Aeterna 2013 Jan; 3:83–101
132. Nojiri S, Odintsov SD, and Oikonomou VK. Modified Gravity Theories on a Nutshell: Inflation, Bounce and Late-time Evolution. Phys. Rept. 2017; 692:1–104. DOI: 10.1016/j.physrep.2017.06.001. arXiv: 1705.11098 [gr-qc]
133. Nojiri S and Odintsov SD. Unified cosmic history in modified gravity: from $f(R)$ theory to Lorentz non-invariant models. Phys. Rept. 2011; 505:59–144. DOI: 10.1016/j.physrep.2011.04.001. arXiv: 1011.0544 [gr-qc]
134. Nojiri S, Odintsov SD, and Sami M. Dark energy cosmology from higher-order, string-inspired gravity and its reconstruction. Phys. Rev. D 2006; 74:046004. DOI: 10.1103/PhysRevD.74.046004. arXiv: hep-th/0605039
135. Pavlov AE. Friedmann Cosmology in Elliptic Functions. Grav. Cosmol. 2021; 27:403–8. DOI: 10.1134/S0202289321040113
136. Pereira SH and Jesus JF. Can Dark Matter Decay in Dark Energy? Phys. Rev. D 2009; 79:043517. DOI: 10.1103/PhysRevD.79.043517. arXiv: 0811.0099 [astro-ph]
137. Perlmutter S et al. Measurements of Ω and Λ from 42 High Redshift Supernovae. Astrophys. J. 1999; 517:565–86. DOI: 10.1086/307221. arXiv: astro-ph/9812133
138. Riess AG et al. Observational evidence from supernovae for an accelerating universe and a cosmological constant. Astron. J. 1998; 116:1009–38. DOI: 10.1086/300499. arXiv: astro-ph/9805201
139. Ritt JF. Integration in finite terms: Liouville's theory of elementary methods. Columbia University Press, 1948
140. Robertson HP. Kinematics and World-Structure. Astrophys. J. 1935; 82:284–301. DOI: 10.1086/143681
141. Robertson HP. Kinematics and World-Structure. 2. Astrophys. J. 1935; 83:187–201. DOI: 10.1086/143716
142. Robertson HP. Kinematics and World-Structure. 3. Astrophys. J. 1936; 83:257–71. DOI: 10.1086/143726
143. Rosenlicht M. Liouville's theorem on functions with elementary integrals. Pacific Journal of Mathematics 1968; 24:153–61
144. Sadjadi HM and Alimohammadi M. Cosmological coincidence problem in interactive dark energy models. Phys. Rev. D 2006; 74:103007. DOI: 10.1103/PhysRevD.74.103007. arXiv: gr-qc/0610080
145. Saridakis EN, Lazkoz R, Salzano V, Vargas Moniz P, Capozziello S, Beltrán Jiménez J, De Laurentis M, and Olmo GJ, eds. Modified Gravity and Cosmology: An Update by the CANTATA Network. Springer, 2021. DOI: 10.1007/978-3-030-83715-0. arXiv: 2105.12582 [gr-qc]
146. Schutz B. A first course in general relativity. Cambridge university press, 2022
147. Semenaite A, Sánchez AG, Pezzotta A, Hou J, Eggemeier A, Crocce M, Zhao C, Brownstein JR, Rossi G, and Schneider DP. Beyond – ΛCDM constraints from the full shape clustering measurements from BOSS and eBOSS. Mon. Not. Roy. Astron. Soc. 2023; 521:5013–25. DOI: 10.1093/mnras/stad849. arXiv: 2210.07304 [astro-ph.CO]
148. Sonego S and Talamini V. Qualitative study of perfect-fluid Friedmann-Lemaître-Robertson-Walker models with a cosmological constant. Am. J. Phys. 2012; 80:670–9. DOI: 10.1119/1.4731258. arXiv: 1112.4319 [physics.ed-ph]
149. Sotiriou TP and Faraoni V. f(R) Theories Of Gravity. Rev. Mod. Phys. 2010; 82:451–97. DOI: 10.1103/RevModPhys.82.451. arXiv: 0805.1726 [gr-qc]
150. Strogatz SH. Nonlinear dynamics and chaos: with applications to physics, biology, chemistry, and engineering. CRC press, 2018

151. Takebe T. Elliptic Integrals and Elliptic Functions. Springer, 2023
152. Tamanini N. Dynamics of cosmological scalar fields. Phys. Rev. D 2014; 89:083521. DOI: 10.1103/PhysRevD.89.083521. arXiv: 1401.6339 [gr-qc]
153. Tamanini N. Phenomenological models of dark energy interacting with dark matter. Phys. Rev. D 2015; 92:043524. DOI: 10.1103/PhysRevD.92.043524. arXiv: 1504.07397 [gr-qc]
154. Tchebichef P. Sur l'intégration des différentielles irrationnelles. Journal de mathématiques pures et appliquées 1853; 18:87–111
155. Temme NM. Special functions: An introduction to the classical functions of mathematical physics. John Wiley & Sons, 2011
156. Tolman RC. Effect of inhomogeneity on cosmological models. Proceedings of the National Academy of Sciences 1934; 20:169–76
157. Tsujikawa S. Quintessence: A Review. Class. Quant. Grav. 2013; 30:214003. DOI: 10.1088/0264-9381/30/21/214003. arXiv: 1304.1961 [gr-qc]
158. Ureña-Lopez LA. Scalar fields in Cosmology: dark matter and inflation. Journal of Physics: Conference Series 2016 Oct; 761:012076. DOI: 10.1088/1742-6596/761/1/012076
159. Ureña-López LA and Roy N. Generalized tracker quintessence models for dark energy. Phys. Rev. D 2020; 102:063510. DOI: 10.1103/PhysRevD.102.063510. arXiv: 2007.08873 [astro-ph.CO]
160. Uzan JP and Lehoucq R. A dynamical study of the Friedmann equations. European Journal of Physics 2001; 22:371
161. Vagnozzi S, Di Valentino E, Gariazzo S, Melchiorri A, Mena O, and Silk J. The galaxy power spectrum take on spatial curvature and cosmic concordance. Phys. Dark Univ. 2021; 33:100851. DOI: 10.1016/j.dark.2021.100851. arXiv: 2010.02230 [astro-ph.CO]
162. Vagnozzi S, Loeb A, and Moresco M. Eppur è piatto? The Cosmic Chronometers Take on Spatial Curvature and Cosmic Concordance. Astrophys. J. 2021; 908:84. DOI: 10.3847/1538-4357/abd4df. arXiv: 2011.11645 [astro-ph.CO]
163. Valiviita J, Maartens R, and Majerotto E. Observational constraints on an interacting dark energy model. Mon. Not. Roy. Astron. Soc. 2010; 402:2355–68. DOI: 10.1111/j.1365-2966.2009.16115.x. arXiv: 0907.4987 [astro-ph.CO]
164. Wainwright J and Ellis GFR. Dynamical systems in cosmology. Cambridge University Press, 1997
165. Wald RM. General Relativity. Chicago, USA: Chicago Univ. Pr., 1984. DOI: 10.7208/chicago/9780226870373.001.0001
166. Walker AG. On Milne's Theory of World-Structure. Proc. Lond. Math. Soc. s 1937; 2–42:90–127. DOI: 10.1112/plms/s2-42.1.90
167. Weinberg S. The Cosmological Constant Problem. Rev. Mod. Phys. 1989; 61. Ed. by Hsu JP and Fine D:1–23. DOI: 10.1103/RevModPhys.61.1
168. Whittaker ET and Watson GN. A course of modern analysis: an introduction to the general theory of infinite processes and of analytic functions; with an account of the principal transcendental functions. University press, 1920
169. Wiggins S. Introduction to Applied Nonlinear Dynamical Systems and Chaos. Texts in Applied Mathematics. Springer New York, 2003
170. Will CM. Theory and Experiment in Gravitational Physics. Cambridge University Press, 2018 Sep
171. Yang W, Pan S, Di Valentino E, Mena O, and Melchiorri A. 2021-H0 odyssey: closed, phantom and interacting dark energy cosmologies. JCAP 2021; 10:008. DOI: 10.1088/1475-7516/2021/10/008. arXiv: 2101.03129 [astro-ph.CO]
172. Zlatev I, Wang LM, and Steinhardt PJ. Quintessence, cosmic coincidence, and the cosmological constant. Phys. Rev. Lett. 1999; 82:896–9. DOI: 10.1103/PhysRevLett.82.896. arXiv: astro-ph/9807002